The characterisation of road surface friction as a factor in vehicle safety

Peter David Sanders

Belfast School of Architecture and the Built Environment

Ulster University

A thesis submitted for the degree of

Doctor of Philosophy

Word count: 19,939

March 2022

For Robin ... I don't understand it either.

Acknowledgements

Disclaimer

The works supporting this thesis were produced at TRL Limited (TRL) under the commission of the Highways Agency (currently National Highways (NH)), and Highways England (currently NH). The novel work presented in this thesis (Chapters 1, 2, 6, 7, and 8) was produced independently of both TRL and National Highways by this thesis author. The novel work, analysis, and conclusions presented in this thesis do not necessarily represent those of TRL or NH.

Contributions to supporting documents

This section summarises the contributions of the authors to the supporting works for this thesis. The following paragraphs detail the activities carried out by the co-authors to those works. All other activities were carried out by this thesis author, P. D. Sanders, and Table 1 details the contributions made by them, expressed as a percentage of the work carried out[1].

The supporting documents to this thesis were produced at TRL and, with the exception of the collection of Computed Tomography data detailed in PPR894 (Sanders, 2017), all activities completed as part of those works were carried out by TRL members of staff.

Chapter 3 is based on two documents: **PPR727 Road surface properties and high speed friction** by P. D. Sanders, K. Morosiuk and J. R. Peeling (Sanders et al., 2014), and **PPR894 Road surface properties and high speed friction - the effect of permeability** (Sanders, 2017).

For PPR727 J. R. Peeling collected data relating to tyre/road surface pressure distributions and digitised this information. Software to convert the digitised pressure distributions into numerical matrices and the initial processing thereof was scripted by K. Morosiuk.

Chapter 4 is based on **PPR815 Better understanding of the tyre surface interface** by P. D. Sanders, M. Militzer and H. E. Viner (Sanders et al., 2017b). For this work M. Militzer carried out an initial review of the literature. The work was reviewed by H. E. Viner who also provided overall guidance and support.

Chapter 5 is based on three documents: **PPR768 Performance review of skid measurement**

---

[1] Where P. D. Sanders is the sole author, a percentage of 95 is given to acknowledge the contribution of support staff.

devices by P. D. Sanders, S. Brittain and A. Premathilaka (Sanders et al., 2017a), **PPR957 Characterising the measurement characteristics of sideway-force skid resistance measurement devices - A desk study and proposal for an experimental study** by P. D. Sanders and C. Browne (Sanders & Browne, 2020), and **PPR980 Characterising the measurement characteristics of sideways-force skid resistance measurement devices - An experimental study** (Sanders, 2021).

For PPR768, S. Brittain conducted the desk study reported in section 3.1 and A. Premathilaka carried out a review of the document. For PPR957, C. Browne carried out an independent verification of the work and authored Appendix A of the document.

The final chapter of this thesis presents a study reported in **PPR988 The relationship between vehicle data, collision risk and skid resistance** (Hammond et al., 2021), whilst omitted as a supporting document to this thesis, P. D. Sanders is a co-author, and developed the research concept for this work, reviewed the document, and provided technical input to the co-authors who carried out the bulk of the study.

Table 1: P. D. Sanders contribution to supporting documents

Document title	% Contribution
PPR727 Road surface properties and high speed friction	85
PPR894 Road surface properties and high speed friction - the effect of permeability	95
PPR815 Better understanding of the tyre surface interface	80
PPR768 Performance review of skid measurement devices	90
PPR957 Characterising the measurement characteristics of sideway-force skid resistance measurement devices - A desk study and proposal for an experimental study	85
PPR980 Characterising the measurement characteristics of sideways-force skid resistance measurement devices - An experimental study	95

Abstract

The relationship between road surface friction and vehicle safety is self evident. This relationship means that the effective management of friction is critical in maintaining a safe environment for all road users. Many road authorities measure low speed friction with devices utilising the sideway-force measurement principle, and assess texture depth as a proxy for high speed friction.

This thesis concludes that whilst effective for a time, road surface friction management policies based on measurements made by sideway-force devices are in need of radical reform in order to achieve a link between the management of road friction and vehicle safety.

This conclusion is of particular significance to the Australian, Belgian, Czech, English, French, German, Hungarian, Irish, New Zealand, Northern Irish, Scottish, Slovenian, Spanish, and Welsh, road authorities but will also be of interest to other authorities currently using, or investigating the use of, sideway-force friction measurement devices.

This thesis presents the results of a decade of study into road surface friction characterisation and how it pertains to vehicle safety. Six research reports are presented which detail:

- the relationship between road surface properties and the generation of tyre / road friction;

- a statistical model for predicting the friction generated between a road surface and tyre at all possible friction parameters; and

- an assessment of sideway-force devices to determine their measurement parameters.

Chapter 7 of this thesis presents an alternative friction management policy based on the use of crowd sourced in-vehicle data, which has undergone a promising proof of concept study.

This thesis demonstrates a correlative, and causal, disassociation between the friction parameters exploited by road vehicles, and those measured (or inferred) for engineering purposes on the English trunk road network. This disconnect is a significant and unique finding which supports the main conclusion of this thesis.

This thesis also demonstrates the need to include advanced research methodologies into road friction research portfolios, such as, the application of a multivariate approach to the prediction of friction between a tyre and road surface, or the use of advanced statistical methods such as artificial intelligence or machine learning to identify influencing factors not currently understood.

List of Figures

List of Tables

Abbreviations

3DSVV	3 Dimensional Surface Void Volume
ABS	Anti-lock Braking System
ACW	Anti-ClockWise
ASTM	American Society for Testing and Materials
BC	Brushed Concrete
BBA	British Board of Agrément
CAN	Controller Area Network
CAUTS	Cold Applied Ultra Thin Surface course system
CSC	Corrected Skid-resistance Coefficient
CAVs	Connected and Autonomous Vehicles
CT	Computed Tomography
CTI	Computed Tomography Imaging
CW	ClockWise
CWA	Critical Wheel Angle
DMRB	Design Manual for Roads and Bridges
ESC	Electronic Stability Control
E-SCRIM	Equivalent SCRIM Coefficient
EU	European Union
GDPR	General Data Protection Regulation
GN	Grip Number
GPS	Global Positioning System
GSTD	Glass Spheres Texture Depth
HAPAS	Highways Agency Pavement Assessment Scheme

HAPMS   Highways Agency Pavement Management System

HE   Highways England

HERMES   Harmonisation of European Routine and research Measuring Equipment for Skid resistance

HFS   High Friction Surfacing

HP   Horizontal Permeability

HRA   Hot Rolled Asphalt

IL   Investigatory Level

LA   Local Authority

L-FnX   Locked-wheel Friction at operational velocity "X" [km/h]

MCHW   Manual for Contracts for Highways Works

MIRA   Motor Industry Research Association

MPD   Mean Profile Depth

MTD   Mean Texture Depth

NH   National Highways

OEM   Original Equipment Manufacturer

P-FnX   Peak Friction at at operational velocity "X" [km/h]

PFT   Pavement Friction Tester

RADAR   RAdio Detection And Ranging

RMSTD   Root Mean Squared Texture Depth

RRL   Road Research Laboratory

PPA   Percentage Pressed Area

PPR   Published Project Report

ROSANNE   ROlling resistance, Skid resistance, ANd Noise Emission measurement standards for road surfaces

PSV   Polished Stone Value

SC   SCRIM Coefficient

SCRIM   Sideway-force Coefficient Routine Investigation Machine[2]

SD   Surface Dressing

SkReDeP Skid Resistance Development Platform

SMTD   Sensor Measured Texture Depth

SRN   Strategic Road Network

SRT   Skid Resistance Tester

TPD   Tyre Penetration Depth

TRL   Transport Research Laboratory

TSCS   Thin Surface Course System

TYROSAFE TYre and ROad SurfAce optimisation for skid resistance and Further Effects

UK   United Kingdom

UTSCS   Ultra Thin Surface Course System

VVBT   Volume of Void Below Tyre

VVOT   Volume of Void Occupied by Tyre

---

[2]Within this thesis, "SCRIM" is an abbreviation of the words "Sideway-force Coefficient Routine Investigation Machine" and does not refer to a trademark owned by WDM Limited.

Definitions

Skid resistance and friction

The term "skid resistance" is often defined as the contribution of the road surface to the generation of friction between the road and a vehicle tyre. A key theme of this thesis is to move towards a concept of friction as a context dependent parameter rather than a ubiquitous material property. The term "friction" will therefore be used in preference to "skid resistance" to reinforce this theme.

Vehicle speed and operational velocity

The term "vehicle speed" within the context of friction measurement devices is defined as:

> *"The speed at which the device traverses the test surface"* - British Standards Institution (2009b)

For this work, this definition of vehicle speed is used. In addition to vehicle speed, it is important to introduce a second term to the lexicon of friction measurement; the "operational velocity". The operational velocity is defined as:

> *The speed at which the rotational axis of the tyre moves with respect to the direction of friction measurement.*

% wheel slip

An important concept regarding the characterisation of road surface friction is % wheel slip. This is sometimes referred to as "wheel slip percentage", "percentage slip", "% slip", or similar. For the purposes of consistency "% wheel slip" is used throughout this thesis and is defined as:

> *The speed at which the tyre/surface contact patch moves with respect to the direction of friction measurement, expressed as a percentage of the operational velocity.*

Published Project Reports (PPRs) and original works

The works supporting this thesis were produced at and published by TRL. All reports published by TRL are assigned a unique Published Project Report (PPR) number which is referenced in the report titles. This thesis uses PPR numbers as shorthand for report titles throughout.

The works supporting this thesis are henceforth referred to as the "original works[3]".

---

[3]At the time of writing the original works are available from the TRL website (www.trl.co.uk).

Contents

Chapter 1   Introduction

1.1   Foreword

This thesis presents the results of a decade of study into road surface friction characterisation and how it pertains to vehicle safety. This document can be read as a summary of six research reports (the original works) produced as part of the development of the UK friction management policy:

- PPR727 Road surface properties and high speed friction (Sanders et al., 2014);

- PPR894 Road surface properties and high speed friction - The effect of permeability (Sanders, 2017);

- PPR815 Better understanding of the surface tyre interface (Sanders et al., 2017b);

- PPR768 Performance review of skid resistance measurement devices (Sanders et al., 2017a);

- PPR957 Characterising the measurements made by sideways-force skid resistance devices: A desk study (Sanders & Browne, 2020); and

- PPR980 Characterising the measurements made by sideways-force skid resistance devices: An experimental study (Sanders, 2021).

The collective assessment of the original works offers insight not available in the individual reports and provides a substantial contribution to knowledge. The conclusions drawn from this insight are radical, and support an overhaul of the current friction management policy in the UK, and many other nations. In this way, this thesis is greater than the sum of its parts and broadens the overall contribution of the original works.

This chapter defines the research questions, aim, hypotheses, and objectives.

1.2   Research questions and hypotheses

The research questions for the original works were not formalised at the time of writing those documents, but are retrospectively presented below:

Q1. Can the high speed, locked-wheel friction properties of all road surface materials be inferred from their geometric properties (PPR727)?

Q2. Can the permeability of road surface materials affect high speed, locked-wheel friction (PPR894)?

Q3. To what level of accuracy can the friction of non-porous road surfaces at all % wheel slips and operational velocities be inferred using data currently collected on the road network (PPR815)?

Q4. Can the current speed correction formula for SCRIMs be expanded to validate measurements made below 25km/h (PPR768)?

Q5. Are there devices other than the currently used SCRIMs that could be used for the direct measurement of road surface friction in the UK at a network level (PPR768)?

Q6. What are the measurement properties of the current SCRIMs as expressed in terms of operational velocity and % wheel slip (PPR957 and PPR980)?

This thesis considers the answers to these research questions and posits the following overall question[4]:

QT. Is the characterisation of highway friction using sideway-force devices, and the inference of high speed, locked-wheel friction, conducive to maintaining or improving vehicle safety?

The hypotheses for the original works were not formalised at the time of writing those documents, but are retrospectively presented[5] in the form of null hypotheses[6] below:

$H_0$1. The high speed, locked-wheel friction properties of all road surface materials cannot be inferred from their texture depth properties and the static pressure distribution between the tyre and road surface (PPR727).

$H_0$2. The high speed, locked-wheel friction properties of all road surface materials cannot be inferred from their texture depth, low speed friction, and permeability properties (PPR894).

$H_0$3. The friction of non-porous road surfaces cannot be inferred at all % wheel slips and operational velocities using data currently collected on the road network (PPR815).

---

[4]The suffix "T" has been used for "QT", and "H_0T" to highlight that these are related to this thesis and represent a question and hypothesis not posited in the original works.

[5]Hence the specificity of $H_0$4 and $H_0$7.

[6]In this thesis null hypotheses are used within a philosophical paradigm rather than a statistical one. An important factor for consideration is that the non-falsification of a null hypothesis does not "prove" the hypothesis true. This allows the hypotheses to be challenged as part of future works.

$H_0$4. The inferences made (from $H_0$3) will not be accurate to 10 units using a 95% confidence limit[7] (PPR815).

$H_0$5. The current speed correction formula for SCRIMs cannot be safely expanded to validate measurements made below 25km/h (PPR768).

$H_0$6. There are no other devices than SCRIM that could be used for the direct measurement of road surface friction in the UK (PPR768).

$H_0$7. SCRIMs do not make measurements at 100% wheel slip and 17.1km/h operational velocity (PPR957 and PPR980).

The null hypothesis for this thesis is as follows:

H_0T. **The characterisation of highway friction using sideway-force devices, and the inference of high speed, locked-wheel friction, is not conducive to maintaining or improving vehicle safety.**

1.3 Research aim and objectives

This thesis has the following aim:

Improve the understanding of road surface friction characterisation as it relates to friction demand, such that the ability of the current UK friction management policy to affect vehicle safety can be evaluated.

The following objectives were fulfilled in the original works:

1. Understand the value of surface texture measurements, and pavement permeability measurements in the generation of high speed, locked-wheel friction (PPR727 and PPR894).

2. Analyse historical friction data to create friction profiles for multiple material types, and evaluate these friction profiles to determine typical behaviours for various surfacing materials (PPR815).

3. Understand the power of measurements of SC and SMTD in predicting the friction of a given material at all % wheel slips and operational velocities (PPR815).

---

[7]The accuracy of the TRL367 model.

4. Evaluate the performance of various skid resistance measurement devices under various testing conditions to understand the applicability of these devices in characterising the friction of road networks (PPR768).

5. Analyse the measurements made by various friction test devices to evaluate if current speed correction methodologies could be extended to lower vehicle speeds, or altered to accommodate lower vehicle speeds (PPR768).

6. Understand the measurement characteristics of SCRIMs in the context of % wheel slip and operational velocity (PPR957 and PPR980).

In addition to those objectives, this thesis was produced to fulfill the following overall objective:

Evaluate current and historical works to understand if the current friction management policy affects vehicle safety.

1.4   Thesis outline

Chapter 1 - Introduction

Presents research questions, the aim, and objectives of the study.

Chapter 2 - Background

Presents the background to the work described in this thesis. A comprehensive summary of the current UK friction management policy, the measurement devices used under that policy, and a summary of historical works.

Chapter 3 - Factors affecting road surface friction

Summarises the works reported in PPR727 and PPR894. Those works focused on the identification of texture depth characterisation methods that correlate with high speed, locked-wheel friction for all road surfacing materials. This chapter presents the texture depth and friction measurements made, some of which are standard techniques and some were unique to this work. The work also assessed the horizontal permeability and collected radiographic images of the internal structure of a sub-set of materials such that the inter-connected void network of those materials could be analysed.

Chapter 4 - Friction as a context dependent parameter

Summarises the work reported in PPR815. That work focused on understanding the relationships

between two crucial contextualisations relating to the measurement of road surface friction, namely operational velocity and % wheel slip. This chapter presents the results of a modelling exercise carried out to predict the friction of any given, non-porous, road surface at any operational velocity and % wheel slip.

Chapter 5 - The contextual framework of the UK's friction measurement devices

Summarises work reported in PPR768, PPR957 and PPR980. The work reported in PPR768 focused on understanding the practical applications of friction testing devices available in the UK at the time of writing. Under this work practical assessments of three devices were carried out on a closed test track to replicate the worst case test scenarios.

PPR957 and PPR980 focused on understanding the measurement properties of the SCRIM and describing these properties in terms of operational velocities and % wheel slip. This work was undertaken in two parts, a desk study which lead to four characterisations of the SCRIM. And the challenging of these characterisations through practical assessment.

Chapter 6 - Discussion and conclusions

Discusses the results of the research in relation to each of the research objectives. The chapter provides a summary of the key findings and frames them within the context of other research. This chapter derives the conclusions of the thesis through the use of a formal syllogism.

Chapter 7 - The way forward

Is based on the findings of a proof of concept study carried out by Hammond et al. (2021) into the use of crowd sourced vehicle data for the identification of friction deficient areas on road networks. This chapter expands on that study to present an outline policy for the characterisation of road surface friction in a way that is directly related to the experience of road vehicles.

Chapter 8 - Recommendations for future work

Presents recommendations for future works based on the conclusions of this thesis and the discussions presented in Chapter 7.

Bibliography

Appendices

Present the original works.

Chapter 2   Background

2.1   Foreword

The friction developed between the road surface and vehicle tyres provides road users with the reaction forces necessary for performing manoeuvres. Regardless if the manoeuvre is mundane, such as traversing a bend, or extreme, such as an emergency stop, friction is usually the only appreciable factor allowing vehicle manoeuvres to be performed[8]. Maintaining appropriate and predictable friction conditions is therefore a fundamental contributor to road user safety.

The friction characteristics of the UK Strategic Road Network (SRN) are managed using techniques and policies which have remained largely unchanged since their inception in 1988. This chapter summarises those techniques and policies, and the historical literature, which underpin the current UK friction management policy.

2.2   The contextualisation of friction measurements

Secondary education physics materials will typically describe friction as a force which resists the motion of moving objects.

> *"When two surfaces slide past each other, the interaction between them produces a force of friction. Friction is a force that opposes motion."* - (GCSE Bitesize, 2021)

More complete texts define the friction generated between two solid, non-rotating bodies as being in one of two states, namely:

- Static friction - *"In static friction, the frictional force resists force that is applied to an object, and the object remains at rest until the force of static friction is overcome."* - (Britannica, 2021)

- Kinetic friction - *"In kinetic friction, the frictional force resists the motion of an object."* - (Britannica, 2021)

---

[8]Wind resistance and road geometry can, in some cases, aid in the performance of vehicle manoeuvres.

Undergraduate physics textbooks often consider the friction generated between a rotating solid body, and a static plane, such as a cylinder rolling down a slope. Within the context of formal education, this is typically the point at which the exploration of friction stops[9].

Friction generation is however far more complex than is typically taught in the classroom. Vehicle tyres for example, are manufactured from viscoelastic materials that allow a rotational speed gradient to persist within a vehicle tyre. The combination of the rotational speed and translational speed of a body combine to create an additional contextualising parameter; slip speed. The slip speed of a friction measurement test tyre is defined in BS CEN/TS 15901-6-2009 as the:

> *"relative speed between the test tyre and the travelled surface in the contact area"* - (British Standards Institution, 2009b)

The contextualisation of friction is further complicated in the presence of contaminants. Traditional road surfaces contaminants are vehicle fluids (such as engine oil, brake fluid or fuel), water (from rain, ice and snow), and other nondescript road detritus. Such contaminants act as a barrier between the road and tyre, affecting the ability of those materials to interact and generate friction.

2.3 The characterisation of road surface friction

Road surface friction can be characterised using a large range of standard devices, each of which operates using one of three measurement principles:

- Longitudinal fixed slip. A test wheel mounted in the same orientation as the vehicle wheels which is forced to rotate at a fixed percentage of the vehicle speed.

- Longitudinal variable slip. A test wheel mounted in the same orientation as the vehicle wheels which alternates between a freely rotating and a fully locked (or peak friction) state.

- Sideway-force. A test wheel mounted at an angle to the vehicle wheels which is allowed to freely rotate.

A comprehensive list of full scale test devices, and descriptions thereof are provided in TYROSAFE Deliverable D04 (Do et al., 2008). The work described in this thesis was primarily conducted

---

[9]Some specialist automotive university or industry courses may cover the topics discussed below.

using two devices, one operating under the sideway-force measurement principle, and the other operating under the longitudinal variable slip principle.

A key similarity between the majority of friction characterisation devices is that they seek to replicate the "worst case scenario" for road users. In the UK this is typically defined as using a bald tyre under wet, but not aquaplaning conditions. It should be noted that all of the friction measurements presented within this thesis were conducted under these conditions.

2.3.1   Sideway-force devices

At the time of writing, various devices operating under the sideway-force principle are used by many road authorities:

- In the UK, the Sideways-force Coefficient Routine Investigation Machine (SCRIM) is used;

- in Germany the SeitenKraftMessverfahren (SKM) is used;

- in Belgium Odoliograph is used; and

- in Australia the intelligent Safety Assessment Vehicle (iSAVe) is used.

The use of SCRIMs in the UK is defined in British Standard BS 7941-1-2006 (British Standards Institution, 2006) and CS 228 (Highways England et al., 2020a). The SCRIM uses a smooth test tyre installed in the nearside wheel path of the vehicle angled at 20 degrees to the direction of travel, which is mounted on an instrumented axle. The skid resistance value is determined by calculating the average ratio between the horizontal (along the axis of wheel rotation) and vertical forces, multiplied by 100 (Figure 2.1).
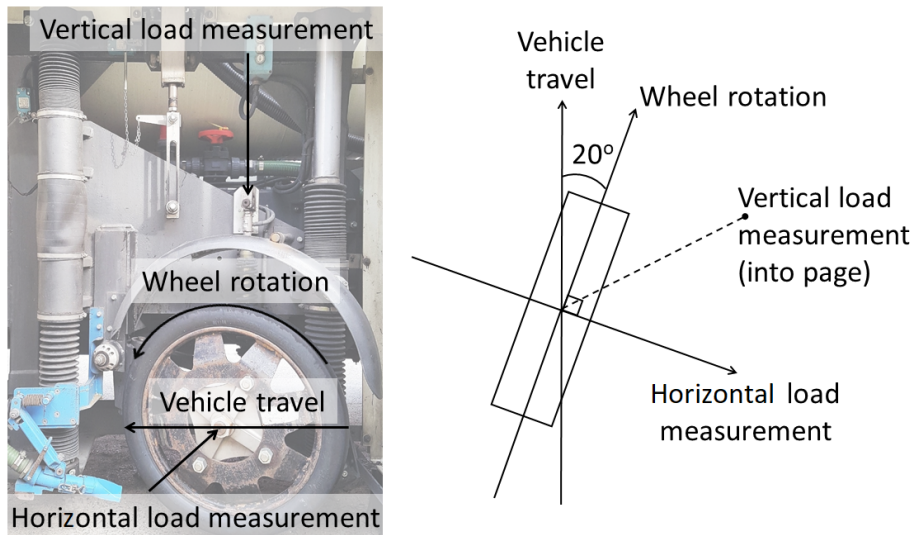
Figure 2.1: The SCRIM measurement principle, an annotated view of the SCRIM measurement wheel (left) and a diagram showing an annotated plan view of the SCRIM wheel (right).

The Skid Resistance Development Platform (SkReDeP) is a research tool used by National Highways (NH) (formerly Highways England). The SkReDeP (Figure 2.2) incorporates sideway-force measurement equipment conforming to the standards for SCRIMs and was a key tool used throughout the research presented in this thesis.

Figure 2.2: The National Highways Skid Resistance Development Platform.

2.3.2 The Pavement Friction Tester

The Pavement Friction Tester (PFT) is a longitudinal variable slip device comprised of a tow vehicle and trailer (Figure 2.3). The trailer holds the test wheel, which is mounted on an instrumented axle and can be braked independently of the vehicle wheels. The vertical and longitudinal (in the direction of vehicle travel) forces acting on the test wheel are measured and the ratio of the forces used to determine the friction between the test tyre and road surface.

Figure 2.3: The Pavement Friction Tester.

A key difference between the PFT and the SCRIM is that the PFT tyre slides over the surface in line with the driving direction of the tow vehicle. The slip differential between the test tyre and tow vehicle are therefore known and measurable.

The use of the PFT is defined in American Society for Testing and Materials (ASTM) standards E274 (ASTM International, 2011) and E524 (ASTM International, 2008).

2.3.3 The inference of friction from pavement properties

Understanding the physical properties of roads that help in the production of friction is critical in the effective management[10] of road surface friction.

---

[10]For the purposes of this thesis, friction management is considered effective if it has a positive and direct effect on vehicle safety.

Multiple studies have been conducted with the aim of correlating the physical characteristics of the road with various friction parameters. Some such studies are Bradley & Allen (1930), Bird & Scott (1936), Bird & Miller (1937), Sabey (1966), Hosking & Woodford (1976a), Hosking & Woodford (1976b), Leu & Henry (1978), Roe et al. (1998), Hall et al. (2009), and Roe & Dunford (2012). The work presented in this thesis focuses on two surface properties which are also explored in the above works; texture depth and permeability.

Texture depth

Texture depth describes the magnitude of the surface texture of road surfaces on the order of millimeters. Multiple characterisations of texture depth exist for road surfaces:

- Sensor Measured Texture Depth (SMTD) as defined in the SCANNER user guide and specification Volume 5 (Department for Transport, 2009);

- Mean Profile Depth (MPD) as defined in BS EN ISO 13473-1:2004 (British Standards Institution, 2004);

- Mean Texture Depth (MTD) as defined in BS EN 13036-1:2010 (British Standards Institution, 2010); and

- Route Mean Squared Texture Depth (RMSTD) (Calculated in the usual way).

Permeability

Permeability is the ability of a pavement to move water through its surface layers rather than over it, which is one of the functions of texture depth. Currently there are no overarching performance requirements for pavement permeability in the UK, but porous materials (materials which generally have higher levels of permeability) are marketed as such for use in specific cases. The permeability of pavement materials can be quantified using the procedures defined in BS EN 12697-19:2012 (British Standards Institution, 2012).

2.4 The management of road surface friction in the UK

2.4.1 The direct measurement of friction

The first standard for the assessment of road surface friction in the UK was introduced in 1988 (Roe & Caudwell, 2008). This standard attempted to normalise the skidding risk to motorists

across all areas of the strategic road network using a methodology originally proposed by Salt and Szatkowski in 1973 (Salt & Szatkowski, 1973). The current friction management standards in the UK are based on this methodology.

Document CS 228 of the Design Manual for Roads and Bridges (DMRB) (Highways England et al., 2020a) details the policy in place at the time of writing. Road networks under the purview of Local Authorities (LAs) may have other policies in place but it is the authors understanding that the majority of LAs, with friction management policies, adopt CS 228 as best practice.

The current policy can be summarised as making annual skid resistance measurements of the road network using SCRIMs and comparing these with values known as Investigatory Levels (ILs). Lengths of the network that are found to be at or below the IL for prolonged periods of time are subject to further investigation to determine what actions would be beneficial at those locations.

The IL for any given section of carriageway is determined by the risk posed to road users[11]. Table 2.1 has been recreated from CS 228 and provides the ILs[12] related to the different site categories used in the UK.

---

[11] The risk posed to road users being determined through accident studies.
[12] ILs are presented as values of Corrected Skid-resistance Coefficient (CSC) which represent measurements made using the SCRIM corrected for speed and seasonal effects.

Table 2.1: Site category investigatory levels reproduced from (Highways England et al., 2020a) LR: Lower Requirement, and ST: STandard requirement.

	Site category and definition	0.30	0.35	0.40	0.45	0.50	0.55
		IL for CSC					
A	Motorway	LR	ST				
B	Non-event carriageway with one-way traffic	LR	ST	ST	-	-	-
C	Non-event carriageway with two-way traffic	-	LR	ST	ST	-	-
Q	Approaches to and across minor and major junctions, approaches to roundabouts and traffic signals	-	-	-	ST	ST	ST
K	Approaches to pedestrian crossings and other high risk situations	-	-	-	-	ST	ST
R	Roundabout	-	-	-	ST	ST	-
G1	Gradient 5-10%, longer than 50m	-	-	-	ST	ST	-
G2	Gradient >10%, longer than 50m	-	-	LR	ST	ST	-
S1	Bend radius <500m – carriageway with one-way traffic	-	-	ST	ST	-	-
S2	Bend radius <500m – carriageway with two-way traffic	-	-	LR	ST	ST	-

2.4.2   The management of texture depth

Salt and Szatkowski (1973) summarise the findings of research into the effect of texture depth on friction:

> *"Skidding resistance changes with the speed of the vehicle and the rate of change depends on texture depth."* - (Salt & Szatkowski, 1973)

This observation and the accompanying data lead to the recommendation for a texture depth standard for high speed roads, and that resulted in the texture depth management standards used today. There are four key texture depth standards in operation in the UK:

- MCHW 921 (Department for Transport, 2019b) defines the texture depth requirements for newly laid asphalt roads with either a Cold Applied Ultra Thin Surface course system

(CAUTS), Ultra Thin Surface Course System (UTSCS), or, Hot Rolled Asphalt (HRA) surface construction (Table 2.2).

- MCHW 942 (Department for Transport, 2019b) defines the texture depth requirements for newly laid asphalt roads with a Thin Surface Course System (TSCS) surface construction (Table 2.2).

- MCHW 1026 Series (Department for Transport, 2020a) defines the texture depth requirements for newly laid concrete roads (Table 2.2).

- CS 230 (Highways England et al., 2020c) defines the in-service texture depth requirements for the UK SRN which are based on measurements of SMTD (Table 2.3).

The texture depth standards within the MCHW are complex and, for clarity, have been summarised in Table 2.2, which shows the texture depth requirement for different road and surfacing types. The reference to the standard, and table within that standard where these values are reported, are also presented.

Table 2.3 presents the texture depth requirements in CS 230 (Highways England et al., 2020c).

Table 2.2: Texture depth requirements for the UK road network, derived from Department for Transport (2019b) and Department for Transport (2020a).

Road type	Surfacing type	921 T9/3 Initial	924 T9/12 Initial	924 T9/13 Initial	924 T9/14 ≤2 years	1026 T10/8 ≤6 weeks
		MTD (mm)				
High Speed	CAUTS to 923	1.2	-	-	-	-
	Non-942 asphalt materials	1.2	-	-	-	-
	14mm TSCS to 942	1.2	-	-	0.9	-
	10mm TSCS to 942	1.2	-	-	0.8	-
	6mm TSCS to 942	1.2	-	-	0.7	-
Low Speed	CAUTS to 923	1.2	-	-	-	-
	Non-942 asphalt materials	1.0	-	-	-	-
	≤14mm TSCS to 942	-	0.9	-	-	-
Roundabouts on high speed roads	Non-942 asphalt materials	1.0	-	-	-	-
	10mm TSCS to 942	-	0.9	-	-	-
Roundabouts on low speed roads	Non-942 asphalt materials	0.9	-	-	-	-
	10mm TSCS to 942	-	0.9	-	-	-
	6mm TSCS to 942	-	0.9	-	-	-
A category roads ≥ 50mph	All 942 materials	-	-	0.9	0.7	-
A category roads ≤ 50mph	All 942 materials	-	-	0.7	0.6	-
B, C and U category roads ≥ 50mph	All 942 materials	-	-	0.7	0.6	-
All	Concrete materials	-	-	-	-	$1.00^{+0.25}_{-0.10}$

Table 2.3: Texture depth requirements for the UK SRN, reproduced from Highways England et al. (2020c).

	Road surface condition category & description	SMTD (mm)	
		High friction surfacing	All other surfacing types
1	Sound - negligible deterioration	>0.6	>1.1
2	Some deterioration - low level of concern.	≤0.6	0.8< [SMTD] ≤1.1
3	Moderate deterioration – warning level of concern.	N/A	0.4< [SMTD] ≤0.8
4	Severe deterioration – intervention level of concern.	N/A	≤0.4

Investigating Tables 2.2 and 2.3, the following observations can be made:

- The in-service texture depth requirements reported in Table 2.3 do not differentiate between TSCS materials and other material types, most notably concrete materials;

- the newly laid texture depth requirements differentiate between road types and nominal vehicle speed, whereas the in service criteria do not; and

- the in-service requirements require texture depth to be characterised using the SMTD method[13] but, the newly laid requirements characterise texture depth as MTD[14].

2.5   The relationship between road surface friction and vehicle safety

To the authors knowledge, the first exercise correlating road surface friction and vehicle safety was conducted by Giles (1957) who concluded their work by proposing levels of friction (as measured using the predecessor to modern SCRIMs) that could be considered to provide a "satisfactory" level of skidding risk to motorists. Since then, studies comparing road surface friction and vehicle safety in the UK have been conducted by; Sabey & Storie (1968), Hosking (1986), Roe et al. (1991), Parry & Viner (2005), and Wallbank et al. (2016).

The two most recent studies offer the most relevant insight into the relationship between friction and safety, as these studies had access to the largest quantities of data and were based on the current friction management policy. Summary data from TRL622 (Parry & Viner, 2005) and

---

[13]A methodology that uses optical devices that rely on line of site to the target in order to measure texture depth.
[14]A methodology that uses a known volume of glass beads to "fill up" the texture depth and therefore does not require line of sight.

PPR806 (Wallbank et al., 2016) have been reproduced from original figures and reported together in Figures 2.4 and 2.5.
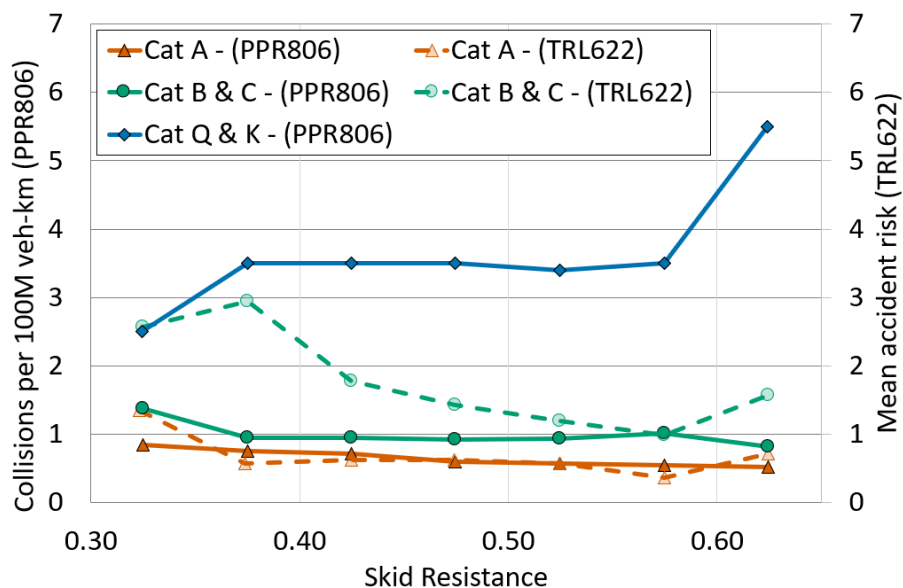
Figure 2.4: Relationships between vehicle incidents under wet conditions and measured friction for category A, B & C, and Q & K sites, derived from Parry & Viner (2005) and Wallbank et al. (2016).

Figure 2.4 shows that for low risk sites (Categories A, B and C) the 2005 data (TRL622) show a slight trend for collision rate to reduce as skid resistance is increased. Comparative data from 2016 (PPR806), shows a very subtle trend for incidents to reduce with increasing skid resistance for Category A sites only, whereas Category B, C, Q & K sites show no correlation between accident rate and skid resistance.
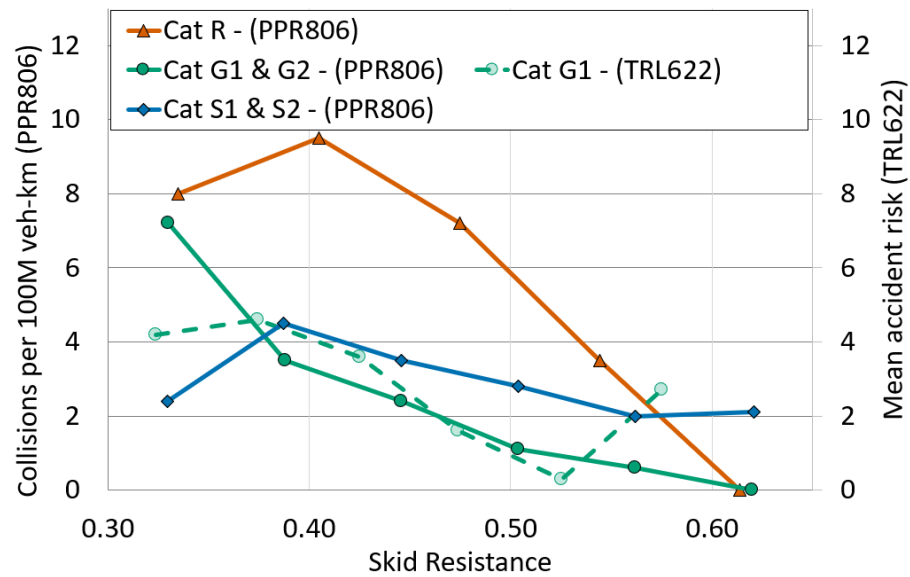
Figure 2.5: Relationships between vehicle incidents under wet conditions and measured friction for category R, G1 & G2, and S1 & S2 sites, derived from Parry & Viner (2005) and Wallbank et al. (2016).

Figure 2.5 shows that high risk sites involving bends or gradients [15] (Categories R, G1, G2, S1 and S2) show a strong negative correlation between collision rate and skid resistance, this correlation prevails regardless of when the survey was carried out.

To further contextualise the data presented in figures 2.4 and 2.5 the percentage of the English trunk road network defined as each site category at the time of writing Parry & Viner (2005) and Wallbank et al. (2016) is presented in figure 2.6.

---

[15]Data for category R, S1 and S2 sites were not available in TRL622.
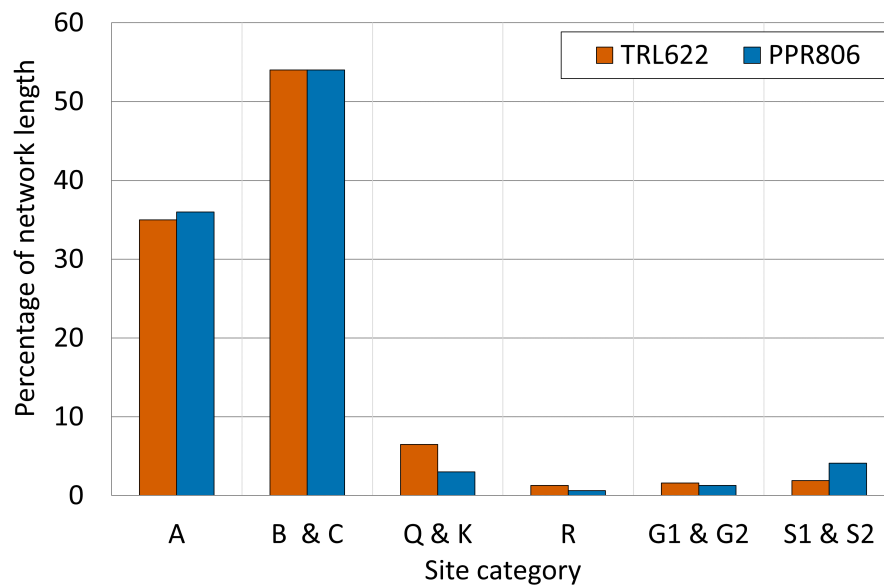
Figure 2.6: The percentage of the English trunk road network defined as each site category at the time of writing Parry & Viner (2005) and Wallbank et al. (2016).

Figure 2.6 shows that for those site categories for which comparable data are available (A, B & C, and G1 & G2) the distribution of site categories across the networks are similar and comparisons between the two networks are therefore valid.

Chapter 3   Factors affecting road surface friction

3.1   Foreword

Fundamental research into road surface properties and their effect on friction generation was carried out in 1966 and is reported in RRL report No. 20 (Sabey, 1966). This research demonstrated a tentative correlation between the texture depth of road surfaces (measured using the volumetric patch test), and friction (measured using the small braking force trailer[16]). Based on these measurements, Sabey concluded that:

> *"Very large decreases in [friction] coefficient between 30 and 80 mile/h can be expected when the texture depth is less than 0.010 in, however high the coefficient is at 30 mile/h. In order to restrict the decrease to 25 percent it appears that, on average, texture depths greater than 0.025 in are desirable." - (Sabey, 1966).*

Further research conducted by Roe et al. (1998), reported in TRL report 367, consisted of making measurements of texture depth (using the SMTD method), side-force friction coefficient (using the SCRIM) and high speed friction (using the PFT). The measurements made were used to develop a model capable of predicting locked-wheel friction at 100km/h (L-Fn100) (Equation 3.1).

$$L - Fn100 = aSR + b\left[1 - \exp(SMTD)\right] + c \tag{3.1}$$

Where:

SR represents the side-force coefficient measured using the SCRIM,
SMTD is the texture depth of the surface measured using the SMTD method,
a, b and c are the model coefficients[17].

The results of the work reported in TRL367 have been reproduced in Figure 3.1, which shows a concentration of friction measurements in a narrow band which increases linearly between 0 and 0.8mm SMTD and is flat thereafter. However, a group of points (primarily comprised of porous asphalt materials) at approximately 0.7mm SMTD and 0.50L-Fn100 are outlying from the main band of measurements; these are highlighted in the broken ellipse. The report authors noted that:

---

[16]A single wheeled braked trailer device with a similar function to the PFT.
[17]The model coefficients were not published in the original works, but have since been made publically available: a = 0.00337, b= 0.411 and c = -0.151.

"...such surfacings have clearly have a greater drainage potential than SMTD (or sand patch) measurements of texture depth can quantify." - (Roe et al., 1998)

Research reported in TRL report PPR564 (Roe & Dunford, 2021) identified another material type, a 6mm TSCS, which displayed similar properties to the porous asphalt identified in TRL367. A summary of the measurements made as part of PPR564 is replicated from the original data in Figure 3.1. This figure shows that, of the materials assessed in PPR564, the materials constructed from 10mm nominal aggregate sizes, or larger, are performing within the range of the results from the study reported in TRL367. The materials using a nominal 6mm aggregate size are showing a similar performance to the outlying TRL367 results (the broken ellipse).
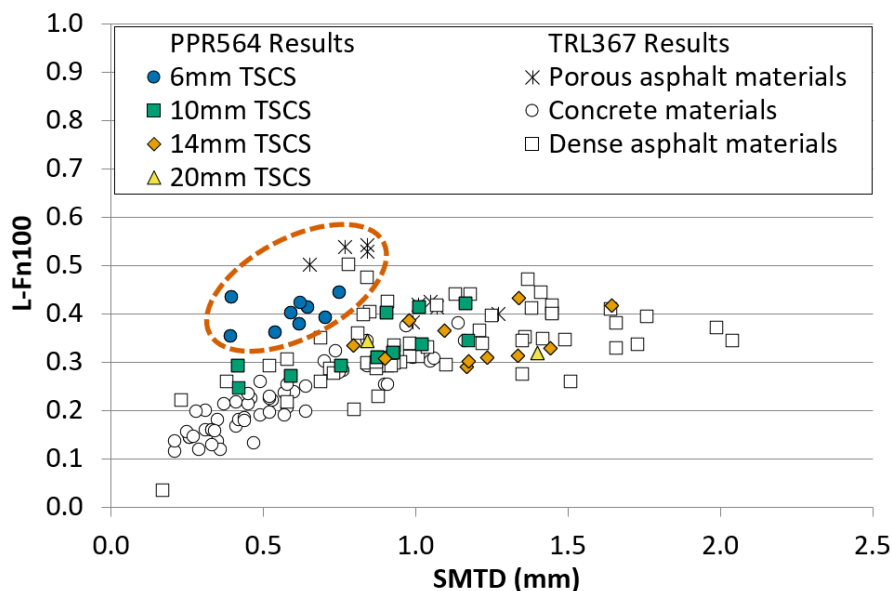
Figure 3.1: The relationship between SMTD and L-Fn measured at 100km/h derived from TRL367 (Roe et al., 1998) and PPR564 (Roe & Dunford, 2012). The dimensional units show the nominal aggregate sizes of the TSCSs.

Motivated by these observations, further work was conducted with the aim of developing a new texture measure capable of predicting the high speed locked-wheel friction characteristics of all pavement materials.

3.2 The original works

The work detailed in the remainder of this chapter is reported in two of the original works; PPR727 (Sanders et al., 2014) and PPR894 (Sanders, 2017). PPR727 is presented in full in Appendix A and presents a study seeking a statistical correlation between texture depth measurements and friction for various material types. PPR894 is presented in full in Appendix B and presents a study assessing the internal permeability characteristics of pavement materials subject to investigation in PPR727. The work presented in PPR894 followed on directly from PPR727 and so these papers are summarised together in this chapter.

3.3 Experimental methodologies

The methodologies utilised for this study are detailed in full in Appendices A & B and can be summarised as making measurements of high speed friction on a number of material types using the PFT. These measurements were compared with the following texture depth characterisations:

- Standard texture depth measurements typically used in the management of road surface friction, MTD, MPD, and RMSTD (as detailed in Chapter 2).

- New surface characterisation techniques developed as part of PPR727:

    Percentage Pressed Area (PPA);

    3D Surface Void Volume (3DSVV);

    Tyre Penetration Depth (TPD);

    Volume of Void Below Tyre (VVBT);

    Volume of Void Occupied by Tyre (VVOT); and

    Glass Spheres Texture Depth (GSTD).

- Characterisations of material permeability as detailed in PPR894:

    Horizontal Permeability (HP); and

    Computed Tomography Images (CTI) of the specimens internal structure.

The measurements listed above were made on road surface specimens in the form of 225mm diameter, 50mm thick cylinders extracted from the sites assessed with the PFT.

The data used were collected from multiple research works (including the original works) and some measurements were made on some specimens and not others. Table 3.1 clarifies the measurements made, and the works under which the measurements were made.

Table 3.1: Materials assessed and measurements made. The PPR referring to the work through which the measurements were made is provided in the table cells. Where measurements were made on a sample of specimens, the number of specimens assessed are provided in parenthesis.

Material & number of specimens assessed		Measurements made & publication reference												
		L-Fn100	SMTD	MTD	MPD	RMSTD	PPA	3DSVV	TPD	VVBT	VVOT	GSTD	HP	CTI
6mm TSCS	19	–	PPR564					PPR727					PPR727 (4) & PPR894 (15)	PPR894 (2)
10mm TSCS	15	–	PPR564					PPR727					PPR727 (5) & PPR894 (10)	PPR894 (2)
14mm TSCS	21	–	PPR564					PPR727					PPR727 (5) & PPR894 (16)	N/A
20mm TSCS	4	–	PPR564					PPR727					PPR727 (1) & PPR894 (3)	PPR894 (1)
Calcined flint surface dressing	3	PPR727	N/A					PPR727						N/A
Hot rolled asphalt	3	PPR727	N/A					PPR727						N/A
Sawn concrete	1	PPR727	N/A					PPR727						N/A
Brushed concrete	3	PPR727	N/A					PPR727						N/A

3.4   Results

A full set of results can be found in the original works, the key findings are presented in Figures 3.2 to 3.5.

Figures 3.2 and 3.3 present the relationships between the GSTD, 3DSVV and L-Fn100 respectively. The broken ellipse encompassing the outlying points in Figure 3.1 has been included in these figures for reference. Figure 3.2 shows a relationship between 3DSVV and L-Fn100 that demonstrates an improvement over those shown in Figure 3.1. Whilst 3DSVV improves the relationship with L-Fn100 over SMTD there are nonetheless some outlying points that do not follow the general relationship.
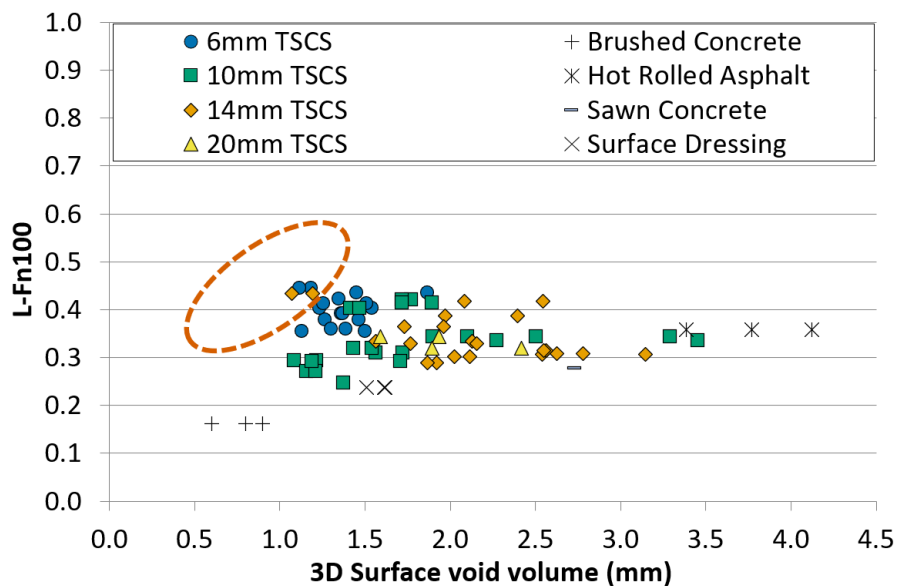
Figure 3.2: 3DSVV Vs L-Fn100. The broken ellipse presents the area within which outlying measurements were originally observed. Reproduced from PPR727 (Sanders, 2014).

Figure 3.3 presents the relationship between GSTD and L-Fn100. These data show the same general relationship for all material types and that the outlying 6mm TSCS materials, have moved out of the broken ellipse and been absorbed into the main relationship. An aspect of the measurement principle of the GSTD method is that the size of the spheres used to determine texture depth were very small. In using these spheres, they displayed properties more analogous to a liquid than a collection of spheres.
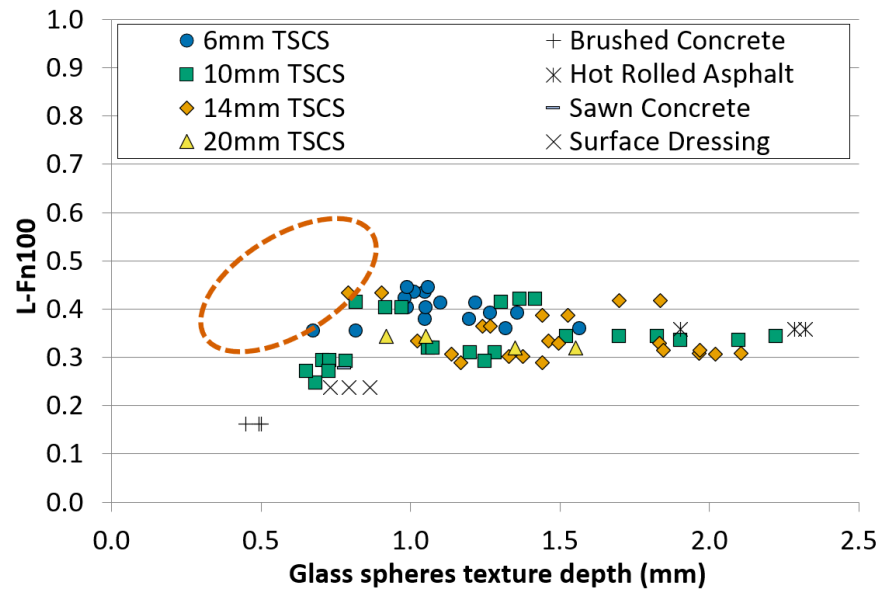
Figure 3.3: GSTD depth Vs L-Fn100. The broken ellipse presents the area within which outlying measurements were originally observed. Reproduced from PPR727 (Sanders et al., 2014).

A hypothesis based on these observations is that the GSTD parameter is characterising the texture depth of materials by accessing areas unavailable to optical methods; the glass beads are accessing areas within the surface of the material itself. Whilst correlations between 3D texture information and friction seem to be stronger than those between 2D texture information and friction, an understanding of the areas of texture unseen by optical measurement methodologies seems to offer superior relationships between the geometric properties of road surfaces and friction than texture depth alone.

To test this hypothesis, HP measurements were combined with SMTD measurements to assess if the areas of texture unseen by optical methods (which it has been assumed can be characterised by HP) can account for the outlying data in a similar way to the GSTD parameter.

This was achieved by augmenting the relationship between SMTD and L-Fn100 in TRL367 (Roe et al., 1998) by "adding" the results from HP tests onto the SMTD variable. Figure 3.4 presents the results of this analysis[18] which shows a similar relationship between the combined SMTD and HP metric and L-Fn100 as was shown between the GSTD parameter and L-Fn100.

---

[18]The constant 10201 was derived from a regression analysis to account for variations in the magnitude of measurements of SMTD and HP.
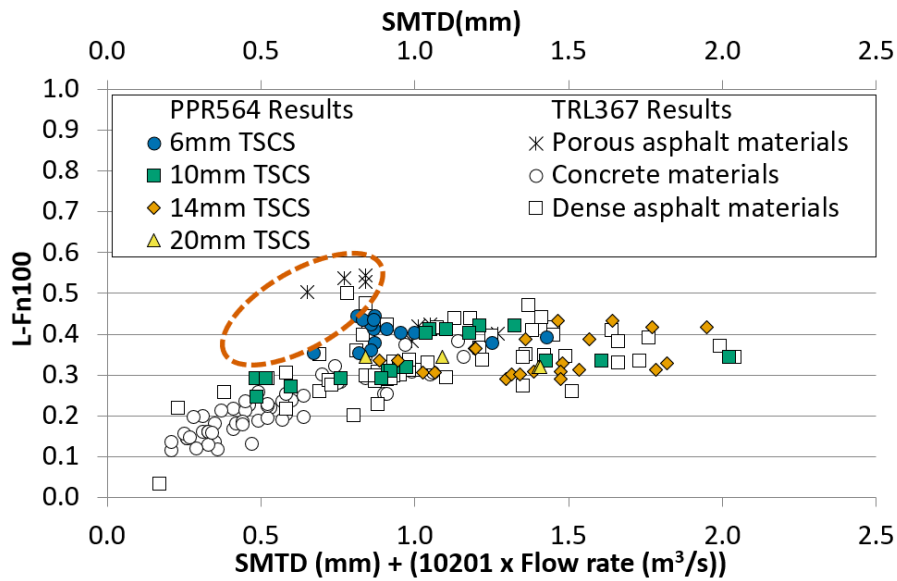
Figure 3.4: SMTD Vs L-Fn100 data from TRL367 (Roe et al., 1998) (the open series), and SMTD + flow rate Vs L-Fn100 (the solid series). The broken ellipse presents the area within which outlying measurements were originally observed.

These observations lead to the conclusion that the combination of surface texture depth and the internally connected void structure of a material work together in removing water from the pavement surface. To fully support this conclusion and to develop a more practical understanding of the effect of permeability on L-Fn100, the results from CT imaging were used to demonstrate the relationship between HP and interconnected voids (Figure 3.5). The solid series represents the average of the individual data points, represented by the open series.
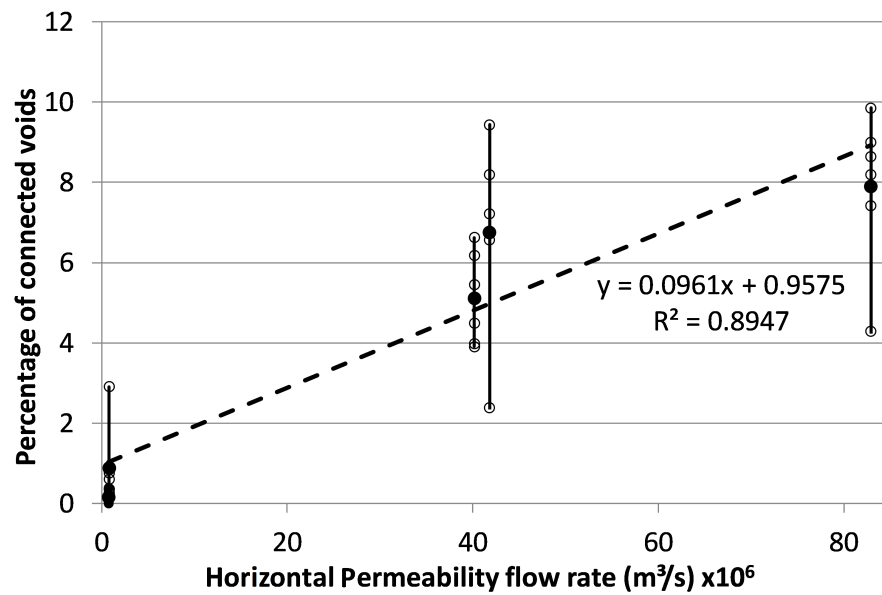
Figure 3.5: Correlation between HP and percentage of connected voids. The solid series are the average of the individual data points, represented by the open series. Reproduced from PPR894 (Sanders, 2017).

This figure shows a strong linear correlation between HP and the percentage of the connected voids within the structure of the material. This observation leads to the conclusion that texture depth and pavement permeability work together to influence high speed friction. This observation also demonstrates that it is impossible, using current optical methods, to characterise texture depth in a way that allows the prediction of L-Fn100 for all material types, as these methodologies cannot characterise permeability.

Chapter 4   Friction as a context dependent parameter

4.1   Foreword

In the foundational stages of research into pavement friction, it has been demonstrated that the way in which friction is measured affects the result. Works by Bradley & Allen (1930), Bird & Scott (1936), and Bird & Miller (1937) demonstrated the general relationships between:

- test vehicle speed and friction;

- wheel angle and friction (for sideway-force devices); and

- % wheel slip and friction.

Later works by Sabey & Storey (1968) and Hosking & Woodford (1976b) investigated the relationships between the properties of friction measurement devices and the friction measured, such as test tyre properties, and water flow rate.

Concurrent to and following these works, the physical properties of the road surface influencing friction were investigated, this work lead to the development of friction prediction models. Several models exist for predicting pavement friction as a function of the vehicle speed, % wheel slip and road characteristics. The most common are:

- the Rado model (Equation 4.1);

- the Penn State model;

- the PIARC model;

- the HERMES model; and

- the ROSANNE model (Equation 4.2).

The Rado model predicts friction as a tyre proceeds from a rolling to locked-wheel condition, at a single vehicle speed.

$$\mu = \mu_{peak} \cdot \exp\left[-\frac{ln\left(\frac{V_s}{S_{peak}}\right)^2}{C^2}\right]$$
(4.1)

Where:

μ_{peak} is the peak friction,

V_s is the slip speed,

S_{peak} is the slip speed at the peak,

C is the Shape factor – mainly dependent on surface texture.

The Rado model describes two phases during the braking process. In the first phase, the tyre moves from a free rolling to peak friction state. Subsequently, the % wheel slip increases to the locked-wheel state (100% wheel slip). The corresponding friction coefficient therefore increases to the peak friction level, and then decreases with increasing slip speed (Wang et al., 2010).

The Penn State, PIARC, HERMES, and ROSANNE models were developed from one another respectively. The Penn State model was developed by Leu & Henry (1978) and describes the relationship between friction and % wheel slip speed as a function of texture depth.

The PIARC experiment was conducted in 1992 resulted in the development of the PIARC model and the International Friction Index (IFI), the aim of which was to allow friction to be measured using any friction measurement device and reported on a common scale. Tyrosafe D05 (Vos et al., 2009) reported that the precision of the IFI scale was not sufficient for practical application.

Descornet (1998) examined the IFI with a view to refining this measure to better reflect the test devices used in Europe. This resulted in the development of the European Friction Index (EFI). The EFI was further refined into the HERMES model in 2006 through the Harmonisation of European Routine and Research Measuring Equipment for Skid Resistance (HERMES) project (Descornet, 2006).

The ROSANNE model was developed by Cerezo et al. (2015) from the ROlling resistance, Skid resistance, ANd Noise Emission measurement standards for road surfaces (ROSANNE) experiment. The ROSANNE experiment used a similar methodology to the PIARC and HERMES experiments but, split the analysis of friction measurement devices into three device families and derived a new Skid Resistance Index (SRI) for each device family:

- SRI$_{SF}$ for sideway-force devices;

- SRI$_{LFLS}$ for longitudinal low % wheel slip devices; and

- SRI$_{LFHS}$ for longitudinal high % wheel slip devices.

The segregation of devices into device families improved the predictive power of the ROSANNE model over its predecessors, but is also illustrative of the difficulties inherent in designing a ubiquitous friction index.

$$SRI_{\text{x}} = B_{\text{x}} \cdot F \cdot \exp \left[\frac{S - S_{\text{ref}}}{a_{\text{x}} \cdot MPD^{\text{b}_{\text{x}}}} \right] \tag{4.2}$$

Where:

SRI$_{\text{x}}$ is the Skid Resistance Index for device family x,

a$_{\text{x}}$, b$_{\text{x}}$, and B$_{\text{x}}$ are parameters related to device family x,

F is the measured skid resistance value,

S is the vehicle speed,

S$_{\text{ref}}$ is the reference speed at which SRI$_{\text{x}}$ is reported,

MPD is the texture depth of the pavement, determined using the Mean Profile Depth method.

4.2   The original works

The work detailed in the remainder of this chapter was originally reported in PPR815 (Sanders et al., 2017b). This study is provided in Appendix C and presents a desk study which lead to the production of a model that predicts the friction of a material at any operational velocity and % wheel slip based on skid resistance and texture measurements made using the SCRIM.

4.3   Experimental methodologies

A full description of the experimental methodologies used for this work are presented in the original works (PPR815), what follows is a brief summary of the methodologies used to develop the friction prediction model.

4.3.1   Generation of a friction database

This work was a desk study that utilised friction data collected from 2,468 PFT measurements,

and SC and SMTD from ≥200 measurements from SCRIMs. Data collected using the PFT were gathered in their raw state such that each individual determination of friction over the whole braking cycle was available. The data collation exercise resulted in the generation of a database of values for the following material types; the values shown in parentheses represent the number of individual surfaces assessed, and therefore the number of friction profiles generated:

- Concrete (41),

- HRA (17), and,

- TSCS with the following coarse aggregate sizes; 6mm (9), 8mm (4), 10mm (17), 14mm (5), and Unknown (20).

- Porous materials were deliberately omitted from this study based on the conclusions from PPR727 and PPR894 (Chapter 3).

4.3.2   Generation of friction profiles

A key task of this work was to develop a methodology capable of characterising the friction performance of road surfacing materials at all operational velocities and % wheel slips. The approach was to represent the performance of individual surfaces as a matrix of values where the position of a value in the matrix described its operational velocity and % wheel slip, and the magnitude of the value represented the tyre/surface friction. This is illustrated in Figure 4.1 where the matrix is plotted as a three dimensional profile where the x, y and z axes represent the % wheel slip, operational velocity, and friction respectively. This is referred to as a friction profile.
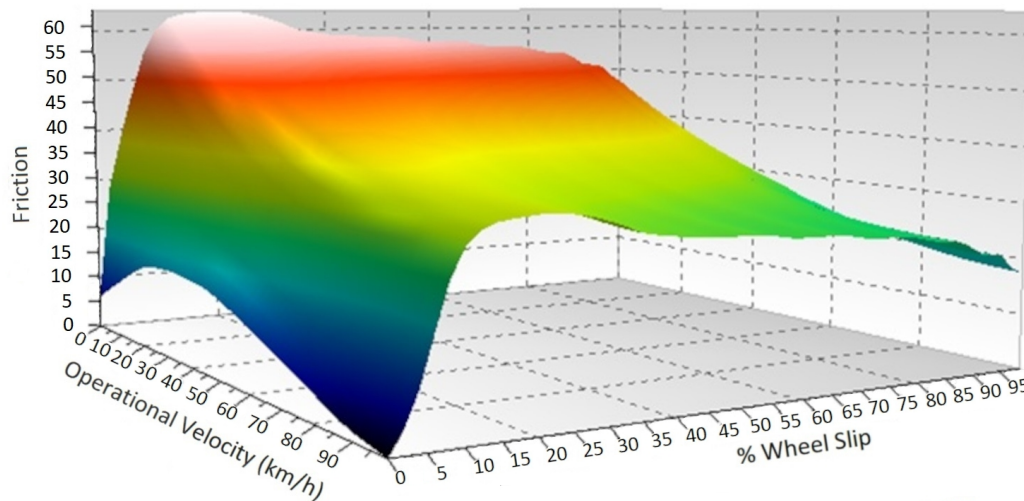
Figure 4.1: An example of a friction profile: The relationship between friction (z-axis), % wheel slip (x-axis) and operational velocity (y-axis) for a given material. Profile shown is for a TSCS.

4.3.3 Prediction of friction profiles

A statistical model (the friction model) was created using the multiple linear regression method. The dependent variable was pavement friction (using the friction profiles generated from the previous stage), and the independent variables were % wheel slip, operational velocity, and the SC and SMTD of the material for which friction is being predicted.

4.3.4 Validation of the friction model

The friction model was validated through an assessment of residual values[19] where model predictions were compared with raw friction measurements made using the PFT. This approach allowed comparisons to be made with a total of 122,018 values. Owing to the scope of the work it was not possible to collect independent data for the purposes of model validation so to add context to the analysis of residual values, a comparison was made with the TRL367 model. This consisted of calculating the distribution of the residual values generated by the TRL367 model on the data used to build that model (Roe et al., 1998).

---

[19]The difference between measured values and values predicted by the model.

4.4   Results

The regression analysis was carried out using the data analytics package in Microsoft Excel (Microsoft, 2017). The analysis showed no correlation between % wheel slip and friction. Owing to this, a separate regression was carried out at each % wheel slip. The results of the analyses were then consolidated into a simple programme where they were used to construct a lookup table such that the friction of a surface with the following input parameters of SC(50), SMTD, operational velocity and, % wheel slip, could be estimated.

The overall form of the model is shown in Equation 4.3.

$$Fn_x = [a_x \cdot \ln(\ln(V))] + [b_x \cdot \ln(SMTD)] + [c_x \cdot SC(50)] + d_x \tag{4.3}$$

Where:

Fn$_\chi$ is the friction at % Slip χ,

a$_\chi$ **b**$_\chi$ **c**$_\chi$ **and d**$_\chi$ are coefficients at % slip x determined by the regression analysis,

V is the operational velocity relating to the friction value in km/h,

SMTD is the SMTD texture depth of the surface in mm,

SC(50) is the friction of the surface measured using SCRIM and reported as a value of SC(50).

Figure 4.2 shows the distribution of the residual values and the 1, 2 and 3 standard deviation ranges. The distribution of residuals forms a bell curve with a mean value of zero. The 1, 2 and 3 standard deviation ranges represent the 68%, 95% and 99.7% likelihood of the residual of any value falling within the ranges indicated by the x-axis. In this case there is a 68%, 95% and 99.7% likelihood that the friction prediction will fall within approximately 10, 20 and 30 units respectively of the actual friction value.
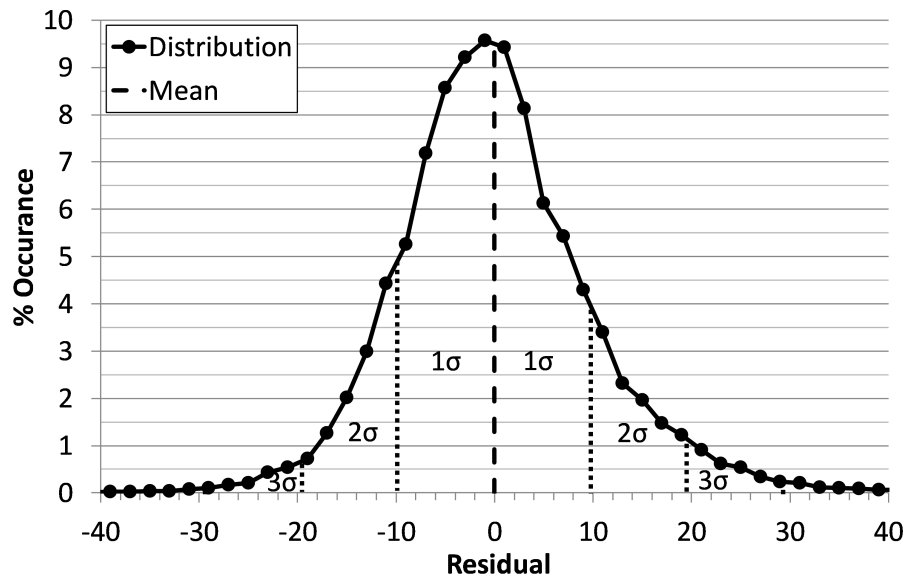
Figure 4.2: Distribution of residuals and standard deviation ranges for friction model. Reproduced from PPR815 (Sanders et al., 2017b).

By way of comparison, the distribution of residual values for the TRL367 model is shown in Figure 4.3. This figure shows that the TRL367 model has 1, 2 and 3 standard deviation ranges of approximately 6, 12 and 18 units. The accuracy of the TRL367 model is therefore notably greater than that of the friction model. However the TRL367 model is limited to estimating friction at one operational velocity and one % wheel slip only.
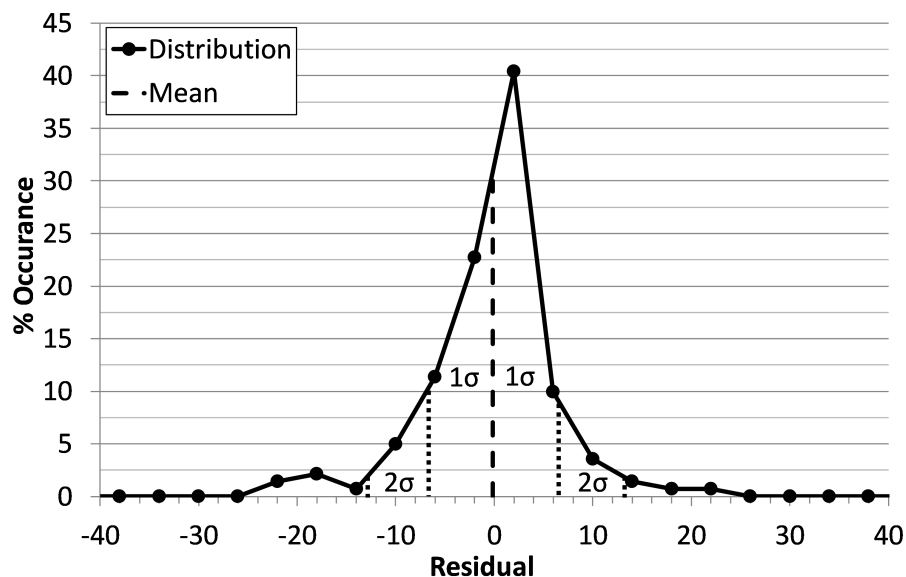
Figure 4.3: Distribution of residuals and standard deviation ranges for TRL367 model. Reproduced from PPR815 (Sanders et al., 2017b).

Chapter 5   Contextualising the UK's friction measurement devices

5.1   Foreword

The first skid resistance testing equipment utilising the sideway-force measurement method was developed in the UK in the early 1930's. The concepts of % wheel slip and vehicle speed were understood during this period, and during the subsequent development of the SCRIM, but the literature is unclear as to how SCRIM measurements can be described in these terms.

Some sources refer to SCRIM measurements as "sideway force skid resistance" whereas other sources strongly allude to the SCRIM as a quasi-locked-wheel device (100% wheel slip), and the FEHRL Report 2006/01 (Descornet et al., 2006) describes the SCRIM as making measurements at 34% wheel slip and 50km/h.

The ambiguity in the measurement characteristics of the SCRIM has hampered discussion into its appropriateness as a tool for assessing vehicle safety. In other words, without knowing where SCRIMs and sideway-force devices in general, sit on a friction profile, it is impossible to fully understand their measurements within the context of vehicle safety.

5.2   The original works

The works described in the remainder of this chapter are reported in three of the original works: PPR768 (Sanders et al., 2017a), PPR957 (Sanders & Browne, 2020), and PPR980 (Sanders, 2021). These publications are presented in full in Appendix D, E, and F respectively. PPR768 presents the results of a practical assessment of skid resistance measurements devices available for use in the UK. PPR957 and PPR980 present a study which identifies the measurement characteristics of sideway-force devices in terms of their operational velocity and % wheel slip.

5.3 Experimental methodologies

Three experimental studies were conducted to fulfill the aim of this work, namely:

- A desk study assessing the properties of SCRIMs leading to the generation of characterisation hypotheses,

- an experiment to compare measurements made using SkReDeP and the PFT to test the aforementioned hypotheses; and

- a critical analysis of alternative skid devices to the SCRIM which are available in the UK, for the purposes of network level assessments.

5.3.1 A desk study to characterise measurements made by SCRIMs

PPR957 (Sanders & Browne, 2020) presents a desk study which assessed the ways in which measurements made using SCRIMs could be described in terms of % wheel slip and operational velocity. The methodology used was to resolve the forces acting on a SCRIM wheel based on the geometry of the device and standard vehicle speed in various directions and describe the resolved forces in terms of % wheel slip and operational velocity.

A full description of this process is presented in Appendix D. In summary, four characterisations were identified each based on the same physical properties of the SCRIM and as such were found to be equally valid[20].

The results of the desk study have been presented in Table 5.1 (instead of the results section) as knowledge of them is important for a full introduction to the experimental methodology.

---

[20]With the exception of the co-axial characterisation which has been included for completeness.

Table 5.1: Characterisations derived from the desk study reported in PPR957 (Char.: Characterisation, and Op. vel.: Operational velocity).

Char.	Description	% wheel slip	Op. vel. (km/h)
Current	The operational velocity defined as the vehicle speed, and the slip speed is defined as the vehicle speed resolved orthogonal to the direction of wheel rotation.	32.4	50
Scalar	The operational velocity is defined as the vehicle speed, and the slip speed is calculated from the wheel speed (which is calculated by resolving the vehicle speed in line with the direction of wheel rotation), and vehicle speed.	6.04	50
Vector	The operational velocity and slip speed are considered to act along the axis of wheel rotation.	100	17.1
Co-Axial	The operational velocity is defined as the velocity of the vehicle and the wheel speed resolved in to the direction of travel.	11.7	50

5.3.2 An experimental study to challenge the characterisations

To challenge the characterisations derived from the desk study, an experiment was carried out to make comparative measurements with the PFT and SkReDeP. Measurements made with the PFT were used to generate friction profiles for the materials tested, and these were used to compare the performance of SkReDeP with areas of the friction profiles that correlate to the characterisations derived from the desk study. The work presented in Appendix E details the methodology in full which is summarised below:

- Modify the PFT to reflect the properties of SCRIMs - so that direct comparisons could be made between SkReDeP and the PFT, and to control for differences in tyre effects. Table 5.2 shows the differing properties of SkReDeP and the PFT which were addressed by the PFT modifications.

Table 5.2: Comparison of the properties of SkReDeP and the PFT.

Property	SkReDeP	PFT
Vertical load at test axle (kg)	200 ± 8	489.5 ± 6.6
Test tyre used	BS 7941-1-2006 (British Standards Institution, 2006)	ASTM E524 - 08 (ASTM international, 2008)
Water film thickness (mm)	0.5	1.0

- Identify materials to be assessed - The experimental work required the determination of the friction properties of materials with different nominal friction levels, at a wide range of vehicle

speeds, and with multiple measurements being made at each vehicle speed. To this end measurements were made on a closed test track containing the following material types:

Basalt tiles (BT) – A smooth surface constructed from basalt tiles,

Delugrip 1 and 2 (DG1 and DG2) – Propriety asphalt materials,

ISO 1 and 2 (ISO1 and ISO2) – Asphalt surfaces used in standardised braking tests,

Bridport Pebel (BP) – An asphalt material with bridport pebel aggregate.

- Make measurements using a SCRIM and the modified PFT - as summarised in Table 5.3.

Table 5.3: Number of measurements made with the modified PFT and SkReDeP.

Material	SkReDeP measurements at vehicle speeds (km/h):			PFT measurements at vehicle speeds (km/h):		
	30	50	80	30	50	80
BT	8	10	8	24	28	43
DG1	8	8	7	27	26	22
ISO1	8	8	8	20	26	25
BP	8	8	8	16	13	4
ISO2	8	8	8	27	27	18
DG2	6	5	6	39	46	42

5.3.3   A critical assessment of SCRIM alternatives

The final task of this work was to consider the efficacy of alternatives to the SCRIM as network level test devices. This was achieved by undertaking an assessment of alternatives to the SCRIM, namely:

- The Pavement Friction Tester - measuring locked wheel friction; and

- GripTester - measuring fixed slip skid resistance.

Whilst there are numerous other friction measurement devices (Descornet at al., 2006), the majority of these devices were not considered during this study. This was owing to pragmatism as an exhaustive study would have been fiscally untenable, and the results of the work should be implementable, and therefore would not be conducive with adopting a device not available in the UK.

The focus of the work was twofold:

1. To stress test the speed correction formula applied to SCRIM data to identify if its scope could be expanded to include measurements made at lower speeds. Demonstrating this would have enabled the validation of measurements made on high risk sites which would have normally been considered invalid.

2. To identify the influence of site geometry (bends) and test vehicle manoeuvres (braking) on measurements made by SCRIMs, the PFT, and GripTester.

The work presented in Appendix F details the methodologies used for this study which are summarised below:

Stress testing of the speed correction formula was carried out by assessing the friction of a number of surfaces at the HORIBA-MIRA proving ground, using SkReDeP, GripTester, and the PFT at vehicle speeds between 20 and 100km/h. The friction values collected using SkReDeP and GripTester were compared with the current speed correction formulas.

For the assessment of the effect of vehicle manoeuvres on friction measurements, the PFT was omitted. This was owing to safety concerns regarding testing using the PFT around bends. To assess the effect of braking manoeuvres, measurements were made with SkReDeP and GripTester under braking conditions at initial speeds of 25, 50 and 80km/h. The measurements made under these conditions were then compared to measurements made under non-braking conditions.

The effect of cornering manoeuvres was conducted in two parts; the first was to simulate testing on roundabouts. To this end, SkReDeP and GripTester were used to make measurements in both directions of a circular path at speeds between 10 and 35km/h. Measurements were made in the clockwise (CW) and anti-clockwise (ACW) directions and friction measurements compared between the two directions.

The second part of the cornering testing was to assess a vehicle transitioning from a CW to ACW curve in a figure of eight test path. Measurements were made with SkReDeP and GripTester in each direction of a figure eight path between 10 and 25km/h in 5km/h increments.

5.4   Results

5.4.1   Characterisation of friction measurements made using SCRIMs

Figures 5.1 and 5.2 present measurements made using SkReDeP (the vermilion square series (SR)) with those made using the modified PFT (the blue circle series (Fn)). Solid series represent average values at each operational velocity and open series represent individual measurements. Lines of best fit are shown in relation to average values. The critical parameter in these figures is the % wheel slip of measurements made using the modified PFT, which is shown in the legends.

In the original work (PPR980 (Sanders, 2021)) one figure of this type was generated for each material and characterisation assessed, and as such 24 such figures are presented in that work. For simplicity, this thesis presents two of these figures to demonstrate the key observations made. Figure 5.1 presents the results collected on the DG1 material, but, represents the overall behaviour observed on five of the six materials assessed. Figure 5.2 presents the results collected on the DG2 material, which was the only material which demonstrated a different overall behaviour to the other materials assessed.

The agreement between measurements made using SkReDeP and the modified PFT was quantified using the R^2 value for the "All" series. This parameter was used to identify the cases where measurements made using the SkReDeP and modified PFT most closely matched, i.e. those cases where measurements made using the modified PFT best represented those made by the SkReDeP, these cases are represented here. Figure 5.1 shows the overall behaviour observed[21], measurements made with SCRIM and the modified PFT most closely match with the 100% wheel slip case (the vector case).

---

[21] It should be noted that Figure 5.1 represents the overall behaviour of the cases referenced only, the absolute measurements made on other materials were markedly different and are available in the original work.
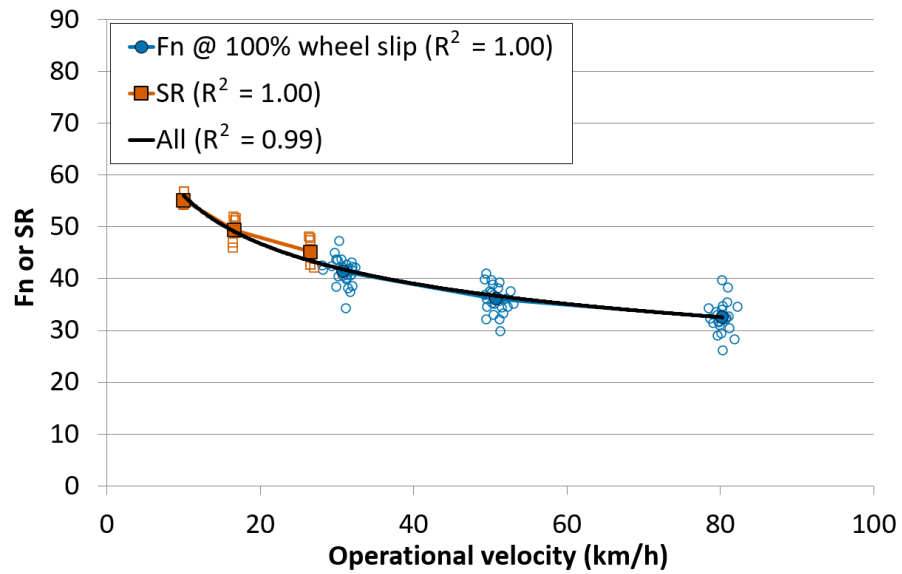
Figure 5.1: SCRIM and modified PFT measurement made on the *DG1* material. Solid series indicate average values, and hollow series represent individual data points. The general behaviour[22]was also observed on the BP, ISO1, ISO2, and BT materials. Reproduced from PPR980 (Sanders, 2021).

Measurements made on the DG2 material (Figure 5.2), most closely match with the 34% wheel slip case (the current case). It is noteworthy that these measurements were made on the surface with the highest nominal friction values.
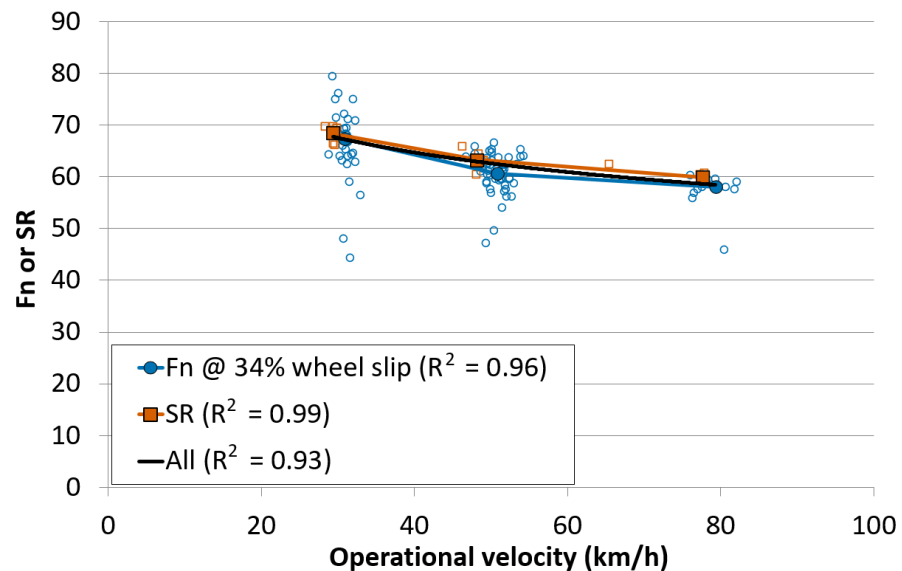
Figure 5.2: SCRIM and modified PFT measurement made on the *DG2* material. Solid series indicate average values, and hollow series represent individual data points. Reproduced from PPR980 (Sanders, 2021).

---

[22]That SkReDeP measurements most closely match with modified PFT measurements at 100% wheel slip.

5.4.2 Performance review of friction measurement devices

Amount of the UK network assessed using SCRIM

Figures 5.3 and 5.4 show the results of the desk study. The percentage of the English trunk road network made at different vehicle speeds are shown in each graph. The letters in the legend refer to road categories as defined in CS 228 (Highways England, 2020a).

Figure 5.3 shows the percentage of the network measured below 25km/h (the limit of the SCRIM speed correction at the time of writing) for each site category. Figure 5.4 shows the percentage of the English trunk road measured below 10km/h, this has been provided to demonstrate the potential effect in reducing the lower limit of the speed correction formula to 10km/h.
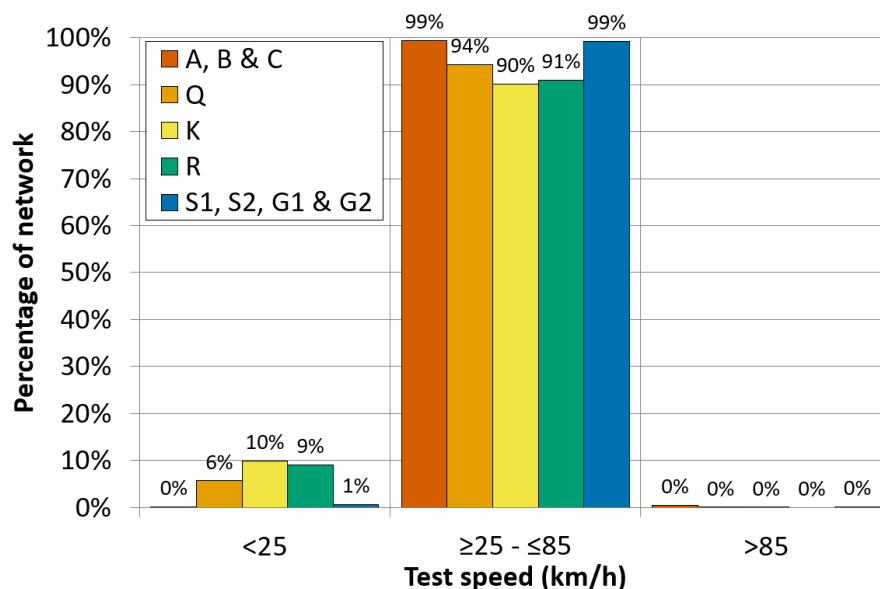
Figure 5.3: Amount of English Trunk road network for which friction measurements were made between 25 and 85km/h by site category (the letters in the legend (Highways England, 2020a)) in 2013. Reproduced from PPR768 (Sanders et al., 2017a).

Figure 5.3 demonstrates that between 6 and 10 percent of category Q, K and R sites (all of which are high risk sites) are measured below the threshold of the speed correction formula and are therefore considered invalid.
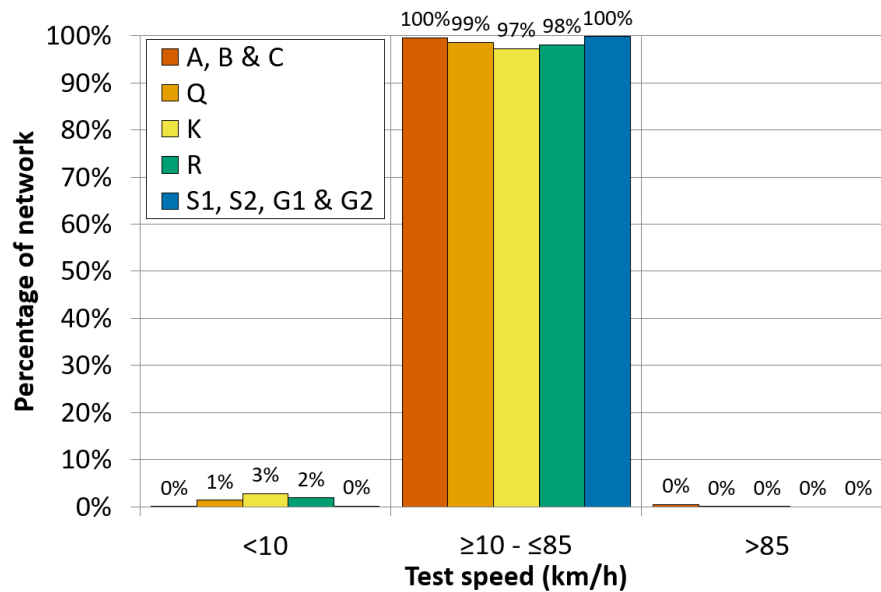
Figure 5.4: Amount of English Trunk road network for which friction measurements were made between 10 and 85km/h by site category (the letters in the legend (Highways England, 2020a)) in 2013. Reproduced from PPR768 (Sanders et al., 2017a).

Figure 5.4 shows that reducing the limit of the speed correction formula to 10km/h would have reduced the amount of invalid measurements made in 2013 for these sites to between 1 and 3 percent.

Speed correction of friction measurements

Relating to the results presented in the previous sub-section are those shown in Figure 5.5[23]. This figure shows the values of SC collected at different speeds and on different materials normalised to converge at point 10km/h and 0.7SC. Measurements expected based on the speed correction formulas provided in HD28/15 (Highways England et al., 2015), the active standard at the time of writing PPR768 (Sanders et al., 2017a), and CS 228 (Highways England et al., 2020a), the active standard at the time of writing this thesis are also provided for reference. The speed correction formulas in HD28/15 and CS 228 are identical and so only that relating to CS 228 is referenced.

---

[23]Results from Surface 2 have been omitted as they were invalid.
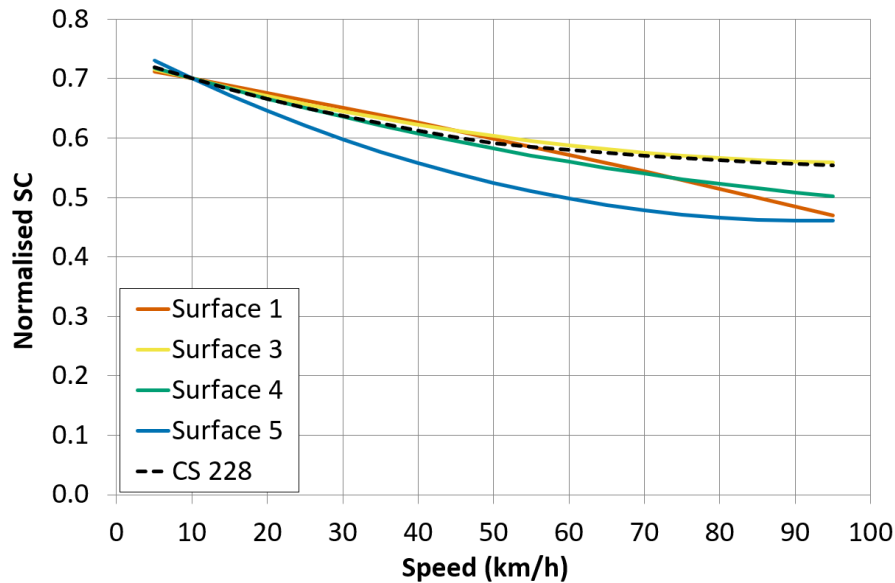
Figure 5.5: Friction measurements made using *SkReDeP* at various speeds and on various surfaces, normalised to converge at point 10km/h and 0.7SC. Reproduced from PPR768 (Sanders et al., 2017a).

Figure 5.5 shows that at lower speeds, the results from Surface 5 deviate from those from the other materials and those expected by the speed correction. This deviation represents a fail-unsafe position as using the speed correction would result in a larger estimated friction than is actually available.

Normalised measurements made at different speeds on different surfaces with GripTester are shown in Figure 5.6. Whilst there is no standardised speed correction for GripTester, in practice, measurements made using GripTester are commonly converted to estimated sideway-force device values using the relationship presented in TRL report PPR497 (Dunford, 2009)[24].

Given that this practice takes place, it is prudent to include the speed correction formula stated in CS 228. These results show a similar behaviour between the speed correction and the measurements made at speeds below approximately 40km/h. Measurements made at higher speeds deviate as the rate of change in friction with speed reduces.

For the majority of materials, this creates the fail-safe position whereby the speed correction would underestimate actual measurements at higher speeds. But, a fail-unsafe condition is met on Surface 1 at higher speeds.

---

[24]SC = 0.89 x GN
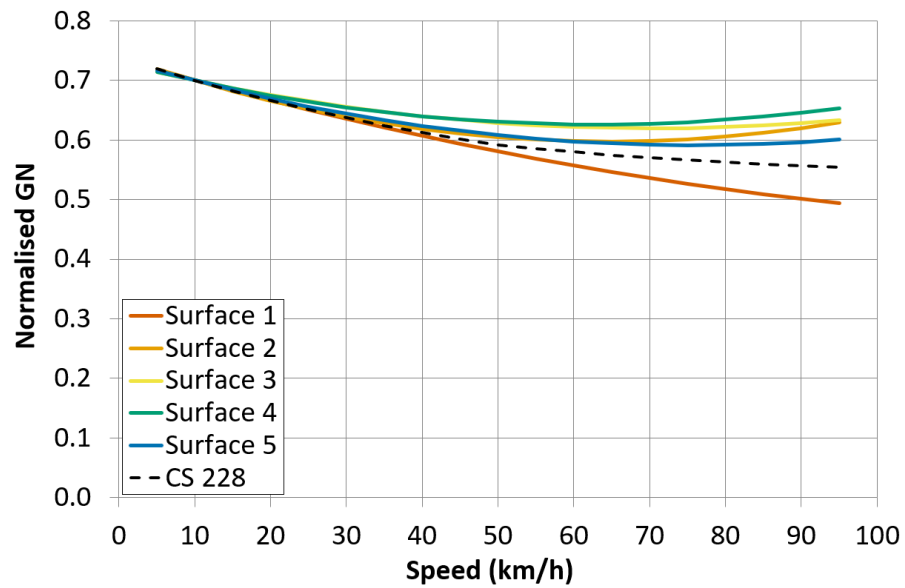
Figure 5.6: Friction measurements made using *GripTester* at various speeds and on various surfaces, normalised to converge at point 10km/h and 0.7GN. Reproduced from PPR768 (Sanders et al., 2017a).

Measurements made at different speeds on different surfaces using the PFT are shown in Figures 5.7 and 5.8, measurements made in a locked-wheel condition (100% wheel slip) are shown above those made at peak friction. There is currently no standard speed correction for measurements made with the PFT and so none is shown. Measurements in both locked-wheel and peak friction conditions show divergence from one another, particularly between Surface 1 and the other surfaces. This suggests that developing a reliable, ubiquitous, speed correction formula for measurements made using the PFT would be challenging.
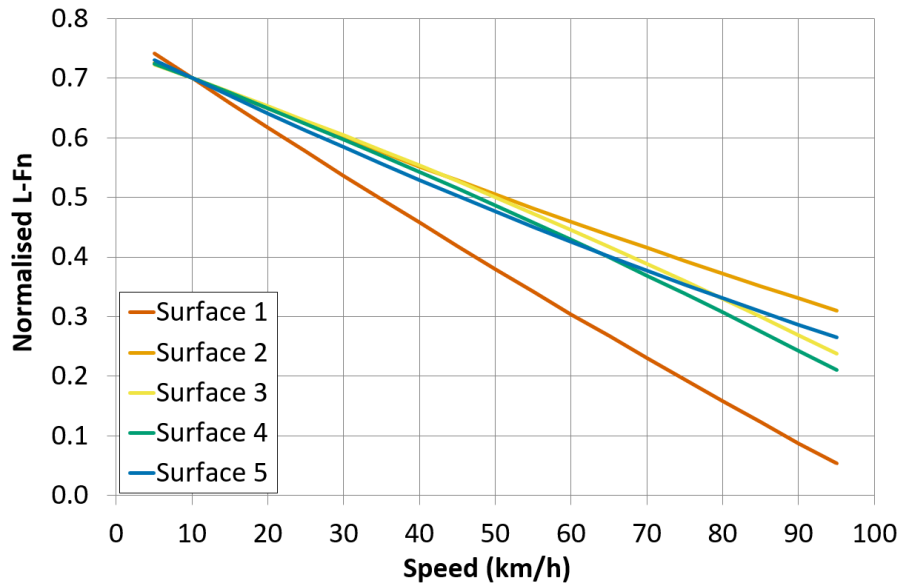
Figure 5.7: Locked-wheel friction measurements made with the PFT at various speeds and on various surfaces, normalised to converge at point 10km/h and 0.7L-Fn. Reproduced from PPR768 (Sanders et al., 2017a).
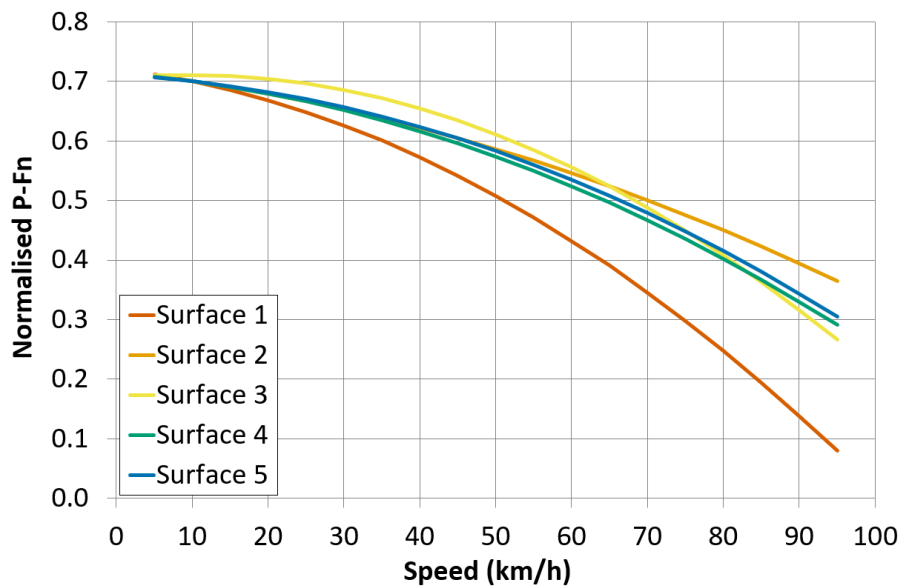
Figure 5.8: Peak friction measurements made with the PFT at various speeds and on various surfaces, normalised to converge at point 10km/h and 0.7P-Fn. Reproduced from PPR768 (Sanders et al., 2017a).

Effect of manoeuvres on friction measurements

Braking manoeuvres

Measurements made using SkReDeP and GripTester whilst conducting a breaking manoeuvre are

shown in Figures 5.9 and 5.10 respectively. In each graph, the broken lines represent vehicle speed with respect to distance traveled (Chainage), and the solid lines represent the speed corrected friction.
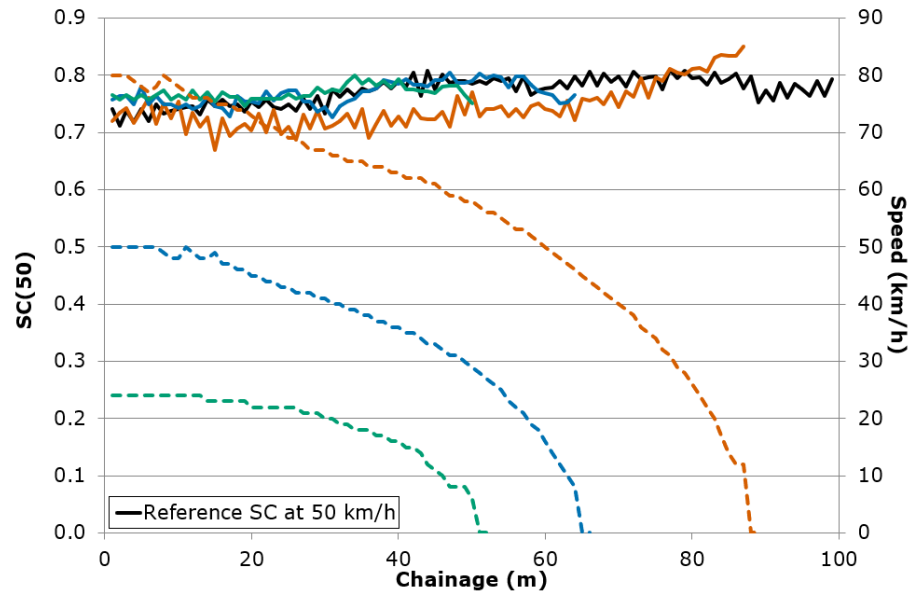
Figure 5.9: Friction measurements made using *SkReDeP* under a straight line braking manoeuvre. Broken lines refer to speed and solid lines refer to SC(50). Reproduced from PPR768 (Sanders et al., 2017a).

A stark difference in performance is shown between the two devices. SkReDeP produces friction values that are largely comparable at all speeds. At lower speeds this is also true of GripTester, but at higher speeds, large differences in friction value are observed. At 80km/h the GripTester wheel was observed leaving the ground, which would account for the large variations in GN at this speed.
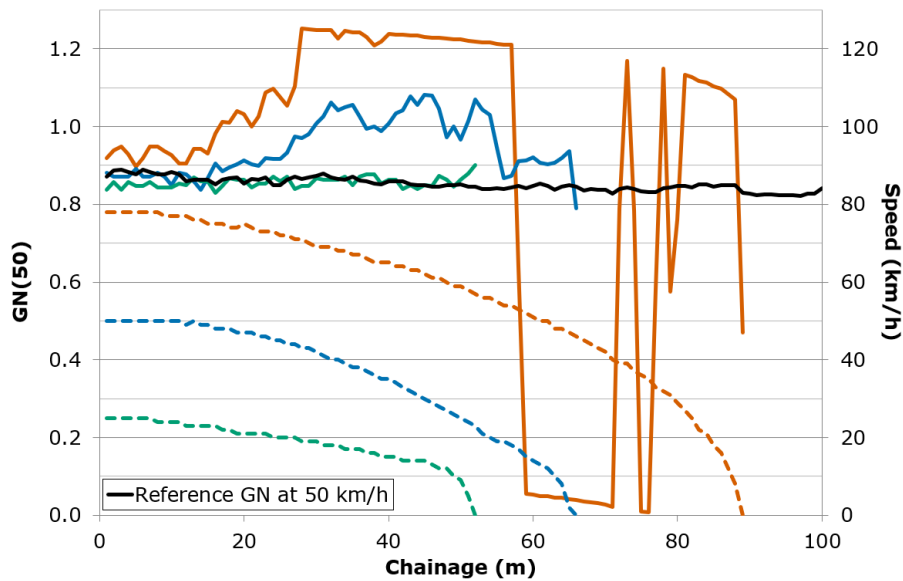
Figure 5.10: Friction measurements made using *GripTester* under a straight line braking manoeuvre. Broken lines refer to speed and solid lines refer to GN(50). Reproduced from PPR768 (Sanders et al., 2017a).

Roundabouts

The data collected whilst testing a roundabout analogue were analysed to produce histograms of the difference in skid resistance, calculated using measured vertical load and an assumed constant vertical load. Differences in the histograms between the CW and ACW directions would demonstrate the effects of load transfer on the skid resistance values. Included within the histograms is the distribution of measurements made in a straight line, so that the performance of the machines testing in both scenarios can be compared. These data are shown in Figure 5.11 for SkReDeP and Figure 5.12 for GripTester.

Figure 5.11 shows that measurements made with the SkReDeP in both directions are providing similar distributions. This shows that the effect of load transfer on the results is the same regardless of the direction of travel.
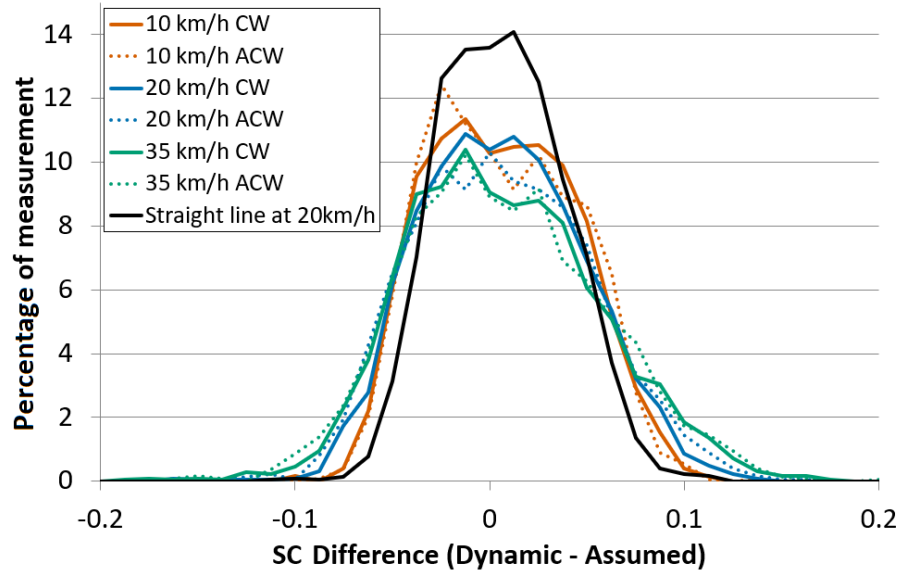
Figure 5.11: The difference between friction measurements made using *SkReDeP* with a dynamic and assumed vertical load on roundabout analogue. Reproduced from PPR768 (Sanders et al., 2017a).

Broadly, the same behaviours are shown in the GripTester results as in the SkReDeP results. There is however an additional phenomenon shown in the results gathered at 35km/h using GripTester by the presence of a peak in the ACW results at approximately -0.15GN difference. It is hypothesised that this behaviour is related to an increase in vertical load experienced by some dynamic effects of travelling in an ACW direction with the machine attached on the nearside of the vehicle.
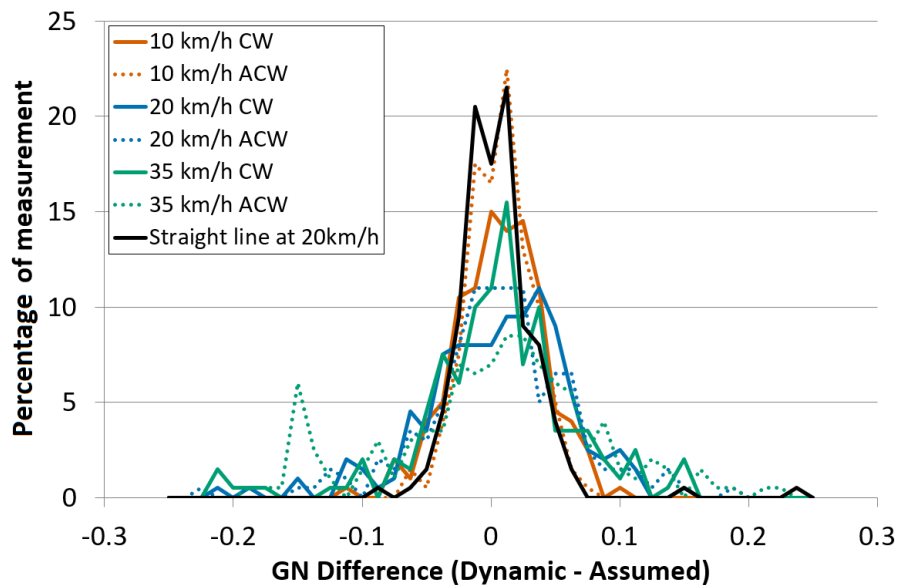
Figure 5.12: The difference between friction measurements made using *GripTester* with a dynamic and assumed vertical load on roundabout analogue. Reproduced from PPR768 (Sanders et al., 2017a).

Figure eight

Data collected from the figure of eight testing were analysed by comparing the difference in values generated from testing at 10 and 25km/h along the length of the test path. If load transfer was affecting the results it would be expected to see changes in this difference at the crossover point and apexes of the circles.

Figures 5.13 and 5.14 show the difference in skid resistance values measured using SkReDeP and GripTester at 10 and 25km/h from a single test run (the blue line). Included in the Figures are the radii being traversed (the black line) and the range of values measured in a straight line (the vermillion lines) for reference.

Measurements made with SkReDeP are relatively consistent and load transfer does not appear to affect the results.
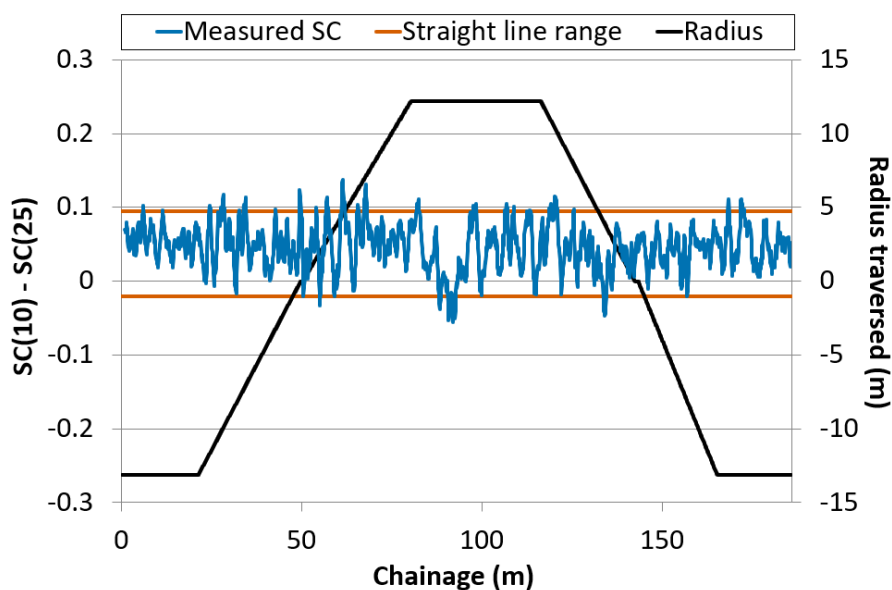
Figure 5.13: The difference between friction measurements made using _SkReDeP_ at 10km/h and 25km/h during a figure 8 manoeuvre. Reproduced from PPR768 (Sanders et al., 2017a).

Results gathered using GripTester are noisy and some data have been removed owing to insufficient vertical load. Despite this, there is no obvious trend for the values to change as a result of the figure of eight path.
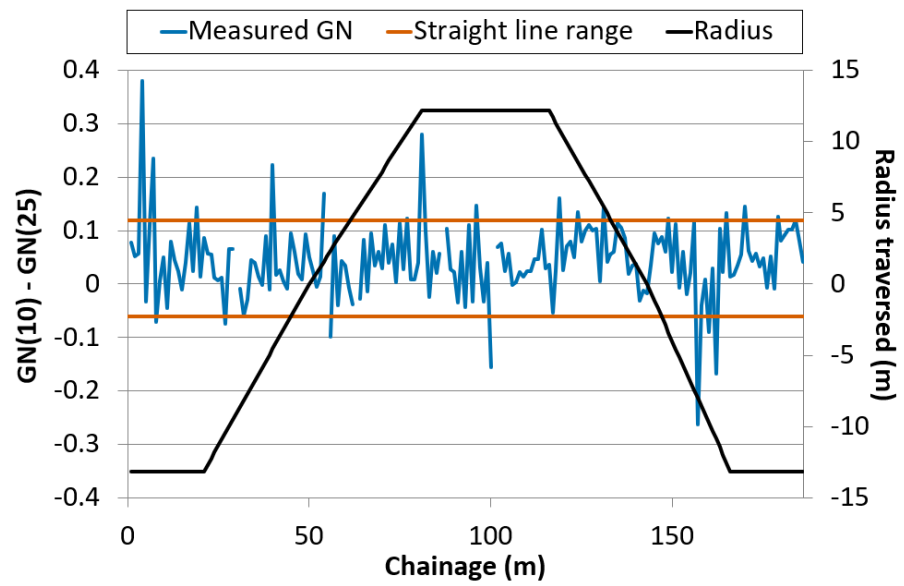
Figure 5.14: The difference between friction measurements made using *GripTester* at 10km/h and 25km/h during a figure 8 manoeuvre. Reproduced from PPR768 (Sanders et al., 2017a).

Chapter 6   Discussion and conclusions

6.1   Foreword

This chapter discusses the findings of the works presented in the previous chapters within the context of the research aim. The research questions and null hypotheses presented in Chapter 1 are addressed in Section 6.2. In Section 6.3 a formal deductive argument[25] is presented which summarises the work carried out and leads to the main conclusions. Evidence supporting the premises is given in Section 6.4, and a discussion and the conclusions are presented in Section 6.5.

6.2   Answering the research questions & falsifying the null hypotheses

Q1: Can the high speed, locked-wheel friction properties of all road surface materials be inferred from their geometric properties?

H_o1: The high speed, locked-wheel friction properties of all road surface materials cannot be inferred from their texture depth properties and the static pressure distribution between the tyre and road surface.

This research question, and null hypothesis, was addressed by the work presented in Appendix A, and summarised in Chapter 3, (PPR727 (Sanders et al., 2014)). If the geometric properties of the road surface are limited to those which can be quantified using line of sight dependent tools, then the answer to the research question is; they cannot be.

If the geometric properties of the road surface includes those which can be characterised using non-line of sight dependent measurement methodologies then this question can be answered by stating that:

---

[25]Also known as a syllogism a formal deductive argument consists of: Premises (P), statements of fact which are supported by evidence; Minor Conclusions (c), conclusions which logically follow from the premises and break the argument into different themes; and Major Conclusions (C), the results of the argument which follow from the minor conclusions and/or premises. An important feature of a deductive argument is that if all premises are true, and all conclusions logically follow from those premises (that is, without the use of fallacious logic), then the conclusions must also be true.

The high speed, locked-wheel friction of all road surface materials can be inferred from the texture depth and permeability properties of such materials, if, the low speed friction properties of those materials are also known.

H_o1 was *not falsified*.

Q2: Can the permeability of road surface materials affect high speed, locked-wheel friction?

H_o2: The high speed, locked-wheel friction properties of all road surface materials cannot be inferred from their texture depth, low speed friction, and permeability properties.

This research question and hypothesis was answered by the results of the study presented in Appendix B, and summarised in Chapter 3, (PPR894 (Sanders, 2017)). This demonstrated that in order to characterise the high speed, locked-wheel friction properties of all road surfaces, one must have knowledge of the internal structure of the road surface.

Knowledge of the internal structure of the road surface is not necessary for non-porous materials, therefore if one has confidence that the materials assessed are non-porous, then the effect of permeability does not need to be considered when predicting high speed, locked-wheel, friction.

H_o2 was *falsified*.

Q3: To what level of accuracy can the friction of non-porous road surfaces at all % wheel slips and operational velocities be inferred using data currently collected on the road network?

H_o3: The friction of non-porous road surfaces cannot be inferred at all % wheel slips and operational velocities using data currently collected on the road network.

H_o4: The inferences made (from H_o3) will not be accurate to 10 units using a 95% confidence limit.

The works reported in Appendix C, and summarised in Chapter 4, (PPR815 (Sanders et al., 2017b)) have answered this question and addressed the null hypotheses. That work demonstrated that the friction performance of the non-porous road surfacings assessed could be predicted to within 20

units at a confidence level of 95%.

H_o3 was *falsified*, and H_o4 was *not falsified*.

Q4: Can the current speed correction formula for SCRIMs be expanded to validate measurements made below 25km/h?

H_o5: The current speed correction formula for SCRIMs cannot be safely expanded to validate measurements made below 25km/h.

The work presented in Appendix D, and summarised in Chapter 5, (PPR768 (Sanders et al., 2017a)) has shown that expanding the scope of the current speed correction formula for SCRIMS would result in a fail-unsafe situation and therefore its expansion to include measurements below 25km/h is inappropriate.

H_o5 was *not falsified*.

Q5: Are there devices other than the currently used SCRIMs that could be used for the direct measurement of road surface friction in the UK at a network level?

H_o6: There are no other devices than the SCRIM that could be used for the direct measurement of road surface friction in the UK at a network level.

The work presented in Appendix D, and summarised in Chapter 5, (PPR768 (Sanders et al., 2017a)) has shown that the influence of road geometry and/or vehicle manoeuvres can affect the measurements made by GripTester devices in a way non-conducive to their adoption as a tool for the assessment of the entire road network. However, within their envelope of valid operation, it would be possible to adopt the use of these devices for the characterisation of friction on some parts of the road network.

A similar statement could be made for the PFT. Whilst the ubiquitous adoption of the PFT on the UK road network is not feasible, its use in specific situations could provide high resolution information in areas requiring detailed investigation. This may be of particular pertinence for the investigation of accidents, or new road constructions.

H_o6 was *falsified* in that the other tools assessed could not be used for network level assessment,

but it should be noted that devices other than the SCRIM can be used in specific locations and instances.

Q6: What are the measurement properties of the current SCRIMs expressed in terms of operational velocity and % wheel slip?

H_o7: SCRIMs do not make measurements at 100% wheel slip and 17.1km/h operational velocity.

The works reported in Appendices E and F, summarised in Chapter 5, (PPR957 (Sanders & Browne, 2020) and PPR980 (Sanders, 2021)) have demonstrated that SCRIMs make friction measurements at 100% wheel slip and an operational velocity of 17km/h when travelling at a speed of 50km/h.

H_o7 was *falsified*.

QT: Is the characterisation of highway friction using sideway-force devices, and the inference of high speed, locked-wheel friction, conducive to maintaining or improving vehicle safety?

H_oT: The characterisation of highway friction using sideway-force devices, and the inference of high speed, locked-wheel friction, is not conducive to maintaining or improving vehicle safety.

This question is at the core of this thesis. To answer it simply, the characterisation of highway friction using sideway-force devices and the inference of high speed, locked-wheel friction through the measurement of texture depth, is in some limited cases, conducive to affecting vehicle safety. However, in the vast majority of cases these measurements are non-conducive to affecting vehicle safety.

H_oT was *not falsified* for the majority of locations on the UK trunk road network. In some, small number of cases, H_oT was *falsified*. But overall, the null hypothesis stands.

The reasoning leading to this answer and a more detailed response is provided by the summary argument laid out in the next section.

6.3 The summary argument

The following argument summarises the main points of this thesis and provides a clear and evidenced rationale supporting the conclusions of this work.

P1. The friction supplied to motorists by the UK road network is managed with the goal of maintaining vehicle safety (Highways England et al., 2020a).

P2. The friction demand placed on the UK road network by motorists is determined by, inter alia, the type of vehicle manoeuvre being attempted, and the severity of that manoeuvre.

P3. Based on the vehicle manoeuvre being carried out, and the severity of that manoeuvre, the areas of the friction profile used (the % wheel slip and operational velocity) will differ.

c1. *So, in order to maintain vehicle safety, friction should be measured, or inferred, at the areas on the friction profile used by vehicles.*

P4. Peak friction exploiting driver aides, utilise friction at % wheel slips between approximately 10% and 20% (Bullas et al., 2020).

P5. Peak friction exploiting driver aides were made a legal requirement on all new production vehicles[26] in the EU in 2004[27] (European Parlament and Council, 2003).

P6. In 2019, $79.5^{+1.6}_{-0.0}$% of cars registered to operate on the UK road network were registered after 2004 (Department for Transport, 2019a).

c2. *So, at least 79.5% of cars operating on the UK road network in 2019 were equipped with peak friction exploiting driver aides, and would have demanded friction in the approximately 10% and 20% wheel slip range when conducting emergency manoeuvres.*

P7. In the UK, measurements of road surface friction are made primarily using SCRIMs, and, a proxy for high speed friction is used through texture depth measurements. (Highways England et al., 2020a).

P8. The SCRIM characterises friction at 17km/h operational velocity and 100% wheel slip.

---

[26]With the exception of motorcycles.
[27]At the time of writing peak friction exploiting driver aides are also a legal requirement in the UK.

P9. SCRIM and texture depth measurements can be used to predict the friction properties of non-porous road materials at all % wheel slips and operational velocities with an uncertainty of approximately 20% at a 95% confidence limit.

c3. So, in 2019, the combined use of SCRIM and texture measurements could infer the friction demanded of at least 79.5% of cars in emergency situations with an uncertanty of 20% at a 95% confidence limit on non-porous road surfaces only.

P10. Relationships between friction measurements made using the SCRIM, and accident incidence have eroded between 2005 and 2016 on all road types, except for roundabouts and bends (Figure 2.4 and Figure 2.5).

P11. Roundabouts and bends make up approximately 5.4% of the total length of the English trunk road network (Highways England, 2021).

c4. So, relationships between SCRIM measurements and accident incidence have not been demonstrated on 96.6% of the English trunk road network.

C1. Therefore, SCRIM measurements alone, or the combination of SCRIM and texture depth measurements, cannot be used to accurately infer the friction demanded by the majority of vehicles operating on the UK road network undertaking emergency manoeuvres, and are non-conducive to the detailed management vehicle safety.

P12. Crowd sourced in-vehicle sensor data can be used to identify areas on the UK road network where vehicles experienced near to ABS activation.

P13. The methodology used in Hammond et al. (2021) identified areas on the network not identified using SCRIM and texture measurements.

C2. Therefore, an appropriate alternative / addition to the current UK friction management policy can be generated based on crowd sourced in-vehicle data.

6.4   Supporting the premises

The majority of the premises presented in the summary argument are supported by historical works or publicly available data. This thesis has demonstrated the validity of premises 2, 3, 8, and 9[28]. This section discusses the work presented in the previous chapters and how it supports the premises.

P2. The friction demand placed on the UK road network by motorists is determined by, inter alia, the type of vehicle manoeuvre being attempted, and the severity of that manoeuvre.

P3. Based on the vehicle manoeuvre being carried out, and the severity of that manoeuvre, the areas of the friction profile used (the % wheel slip and operational velocity) will differ.

Friction profiles describing the relationship between % wheel slip, operational velocity, and friction, for any given surface were used throughout the work summarised in Chapter 4. The friction profiles generated, and the friction model derived from them, has shown that the friction generated between a vehicle tyre and a wetted road surface is dependent upon the operational velocity and the % wheel slip; a friction profile is three dimensional.

Even if only two dimensions of a friction profile are considered, it is clear that friction is related to operational velocity (for straight line manouveres this is the same as the vehicle speed). The use of peak friction exploiting driver aides, or certain driving techniques such as brake pumping[29], demonstrates that manoeuvre type and severity can affect the areas of the friction profile accessed by vehicles. Should it not, such devices would not work.

These premises demonstrate a need to understand in some detail the demand for friction placed on the road network, and likewise to understand the friction supplied by roads which correlate with friction demand. These premises also show that the friction demanded from, and supplied by road surfaces to vehicles is complex and highly context dependent. With this in mind, the following questions are key in the practical assessment and interpretation of friction:

- Which areas of the friction profile are used by vehicles, and under which conditions?

- Which areas of the friction profile can be directly measured at network level scales?

---

[28]The validity of premises 12 and 13 is demonstrated in the next chapter.
[29]Which exploits peak friction.

- Can the friction at the speed, slip friction intersections used by vehicles, but not captured by measurement, be estimated using measurements?

- What is the range of friction values on road surfaces at different speed, slip, friction intersections?

- What is the likely impact of this range on vehicle safety?

Whilst it is outside the scope of this thesis to answer the first, Chapter 4 of this thesis has answered the remaining questions:

- Routinely gathered road surface condition information can be used to predict the high speed, locked wheel friction properties of road surfaces to within approximately 12 units at 95% confidence,

- the friction model, designed to predict friction at all % wheel slip and operational velocity combinations has a lower predictive power than models predicting friction at discrete % wheel slip and operational velocities. Namely, 20 units at 95% confidence, and,

- the uncertainty observed in the friction model validation exercise (20 units at 95% confidence) demonstrates that inferring friction properties from the current standard friction and texture measurements is not practically applicable to highways engineering (see Figure 6.1).

P8. The SCRIM characterises friction at 17km/h operational velocity and 100% wheel slip.

Chapter 5 of this thesis has shown that in the vast majority of cases the SCRIM characterises friction at 100% wheel slip and 17km/h operational velocity. One of the observations made demonstrated that in some cases the SCRIM appears to characterise friction at a region closer to 50km/h operational velocity and 32.4% wheel slip. It is hypothesised (in PPR980 (Sanders, 2021)) that this is due to the SCRIM making measurements below the Critical Wheel Angle (CWA)[30].

A key assumption associated with the SCRIM is that it always makes measurements above the CWA. Should measurements be made below the CWA, or indeed there be a suspicion that some measurements are made below the CWA, then one can have little confidence that the SCRIM is characterising road surface friction in a way which is internally consistent. At the very

---

[30]The angle between the direction of travel and test wheel above which no relationship between increasing wheel angle and friction is observed.

least, measurements made by any tool should be internally consistent such that they can be directly compared[31]. Falsifying this hypothesis is therefore essential to have confidence in the measurements made using the SCRIM.

Within the EU[32], Anti-lock Braking Systems (ABS) have been mandatory on all new vehicles since 2004, and Electronic Stability Control (ESC) has been mandatory since 2015. Both of these systems are designed to ensure that the wheels of a vehicle utilise peak friction. Given that the SCRIM measures at 100% wheel slip, friction measurements made using SCRIMs do not correlate with the friction exploited by vehicles with peak friction exploiting driver aides in the majority of cases[33].

P9. SCRIM and texture measurements can be used to predict the friction properties of non-porous road materials at all % wheel slips and operational velocities with an uncertainty of approximately 20%.

Chapter 4 presents a new procedure for estimating the friction supplied by a road surface at all % wheel slips and operational velocities (the friction model). This work supplements that reported in TRL367 which carried out a similar exercise for all operational velocities but at 100% wheel slip only (the TRL367 model). Both models predict friction using the tools currently available for network level assessments in the UK and the data which these tools deliver, namely SC and SMTD.

An analysis of the predictive power of these models through an assessment of residual values has shown that with a 95% confidence limit, the friction model has an uncertainty of approximately 20 units and the TRL367 model an uncertainty of approximately 12 units.

This level of uncertainty makes detailed decisions based on these data and models inappropriate, as their predictive power are only conducive to a broad assessment of road surface friction. As a worked example let it be assumed that the friction properties of two surfaces wish to be inferred at an operational velocity of 50km/h and a % wheel slip of 18:

---

[31]As an example, imagine using a tape measure that sometimes has a scale of cm, sometimes inches, and sometimes decacubits, but you never know which. Clearly the measurements from such a device cannot be used in practical engineering.

[32]During 2004 and 2015 UK was an EU member state and so subject to the following legislation.

[33]In extreme conditions, such as on snow or ice, some peak friction exploiting driver aides do not work and so vehicles will have a higher tenancy to access 100% wheel slip.

- Surface one is a motorway and has an IL of 0.35CSC;

- surface two is an approach to a pedestrian crossing and has an IL of 0.55CSC; and

- both materials are non-porous asphalts with a texture depth of 0.95mm SMTD.

This scenario represents the greatest possible variability in friction requirements under the current friction management policy.

Figure 6.1 presents the estimated friction values as calculated using the friction model, the series markers present the average value and the error bars represent the uncertainty of the model. Here it can be seen that the error bars for each material overlaps the average value for the other by approximately 5 units. This clearly demonstrates, even with this generous example, the inappropriateness of using the current friction management policy to make the types of decisions that it is currently employed to make.
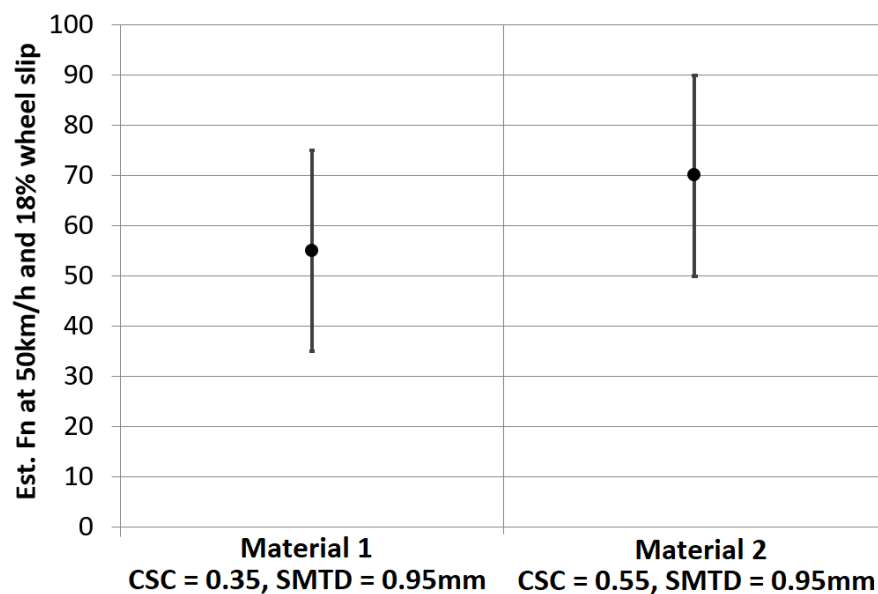
Figure 6.1: A comparison of predictions of friction at 50km/h and 18% wheel slip using the friction model for two materials. The error bars represent a 20 unit uncertainty at a 95% confidence limit.

6.5 Discussion and Conclusions

6.5.1 Overall conclusions

By providing evidence to support premises 2, 3, 8, and 9 of the argument, and because C1 of the argument logically follows from the minor conclusions, C1 is shown to be true. It should be noted that the work leading to this conclusion represents a substantial and sustained effort to use the current tools (the SCRIM and texture depth assessments) to manage road surface friction with a view to affecting vehicle safety. Given that this is the case, it should also be concluded that:

C3. Re-linking friction assessment with vehicle safety, will require a radical reform of the current friction management policy.

The use of SCRIM and texture depth measurements may however be useful in providing a "safety net" friction characterisation. For example it may be effective to set a single performance requirement for the whole network below which no area should fall. But in terms of managing the friction supplied by the network, with the goal of normalising the skidding risk across it, the use of SCRIM and texture depth measurements are inappropriate.

Given that the effective management of road friction is an essential part of vehicle safety, the conclusion of this thesis demonstrates a pressing and safety critical need to find a suitable alternative to the current skid resistance policy in the UK. The following chapter (Chapter 7) presents a potentially suitable alternative.

6.5.2 Additional discussion, conclusions and recommendations

Application of the findings to all network types

The main conclusion of this thesis was based on an assessment of a skid resistance characterisation tool and the friction demanded by vehicles. The findings of this thesis are therefore network independent and applicable to all network types. Local authority networks are often very different to national networks and vehicles operating on these networks can have a larger frictional demand than on national networks owing to the types and severity of manoeuvres carried out. It is therefore recommended that:

All road authorities are encouraged to review their friction management policies in line with the findings of this thesis.

Application of the findings to countries other than the UK

The findings of this work are directly applicable to the friction management policies based on the use of sideway-force devices and/or texture depth measurements. Road owners who use such policies should consider how the results of this work apply to their networks, and reflect on if they need updating. Section 2.3.1 lists some countries whose friction management policies utilise sideway-force devices but to the authors knowledge, the use of such devices is more widespread.

The following chapter provides an alternative that would benefit from an international collaborative approach, it is therefore recommended that:

> *Road authorities utilising sideway-force friction characterisation devices and / or texture depth, should review their friction management policies to critically analyse their effectiveness in terms of maintaining vehicle safety, and make amendments as necessary.*

> *Road authorities, vehicle manufacturers, data suppliers, and governments, are encouraged to work together to facilitate the widespread adoption of crowd sourced vehicle data for the purpose of roadway management.*

Application of findings to other fields

The work presented in this thesis focused specifically on the relationship between friction and vehicle safety on roadways. The characterisation of friction as considered here is however important in other areas, for example, aviation (airport runways and taxiways), pedestrian areas (such as footways or transport hubs), cycleways, car parks, sporting facilities (athletic tracks, velodromes, and fields of play), and motorsport (racetracks).

The principles of the works presented in this thesis (the consideration of the areas on a friction profile demanded by the user, and that assessed by the characterisation method), could likewise be applied to these other industries to identify where improvements to the friction management techniques used in those industries could be made. It is therefore recommended that:

> *Leaders in industries which rely on the characterisation of friction, should consider the principles of this thesis and how they can be applied to their industries.*

The use of alternative friction characterisation devices

Do et al. (2008) list 25 devices that were available in 2008 for the characterisation of roadway friction. Whilst this thesis has focused on the measurements made by the SCRIM, it has only

done so because this is the standard device used in the UK. The tenants of this thesis are equally applicable to the assessment of the other 24 devices mentioned by Do et al. (2008) as well as any other devices as and when they become available.

Road surface friction measurements are not intrinsically valuable or useful, they only become useful when they can be used to predict and manage vehicle safety. This in turn requires friction to be measured, or inferred, at the areas on the friction profile used by vehicles. To this end, the measurement characteristics of friction devices should be considered within the context of their friction characterisation properties (where on the profile do they measure friction) and where vehicles are likely to operate. Likewise, it should be considered if the measurements made by any given device can be combined with other data sources to reasonably infer friction on the areas of the friction profile exploited by vehicles. This leads to the following additional conclusions:

C4. Further research into the friction demanded by vehicles under various scenarios is essential for the effective adoption, or development, of friction characterisation equipment.

C5. When selecting friction assessment equipment for use, it is critical to understand where such equipment makes measurements on the friction profile.

The prediction of pavement friction

Owing to the constraints of measuring friction directly, multiple attempts have been made to predict the frictional behaviour of road surfaces. Such attempts can be broadly sorted into two categories: the inference of friction from other pavement properties, and the correlation of friction measurements made by different devices to a common scale. The work presented in this thesis is directly applicable to both of these categories.

Chapter 3 of this thesis has demonstrated the limitations associated with predicting friction based on the geometric properties of road surface materials. This work also included an analysis of the pressure distribution between the tyre and the surface, crucially, the addition of this parameter did not improve the ability of models to predict friction. This finding is applicable to research works carried out into tyre/road enveloping.

Enveloping is the study of how tyres envelop the texture of road surfaces to produce, inter alia, friction, rolling resistance, and noise. Chapter 3 presented a basic enveloping analysis under static conditions. More modern approaches could add value to the prediction of road surface friction, but

it should be anticipated that to accurately predict the friction generated between a tyre and road, many more variables should be taken into account than those discussed thus far.

Attempts have been made to correlate the measurements made by different friction devices with one another, and to a common scale, the key projects to have made these attempts are:

- Harmonisation of European Routine and research Measuring Equipment for Skid resistance (HERMES) (Descornet et al., 2006);

- TYre and ROad SurfAce optimisation for skid resistance and Further Effects (TYROSAFE) (Scharnigg et al., 2010); and

- ROlling resistance, Skid resistance, ANd Noise Emission measurement standards for road surfaces (ROSANNE) (Green & Kokot, 2017).

These works made substantial progress in understanding the relationships between measurements made with different friction test devices, but, a universal and ubiquitous relationship was not identified as part of those works.

As with the characterisation of friction from pavement properties, it is clear that the harmonisation of friction measurements cannot be carried out using only the properties of measurement devices and the measurements that they provide. Instead, other information is required such as pavement texture depth, pavement microtexture[34], or surface permeability. In this way, a multivariate analysis would progress this research stream further.

Moreover, it is probable that factors outside of the current understanding influence friction generation and identifying such factors could be achieved using advanced statistical methodologies. This leads to the following additional conclusion:

C6. The application of a multivariate approach to the prediction of friction between a tyre and road surface, or the transposition of friction measurements to a common scale, should be carried out. This should include the use of advanced statistical methods such as artificial intelligence or machine learning to identify influencing factors not currently understood.

---

[34]The texture of the surface on the micron scale.

Chapter 7   The way forward

7.1   Foreword

The direct measurement of pavement friction using a single device typically limits one to making an assessment of friction at a single location on the friction profile[35]. In designing or selecting a device for the assessment of pavement friction it is important that the device characterises friction at locations on the friction profile used by vehicles.

The complication is that vehicles access different areas on the friction profile depending on the manoeuvre being carried out and the severity of that manoeuvre. Furthermore, the development of different vehicle technologies has the potential to change the areas on the friction profile accessed. This paints the picture of friction demand being highly dynamic, and it should therefore be sought to manage the friction available to motorists in a similarly dynamic way.

The effective management of road surface friction requires the consideration of the following factors.

Material specifications are based on their physical and chemical properties, a link between the properties of road surfaces and friction supply is therefore required.

Road owners need accurate and up to date information. For physical parameters, such information can only be obtained through the scientific method.

Science

Materials

Policy

Policy specifies the friction performance required of the network, to inform the specification of materials, and, to determine an appropriate friction measurement and interpretation protocol.

Figure 7.1: Factors to be considered when designing a friction management policy

---

[35]Some devices are capable of making measurements over multiple locations on the friction profile and these devices come with drawbacks, typically they make discrete rather than continuous measurements, or require multiple measurements to be made on a single surface.

As already stated in this thesis, the current friction management policy is in need of radical change. There are multiple ways to develop an appropriate friction management policy, one of which is presented in this chapter:

1. Crowd source in-vehicle sensor data from vehicles operating on the road network (science / policy (Figure 7.1));

2. interpret these data to identify areas where vehicles are experiencing deficiencies in friction (science (Figure 7.1));

3. measure the friction at such areas using equipment capable of producing a friction profile (such as the PFT) (science / policy (Figure 7.1));

4. determine the physical properties of the road surface which correlate with the friction parameters used by vehicles (science / materials (Figure 7.1)); and

5. compare measurements of friction with standards similar to those currently used (policy / materials (Figure 7.1)).

A proof of concept study into the first two points has been completed by Hammond et al. (2021) in their work PPR988. This showed that the methodology used can identify areas on the network where the friction demand of motorists is greater than the friction supplied by the road surface which would not have been identified using the current UK friction management policy.

7.2   Crowd sourcing in-vehicle data

Modern vehicles are fitted with a vast array of sensors. Figure 7.2 provides some examples of sensor applications on modern vehicles.
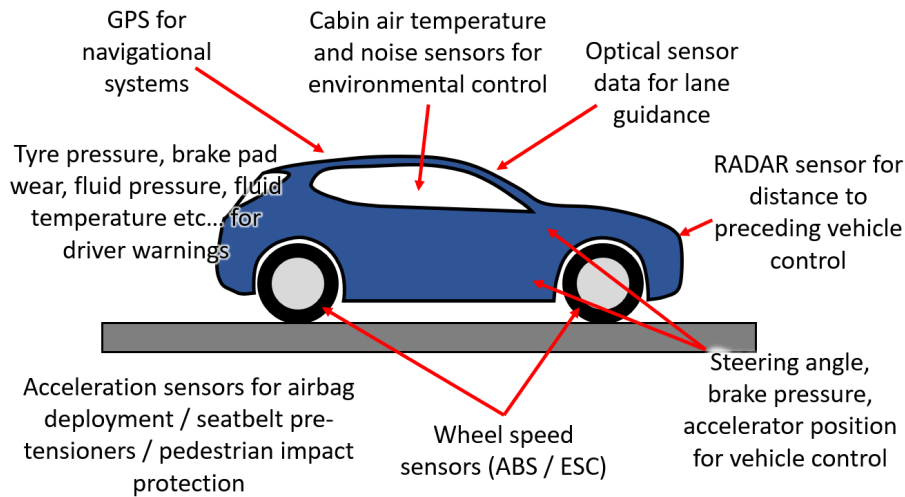
Figure 7.2: Examples of vehicle sensor use on modern automobiles.

Approximately 58,240vehicle/km/day are driven on the UK trunk road network (Department for Transport, 2020b), and the UK trunk road network is approximately 6,880km in length (Highways England, 2021). Using a conservative estimate for the proportion of vehicles operating on the network with sensors arrays similar to those described in Figure 7.2 of 33%, it can be estimated that the length of the UK trunk road network would be traversed by such vehicles approximately 1,000 times per year[36]. This represents a data set three orders of magnitude larger than that collected currently as surveys of the UK trunk road network are carried out once annually.

Data collection using vehicle sensor data poses a number of challenges, not least surrounding access to data. Currently, data collected by the Original Equipment Manufacturers (OEMs) typically comprise post Controller Area Network-bus (CAN-bus) data and as such are heavily processed. Obtaining raw sensor data (as was used by Hammond et al. (2021)) will require additional digital infrastructure to collect and transmit raw sensor data. Additional considerations are that of:

- data infrastructure, the volume of data is likely to be very large and may require additional data infrastructure development / implementation;

- data handling, management, processing and quality assurance procedures will require development;

- data security, such data could be considered personal data, requiring compliance with legislation such as the General Data Protection Regulation (GDPR); and

---

36 $\frac{58,240 \cdot 365 \cdot 0.33}{6,880} = 1,020$

- data property, whilst OEMs currently collect some data relating to vehicle use, it is unclear as to who owns these data.

The first of the considerations listed above is somewhat moot. Organisations such as vehicle OEMs and internet based services (navigation, search engines, social and other networks), are already collecting, processing, and using data in the magnitudes which would be required to implement the crowd sourcing of vehicle data.

The second and third points are largely associated with the legislation around data handling and ownership. There is an emerging trend for organisations to work together to facilitate the more widespread use of vehicle data. An example of this is the European Data Task Force (European Data Task Force, 2020), a public-private partnership with the aim of furthering the exchange of vehicle data in the field of safety related traffic information. At the time of writing the following organisations are partners in the European Data Task Force:

- Bundesministerium für Verkehr und digitale Infrastruktur in Germany;

- Ministry of Infrastructure and Water Management in the Netherlands;

- The Government of the Grand Duchy of Luxembourg in Luxembourg;

- Dirección General de Tráfico in Spain;

- TRAFICOM in Finland;

- National Highways in England; and

- Liikenne- ja Viestintäministeriö in Finland.

7.3   The interpretation of in-vehicle data

Hammond et al. (2021) have shown that the use of vehicle sensor data can identify areas of the road network where the friction required by vehicles is either not being met, or is very close to not being met. Hammond et al. (2021) were provided vehicle sensor data from a third party; Synaptiv. These data were collected over an 18 month period from approximately 30 vehicles and contained 220 skidding events. Hammond et al. (2021) defined a skidding event as areas on the road network where the ABS system was in a "nearly activated state" referred to as pre-ABS activation. Such events were determined based on an propriety algorithm developed by Synaptiv that could predict the activation of ABS events to an accuracy of 97%.

Based on these data Hammond et al. (2021) identified areas on the English road network (data from the trunk road and local authority networks were included) where clusters of pre-ABS activations were observed. When areas showing clustering were investigated using the current friction management policy, they were found to not require further investigation. This shows that the current friction policy was not able to identify these areas of interest, whereas the analysis carried out by Hammond et al. (2021) was.

7.4 The measurement of friction in targeted locations

It has been shown in the previous chapters that friction is a three dimensional parameter, and in order to fully characterise a road surface, friction should be measured at multiple % wheel slips and operational velocities. At the time of writing, there are three devices capable of measuring friction in a way in which a full friction profile can be generated, The PFT, ADHERA 2[37], and the SRT-3[38]. All of these devices are longitudinal variable slip, trailer based systems and as such there are safety concerns regarding their use on bends.

If however, the relationship between vehicle manoeuvres and friction use is well understood, and the prevalence of vehicle manoeuvres in different locations on the network are understood, then specific areas (measurements at a single % wheel slip and operational velocity) on the friction profile could be targeted for direct measurement, or new models developed to predict friction at those % wheel slips and operational velocities. Fulfilling the criteria for making measurements at a single % wheel slip and operational velocity[39] would require a substantial effort on the part of researchers in the fields of vehicle dynamics, and road surface friction, and a similar commitment from the relevant funding authorities.

An example of the type of exercise to be carried out is presented in Figure 7.3 which shows a friction profile which has been annotated with a hypothetical braking event using ABS (the black line). It should be noted that the braking event is not based on real world data and is presented only as an example. The position of the line on the graph shows the areas on the friction profile used, and the spacing of the broken lines represent the length of time during which each area on the friction profile is accessed. A dotted line represents time passing more quickly, and a solid line represents time passing more slowly.

---

[37]A two wheeled friction tester used for research purposes in France.
[38]A single wheel trailer used in Poland.
[39]Understanding the relationship between friction and vehicle manoeuvres, and the prevalence of manoeuvres across the road network.
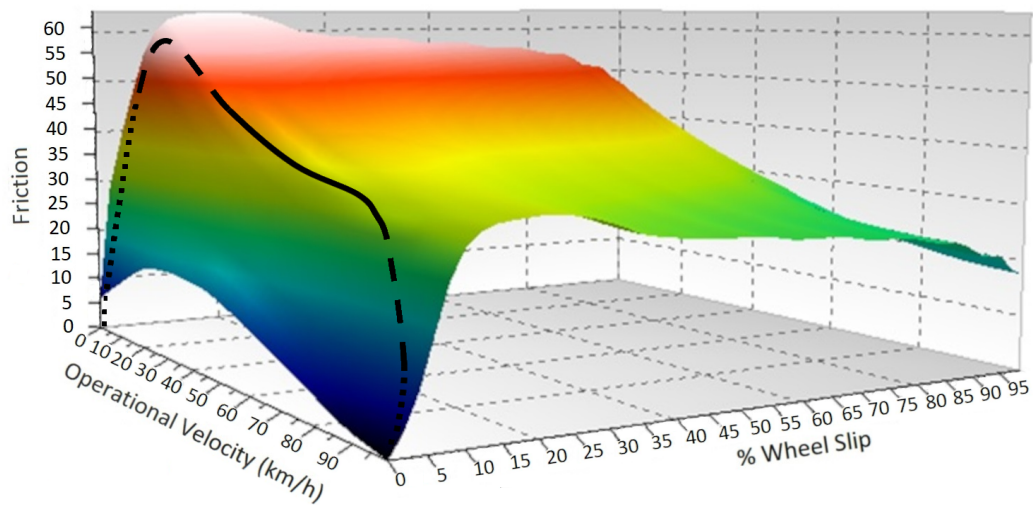
Figure 7.3: A friction profile annotated with a hypothetical straight line emergency braking event using ABS. The type of line represents the passage of time, a dotted line represents time passing quickly, a solid line represents time passing slowly.

With appropriate research, an accurate model of a straight line braking manoeuvre can be developed, as well as similar models for other manoeuvres e.g. cornering, traversing a slope, lane changing etc.

One of the key limitations of the proposed methodology is ensuring that 100% of the network is assessed. This of course cannot be guaranteed using crowd sourced data. With this in mind, it is proposed that measurements continue to be made with the SCRIM as a "safety net" to ensure that the whole of the network is assessed, and that a single friction criterion be set based on SCRIM measurements below which none of the network should fall.

7.5 Determining the correlation between physical properties and friction

The determination of the correlation between the physical properties of road surfacing materials and various friction measurements is an area of research that has been active since the development of the first friction measurement methods. Chapter 3 has presented works on the correlation between texture depth, pavement permeability, and friction measured using the PFT at 100% wheel slip and 100km/h. Given the established nature of this work, it should be clear to see how research in this area could be expanded to generate similar correlations for other friction parameters.

7.6 Comparing measurements to appropriate standards

In summary[40], the current UK friction management methodology requires the demonstration of frictional performance at three stages:

- before acceptance for use on the network through a type approval process[41];

- at application on site by defining either the friction of the material as measured directly, or inferred from texture depth measurements; and

- during use using the procedures outlined in Chapter 1.

Assessing road surfacing products in this way ensures that performance standards are met throughout the life of a material, but prompts the following questions: what are acceptable performance criteria? And how do these criteria relate to vehicle safety?

Taking the approach to the assessment of pavement friction outlined in this chapter will allow the development of performance standards that will always be linked to vehicle safety.

---

[40]Actual procedures differ based on material type but the overall procedures for all road surfacing procedures are similar.
[41]Such assessments are typically carried out through the British Board of Agrément (BBA) Highways Agency Pavement Assessment Scheme (HAPAS).

7.7   Benefits of the proposed friction management methodology

Whilst requiring considerable effort, the friction management policy proposed in this chapter would yield substantial benefits for all stakeholders.

The most direct benefit will be to improve vehicle safety, the major beneficiaries being road users (and their families), vehicle OEMs, and road owners. Because the standards used to implement this policy are based on criteria which are directly related to vehicle safety, it follows that the "correlation problem[42]" would be solved. Solving the correlation problem allows the friction on the road network to be managed dynamically in line with changes to the vehicle fleet, driving behaviour, road layout and design etc... rather than having to react to these phenomena.

Solving the correlation problem also allows confidence in new road materials and treatment options to be gained at development or design stage, rather than at the implementation stages. This is owing to the link between material properties and vehicle safety offered by the proposed methodology. For example, once sufficient models exist it would be possible to predict that change in material property x has effect y on vehicle safety. This could therefore lead to the fine tuning of materials for specific applications which would be of particular benefit to material producers and highways engineers who would be able to "custom fit" a material to a particular situation.

A follow on from the previous point is one of environmental benefit. With an increased confidence in changes to material properties and their effect on vehicle safety, it would be possible to provide engineers with the information needed to produce more sustainable materials. The example of the use of calcined bauxite in High Friction Surfacings (HFS) is particularly pertinent. Calcined bauxite is a non-native material to the UK requiring import from Asia or Africa at substantial environmental (and economic) cost. Being able to use such materials only in locations where there is no other alternative, i.e. in those locations where the demand for friction exceeds all other material possibilities, would have an intrinsic environmental benefit. A similar argument could be made regarding the use of high Polished Stone Value (PSV) materials native to the UK for which there is limited supply.

A final benefit is in the field of vehicle engineering. Because the proposed policy is based on the assessment of actual vehicle data, it is possible to envision a scenario in which the vehicle becomes not only a source of data, but also, a user of it. With suitable communications infrastructure it

---

[42]That friction measurements made with the SCRIM no longer correlate with vehicle safety for the majority of site categories.

would be possible for vehicles to transmit live sensor data to a database to enable the experience of vehicles to be assessed in real time in order to generate a heat map of the road network highlighting locations where friction could be a potential issue[43]. With access to this heat map vehicles could take appropriate actions to improve driver safety, for example, CAVs could adjust headway, stopping distances, or cornering speeds appropriately and/or warnings could be provided to motorists regarding low friction conditions.

It should be noted that such an approach can be applied to other characteristics such as; ride quality, surface defects, noise, and geometry.

A live database of vehicle safety and friction conditions would also have benefits to road management authorities, for example these data could be used to plan and prioritise winter maintenance activities, or amend traffic conditions on smart motorways (imposing temporary speed restrictions or lane reductions/additions). In extreme cases such data could also be used in the management of emergency responses to accidents, or in the early identification of serious incidents.

---

[43]This is analogous to navigation systems that can provide motorists with real time information regarding traffic flow or road closures whereby sections of the network with poor traffic flow are displayed.

Chapter 8   Recommendations for future work

8.1   Foreword

This chapter presents recommendations for future works based on the conclusions of this thesis and the discussion presented in Chapter 7.

8.2   Further develop the crowd-sourcing method

This section addresses Conclusions 1, 2, and 3, and builds on the work of Hammond et al. (2021) and the discussion of the way forward presented in Chapter 7.

The crowd-sourcing vehicle data methodology shows promise as an addition to, or replacement of, the current UK friction management policy. It is recommended that this methodology is developed into a procedure that could be applied to the whole of the UK network through the following research activities are recommended:

- **Understand the volume of data required to produce robust results** by assessing the quality and network coverage of crowd-sourced vehicle data to allow inferences to be made regarding the quantity of data required for network level application.

- **Investigate routes to obtaining crowd-sourced vehicle data** by approaching data providers, vehicle OEMs, or organisations like the European Data Task Force to understand the quantity, quality, and cost of the data that they can provide.

- **Perform a network level investigation using crowd-sourced vehicle data** to identify areas on the network that are potentially friction deficient and compare the results with the current friction management policy to demonstrate the differences between the new approach and the existing one.

8.3   Investigate the link between vehicle manoeuvres and friction demand

This section addresses Conclusions 4 and 5, and the discussion presented in Section 7.4 relating to the assessment of friction in targeted locations.

Understanding the link between vehicle manoeuvres and friction demand is key in assessing

the applicability of friction characterisation methodologies in determining the friction supplied by road surfaces in the regions of the friction profile where friction demand is most prevalent and would allow the targeted deployment of alternative friction measurement methodologies in specific locations. The following research activities are recommended:

- **Understand the locations on the friction profile accessed during vehicle manoeuvres** by carrying out experiments with vehicles modified with appropriate sensing equipment and conducting various manoeuvres on different surface types.

- **Analyse the prevalence of manoeuvrers at different locations on the network** by carrying out studies to understand the prevalence of vehicle manoeuvres at different locations on the network (site categories).

- **Use the results of the above activities to support friction policy** by inferring the locations on the friction profile accessed by vehicles on different areas of the network. This information should be used to select existing, or design new, friction measurement devices which operate at those locations on the friction profile.

8.4   Understand the relationship between vehicle data and material properties

This section addresses Conclusion 6 and the discussion presented in Section 7.5 relating to the connection between friction and road surface properties.

The management of road surface friction is carried out by manipulating the physical properties of road surfaces that affect the friction generated between road surfaces and vehicle tyres. A challenge associated with the crowd-sourced vehicle data method is that changes to the vehicle fleet could produce results that may not will always correlate in the same way with the physical properties of pavements. To this end the following research activities are recommended:

- **Understand the relationship between crowd-sourced vehicle data, friction, and material properties** by carrying out friction and material property measurements on areas of the network demonstrating differences in performance, and modelling their relationship with crowd-sourced vehicle data. This research should be repeated periodically to identify instances in which these relationships change, and in such cases what the new correlative factors are.

- **Carry out a multi-variate analysis of material and vehicle properties** thorough the development of a statistical model using advanced data science techniques to develop a new friction prediction model.

8.5   Update the UK friction management policy

This section addresses the discussion presented in Section 7.6 relating to the comparison of friction measurements with appropriate standards.

The ultimate purpose of the works outlined in this Chapter is to inform the amendment of friction management policy. The UK friction management policy is described in standards relating to:

- **Material specifications for new pavements** specified through the MCHW, namely the 900 series (Department for Transport, 2019b) and 1000 series (Department for Transport, 2020a). These documents should be updated in line with the results of the activities described in Section 8.4.

- **Material assessment and in service performance** described in National Highways documents CS228 (Highways England, Transport Scotland, Welsh Government, Department for Infrastructure, 2020a) and CS230 (Highways England, Transport Scotland, Welsh Government, Department for Infrastructure, 2020c). These documents should be updated in line with the results of the activities described in Sections 8.3 and 8.2.

- **Measurement equipment**, which are managed by various national and international standards organisations; BSi, CEN, DIN, ASTM, etc.... Should new friction measurement equipment be developed through the activities detailed in Section 8.3 appropriate equipment standards should be produced.

References

Ally, A. A., Zeidan, E. S., Hamed, A. & Salem, F. (2011), 'An antilock-braking systems (abs) control: A technical review', *Intelligent Control and Automation* **2**(3), 186–195.

ASTM International (2008), *Standard specification for standard smooth tire for pavement skid resistance tests*, E524-08, ASTM International, USA.

ASTM International (2011), *Standard test method for skid resistance of paved surfaces using a full-scale tire*, E274/E274M-11, ASTM International, USA.

ASTM International (2015a), *Standard test method for measuring pavement macrotexture depth using a volumetric technique*, E965-15, ASTM International, USA.

ASTM International (2015b), *Standard Test Method for Skid Resistance of Paved surfaces Using a full-Scale Tire*, E1845-15, ASTM International, USA.

Bird, G. & Miller, R. A. (1937), *Studies in road friction II: An analysis of the factors affecting measurement*, Transport and Road Research Laboratory, London.

Bird, G. & Scott, W. J. O. (1936), *Studies in road friction I: Road surface resistance to skidding*, Transport and Road Research Laboratory, London.

Birkner, C., Adesiyun, A., Greene, M., Conter, M., Schmidt, B., Sandberg, U. & Scharnigg, K. (2016), *ROSANNE Final summary report 2016*, ROlling resistance, Skid resistance, ANd Noise Emission measurement standards for road surfaces (ROSANNE project), Available at: https://rosanne-project.eu/.

Bradley, J. & Allen, R. F. (1930), Factors affecting the behaviour of rubber-tyred wheels on road surfaces, *in* 'Proceedings of the Institution of Automobile Engineers', Volume 25, Issue 1, Institution of Automobile Engineers, Available at: https://journals.sagepub.com, pp. 62–92.

Britannica (2021), 'Coefficient of friction', https://www.britannica.com/science/static-friction. Accessed: 17/05/2021.

British Standards Institution (2000), *Surface friction of pavements: Part 2: Test method for measurement of surface skid resistance using the GripTester braked wheel fixed slip device*, BS 7941-2:2000, British Standards Institution, London.

British Standards Institution (2004), *Characterisation of pavement by use of surface profiles: Part 1 - Determination of Mean Profile Depth*, BS EN ISO 13473-1:2004, British Standards Institution, London.

British Standards Institution (2006), *Methods for measuring the skid resistance of pavement surfaces: Part 1: Sideways-force coefficient routine investigation machine*, BS 7941-1:2006, British Standards Institution, London.

British Standards Institution (2009a), *Geometrical product specification (GPS) - Surface texture: Profile method - Terms, definitions and surface*, BS EN ISO 4287:1998+A1:2009, British Standards Institution, London.

British Standards Institution (2009b), *Procedure for determining the skid resistance of a pavement surface by measurement of the sideway force coefficient (SFCS): SCRIM*, DD CEN/TS 15901-6:2009, British Standards Institution, London.

British Standards Institution (2010), *Road and airfield surface characteristics - Test methods: Part 1: Measurement of pavement surface macrotexture depth using a volumetric patch technique*, BS EN 13036-1:2010, British Standards Institution, London.

British Standards Institution (2012), *Bituminous mixtures - Test methods for hot mix asphalt: Part 19: Permeability of specimen*, BS EN 12697-19:2012, British Standards Institution, London.

Brittain, S. (2014), *PPR702 Comparision of SCRIM and SKM sideways-force skid resistance devices*, TRL, Wokingham.

Brittain, S. & Viner, H. E. (2017), *PPR818 Development of a high speed friction performance criteriion for asphalt materials*, TRL, Wokingham.

Bullas, J., Andriejauskas, T., Sanders, P. D. & Greene, M. J. (2020), *PPR962 The relationship between connected and autonomous vehicles, and skidding resistance - A literature review*, TRL, Wokingham.

Cerezo, V., Rado, Z. & Kane, M. (2018), *Comparison of european and american methods for harmonizing friction measurements: Results of 1st european pavement friction workshop*, 8th Symposium on Pavement Surface Characteristics: SURF 2018, Brisbane.

Cerezo, V., Viner, H., Greene, M., Schmidt, B. & Scharnigg, K. (2015), *Analysis of data from the first round of tests and initial development of the common scale*, ROlling resistance, Skid resistance, ANd Noise Emission measurement standards for road surfaces (ROSANNE project), Available at: https://rosanne-project.eu/.

Department for Transport (2009), *Technical requirements for SCANNER survey parameters and accreditation*, , SCANNER surveys for local roads, Volume 5,.

Department for Transport (2012), *Revision of SHW Clause 903, Clause 921 and Clause 942*, Interim Advice Note 154/12, Department for Transport, London.

Department for Transport (2019a), 'Licensed cars 2019', https://www.gov.uk/government/statistical-data-sets/veh02-licensed-cars. Accessed: 12/11/2020.

Department for Transport (2019b), *Road Pavements - Bituminous Bound Materials, Manual of Contract documents for Highway Works, Volume 1, Series 900*, Department for Transport, Department for Transport, London.

Department for Transport (2020a), *Road Pavements - Concrete Materials, Manual of Contract documents for Highway Works, Volume 1, Series 1000*, Department for Transport, Department for Transport, London.

Department for Transport (2020b), *Road traffic estimates: Great Britain 2019*, Department for Transport, Department for Transport, London.

Descornet, G. (1998), *Proposal for a European standard in relation with the skid resistance of road surfacings*, Belgian Road Research Centre, Belgian Road Research Centre, Brussels.

Descornet, G., Schmidt, B., Boulet, M., Gothie, M., Do, M. T., Fafie, J., Alonso, M., Roe, P., Forest, R. & Viner, H. (2006), *Harmonisation of European Routine and Research Measuring Equipment for Skid Resistance*, Forum of European National Highway Research Laboratories.

DigitalSurf (2014), 'Mountainsmap universal', Software.

Do, M. T., Roe, P., Vos, E. & Groenendijk, J. (2008), *Report on state-of-the-art of test methods*, TYre and Road surface Optimisation for Skid resistance And Further Effects (TYROSAFE Project), Available at: http://tyrosafe.fehrl.org/.

Dunford, A. (2009), *PPR497 GripTester trial - October 2009 - including SCRIM comparison*, TRL, Wokingham.

Eriksson, O. & Lundberg, T. (2016), *Variation of road surface texture and other geometric properties in transverse direction*, ROlling resistance, Skid resistance, ANd Noise Emission measurement standards for road surfaces (ROSANNE project), Available at: https://rosanne-project.eu/.

European Data Task Force (2020), *Data Task Force Final report and recommendations*, European Data Task Force, Available at: https://www.dataforroadsafety.eu.

European Parlament and Council (2003), *Directive 2003/102/EC of the European Parliament and of the Council*, 2003/102/EC, European Parlament and Council.

Flintsch, G W and McGhee, K K and de León Izeppi, E and Najafi, S (2012), *The little Book of Tire Pavement Friction*, Pavement Surface Properties Consortium.

GCSE Bitesize (2021), 'Friction', https://www.bbc.co.uk/bitesize/guides/zyydmp3/revision/3. Accessed: 02/09/2021.

Giles, C. G. (1957), 'The skidding resistance of roads and the requirements of modern traffic', *The crushed stone journal* **32**(2), 8–11.

Gothie, M., Parry, T. & Roe, P. (2001), *The relative influence of the parameters affecting road surface friction*, 2nd International colloquium on vehicle tyre road interaction, Florence, Italy.

Gottaut, C. & Goubert, L. (2016), *Texture-based descriptors for road surface properties and how they can be used in the appropriate standards*, ROlling resistance, Skid resistance, ANd Noise Emission measurement standards for road surfaces (ROSANNE project), Available at: https://rosanne-project.eu/.

Goubert, L., Do, M. T., Bergiers, A., Karlsson, R., Sandberg, U. & Maeck, J. (2014), *State-of-the-art concerning texture influence on skid resistance, noise emission and rolling resistance*, ROlling resistance, Skid resistance, ANd Noise Emission measurement standards for road surfaces (ROSANNE project), Available at: https://rosanne-project.eu/.

Greene, M. & Kokot, D. (2017), *Draft prEN for harmonised skid resistance measurement for proposal to CEN TC 227/WG5*, ROlling resistance, Skid resistance, ANd Noise Emission measurement standards for road surfaces (ROSANNE project), Available at: https://rosanne-project.eu/.

Greene, M., Viner, H., Cerezo, V., Brittain, S., Kokot, D., Scharnigg, K. & Schmidt, B. (2016), *Analysis of data from the second round of tests and further development of the common scale*, ROlling resistance, Skid resistance, ANd Noise Emission measurement standards for road surfaces (ROSANNE project), Available at: https://rosanne-project.eu/.

Greene, M., Viner, H., Cerezo, V., Kokot, D., Schmidt, B., Do, M. T., Scharnigg, K. & Spielhofer, R. (2014), *Definition of boundaries and requirements for the common scale for harmonisation of skid resistance measurements*, ROlling resistance, Skid resistance, ANd Noise Emission measurement standards for road surfaces (ROSANNE project), Available at: https://rosanne-project.eu/.

Grime, G. (1953), *RN_2029_GG The interpretation of measurements made with the road research laboratory's motorcycle skidding machine*, Road Research Laboratory, Wokingham.

Haider, M. & Conter, M. (2010), *TYROSAFE Project final report*, TYre and Road surface Optimisation for Skid resistance And Further Effects (TYROSAFE Project), Available at: http://tyrosafe.fehrl.org/.

Hall, J. W., Smith, K. L., Tirus-Glover, L., Wambold, J. C., Yager, T. J. & Rado, Z. (2009), *NCHRP Guide for Pavement Friction*, National Cooperative Highway Research Program.

Hammond, J., Bell, M., Wallbank, C. & Sanders, P. D. (2021), *PPR988 The relationship between vehicle data, collision risk and skid resistance*, TRL, Wokingham.

Hart, P. (2003), *ABS Braking Requirements*, Hartwood Consulting Pty Ltd, Victoria.

Henry, J. J. (1983), *Comparison of Friction Performance of a Passenger Tire and the ASTM Standard Test Tires*, American Society for Testing and Materials, Philadelphia, USA.

Henry, J. J. (2000), *Evaluation of pavement friction characteristics - A synthesis of Highway Practice*, Transportation Research Board and National Research Council, Washington DC, USA.

Highways England (2021), 'Highways Agency Pavement Management System (HAPMS)', Database. Accessed: January 2021.

Highways England, Transport Scotland, Welsh Government, Department for Infrastructure (2020a), *Skidding Resistance*, CS 228, Design Manual for Roads and Bridges.

Highways England, Transport Scotland, Welsh Government, Department for Infrastructure (2020b), *Data for pavement assessment*, CS 229, Design Manual for Roads and Bridges.

Highways England, Transport Scotland, Welsh Government, Department for Infrastructure (2020c), *Pavement maintenance assessment procedure*, CS 230, Design Manual for Roads and Bridges.

Highways England, Transport Scotland, Welsh Government, The Department for Regional Development Northern Ireland (2015), *Skidding Resistance*, HD 28/15, Design Manual for Roads and Bridges, Volume 7, Section 3, Part 1.

Hosking, J. R. (1986), *RR76 Relationship between skidding resistance and accident frequency: Estimates based on seasonal variation*, Transport and Road Research Laboratory, Wokingham.

Hosking, J. R. & Woodford, G. C. (1976*a*), *LR738 Measurement of skidding resistance: Part II. Factors affecting the slipperiness of a road*, Transport and Road Research Laboratory, Wokingham.

Hosking, J. R. & Woodford, G. C. (1976*b*), *LR739 Measurement of skidding resistance: Part III. Factors affecting SCRIM measurements*, Transport and Road Research Laboratory, Wokingham.

Kane, M., Scharnigg, K., Conter, M., Roe, P. & Schwalbe, G. (2009), *Report on different parameters influencing skid resistance, rolling resistance and noise emissions*, TYre and Road surface Optimisation for Skid resistance And Further Effects (TYROSAFE Project), Available at: http://tyrosafe.fehrl.org/.

Koskinen, S. & Peussa, P. (2004), *FRICTION - Final Report (FP6-IST-2004-4-027006)*, Information Society Technologies Programme.

Kummer, H. W. (1966), *Unified theory of rubber and tire friction*, Pennsylvania State University College of Engineering, Pennsylvania, USA.

Leu, M. C. & Henry, J. J. (1978), *Unified theory of rubber and tire friction*, Transportation Research Board, Washington DC, USA.

Matsuzaki, R., Kamai, K. & Seki, R. (2015), *Intelligent tires for identifying coefficient of friction of tire/road contact surfaces using three-axis accelerometer*, Tokyo University of Science, Tokyo, Japan.

Microsoft (2017), 'Excel', Software.

Moore, D. F. (1975), *The friction of pneumatic tyres*, Elsevier, Amsterdam, Netherlands.

Nordström, O. & Åström, H. (2001), *Upgrading of VTI friction test vehicle BV12 for combined braking and steering tests under aquaplaning and winter conditions*, 2nd International Coloquium on Vehicle Tyre Road Interaction, Florence, Italy.

Ordnance Survey (2011), 'Ordnance survey open data', www.ordnancesurvey.co.uk/oswebsite/opendata/. Accessed: 2011.

Pacejka, H. B. (2006), *Tire and Vehicle Dynamics: Second Edition*, Society of Automotive Engineers.

Parry, A. R. & Viner, H. E. (2005), *TRL622 Accidents and the skidding resistance standard for strategic roads in England*, TRL, Wokingham, England.

Roe, P. G. & Caudwell, L. (2008), *Skid resistance policy in the UK - Where did it come from and where is it going?*, TRL, Wokingham, England.

Roe, P. G. & Dunford, A. (2012), *PPR564 The skid resistance behaviour of thin surface course systems: HA/MPA/RBA Collaborative Programme 2008-11: Topic 1 Final Report*, TRL, Wokingham, England.

Roe, P. G., Dunford, A. & Crabb, G. (2008), *PPR324 HA/QPA/RBA Collaborative Programme 2004/07: Surface requirements for asphalt roads*, TRL, Wokingham, England.

Roe, P. G., Parry, A. R. & Viner, H. E. (1998), *TRL367 High and low speed skidding resistance: The influence of texture depth*, TRL, Wokingham, England.

Roe, P. G. & Sinhal, R. (1998), *TRL322 The Polished Stone Value of aggregates and in-service skidding resistance*, TRL, Wokingham, England.

Roe, P. G., Webster, D. C. & West, G. (1991), *RR296 The relation between the surface texture of roads and accidents*, Transport and Road Research Laboratory, Wokingham, England.

Sabey, B. E. (1966), *RRL20 Road surface texture and the change in skidding resistance with speed*, Road Research Laboratory, Wokingham, England.

Sabey, B. E. & Storie, V. J. (1968), *LR173 Skidding in personal-injury accidents in Great Britain 1965 - 1966*, Road Research Laboratory, Wokingham, England.

Salt, G. F. & Szatkowski, W. S. (1973), *LR510 A guide to levels of skidding resistance for roads*, Transport and Road Research Laboratory, Wokingham, England.

Sandberg, U. & Goubert, L. (2017), *Reference tyres and road surfaces for skid resistance, noise and rolling resistance measurements*, ROlling resistance, Skid resistance, ANd Noise Emission measurement standards for road surfaces (ROSANNE project), Available at: https://rosanne-project.eu/.

Sanders, P. D. (2017), *PPR894 Road surface properties and high speed friction - The effect of permeability*, TRL, Wokingham, England.

Sanders, P. D. (2021), *PPR980 Characterising the measurements made by sideways-force skid resistance devices: An experimental study*, TRL, Wokingham, England.

Sanders, P. D., Brittain, S. & Premathilaka, A. (2017a), *PPR768 Performance review of skid resistance measurement devices*, TRL, Wokingham, England.

Sanders, P. D. & Browne, C. (2020), *PPR957 Characterising the measurements made by sideways-force skid resistance devices: A desk study and proposal for an experimental study*, TRL, Wokingham, England.

Sanders, P. D., Militzer, M. & Viner, H. E. (2017b), *PPR815 Better understanding of the surface tyre interface*, TRL, Wokingham, England.

Sanders, P. D., Morosiuk, K. & Peeling, J. R. (2014), *PPR727 Road surface properties and high speed friction*, TRL, Wokingham, England.

Scharnigg, K., Cerezo, V., Greene, M. & Kokot, D. (2017), *Quality Assurance Procedures to accompany proposed Common Scale(s)*, ROlling resistance, Skid resistance, ANd Noise Emission measurement standards for road surfaces (ROSANNE project), Available at: https://rosanne-project.eu/.

Scharnigg, K., Schwalbe, G., Conter, M., Kane, M., Kokot, D. & Roe, P. (2010), *Interdependencies of parameters influencing skid resistance, rolling resistance and noise emission*, TYre and Road surface Optimisation for Skid resistance And Further Effects (TYROSAFE Project), Available at: http://tyrosafe.fehrl.org/.

Singh, K. B. & Taheri, S. (2015), 'Estimation of tire-road friction coefficient and its application in chassis control systems', *Systems Science & Control Engineering* **3**(1), 39–61.

The Highways Agency, Scottish Executive, Welsh Assembly Government, The Department for Regional Development Northern Ireland (2004), *Skid Resistance*, HD 28/04, Design Manual for Roads and Bridges, Volume 7, Section 3, Part 1.

The Highways Agency, Scottish Executive, Welsh Assembly Government, The Department for Regional Development Northern Ireland (2008), *Data for pavement assessment*, HD 29/08, Design Manual for Roads and Bridges, Volume 7, Section 3, Part 2.

The Highways Agency, Transport Scotland, Welsh Assembly Government, The Department for Regional Development Northern Ireland (2006), *Surfacing materials for new and maintenance construction*, HD 36/06, Design Manual for Roads and Bridges, Volume 7, Section 5, Part 1.

Viner, H., Abbot, P., Dunford, A., Dhillon, N., Parsley, L. & Read, C. (2006), *PPR148, Surface texture measurements on local roads*, TRL, Wokingham, England.

VolumeGraphics (2014), 'Vgstudio max', Software.

Vos, E., Groenendijk, J., Do, M. T. & Roe, P. (2009), *Report on analysis and findings of previous skid resistance harmonisation research projects*, TYre and Road surface Optimisation for Skid resistance And Further Effects (TYROSAFE Project), Available at: http://tyrosafe.fehrl.org/.

Wallbank, C., Viner, H., Smith, L. & Smith, R. (2016), *PPR806 The relationship between collisions and skid resistance on the strategic road network*, TRL, Wokingham, England.

Wang, H., Al-Qadi, I. L. & Staniculescu, I. (2010), *Effect of Friction on Rolling Tire - Pavement Interaction*, Nextrans.

Wong, J. Y. (1993), *Theory of Ground Vehicles*, John Wiley & Sons, Inc.

Appendix A

Sanders, P. D., Morosiuk, K. and Peeling, J. R. (2014), *PPR727 Road surface properties and high speed friction.* TRL, Wokingham, England.

Transport Research Laboratory
Creating the future of transport
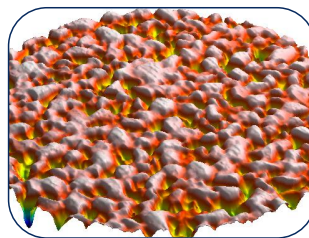
PUBLISHED PROJECT REPORT PPR727

Road surface properties and high speed friction

P D Sanders, K Morosiuk and J R Peeling

Prepared for:	Highways Agency, Pavements
Project Ref:	070/4/45/12 - HALC

Quality approved:

Peter Sanders		Alan Dunford	
(Project Manager)		(Technical Referee)	

Disclaimer

This report has been produced by the Transport Research Laboratory under a contract with Highways Agency. Any views expressed in this report are not necessarily those of Highways Agency.

The information contained herein is the property of TRL Limited and does not necessarily reflect the views or policies of the customer for whom this report was prepared. Whilst every effort has been made to ensure that the matter presented in this report is relevant, accurate and up-to-date, TRL Limited cannot accept any liability for any error or omission, or reliance on part or all of the content in another context.

When purchased in hard copy, this publication is printed on paper that is FSC (Forest Stewardship Council) and TCF (Totally Chlorine Free) registered.

Contents amendment record

This report has been amended and issued as follows:

Version	Date	Description	Editor	Technical Referee
1.0	01/05/2014	1st draft	PS	N/A
2.0	11/07/2014	Amendments made after TR	PS	AD
2.5	04/08/2014	Amendments made after TR	PS	AD
3.0	22/08/2014	Amendments made after TR	PS	AD
4.1	02/10/2014	Amendments made after DPA review	PS	HV

Road surface properties and high speed friction

Contents

Executive Summary

High speed friction generation is an important factor that should be considered by road owners to maintain road user safety. The management of high speed friction on the English strategic road network is based on the specification of surface texture depth. This approach was borne out of work showing that the generation of high speed friction is heavily reliant on the road surface texture depth. It is assumed that the correlation between texture and high speed friction is related to the ability of water to drain away from vehicle tyres through the surface texture.

For the majority of surfacing types, there is a good correlation between texture depth and high speed friction. There are however some exceptions, and some porous asphalt surfacings, and small aggregate thin surface course systems do not follow the same texture/friction relationship as the majority of surfacing types.

The difference in characteristics between surfacings has led to an inconsistency in the specification of surface types for use on the English strategic road network. For the majority of surfaces, texture depth is specified, but for small aggregate thin surface course systems there is a further requirement that high speed friction, measured directly, should also be verified. This extra requirement leads to additional complexity in monitoring the in-service performance, where texture depth is routinely used a as proxy for high speed friction. A better understanding of the relationships between texture, friction, and speed could enable the development of a robust and universal specification for all surface types.

The work described in this report sought to improve the current knowledge by making detailed surface geometry measurements and correlating them with high speed friction. A library of specimens was built up in the form of surface cores representing 8 different surface types. Conventional texture depth measurements were made to assess currently accepted techniques.   To gain more detailed information, the following laboratory measurements were also made:

- 3D surface profile
- Tyre / surface pressure distribution
- Surface void volume

The analysis sought to identify whether new surface characterisation techniques could be developed which improve the correlation between small aggregate thin surfacings and high speed friction. A key finding was that surface void volume measurements gave the best correlation with friction on all surfacing types. Measurements from 3D surface profiles gave a better correlation with friction than traditional texture measurement methods, but the improvement was slight.

The findings suggest that surface void volume offers a universal measure of texture that correlates well with friction for all surfaces. However, the method used is not practical for use on the network as it requires contact with the surface.

It was observed that, for some specimens, the void volume, measured using small diameter glass spheres, was considerably greater than measured with the conventional patch method.   This suggests the presence of fine voids within a complex surface structure. This complexity may not be visible using optical measurements, which rely on establishing line-of-sight.

It is plausible that sub-surface structure could influence high speed friction generation. Just as surface texture provides a pathway for water to drain away from the surface, it is

also likely that small voids within a complex surface structure could also provide conduits, allowing water to be removed from the tyre contact area and improving high speed friction.

To test this theory, hydraulic permeability tests were carried out on a sub-set of specimens. The results from this testing showed that small aggregate thin surfacings generally have a greater hydraulic permeability than the other surfacings tested. A key observation of this work was that when the texture and permeability results were combined, the performance of the small aggregate thin surfacings were better aligned with the other surfacing types. It should be noted that the conclusions borne out by the hydraulic permeability testing are based on a small number of laboratory tests and could be validated by a more robust study.

The results from this work show that by categorising surfaces in terms of the surface void volume, a correlation can be gained with high speed friction for all the surface types assessed. However this approach is not practicable for routine measurement. A wider implication of the work is that the hydraulic conductivity of surfaces may also aid in the generation of high speed friction. The porosity of road surfacings may therefore prompt some further investigation.

Road surface properties and high speed friction

1   Introduction

The aim of this work is to further develop the understanding of road surface properties that contribute to high speed friction. The ultimate goal is to develop a relationship that is applicable to all surface types that could be used to update current requirements with a universal methodology for the assessment of road surface friction.

1.1   Background

Providing adequate levels of low speed skid resistance and high speed friction is an important task for road owners, as a key component for motorist safety. The Highways Agency's skid resistance policy requires direct annual measurement of low speed skid resistance across the whole strategic road network. Direct routine measurement of high speed friction is technically challenging, and so texture is measured as a surrogate for high speed friction according to the following principles.

It is currently understood that high speed friction generation between a tyre and road surface is related to the amount of water present, preventing tyre/road contact. The amount of friction generated between a tyre and road surface reduces with increasing speed, and that the rate of reduction is also dependent on the amount of water present at the tyre/road interface.

The road surface property that has the most influence on the amount of water present at the tyre / road interface is texture depth. High-speed friction can therefore be managed through the specification of texture depth in new surfacing materials and the routine measurement of texture depth in service.

The methodology for the management of high speed friction, by measurement of texture depth, is based on research carried out in the late 1990s, reported in TRL report TRL 367 (Roe, et al., 1998). This work showed that, for the majority of surfaces, should a road have low texture as characterised by sensor measured texture depth (SMTD) (the normal measure for texture on in-service carriageways), then it is also likely to have low high speed friction (Figure 1-1).
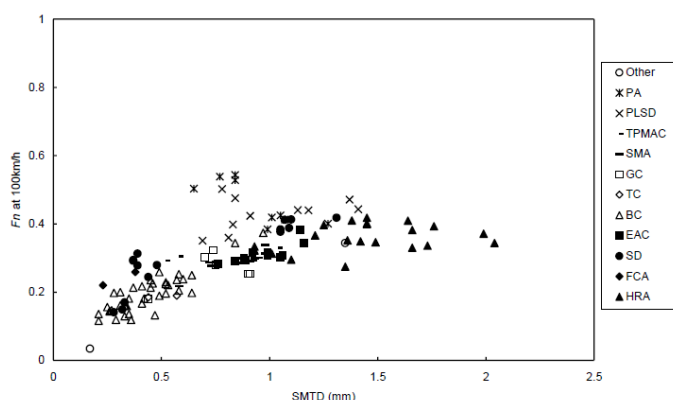
Figure 1-1 SMTD vs locked-wheel friction at 100 km/h (Roe, et al., 1998)

However, there are some exceptions to this relationship. The research described in TRL 367, and further research reported in TRL report PPR 564 (Roe & Dunford, 2012), showed that for some thin surface course systems with 6 mm maximum coarse aggregate size, and porous asphalts, the relationship developed in the 1990s does not apply. In particular, the work described in PPR 564 showed that some 6 mm thin surfacings can have relatively low texture levels, but provide levels of high speed friction greater than would be estimated using the relationships developed in TRL 367 (Figure 1-2).
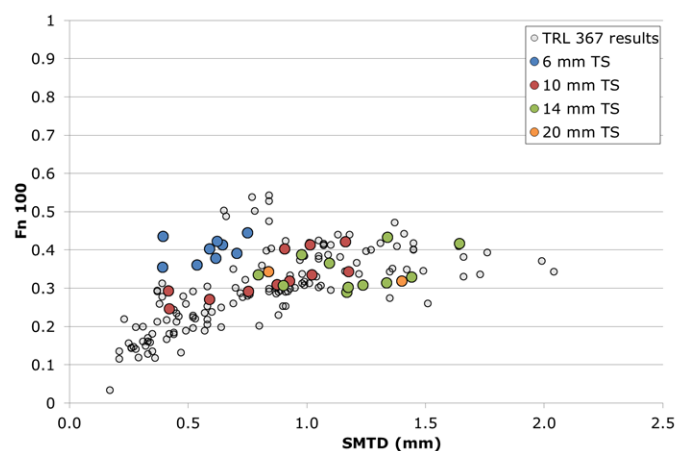
Figure 1-2 SMTD vs high speed friction at 100 km/h for thin surface course systems

Current guidelines permit the use of 6 mm thin surfacings and the specification for initial texture depth was relaxed in Interim Advice Note 154/12 (Department for Transport, 2012). The specification for retained texture depth was also relaxed but a further requirement was added that high speed friction, measured directly, should be verified. This departure from the current policy of measuring texture as a surrogate for high speed friction highlights a gap in the understanding of tyre/road interaction. In order to facilitate the use of 6 mm thin surfacings, and other potentially more durable materials, a better understanding of the relationship between texture, speed and friction is required. This in turn will help the development of a robust methodology for specification and measurement.

1.2   Report outline

Chapter 2 discusses the location and collection of specimens inspected using conventional techniques and more novel laboratory tests. In Chapter 3 the conventional measurement techniques used to gather the following information are discussed:

- High speed friction
- Low speed skid resistance
- Texture depth

The use of a number of alternative laboratory techniques is discussed in Chapter 4. These techniques were used to gather information about:

- 3D surface profile
- Tyre contact pressure
- The total surface void volume, referred to as the glass spheres texture depth

Using this information, new methods for characterising texture depth were devised. The relationships between these new parameters and high speed friction were assessed to find out if the new measures were better able to estimate high speed friction than conventional texture depth measurements.

In addition, some further laboratory testing was carried out to assess the sub-surface properties of the specimens. Hydraulic permeability testing, described in Chapter 6, was carried out to quantify the interconnectivity of the voids in the structure of the surface.

The outcomes from all of the measurements made, and their implications, are discussed in Chapter 7.

2   Surface specimens

A major component of this work was a series of laboratory measurements designed to investigate the properties of a number of surface types. It was therefore necessary to collect a number of road surface specimens.   The specimens used were 225 mm diameter cores cut to a thickness of approximately 50 mm (Figure 2-1).

Figure 2-1 Example of a core specimen

A number of specimens were already available from the work reported in TRL report PPR 564 (Roe & Dunford, 2012). These specimens cover a wide range of proprietary thin surfacing materials, full details of the specimens are available in TRL report in PPR 564 (Roe & Dunford, 2012). 65 specimens were extracted from ten different in-service carriageways; the surfacings were supplied and installed by different contractors and used a variety of different aggregates. For the present work, the most important distinction between the surface constructions is the different maximum coarse aggregate sizes (6 mm, 10 mm, 14 mm and 20 mm).

To supplement these specimens, and to include a wider range of surface types typically found on the UK road network, specimens were also taken from the TRL test track. The following surfaces were included:

- Thin surfacing with nominal maximum coarse aggregate size 6 mm (TS)
- Calcined flint surface dressing (SD)
- Hot rolled asphalt (HRA)
- Sawn concrete (SC)
- Brushed concrete (BC)

Three cores for each of the test track surfaces were taken. After extraction it was only possible to use one specimen of the sawn concrete surface for laboratory testing because two specimens were broken when the cores were being sawn to the correct depth.

3 Conventional assessment of surface properties

This chapter describes the conventional measurements of skid resistance, high speed friction and texture that have been made on the specimens. The vehicle-based techniques, for measuring high speed friction, low speed skid resistance and SMTD, are designed to be used on in-service carriageways and so could not be used to make measurements on the specimens directly. In these cases the value used is the value for the surface from which the specimen was taken (the parent surface).

3.1 High speed friction

Given that the aim of study was to assess the relationships between different surface properties and high speed friction it was important to make high speed friction measurements on each parent surface. These were made using the Pavement Friction Tester (PFT) shown in Figure 3-1.

The PFT is a locked wheel road surface friction testing device owned by the Highways Agency and operated on its behalf by TRL. The PFT comprises a tow vehicle and trailer. The trailer holds the test wheel, which is mounted on an instrumented axle and can be independently braked. The forces acting upon it are measured to determine the friction between the test tyre and road surface.

Figure 3-1 Pavement Friction Tester

During testing, the tyre contact patch slides over the surface at the same speed as the towing vehicle. This device can therefore measure skidding resistance at any practical speed up to about 120 km/h. Whilst testing, the load and drag forces on the tyre are measured every 0.01 seconds throughout the braking cycle. From these measurements, the peak[1] and locked[2] friction are determined. With repeat testing, the PFT allows speed / friction curves to be determined.

---

[1] Peak friction is the maximum friction value reached as the test wheel begins to slip.

[2] Locked friction is the friction value experienced when the test wheel is locked.

Testing was carried out under the guidance of ASTM standards E274/E274M (ASTM, 2011) and E524 (ASTM, 2008). To replicate the worst case scenario for motorists a smooth test tyre and a water film thickness of 1 mm are used.

3.2   Low speed skid resistance

Sideway-force Coefficient Route Investigation Machines are used for the routine monitoring of the skid resistance condition of the UK strategic road network. Figure 3-2 shows the Highways Agency Skid Resistance Development Platform (SkReDeP), which incorporates sideways force measurement equipment. Measurements from this device provide information that can be used to compare the performance of surfacings with the requirements for skid resistance laid out in the DMRB (Department for Transport, 2004).

Figure 3-2 SkReDeP

The machines use a smooth test tyre angled at 20 degrees to the direction of travel, which is mounted on an instrumented axle to record a skid resistance value for every 10 m length of road. The skid resistance value is the average ratio between the measured sideways force and the 200 kg vertical load, multiplied by 100. Readings are speed-corrected if necessary, and converted into values of SCRIM Coefficient (SC) by using a multiple of 0.78.

Measurements are usually made at a standard test speed of 50 km/h in the nearside wheel path. At this speed, since the test wheel is at 20 degrees to the direction of travel, the effective speed at which the tyre contact patch moves over the surface (the slip speed) is 17 km/h. For this reason, the measurements are considered to represent low speed skid resistance.

3.3 Texture

This section describes the three main techniques used to characterise texture on road surfaces.

3.3.1 Sensor Measured Texture Depth

Surface texture is calculated, on a routine basis, using surface profile measurements made at traffic speed with laser based systems fitted to TRACS, SCANNER and some sideways-force coefficient measurement vehicles. Texture measured in this way is normally reported as Sensor Measured Texture Depth (SMTD). The procedure by which SMTD is calculated is detailed in volume 5 of the SCANNER specification (DfT, 2009). For the purposes of this project, SMTD was measured on the parent surface at the same time as low speed skid resistance.

3.3.2 Mean Texture Depth

Often called the sand patch test or volumetric technique, the procedure for calculating Mean Texture Depth (MTD) is detailed in British Standard 13036-1:2004 (British Standards, 2010). The test involves spreading a known volume of glass spheres over a pavement surface in a circular pattern until the spheres are level with the top of the surface. The diameter of the patch created by the glass spheres is then measured and the MTD calculated using the following equation:

$$MTD = \frac{4V}{\pi D^2}$$

Where:

V = the volume of spheres used

D = is the diameter of the circle created

Equation 3-1

This technique is the longest established method of calculating texture depth, and is used to check that new pavements conform to specifications. For this study three determinations of MTD were made on each specimen; the average value is reported for each specimen.

3.3.3 Mean profile depth and root mean squared texture depth

The Circular Texture Meter (CTM) (Figure 3-3) is a portable device designed for measuring the texture depth of road surfaces and road surface specimens. The CTM operates on a similar principal to the texture measurement systems used on traffic speed systems. A triangulation laser is used to measure the distance between the laser source and the specimen surface. The laser is mounted on a rotating arm that, in the case of the device used for this work, moves in a 180 mm diameter circular path.

Figure 3-3 The circular texture meter (CTM)

During one revolution, 1024 distance measurements are made and the CTM software converts these raw distance measurements into values of Mean Profile Depth (MPD) following the principles set out in British Standard 13473-1:2004 (British Standards, 2004), and Root Mean Square (RMS) using the following equation:

$$RMS = \sqrt{\frac{(x_1^2 + x_2^2 + x_3^2 + \cdots x_n^2)}{n}}$$

Where:

x_i = individual texture depth measurements

n = total number of individual measurements

Equation 3-2

101

4   Alternative assessment of surface properties

In order to identify any features of the surface that might account for the behaviour of the 6 mm surfacings, some alternative measurement and characterisation techniques were used to assess surface characteristics for each specimen.

4.1   Measurement techniques

Three measurement techniques were used:

- 3D surface profile
- Tyre / surface pressure
- Glass spheres texture depth

4.1.1   3D Surface profile

Three dimensional computer models of each specimen were created from measurements made using the Breuckmann SmartSCAN HE system. The system is a stereo-imaging device comprising a structured light projector and two high resolution digital cameras (2448 x 2048 pixels) mounted either side of the light source (Figure 4-1). The system produces a representation of the field of view that can be converted to a 3D model in the proprietary software package OPTOCAT 2011 (Breuckmann, Meersberg).

Figure 4-1 Breuckmann SmartSCAN HE System

During image capture the light projector displays a series of eleven linear dark and light patterns onto the specimen and the cameras capture the deformation of these patterns across the surface. A deformation is considered as any pattern that, when analysed, differs from the expected pattern of the projection on a flat plane. Given that the geometry of the system is fixed and known, the surface profile of the specimen can be calculated and modelled.

The 3D capture system was mounted on a tripod with a viewing angle of 53 degrees to the horizontal. During capture ambient light sources were turned off so that the contrast between dark and light areas from the projector would be as great as possible. The specimen was placed on a turntable that allowed it to be rotated between captures whilst remaining in the same place.

Four captures of each specimen were taken with the specimen being rotated by 90 degrees between captures. The images from each capture were then stitched together and combined using the OPTOCAT software to a single model of the specimen surface. Once the four digitized captures were combined, the model was cropped so that only the surface of the specimen remained, as in Figure 4-2. This allowed the specimen surface to be analysed using surface analysis software, MountainsMap Universal (Digital Surf, Besançon).
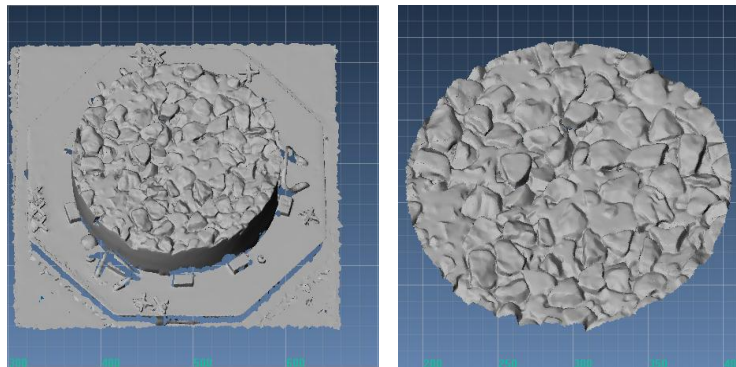
Figure 4-2 3D model of a specimen (left) and cropped model

Three dimensional models were created for each of the surface specimens. The purpose of the 3D modelling was to compare texture values calculated from the 3D models with values obtained from standard texture measurement methods. It was also intended to use the 3D models in conjunction with other measurements, such as pressure distributions, to create new variables based on the tyre's interaction with the surface.

4.1.2 Tyre / surface pressure

The pressure distribution and contact area between surface specimens and a standard ASTM tyre under a static vertical load were measured. These measurements help to investigate the interaction between the tyre and road surface and will be used as inputs during calculation of new surface parameters.

A standard ASTM test tyre used for high speed friction testing was installed on the Instron tensile / compression test machine and a specimen placed directly below it. Fujifilm Prescale pressure measurement film, which produces a pressure distribution "map" under loading, was placed between the tyre and specimen. The measurement set-up is shown in Figure 4-3.

Figure 4-3 Pressure distribution test set-up

The pressure measurement film is composed of two polyester sheets; one coated with a layer of micro-encapsulated colour forming material, "A-Film", and the other with a layer of colour developing material, "C-Film", (Figure 4-4).
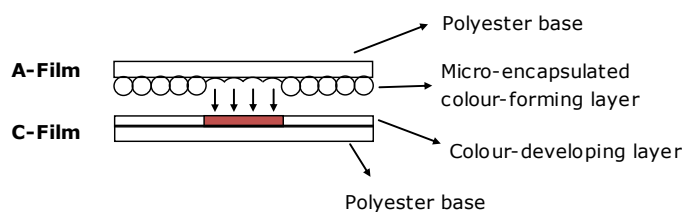
Figure 4-4 Fujifilm Prescale pressure film system

When pressure is applied to the sheets the microcapsules are broken in the A-Film and produce a pressure distribution map similar to that shown in Figure 4-5.
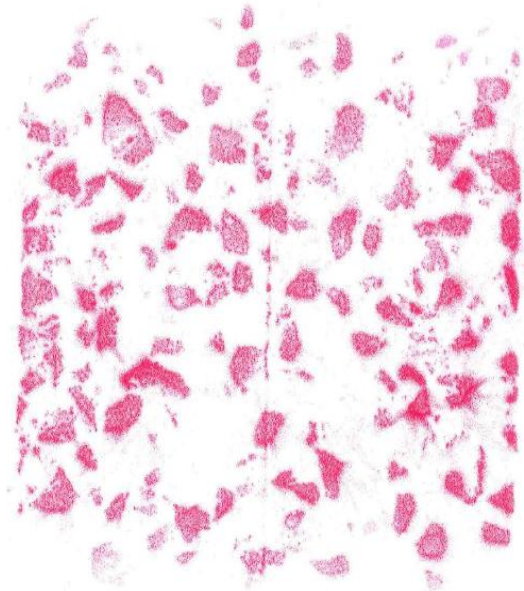
Figure 4-5 Example of pressure distribution "map"

During a test, the machine was set to deliver a force of 5 kN which is representative of the load placed on a PFT tyre during testing. This load was applied for a period of five seconds so that the pressure film could fully develop. The pressure distribution maps were digitized using the software package supplied as part of the pressure measurement system. The software package converts the pixel intensity values in the digitized image to pressure values and outputs a matrix of pressure intensity values that can be used to calculate a number of variables including the percentage pressed area between tyre and surface (the tyre contact patch).

4.1.3 Glass spheres texture depth

The measurement of glass spheres texture depth is an important parameter because it acts as a reference to which the other texture measurement techniques can be compared. The method for determining MTD was adapted to allow the measurement of the glass spheres texture depth of the surface specimens. This involved filling the surface voids with glass spheres of a known density and measuring the change in mass between the filled and un-filled specimen.

The spheres used for the measurement of void volume ranged between 0.025 mm and 0.105 mm in diameter, those used in the determination of MTD are between 0.18 mm and 0.25 mm in diameter. The smaller diameter spheres were chosen for the measurement of glass spheres texture depth so that very fine features in the specimen surface, which may not be captured by the MTD spheres, could be filled.

The procedure for determining the glass spheres texture depth of the specimens is described below and in Equation 4-1:

- The bottom and sides of the specimens were sealed using a silicon compound, to prevent the loss of any spheres through the texture of the specimen

- The specimens were weighed before applying the glass spheres, (m_{ec})

- The glass spheres were evenly applied to the surface of the specimens and vibrated to ensure all the voids were filled

- The glass spheres were levelled to the surface of the specimens using a flat wooden disk (a "sand patch spreader")

- The specimens, now full of spheres, were weighed, (m_{fc})

- The mass of glass spheres used was calculated and the volume inferred by dividing the mass of spheres used by the pre-determined density of the spheres

- The area of each specimen was measured and the void volume of spheres used was divided by the surface area

$$\text{Mass of glass spheres used } (m_s) = m_{fc} - m_{ec}$$

$$\text{Volume of glass spheres (V)} = \frac{m_s}{d_{gs}}$$

$$\text{Glass spheres texture depth} = \frac{V}{A}$$

Where:

d_{gs} = the density of the glass spheres

A = the surface area of the specimen

Equation 4-1

4.2   New surface characterisation techniques

Using the results from the alternative measurement techniques five new surface characterisations were developed:

- Percentage pressed area

- 3D surface void volume

- Tyre penetration depth

- Volume of void below tyre

- Volume of void occupied by tyre

4.2.1   Percentage pressed area

The calculation of percentage pressed area used the pressure distribution matrices gained from the pressure testing described in section 4.1.2. Some noise could be seen in the pressure distribution matrices; pressure points were registered where it appears from the overall pattern that no contact is occurring. It is speculated that the additional points appear where cells in the sheet burst due to the pressure between the tyre and the sheet itself rather than because of the pressure between the tyre and specimen.

A 2D median filter, often referred to as a "salt & pepper" filter, was applied to the pressure matrices to remove this noise and give a more accurate representation of the pressed area. Figure 4-6 shows a filtered and unfiltered image of the same area where red areas represent high pressure. The filter acts on a matrix by replacing an individual value with the median value of its neighbours. The filter was designed to act over a narrow field so that only isolated spots would be affected and measurements made on areas coming into contact with the tyre were relatively unchanged.
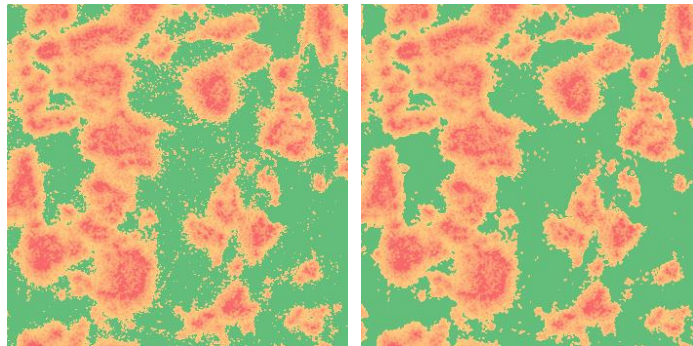
Figure 4-6 Unfiltered image (left) and filtered image

In order to find the percentage of the tyre area that came into contact with the surface a Region of Interest (RoI) was defined to show the physical limits of contact area. The percentage pressed area is then the area of all pressure points indicated by the film divided by the area of the RoI. Quantifying a specific RoI for each specimen would have provided the most accurate results but would have been prohibitively time consuming. An alternative method was used to estimate the RoI for each specimen based on measurements made on a flat steel plate.

The RoI calculated using a flat surface results in a slightly larger RoI than would be expected on a specimen surface. This is due to the voids in the specimen surfaces resulting in higher pressure at the points of contact and therefore a smaller area required to support the load. To account for this, the size and shape of the RoI from the flat surface was used to calculate outer and inner mask areas that, when used together, would estimate the RoI for the specimens.

The outer mask area was defined as the RoI of the steel plate. Because this mask is likely to be larger than the RoI on the specimen surfaces, it was used to calculate the lower limit of the Percentage Pressed Area (PPA_L). The inner mask area was defined as the ROI of the steel plate, excluding the effects of tyre deformation, and is likely to be smaller than the RoI on the specimen surfaces. This mask was used to calculate the upper limit of the percentage pressed area (PPA_U).

The image on the left of Figure 4-7 shows measurements of pressure from a film placed between the test tyre and a flat plate, overlaid with the upper mask area (black outline showing the full extent of potential tyre contact) and the lower mask area (white outline showing a minimum potential contact area). The image on the right of Figure 4-7 shows

how these mask areas are applied to a specimen with a maximum aggregate size of 14 mm.
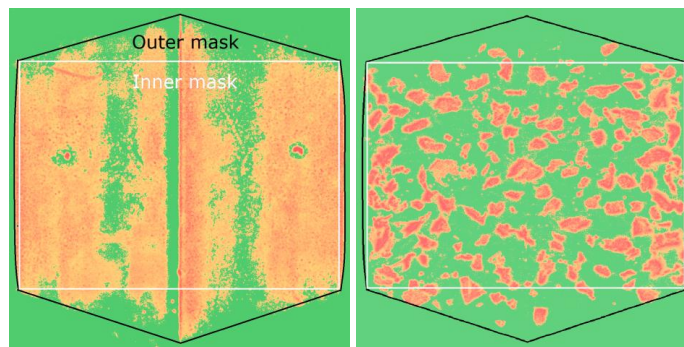
Figure 4-7 Example of outer and inner mask areas calculated from a flat plate (left) and as used on a specimen

The mean Percentage Pressed Area $\left(\frac{PPA_L + PPA_U}{2}\right)$ within each of the two mask areas was used to represent the Percentage Pressed Area (PPA) of the specimen.

4.2.2 3D Surface void volume

Surface analysis software MountainsMap Universal (Digitalsurf, Besançon) was used to calculate the texture of each specimen, based on the 3D surface profiles generated from the Breuckmann system. The 3D surface void volume was defined simply as the total volume of the voids below the highest peak in the profile, divided by the surface area of the specimen (as if it were completely flat). This provides an average texture depth for the specimen expressed in mm^3/mm^2. One drawback to this approach is that the texture value can be overestimated by the presence of a particularly large peak in the profile. When inspecting the 3D profiles of the specimens the peaks were found to be homogeneous enough for this approach to be appropriate.

4.2.3 Tyre penetration depth, volume below tyre and volume occupied by tyre

The "slices" tool in MountainsMap allows a 3D surface to be viewed on a two dimensional plane as though it has been sliced at a specific depth. Figure 4-8 shows an example where the blue areas represent voids present below the selected slice depth, and the yellow areas represent the surface material that has been sliced.

A slice depth was selected so that the "projected area" of material displayed in MountainsMap, matched the percentage pressed area calculated from the pressure distribution tests, for each specimen. If the area pressed by the tyre in the pressure distribution tests is the same as the area of material at a certain depth, then that slice depth may be considered to be representative of the tyre penetration depth.

Because the slice depth represents the tyre penetration depth then the volume of voids below that depth represents the volume into which the tyre does not intrude; the volume

Road surface properties and high speed friction

of voids below tyre. Conversely, any voids above that depth could be filled with tyre, assuming an easily deformed tyre rubber; the volume occupied by the tyre. These two volumes, divided by the area of the surface, are represented by the values indicated in Figure 4-8.

	▉	▉	
Projected Area (%)	33.9	60.1	◄ Percentage pressed area
Volume of void (%)	5.61	77.0	
Volume of material (%)	94.4	23.0	
Volume of void (mm³/mm²)	0.244	0.824	◄ Volume of void occupied by tyre
Volume of material (mm³/mm²)	4.11	0.247	
Mean thickness of void (mm)	0.244	0.824	
Mean thickness of material (mm)	4.11	0.247	
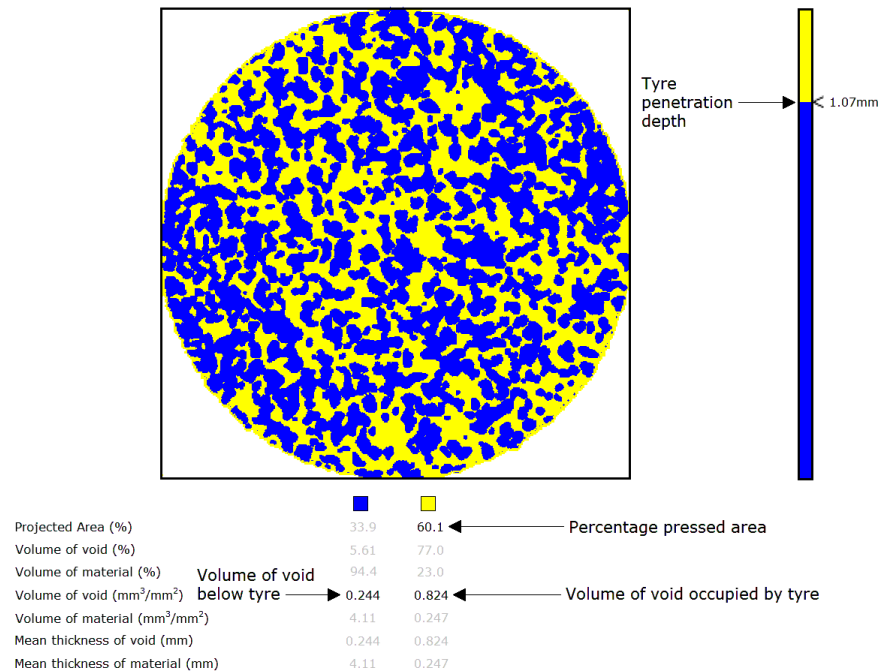
Figure 4-8 Example of slices tool

5   Analysis

This chapter discusses the analysis carried out on the results collected. In order to improve confidence in the results the friction / skid resistance / texture relationship developed in TRL 367 had been repeated. The results collected from the conventional and alternative measurement techniques are then compared and discussed.

5.1   Repetition of TRL 367 relationship

A model for predicting high speed friction was developed and reported in TRL 367 (Equation 5-1).

$$Fn100 = (0.00367 \times SR) + \left(0.411 \times (1 - e^{-SMTD})\right) - 0.151$$

Where:

SR = The surface SCRIM Reading (the unprocessed output from SCRIM)

SMTD = The surface texture as measured using SMTD

Equation 5-1

Equation 5-1 was used to estimate high speed friction, Fn 100, for the surfaces analysed during the present study, using measurements of skid resistance and texture made on the sites. The estimated high speed friction was then compared with high speed friction actually measured on the sites. This comparison is shown graphically in Figure 5-1; previous measurements made during the TRL 367 study are included for reference.
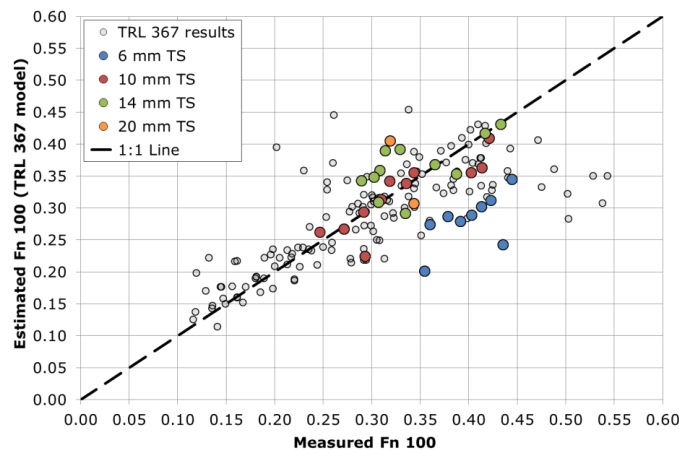
Figure 5-1 Comparison between estimated Fn 100 using Equation 5-1 and measured values

Figure 5-1 shows that there is an agreement with the results from the TRL 367 study. Whilst the 10 mm and 14 mm specimens are scattered around the 1:1 line, the majority

of the 6 mm specimens are clustered below the 1:1 line. The outlying points reported in TRL 367, below the 1:1 line, mainly represent porous asphalt surfaces.

It is possible that the outlying surfaces, porous asphalt and 6 mm thin surfacings, share a common mechanism causing actual high speed friction to be greater than predicted.

5.2   Comparison of texture parameters

Each parameter characterising specimen surface texture (MTD, MPD, RMS and 3D void volume) has been compared with the total surface void volume; the glass spheres texture depth (Figure 5-2 to Figure 5-5). There is no relationship shown with SMTD because the SMTD and RMS measures are very similar and the RMS measure was calculated for each specimen whereas SMTD measurements were made on the specimens' parent surfaces. A broken diagonal line shows the line of unity on each graph.
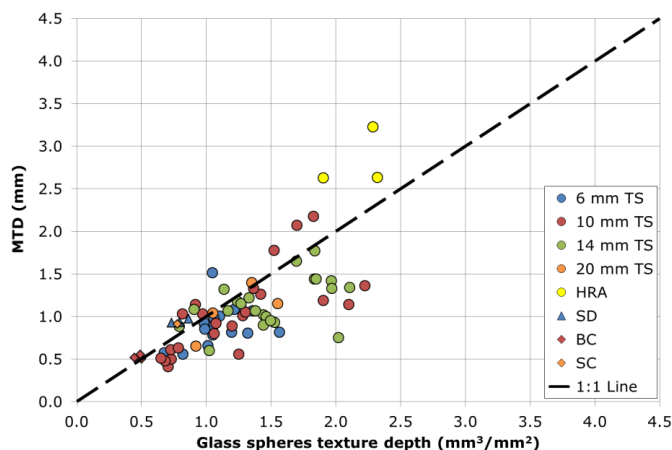
Figure 5-2 Comparison of MTD and glass spheres texture depth
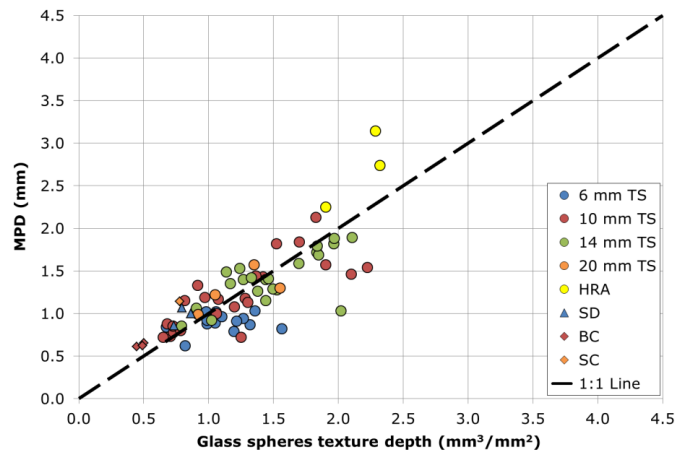
Figure 5-3 Comparison of MPD and glass spheres texture depth
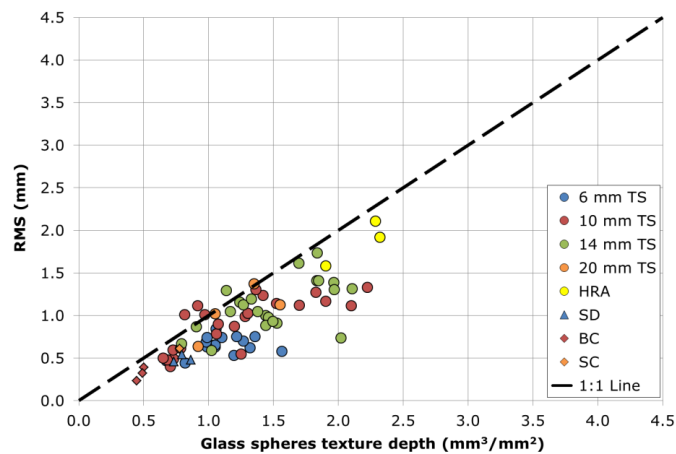
Figure 5-4 Comparison of RMS and glass spheres texture depth
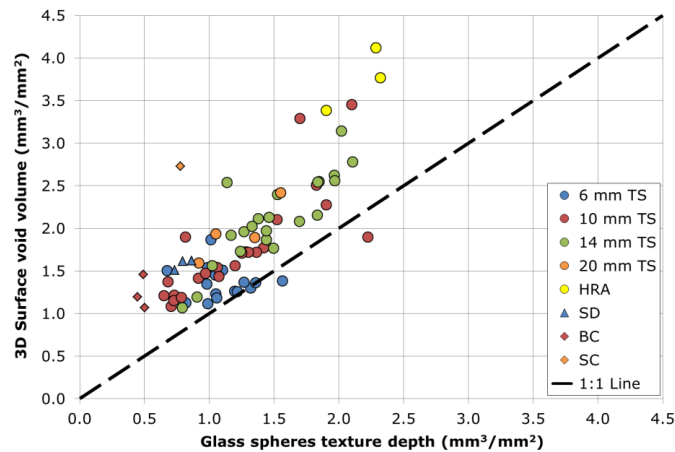
Figure 5-5 Comparison of 3D surface void volume and glass spheres texture depth

For all four variables, the 6 mm specimens are generally found in a cluster in a horizontal line. This is a key observation, and is particularly evident in MPD and RMS results where there is little variation in the y-axis, compared to larger differences in values recorded for the glass spheres texture depth. The 10 mm and 14 mm thin surfacing specimens are more widely spread than the 6 mm specimens and there is generally some correlation for these, and the other surfacing types, between the texture parameter and glass spheres texture depth.

Values of 3D void volume generally sit above the 1:1 line. This shows that the 3D method measures a larger volume than the glass spheres method. This is primarily because the 3D values are referenced from the top of the aggregate chippings whereas the glass spheres method is unable to capture information at the very top of the aggregate chippings. Figure 5-6 is an image of a surface specimen after it had been filled with glass spheres; note the dark protruding aggregate particles.

Figure 5-6 Example of image taken during glass spheres texture depth measurement

5.3   Comparison of alternative parameters with high speed friction

Some of these parameters may be useful in finding a relationship between the outlying 6 mm thin surfacings and high speed friction. To test the new parameters, each one was compared with Fn 100. Graphs showing these relationships can be found in Appendix A.

5.3.1   Percentage pressed area

There is a school of thought that attributes the high speed friction performance of 6 mm thin surfacings to an improvement in tyre contact area as a result of the smaller aggregate size. This stands to reason; a smaller aggregate size would allow for a denser surface, improving the tyre contact area and therefore high speed friction.   The measurement of percentage pressed area (tyre contact area) showed that values from the 6 mm thin surfacings were similar to those from other surfacing types. Furthermore there was no correlation between percentage pressed area and high speed friction.

5.3.2   Tyre penetration depth, volume below tyre and volume occupied by tyre

The analysis of these parameters showed a slight improvement in the position of the outlying 6 mm surfaces compared with the traditional measurement methods. However, the improvements were slight and, based on the limited number of observations none of the parameters provide a substantial improvement over the current relationship.

5.3.3   3D surface void volume and glass spheres texture depth

Figure 5-7 shows the relationship between high speed friction and glass spheres texture depth and Figure 5-8 shows the relationship between high speed friction and 3D surface void volume.

Road surface properties and high speed friction
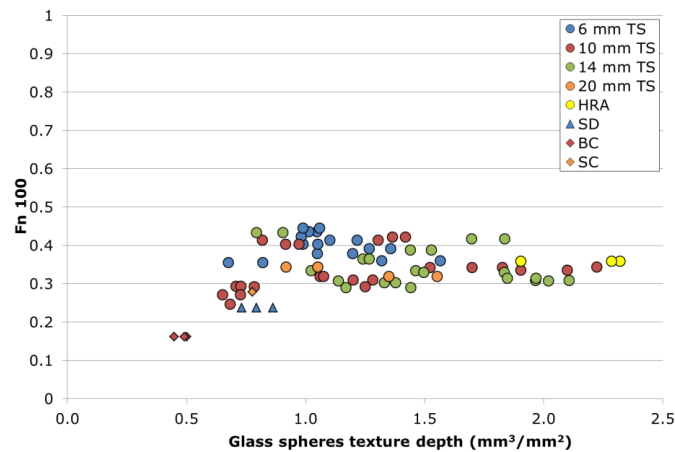
Figure 5-7 Comparison between glass spheres texture depth and Fn 100
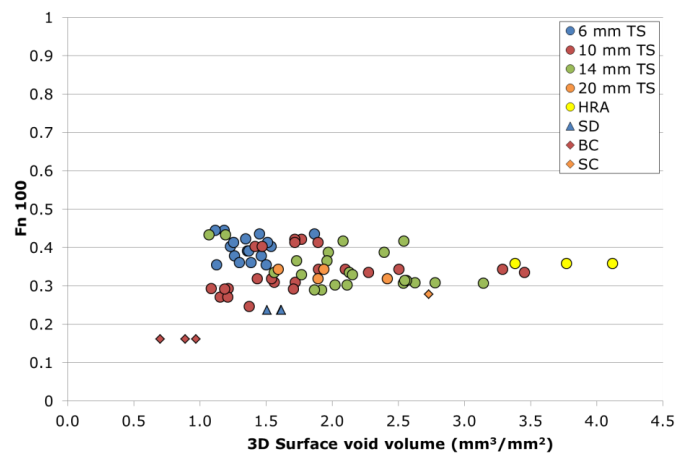
Figure 5-8 Comparison 3D surface void volume and Fn 100

Figure 5-7 shows that the glass spheres measure produces the results with the fewest outliers and the 6 mm specimens share a similar pattern of behaviour to the other surfaces. This indicates that the glass spheres texture depth is showing a clearer correlation for texture and high speed friction than the non-contact measurement methods.

Figure 5-8 shows that the form of the relationship between the 3D surface void volume and high speed friction is similar to that of the SMTD measurements (Figure 1-2), including a cluster of 6 mm surfaces that are outlying from the bulk of results. However, the cluster in Figure 5-8 is less well defined than that in Figure 1-2; more 6 mm specimens appear in the bulk of the measurements.

5.4 Analysis summary

There are many methods for measuring road surface texture and, because of the efficiency associated with making measurements at traffic speed, most use contactless techniques. Contactless measurement systems can be vehicle mounted and collect information in conjunction with other parameters, such as skid resistance or road geometry. All currently used contactless methods characterise texture using a two dimensional texture profile.

When 2D optical methods are used to characterise texture, the 6 mm thin surfacings lie outside of the bulk of the measurements. The analysis has shown that 3D texture measurement systems are capable of capturing a greater amount of textural information than 2D methods and the parameters based on 3D measurement systems improve the relationship with high speed friction, albeit slightly. The glass spheres method is capable of capturing the very small scale texture, deep within the surface of the specimens and provides the best relationship with high speed friction, for all surfaces, of all the measurement techniques.

For the majority of materials, the texture that can be seen from above the surface is representative of the volume available for water to escape the tyre/road interface. But, for some surfaces, such as the 6 mm thin surfacings assessed, there may be an amount of texture that cannot be seen from the surface in the form of interconnected voids or texture that is too deep, or small, for optical systems to characterise.

It is plausible, therefore, that the glass spheres texture depth produces the best relationship with high speed friction because this measurement method is capable of characterising some of the texture that cannot be seen from the surface, including interconnected voids. These voids could provide a pathway for water to be removed from the surface, and could improve the friction characteristics of some surfacings.

6   Hydraulic permeability

In Chapter 1 the influence of water on friction generation was discussed, and in Chapter 5 it was suggested that the interconnected voids within a surface may provide a pathway for water to escape the tyre road interface and therefore aid friction generation. This chapter discusses the experiments carried out to assess the hydraulic permeability of the specimens. This will characterise the specimens' ability to transport water through the interconnected voids within the surface structure.

6.1   Experimental procedure

For this experiment a variation on the technique defined in BS EN 12697-19:2012 (British Standards, 2012) was used, Figure 6-1 represents the experimental setup. A steel tube was bonded to a specimen surface, and the outside edge of the top of the specimen was sealed using silicone sealant to remove the effects of surface texture because they are likely to mask the effects of permeability. The bottom of the specimen was also sealed to reduce any effect of drainage relating to variations in the amount of base course still attached to the surface course. Water with a constant hydrostatic head of 2.94 N/m^2 was fed into the steel tube and allowed to flow through the specimen surface to saturate the voids in the specimen. Once saturated, the water flowing out of the specimen was collected over a known time and the flow rate was calculated using the mass of the collected water.
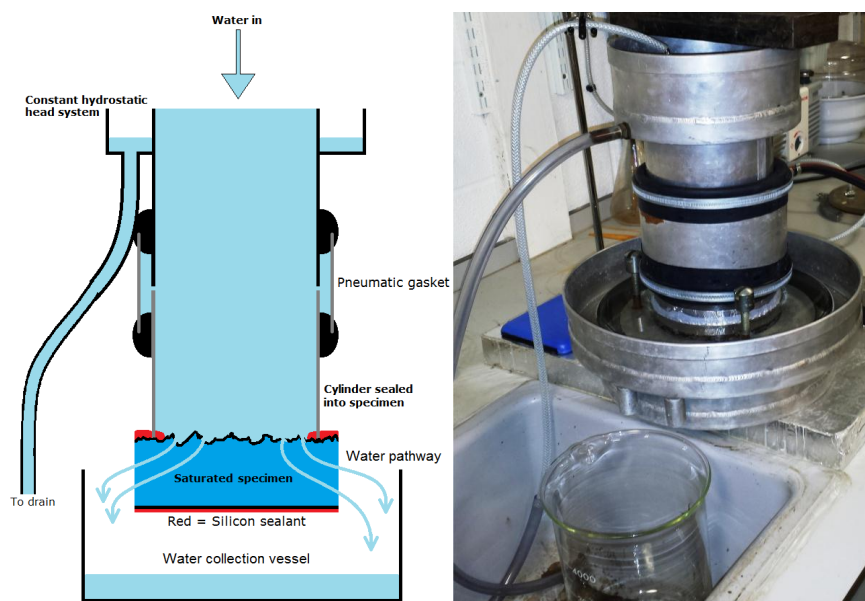
Figure 6-1 Representation of hydraulic permeability setup (left) and the system used

117

To investigate the depth of any inter-connected voids, the experiment was repeated several times for each specimen, with the sides of the specimen sealed to different extents. Firstly, the sides of the specimen were completely sealed with aluminium tape to restrict the water flow. For further repetitions, 5 mm of tape was removed from the bottom of the specimen to reveal progressively more of the specimen's sides, until all of the tape was removed.

A sub-set were chosen for testing based on aggregate size and their position in the friction / texture relationship shown in Figure 6-2; the circular points with solid colours represent the specimens selected for permeability testing and the shaded circular points represent the remainder of the available specimens. TRL 367 results have been included for reference and are represented by the shaded diamond points. The specimens selected were chosen because they represent the range of behaviours observed.
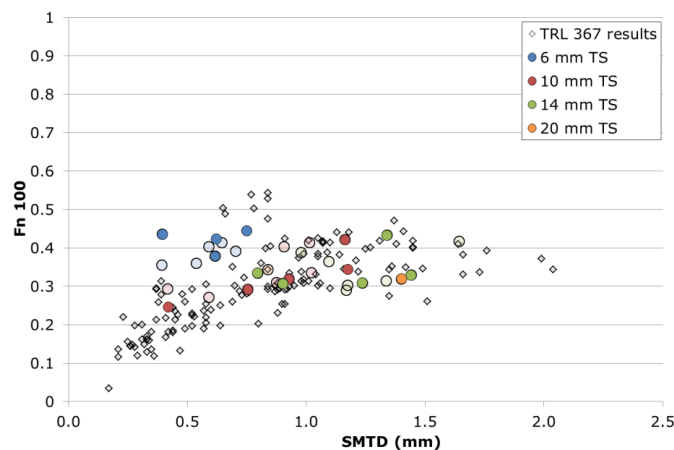
Figure 6-2 Specimens selected for permeability testing

6.2 Results

The testing yielded a permeability profile for each specimen like the one shown in Figure 6-3. The permeability profile shows the flow rate measured at different sealed depths. In Figure 6-2 the flow rate at 35 mm is the rate when all but the bottom 5 mm of the specimen was sealed with aluminium tape, the flow rate at 0 mm is the rate with the sides of the core completely open. A full account of the permeability measurements is given in Appendix B.

Figure 6-3 shows that, as the tape is removed and more of the specimen is revealed, the flow rate increases; this behaviour was similar for all the specimens. In this case, the flow rate remains fairly consistent for measurements made until only the top 20 mm of the surface was sealed. For other specimens this depth differs, but the example suggests that the permeability of the material, at considerable depths below the surface, may influence the flow of water at the surface.
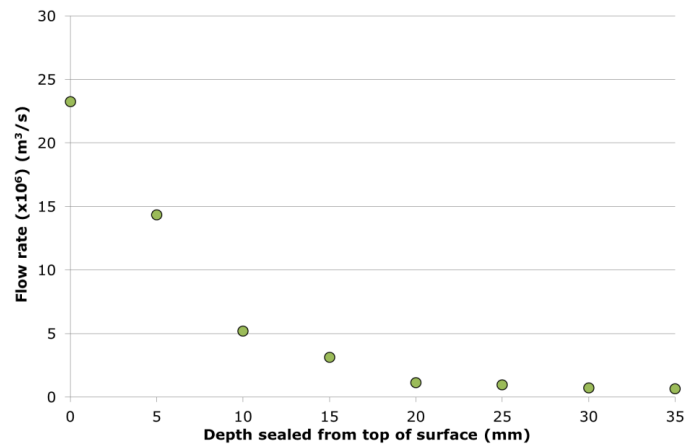
Figure 6-3 Permeability profile for thin surfacing with a maximum aggregate size of 14 mm

For further analysis, the permeability of the specimens without any sealing of the sides was considered in relation to their textural and frictional performance. Figure 6-4 shows the behaviour of the specimens; the position of the points on the graph represents the textural and frictional performance, as before, and the shape of each point represents the specimen's permeability. The TRL 367 results have been included for reference.
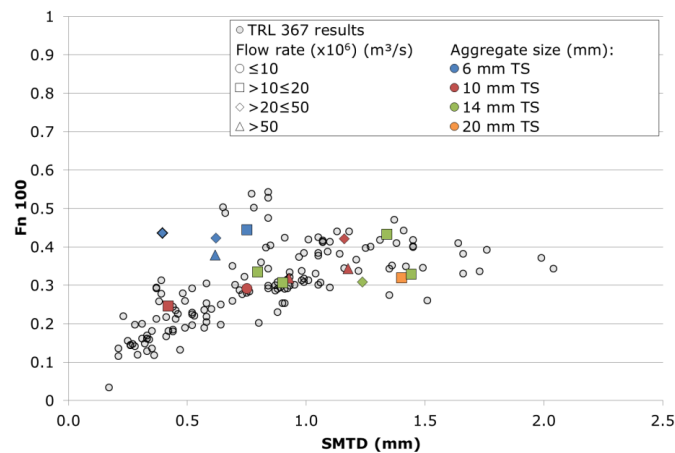
Figure 6-4 Specimens chosen for hydraulic permeability tests

Figure 6-4 shows that the specimens with texture below approximately 1 mm SMTD, which also fall within the bulk of the friction measurements, have low flow rates. Conversely, specimens with texture below 1 mm SMTD, which have higher friction than the bulk of the measurements, generally have higher flow rates. Specimens with

textures greater than approximately 1 mm SMTD have a range of flow rates, although the friction / texture relationship above 1 mm SMTD suggests that an increase in texture does not improve the friction performance, and this may also be true for an increase in flow rate.

A primary function of both texture depth and permeability is to remove water from the tyre/road interface and so their measurements could be considered to be additive. Using this assumption, the sum of values of SMTD and flow rate (multiplied by a constant of 11000, derived using the least squares method) were plotted with the TRL 367 results in Figure 6-5, although since the flow rate for the TRL 367 results is unknown these points have not been adjusted.
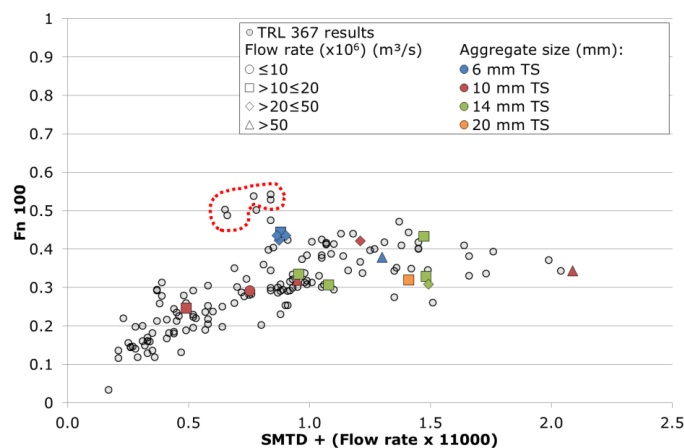
Figure 6-5 The combined effects of texture and permeability

The performance of the outlying specimens is now much closer to the bulk of the measurements. The positions of specimens with high flow rates have been affected greatly whereas the position of specimens with low flow rates have been less affected. Supporting this observation, the group of points surrounded by the broken red line represent porous asphalt surfaces. It is highly likely that these surfaces would have very high flow rates and so if this was taken into account their position on the x-axis would move to >2.5. The overall shape of the point cloud would then be more representative of the bulk of the measurements.

This demonstrates the potential for permeability to be considered as adding texture to the surface, and that when these effects are taken into account the relationship between texture and friction developed in TRL 367 remains valid for the small aggregate thin surfacings that are the focus o7f this study.

It is worth noting at this point that the results are based on a small number of laboratory measurements. The results cannot therefore be definitive and the behaviour shown above may differ significantly for other surfacing types or if measurements were to be made on in-service carriageways.

7 Discussion

Measurements of conventional surface texture parameters have shown that, for the majority of surfaces, at textures below approximately 0.8 mm SMTD, friction increases linearly with texture, and for textures above 0.8 mm SMTD friction changes little with increasing texture. There is an exception to this rule, however, and it has been found that some small aggregate thin surfacings are providing higher levels of friction than would be expected, given their texture characteristics. This is a replication of the findings of TRL 367 which did not assess small aggregate thin surfacings but found that porous asphalt surfacings were providing higher friction levels than expected.

The use of alternative texture measurement techniques has shown that characterising texture using 3D imaging techniques more closely represents surface texture than traditional measurement techniques. The 3D texture measures used were able to reduce the number of outlying points in the Fn 100 / texture relationship, although there were still some outliers.

The Fn 100 / texture relationship that showed the fewest outliers was that using the glass spheres method. This suggests that the ability of the spheres to access areas deeper in the surface that cannot be seen using optical techniques leads to a texture characterisation more closely related to high speed friction.

The relationship between glass spheres texture depth and friction suggests that there may be some features below the surface that are influencing friction generation. Hydraulic permeability measurements were made to characterise the interconnected voids in the surface of the specimens. Results from these measurements have shown that the hydraulic permeability of the 6 mm TS specimens, outlying from the bulk of the points in the Fn 100 / texture relationship, generally have a higher permeability than specimens with similar texture within the bulk of the relationship. Further analysis of the texture and permeability results showed that, when texture and permeability are thought of as additive properties, their combined effects can bring outlying measurements into the bulk of the TRL 367 relationship.

This has implications for the development of a new texture measurement system for routine use because current technology does not allow the remote measurement of permeability and it may not be possible, to fully characterise the pavement properties that influence friction using purely optical techniques.

Although it is possible to develop an improved texture measurement system based on 3D measurement principles, implementing such a system for routine use requires a number of technical challenges to be overcome. Furthermore, the research presented in this report shows that the improvements gained from such a system are likely to be relevant for measurements made on a small number of surfacings, and even then the improvement is slight.

Further understanding of the relationship between permeability and high speed friction could form the basis for the development of a criterion based on glass spheres texture depth or permeability. This could be used in conjunction with traditional texture measurement systems to allow the universal analysis of friction for all road surfacings.

There are also implications for the development of new road surfacing materials as the permeability of materials could be used to provide greater levels of friction, but permeable materials have been shown to be less durable than dense materials and so an improvement in friction could be achieved at the cost of durability.

8   Conclusions

From the work carried out in this study the following conclusions can be made:

- 3D imaging techniques can more accurately characterise road surface texture than traditional methods

- A 3D imaging based texture measurement system slightly improved the form of the texture / friction relationship but some outliers were still present

- The implementation of a 3D based system for routine use on the road network is unlikely to produce substantially improved results over traditional methods

- The hydraulic permeability of road surfaces may be influencing the frictional performance of road surfacings in a manner similar to that of texture

It should be noted that the final conclusion is based on laboratory measurements made on a small sample size and that the characteristics noted above may differ for other material types or in-service carriageways. The assessment of texture, permeability and friction on in-service carriageways of various constructions would be useful in determining the role that permeability plays in friction generation.

References

ASTM, 2008. *E524-08 Standard specification for standard smooth tire for pavement skid-resistance tests,* West Conshohocken: ASTM.

ASTM, 2011. *E274/E274M-11 Standard test method for skid resistance of paved surfaces using a full-scale tire,* West Conshohocken: ASTM.

British Standards, 2004. *BS EN ISO 13473-1-2004 Characterisation of pavement by use of surface profiles - part 1 - determination of MPD,* London: BSI.

British Standards, 2010. *BS EN 13036-1. Road and airfield surface characteristics - test methods. Part 1: Measurement of pavement surface macrotexture depth using a volumetric patch technique,* London: BSI.

British Standards, 2012. *BS EN 12697-19:2012 Bituminous mixtures - test methods for hot mix asphalt part 19: Permeability of specimen,* London: BSI.

Department for Transport, 2004. *HD 28/04 - Skid resistance (DMRB 7.3.1),* London: The Stationery Office.

Department for Transport, 2012. *Interim advice note 154/12,* London: The Stationery Office.

DfT, 2009. *SCANNER specification 2009, Vol 5 - Technical requirements: SCANNER survey parameters and accreditation,* London: UK Roads Board and TRL.

Roe, P. G. & Dunford, A., 2012. *PPR 564 The skid resistance behaviour of thin surface course systems,* Wokingham: HA / MPA / RBA Collabarative Programme 2008-11: topic 1 prepared for Highways Agency, Minerals Products Association and Refined Bitumen Association.

Roe, P. G., Parry, A. R. & Viner, H. E., 1998. *TRL 367 High and low speed skidding resistance: the influence of texture depth,* Wokingham: Prepared for Pavement Engineering Group, Highways Agency.

Road surface properties and high speed friction

Appendix A Relationship between Fn 100 and new texture parameters
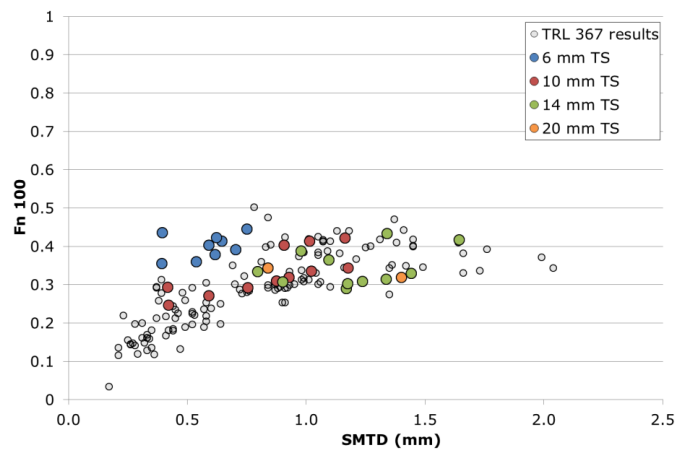
Appendix A-1 Comparison between FN 100 and SMTD
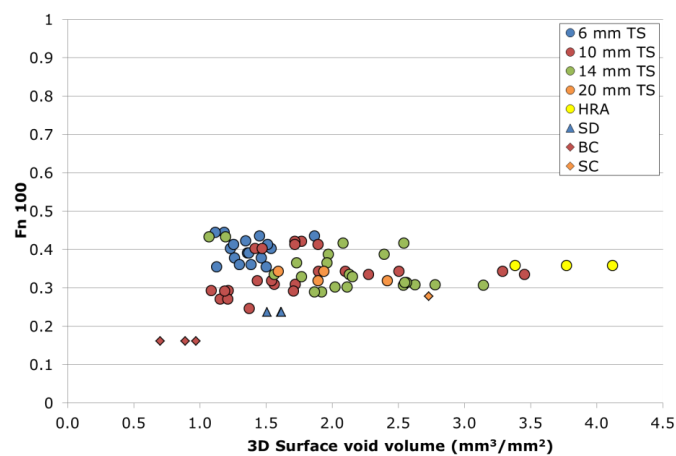
Appendix A-2 Comparison between FN 100 and 3D surface void volume

Road surface properties and high speed friction
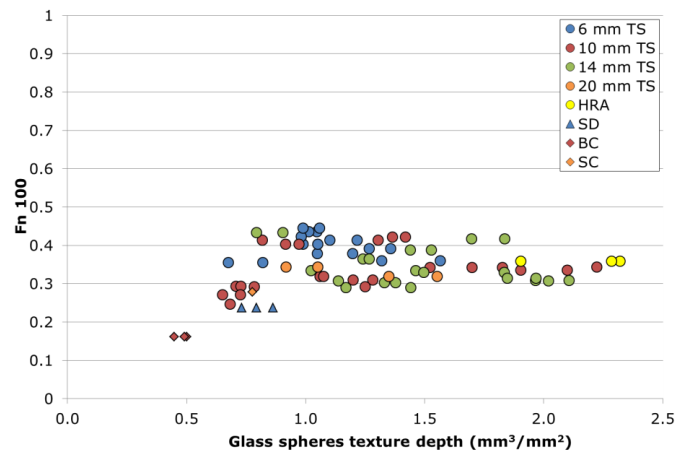
Appendix A-3 Comparison between FN 100 and glass spheres texture depth
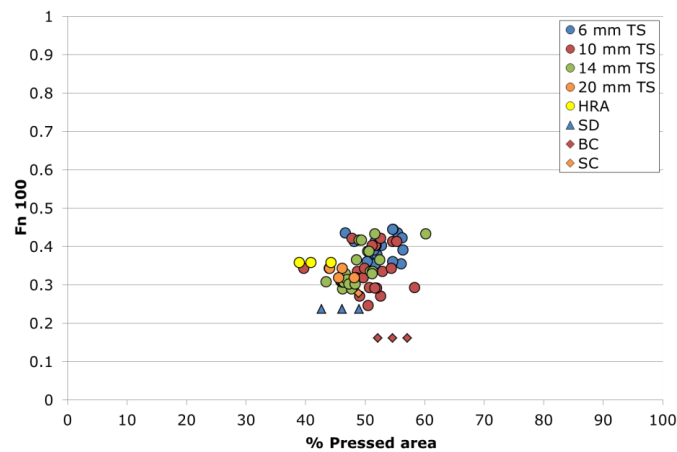
Appendix A-4 Comparison between FN 100 and percentage pressed area

125
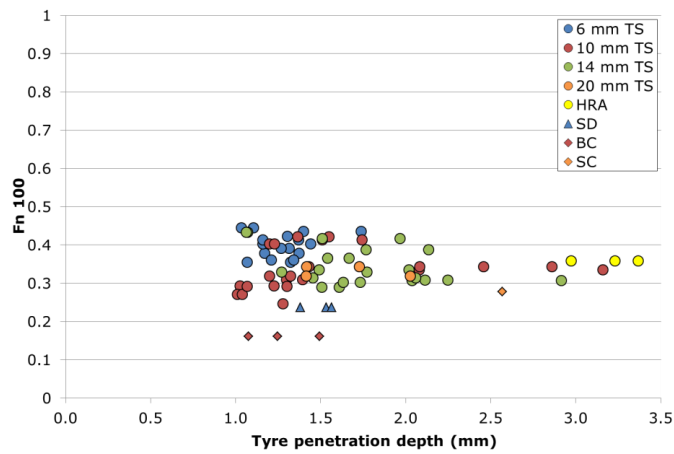
Appendix A-5 Comparison between FN 100 and tyre penetration depth
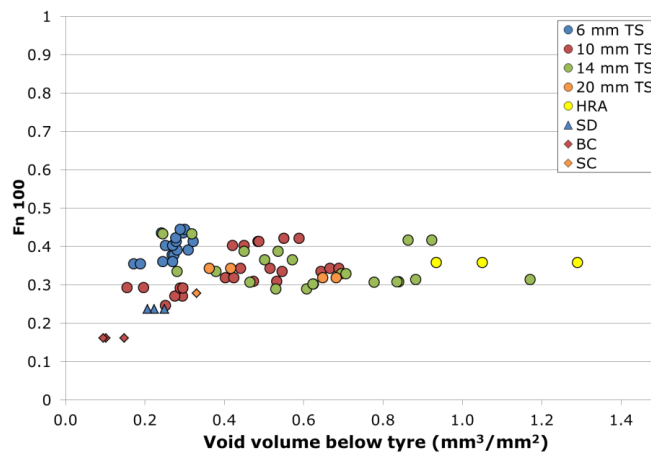
Appendix A-6 Comparison between FN 100 and volume of the void below the tyre
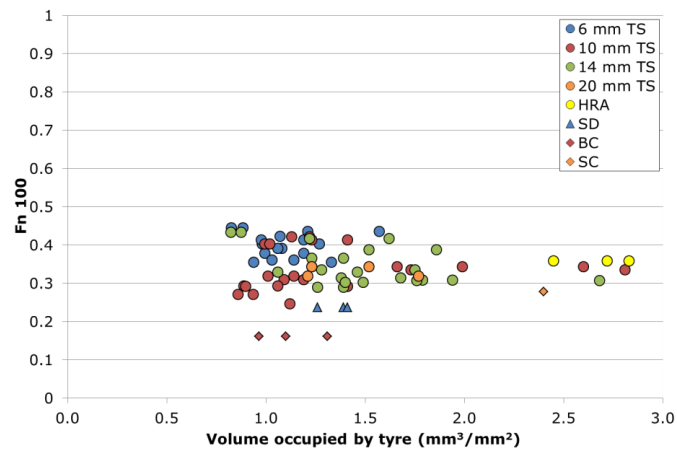
Appendix A-7 Comparison between FN 100 the volume occupied by the tyre

Road surface properties and high speed friction

Appendix B Results of permeability testing

The graphs below show the results of the permeability testing. Tests were primarily carried out on specimens used as part of the collaborative project. The labelling convention for these specimens is: Road name_Lane_Section_maximum aggregate size. Full details of the surfaces are available in TRL report PPR 564 (Roe & Dunford, 2012)
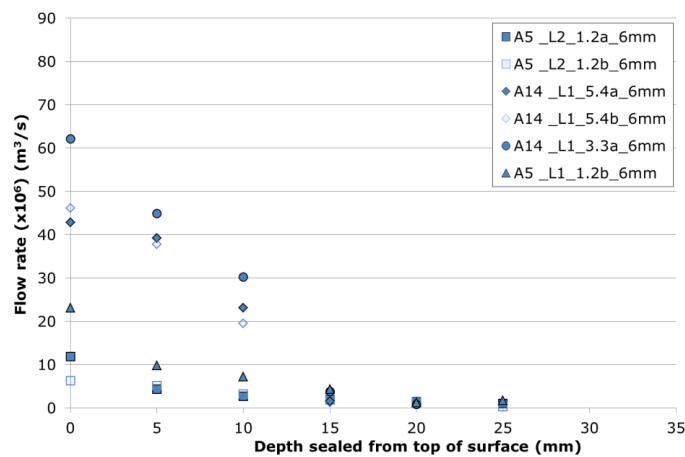
Appendix B-1 Hydraulic permeability measurements for 6 mm thin surfacings
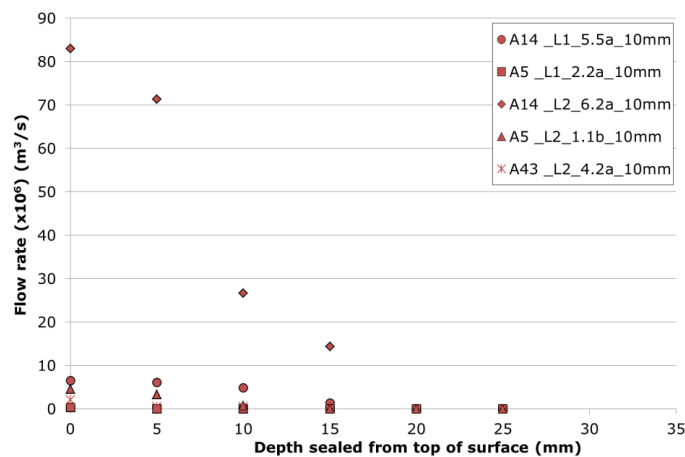
Appendix B-2 Hydraulic permeability measurements for 10 mm thin surfacings

Road surface properties and high speed friction
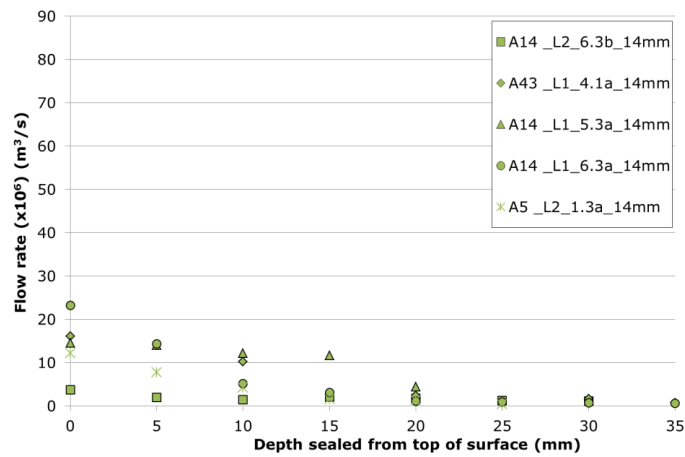
Appendix B-3 Hydraulic permeability measurements for 14 mm thin surfacings
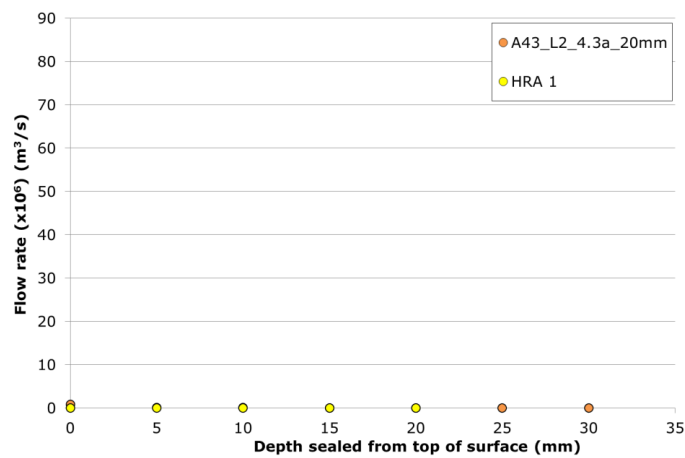
Appendix B-4 Hydraulic permeability measurements for a 20 mm thin surfacing and a HRA surfacing

Appendix B

Sanders, P. D. (2017), *PPR894 Road surface properties and high speed friction - The effect of permeability.* TRL, Wokingham, England.

PUBLISHED PROJECT REPORT PPR894

Road surface properties and high speed
friction - The effect of permeability

P D Sanders

Report details

Report prepared for:	Highways England, Pavements
Project/customer reference:	519(4/45/12)HALC
Copyright:	© TRL Limited
Report date:	2017
Report status/version:	Final
Quality approval:	
Peter Sanders (Project Manager)	**Approved**	Martin Greene (Technical Reviewer)	**Approved**

Disclaimer

This report has been produced by TRL Limited (TRL) under a contract with Highways England. Any views expressed in this report are not necessarily those of Highways England.

The information contained herein is the property of TRL Limited and does not necessarily reflect the views or policies of the customer for whom this report was prepared. Whilst every effort has been made to ensure that the matter presented in this report is relevant, accurate and up-to-date, TRL Limited cannot accept any liability for any error or omission, or reliance on part or all of the content in another context.

When purchased in hard copy, this publication is printed on paper that is FSC (Forest Stewardship Council) and TCF (Totally Chlorine Free) registered.

Permeability and high speed friction

TRL

Table of Contents

Executive summary

In the UK the risk posed to motorists from low levels of pavement skid resistance is managed through a policy that requires direct measurement of sideway-force skid resistance, the inference of high speed friction through the measurement of road surface texture depth, and the provision of appropriately selected aggregates. The ability to infer high speed friction was a result of work published in TRL report 367 (Roe, et al., 1998) which provided a relationship between texture depth and high speed friction.

It has been shown that the relationship developed as part of TRL report 367 is capable of characterising the performance of the majority of surfacing materials, but not all. Some porous asphalt surfacings and small aggregate thin surface course systems do not follow the same texture/friction relationship as the majority of surfacing types, leading to the under-prediction of the performance of these materials.

This study follows on from an initial study into the performance of the materials mentioned above reported in TRL report PPR727 (Sanders, et al., 2014). Based on the work reported in PPR727 the following hypothesis was formed; a pavement may remove water from the tyre road interface either via the surface texture depth or through the internal permeability of the surfacing; both mechanisms aid the pavement in providing high speed locked-wheel friction. It is the aim of the work reported here to test this hypotheses through the following research tasks:

- Completion of a laboratory study initiated as part of the work reported in PPR727. The laboratory testing was aimed at characterising the permeability of a variety of thin surface course systems.

- Quantify the relationship between texture depth, permeability and high speed friction. This was achieved by using the results of the laboratory measurements and from full scale measurements of texture depth and high speed friction.

- Validate the results from the laboratory and full scale testing. This was carried out by imaging the internal structure of the specimens assessed using a CT scanner. The images were used to quantify the amount of voids through which water could escape the tyre surface interface.

From the work carried out the following conclusions can be made:

- A key characteristic influencing high speed locked-wheel friction in wet conditions is the ability of the pavement to remove water from the tyre / road interface.

- The major pathway for water removal from the tyre / road interface is through the surface texture, but the inter-connected void network can provide additional drainage routes.

- There is an indication that pavements with a large percentage of voids inevitably possess a large number of inter-connected voids.

- There is the possibility of amending current standards which require measurements of high speed friction, to allow an inference of high speed friction based on the measurement of texture and permeability.

1 Background and introduction

This chapter summarises salient historical research and current UK standards to add context to the work. The aims of the research are presented at the end of the chapter.

1.1 The relationship between texture depth and high speed friction

Fundamental research into road surface properties and pavement skid resistance was carried out in 1966 and is reported in RRL report No. 20 (Sabey, 1966). This research demonstrated a tentative correlation between the texture depth of road surfaces, (measured using the volumetric patch test), and skid resistance, (measured using the small braking force trailer). Figure 1-1 is a replication of the results reported in RRL20, a positive trend is observed between texture depth and braking force, particularly at higher speeds.
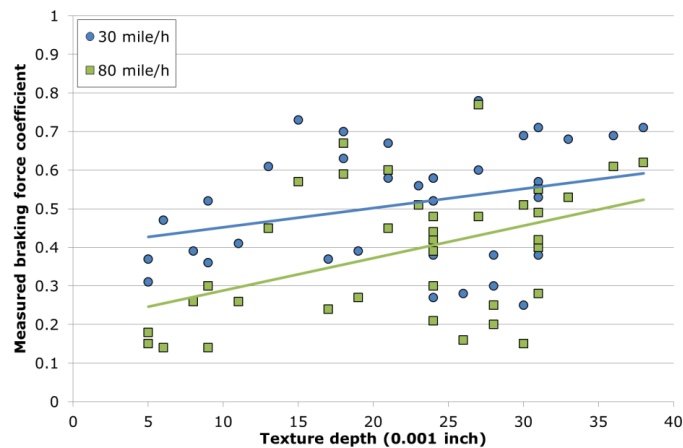
Figure 1-1 Comparison between texture depth and braking force coefficient, replicated from (Sabey, 1966)

Based on these results, Sabey concluded that:

"Very large decreases in coefficient between 30 and 80 mile/h can be expected when the texture depth is less than 0.010 in, however high the coefficient is at 30 mile/h. In order to restrict the decrease to 25 percent it appears that, on average, texture depths greater than 0.025 in are desirable." (Sabey, 1966).

Subsequent research was conducted in the USA in 1978 by Leu and Henry (1978) who conducted a statistical analysis of high speed friction, texture depth and microtexture measurements made on 20 locations in West Virginia in 1976. The researchers found correlations between texture depth, microtexture, speed and friction. The result of the work was the formulation of a friction prediction model commonly known as the Penn State model.

$$SN = SN_0 exp[-(PSNG/100) \times V]$$

Where:

- SN_0 = zero speed intercept (related to microtexture)
- PSNG = Percentage speed number gradient (related to texture depth)

Equation 1-1 The Penn State model (Leu & Henry, 1978)

Further research was conducted in 1998 by Roe, Parry and Viner and is reported in TRL report 367 (Roe, et al., 1998). This work consisted of making measurements of texture depth (using the Sensor Measured Texture Depth (SMTD) method (section 2.4)), side-force coefficient (using the side-force method (section 2.3)) and high speed friction (using the Pavement Friction Tester (PFT) (section 2.2)). The measurements made were used to develop a model capable of predicting locked-wheel friction at 100 km/h (L-Fn100) based on measurements of side-force coefficient and texture depth, Equation 1-2.

$$L - Fn100 = aSR + b(1 - e^{SMTD}) + c$$

Where:

- a, b and c are the model coefficients[1]
- SR represents the side-force coefficient measured using SCRIM
- SMTD is the texture depth of the surface measured using the SMTD method.

Equation 1-2 Prediction for L-Fn100 (Roe, et al., 1998)

It is interesting to note that the exponential function is raised to a power proportional to texture depth in both Equation 1-1 and Equation 1-2.

1.2   The identification of outlying materials

An additional observation from the work reported in TRL367 is shown in Figure 1-2 which shows the individual texture and high speed friction measurements made, categorised by material type. In general the measurements are concentrated in a narrow band which increases linearly between 0 and 0.70 mm SMTD and is flat thereafter. However the group of points at approximately 0.75 mm SMTD and 0.50 Fn at 100 km/h are outlying from the main band of measurements. The report authors noted that:

"It is possible that there are some different mechanisms involved in that way in which these materials interact with the tyre to generate friction. However it is more likely that, however it is that SMTD measures on porous surfacings, this measure of texture depth does not adequately represent the texture. For example, such surfacings have clearly have a greater

---

[1] The model coefficients were not stated in TRL367 but these have been provided by one of the authors, a = 0.00337, b = 0.411 and c = -0.151.

drainage potential than SMTD (or sand patch) measurements of texture depth can quantify."
(Roe, et al., 1998)
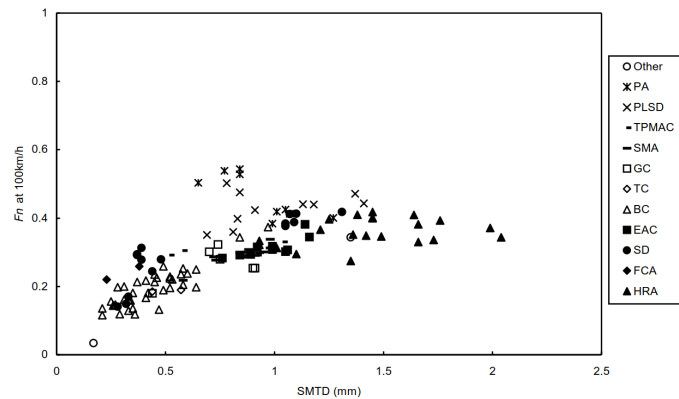
Figure 1-2 Comparison of texture and high speed friction (Roe, et al., 1998)

Research reported in TRL report PPR564 (Roe & Dunford, 2012) has identified another material type, a 6 mm Thin Surface Course System (TSCS), which displays similar properties to the porous asphalt identified in TRL367. This work made measurements of high speed friction (using the PFT) and texture depth (using the SMTD method) on TSCSs with different course aggregate sizes. A summary of the measurements made as part of PPR564 is replicated from the original data in Figure 1-3. Included in this figure are the data from TRL367, represented by the grey series markers.
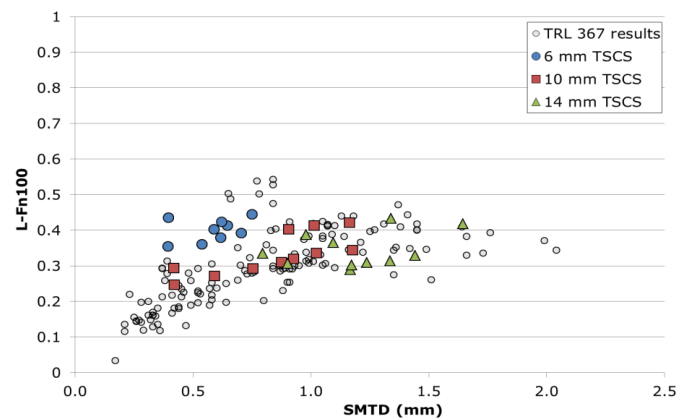
Figure 1-3 Texture and high speed friction on different TSCS materials, replicated from (Roe & Dunford, 2012) and (Roe, et al., 1998)

Figure 1-3 shows that, of the materials assessed, the materials constructed from the 10 mm and 14 mm nominal aggregate sizes are performing within the range of the results from the study reported in TRL367. The materials using a nominal 6 mm aggregate size are showing a similar performance to the outlying measurements to the TRL 367 results in that they are providing higher levels of friction than would be expected from their texture depth values.

1.3 Current UK texture depth requirements

1.3.1 Initial texture depth requirements

In the light of the findings of PPR564 the standards governing the application of TSCS materials, the MCHW 900 series (2008) were updated by way of an Interim Advice Note (IAN) in 2012. IAN 154/12 (2012) allows the use of lower levels of texture depth on 6 mm thin surface course systems than were required before the publication of PPR564. Table 1-1 and Table 1-2 present the pertinent texture information from IAN 154/12; the bold boxes in both tables represent the information pertaining to 6 mm TSCSs.

Table 1-1 Requirements for initial texture depth for trunk roads including motorways (MCHW 900 series) and (IAN 154/12)

Road	Average MTD per 1,000 m section, mm	
	MCHW 900 Series	IAN154
High speed roads Posted speed limit ≥ 50 miles/hr (80 km/h)	≥1.3	≥1.0 and ≤1.5
Lower speed roads Posted speed limit ≥ 40 miles/hr (65 km/h)	≥1.0	≥1.0 and ≤1.5
Roundabouts on high speed roads Posted speed limit ≥ 50 miles/hr (80 km/h)	≥1.2	≥1.2 and ≤1.7
Roundabouts on lower speed roads Posted speed limit ≥ 40 miles/hr (65 km/h)	≥1.0	≥1.0 and ≤1.5

Table 1-2 Requirements for retained texture depth for trunk roads including motorways (MCHW 900 series) and (IAN 154/12)

Surfacing type	Average MTD per 1,000 m section, mm[A]	
	MCHW 900 Series	IAN154
Hot applied thin surface course systems with an upper (D) aggregate size of 14 mm	1.0	0.9
Hot applied thin surface course systems with an upper (D) aggregate size of 10 mm	1.0	0.8
Hot applied thin surface course systems with an upper (D) aggregate size of 6 mm	1.0	0.7[B]

A - or the complete carriageway lane where this is less than 1,000 m.

B - Verification of high speed friction performance required.

Table 1-1 and Table 1-2 demonstrate the relaxing of requirements applied to 6 mm TSCSs; this relaxation was granted on the basis of the research presented at the start of this chapter. However, full confidence in the performance of the 6 mm TSCSs could not be established as part of the previous work and in order to fail safe, the requirement was added for these materials to demonstrate their high speed friction performance after being laid.

1.3.2 *In service requirements*

The in-service performance of road pavements in the UK is governed by the documents comprising the Design Manual for Roads and Bridges (DMRB). HD 29/08 (2008) of the DMRB provides details of the texture depth requirements. In summary a TRAffic speed Condition Survey (TRACS) survey makes SMTD measurements which are compared to threshold values (shown in Table 1-3) which define the deterioration category of the road (described in Table 1-4).

Table 1-3 Texture depth category thresholds (HD 29/08)

Category	1	Threshold value	2	Threshold value	3	Threshold value	4
Texture depth (mm)							
Anti-skid surfacing (HFS)		0.6		N/A		N/A	
All other surfaces		1.1		0.8		0.4	

Table 1-4 TRACS category definitions (HD 29/08)

Category	Description
1	Sound – no visible deterioration.
2	Some deterioration – lower level of concern. The deterioration is not serious and more detailed (project level) investigations are not needed unless extending over long lengths, or several parameters are at this category at isolated positions.
3	Moderate deterioration – warning level of concern. The deterioration is becoming serious and needs to be investigated. Priorities for more detailed (scheme level) investigations depend on the extent and values of the condition parameters.
4	Severe deterioration – intervention level of concern. This condition should not occur very frequently on the motorway and all purpose trunk road network as earlier maintenance must have prevented this state from being reached. At this level of deterioration more detailed (scheme level) investigations should be carried out on the deteriorated lengths at the earliest opportunity and action taken if, and as, appropriate.

As can be deduced from Table 1-3 and Table 1-4, in order for a road to require no further investigation, it must provide a texture depth (SMTD) of 0.8 mm or greater. However as demonstrated by Figure 1-3 only the best performing 6 mm TSCS materials are likely to provide this level of texture depth. Furthermore, there is no mechanism within this

standard to account for the improved high speed friction performance demonstrated by these materials.

1.4 Initial investigation

An initial investigation into the behaviour of these 6mm TSCS materials was commissioned in 2013 with a view to developing a new texture depth characterisation that would account for the discrepancy in friction performance. This work was reported in TRL report PPR727 (Sanders, et al., 2014).

The investigation utilised historical high speed friction measurements collected using the PFT. These measurements were made on a variety of sites containing thin surface course materials. In the work reported in PPR727 these high speed friction measurements acted as reference measurements, against which various pavement parameters would be assessed.

The work showed that it was not possible to identify a texture measurement technique capable of fully characterising the performance of 6 mm TSCS materials. As part of that study a small number of laboratory assessments were carried out into the relationship between the porosity of the specimens and their high speed friction. The results of this aspect of the study were positive and indicated that with further porosity assessments the nature of the performance of 6 mm TSCS materials might be understood. It is the aim of the work reported in this document to complete the further work recommended by the initial investigation.

1.5 Research aims

The hypothesis for this work is that a pavement may remove water from the tyre road interface either via the surface texture depth or through the internal permeability of the material; both mechanisms aid the pavement in providing high speed locked-wheel friction.

Testing of this hypothesis was undertaken through the following research tasks:

- Completion of the laboratory assessments initiated as part of the work reported in PPR727.

- Quantifying the relationship between texture depth, permeability and high speed friction.

- Validating the results from the laboratory and full scale testing by imaging the internal structure of the specimens used in the laboratory testing.

2 Completion of the texture, permeability and high speed friction assessment

The data used for this work were originally collected as part of the works reported in PPR324 (Roe, et al., 2008), PPR564 (Roe & Dunford, 2012) and PPR727 (Sanders, et al., 2014). The following sections present the measurement methods used for each of the material properties and summarise the materials assessed.

2.1 Materials assessed

The materials assessed for this work were originally the subject of research published in PPR324 (Roe, et al., 2008) which provides detailed information for each of the materials. The materials were all laid between 2005 and 2007 at various locations in the UK, detailed site maps are provided in Appendix A and Table 2-1 provides a summary. All of the materials are TSCSs utilising different nominal coarse aggregate sizes.

Table 2-1 Summary of materials assessed

Site Number	Section	Coarse aggregate size (mm)	Lane(s)	Road	Direction	Location
1	1	10	1 & 2	A5	WB	Gibbet Hill, Lutterworth, Leicestershire
	2	6				
	3	14				
2	1	14	1 & 2	A5	WB	Tamworth, Staffordshire
	2	10				
3	1	14	1	A14	WB	Creeting St Mary, Suffolk
	2	10				
	3	6				
4	1	14	1 & 2	A43	NB	Brackley, Northamptonshire
	2	10				
	3	20				
	4	6				
5[2]	1	6	1	A14	EB	Thrapston, Northamptonshire
	2	10				
	3	14				
	4	6				
	5	10				
	6	14				
6	1	6	1 & 2	A14	EB	Stanford-on-Avon, Northamptonshire
	2	10				
	3	14				

[2] This site contains two material types with the same coarse aggregate size.

To allow for laboratory assessment, two specimens (150mm diameter cores) were removed from each section. The specimens were removed after the collection of high speed friction, side-force skid resistance, and texture information. In total, 60 specimens were used in this work for the assessment of pavement porosity. For clarity, the pavement from which individual cores were extracted will be referred to as the parent surface, and the cores, the specimens.

2.2   High speed friction

High speed friction measurements were made on each parent surface with the 1295 Pavement Friction Tester (PFT) (Figure 2-1), a locked-wheel friction testing device owned by Highways England and operated on their behalf by TRL. The PFT consists of a tow vehicle (1995 Chevrolet Silverado), and test trailer which employs the locked-wheel technique allowing it to measure the friction generated between the test tyre and road surface throughout the complete braking cycle. This allows the determination of the peak[3] and locked-wheel[4] friction for the speed at which the test was carried out.

Figure 2-1 The Pavement Friction Tester (PFT)

Measurements were made under the advice of ASTM E-274 (ASTM, 2011) using the tyre specified in ASTM E-524 (ASTM, 2008). Wet conditions were achieved by pumping water (from a tank in the tow vehicle), at a controlled rate. This results in a nominal water film of 1.0 mm between the tyres contact point and pavement surface.

---

[3] The maximum amount of friction generated between the tyre and surface.

[4] The amount of friction generated between the tyre and surface when the test wheel is in the fully locked condition.

Peak and locked-wheel friction were measured at various speeds ranging from 20 km/h to 120 km/h. A regression analysis was then used to identify the locked-wheel friction values at 100 km/h reported as L-Fn100. The use of the L-Fn100 allowed the measurements to be compared with the results of TRL367.

2.3 Side-force coefficient

The Sideway-force Coefficient Routine Investigation Machine (SCRIM) is the standard device for monitoring the side-force coefficient condition of the UK trunk road network, and is also used by many local authorities. Figure 2-2 shows the Highways England SCRIM which was used for this work, this device has now been decommissioned.

Figure 2-2 The Highways England SCRIM device

SCRIM uses a smooth test tyre angled at 20 degrees to the direction of travel, mounted on an instrumented axle to record a SCRIM Reading (SR) for every 10 m length of road. The SR is the average ratio between the measured sideway-force and the vertical load, which is dynamically measured, multiplied by 100. Measurements of sideway-force coefficient were made using SCRIM on each of the parent surfaces. The measurements were made at a test speed of 50 km/h and are reported in this document as SR(50).

2.4 Texture depth

Measurements of texture depth were made on each parent surface using the Sensor Measured Texture Depth (SMTD) method. The SMTD method uses a triangulation laser fitted to a vehicle (the HE SCRIM device) to make measurements of the displacement between the sensor receiver and road surface as the vehicle travels down the road at traffic speed. The distance measurements are combined with speed information to provide a two dimensional profile of the road surface. SMTD values were provided as 10 m average values and the mean of these values was used as the indicative texture depth of each section.

143

2.5   Permeability

The assessment of pavement permeability was carried out on the specimens removed from each of the sites in Table 2-1. The methodology described in BS EN 12697-19:2012 (British Standards, 2012) was used. This methodology can be summarised as applying a constant hydrostatic head of water to the surface of each specimen and allowing the water to exit the specimen through the side only. The permeability of the specimen was calculated by collecting the ejected water over a known period of time and recording the mass of the collected water.

To achieve this, a steel tube was bonded to a specimen surface, and the outside edge of the top of the specimen was sealed using silicone sealant. This isolated the surface texture and allowed water to escape the surface only through the specimen. The bottom of the specimen was also sealed to reduce any effect of drainage relating to variations in the amount of binder course still attached to the surface course.

Water with a constant hydrostatic head of 2.94 N/m^2 was fed into the steel tube and allowed to flow through the specimen to saturate the voids in the specimen. Once saturated, the water flowing out of the specimen was collected over a known period of time and the flow rate calculated using the mass of the collected water. The resulting volumetric flow rate is therefore indicative of the amount of horizontal permeability within the specimen which in turn is a characterisation of the amount of inter-connected voids in the specimen. The equipment used is shown in Figure 2-3.
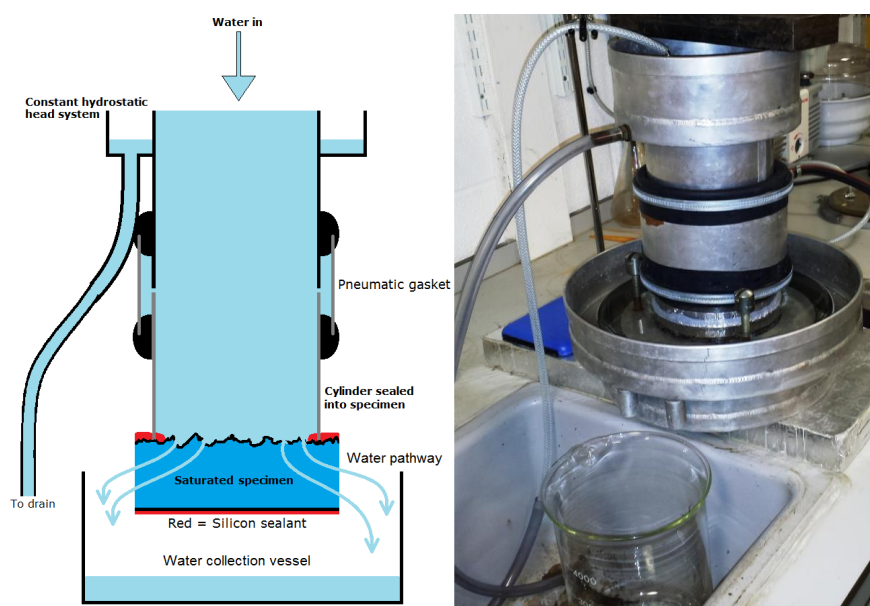
Figure 2-3 Representation of hydraulic permeability setup (left) and the equipment used

3   The relationship between texture depth, permeability and high speed friction

The results from the permeability, high speed friction and texture depth measurements are presented graphically in Figure 3-1, included with these results are the measurements made as part of TRL367 to add context to the data. The colour of the series markers represents the coarse aggregate size and the shape the permeability of the specimen. The cluster of measurements representing the 6 mm TSCS materials has been highlighted by the red circle.
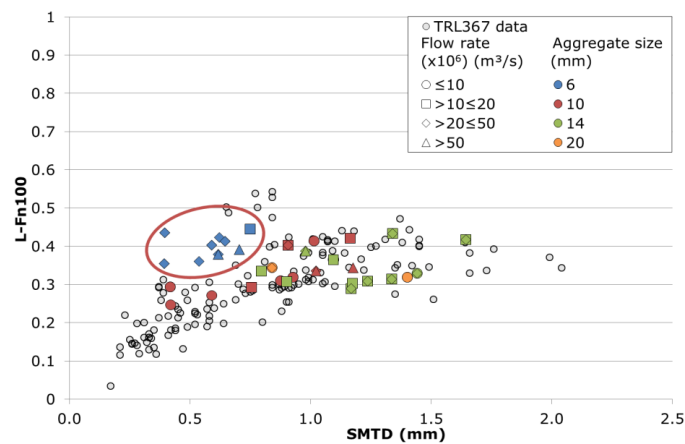
Figure 3-1 Relationship between texture, high speed friction and permeability

If the hypothesis forming the basis of this work is true then it should be expected for the positions of the series markers to move closer to the bulk of the TRL367 measurements when the effects of texture depth and permeability are combined.

This assessment was carried out by augmenting the texture depth, side-force coefficient and friction relationship reported in TRL367 so that the effect of texture depth and permeability are considered additive, this is expressed in Equation 3-1.

$$Predicted\ L - Fn100 = 0.00337SR + 0.411\left(1 - e^{(SMTD+(x \times Flow))}\right) - 0.151$$

Where:

- SR represents the side-force coefficient measured using SCRIM

- SMTD is the texture depth of the (mm)

- x represents the magnitude of the effect of the permeability

- Flow is the flow rate derived from the permeability assessments (mm^3/s).

    Equation 3-1 Prediction of L-Fn100 from SR, SMTD and permeability

The magnitude of the effect of the permeability (x) was derived using the conversion of fixed point iteration process which compared the measured friction values with the friction values predicted from Equation 3-1 whilst varying the "x" constant. The best relationship between the measured and predicted values was identified with an x constant value of 10201 units. This has the following effect on Equation 3-1.

$$Predicted\ L-Fn100 = 0.00337SR + 0.411\left(1 - e^{(SMTD+(10201\times Flow))}\right) - 0.151$$

Equation 3-2 Prediction of L-Fn100 from side-force coefficient, texture depth and permeability with the derived magnitude of flow rate

To demonstrate the effect of permeability, Figure 3-2 shows the friction and texture relationship but the primary x-axis units have been changed to include the flow rate term used in Equation 3-2, the TRL367 data are presented on the secondary x-axis which reports texture depth only. The red circle highlights the position of the 6 mm TSCS when texture depth only is considered so that the change in characterisation can be easily observed.
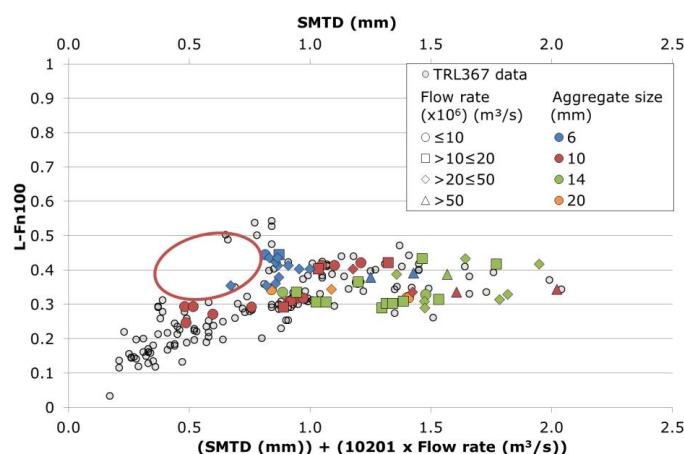
Figure 3-2 Relationship between texture, high speed friction and corrected permeability

The most notable aspect of Figure 3-1 and Figure 3-2 is that the group of 6 mm surfacings (the blue series) have moved out of the red circle and closer to the bulk of the measurements. The positions of other high flow rate materials (the diamond and triangle series) have also moved to the right of the x-axis. Lower flow rate materials however (the round and square series) have moved relatively little.

These observations are in agreement with the original hypothesis and demonstrate a good correlation between the combined effects of texture depth and permeability.

4 Further investigations into permeability

The data presented in Chapter 3 demonstrate a correlation between texture depth, permeability and friction. Furthermore, being a wet test, the horizontal permeability methodology directly links the permeability of the specimens with their ability to remove water from the pavement surface. In order to gain a fuller understanding of permeability, further investigations were carried out into the internal structure of the materials assessed. This chapter presents the findings of a study utilising Computational Topography (CT) to investigate the internal void network of the materials.

This investigation aimed to quantify the relationship between the inter-connectivity of the void network and the total number of voids in the materials assessed. Furthermore this investigation sought to understand the relationship between the interconnectivity of the void network and the flow rates observed from the laboratory testing.

4.1 Materials assessed

Project constraints limited the number of CT assessments that could be carried out, so to gain the most value from the assessments the following specimens were selected:

- Site 6, Section 2, 10mm, Lane 2, Specimen 1 – Highest permeability
- Site 4, Section 3, 20mm, Lane 1, Specimen 2 – Lowest permeability
- Site 5, Section 1, 6mm , Lane 1, Specimen 2 – Permeability closest to the mean
- Site 4, Section 4, 6mm, Lane 1, Specimen 2 – Low texture depth and high friction
- Site 4, Section 2, 10mm, Lane 1, Specimen 1 - Low texture depth and low friction

Figure 4-1 shows the performance of the materials selected. The diamond series markers represent the texture depth performance of the specimen only. The circular markers represent the performance of the specimens when texture depth and permeability are combined, large changes in performance are indicated by the black arrows.
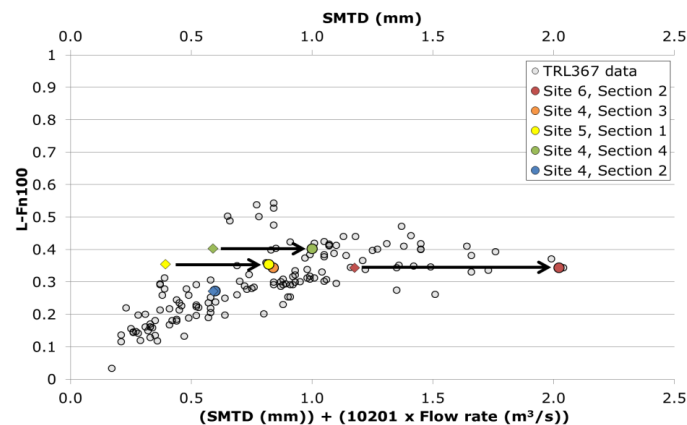
Figure 4-1 Texture depth, permeability and high speed friction of selected specimens

4.2   Measurements made

Computational topography utilises multiple x-ray images which, when combined, provide a three dimensional representation of the internal structure of an object. The collection of x-ray images can be thought of in a similar way to that of photography as both systems utilize the properties of the electro-magnetic spectrum of radiation. In photography a light source emits visible light (wavelength 400 nm to 700 nm) which is partially absorbed and partially reflected by the target object, the reflected light is then captured by a detector in a camera creating a photograph.

The same is true for x-ray imaging, a radioactive source emits x-rays (wavelength 0.01 nm to 10 nm), however because of their shorter wavelength than visible light, some x-rays are absorbed and some pass through the target. The x-rays that pass through a target are captured by a detector creating an image that reveals the internal structure of the target; such an image is known as a radiograph (Figure 4-2). When a number of radiographs are collected at different angles to the target, they can be combined using image processing software to create a three dimensional description of the target.

4.2.1   Specimen preparation and equipment setup

The assessment of road surfacings by CT is relatively rare and so some initial investigations were required to identify the best setup for image collection. Initial imaging was carried out on the specimens used for the permeability testing (150 mm diameter cores). However, it became evident that the density of the specimens was so great that the x-rays could not provide the contrast required for CT. To obtain the required contrast three procedures were carried out:

1. The specimens were mounted at a 30 degree angle to the radiation source to reduce the thickness of material at certain angles of rotation.

2. An 8mm tin filter was added to the radiation source to allow only the highest energy x-rays to be captured by the detector.

3. The specimens were re-sized to a diameter of 100 mm, reducing the overall volume of material.

The effect of these changes was substantial and allowed the collection of high contrast images for analysis.

4.2.2   Image capture

The imaging of the specimens was conducted at the Nikon metrology laboratory in Hertfordshire, UK, using the XT H 450 system. This system utilises a 450 kV radiation source and is capable of producing images to a repeatability and accuracy of 25 microns. To provide sufficient images for CT analysis, 3064 radiographs were made of each specimen by rotating the specimen about an axis perpendicular to the source; one radiograph was therefore made every 0.12 degrees. An example of this is given in Figure 4-2.

Figure 4-2 Example of a captured radiograph (Site 4, Section 3)

The collection of radiographs were then combined using Volume Graphics VGStudio MAX software to create a three dimensional representation of the specimen, this is known as a reconstruction. Figure 4-3 gives an example of the reconstruction for the Site 4, Section 3 specimen. The bottom right panel provides a representation of the exterior of the specimen. The top left, top right and bottom left panels represent the top, side and front view of the specimen in relation to the orientation shown in the bottom right panel. Each slice represents the internal structure of the material at a certain plane in the specimen's depth.
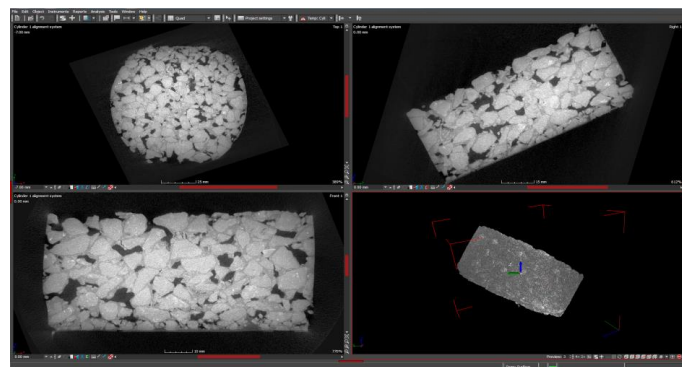
Figure 4-3 Reconstruction of the Site 4, Section 3 specimen

The front slice of the reconstruction is presented in larger scale in Figure 4-4. This level of detail clearly shows the three elements of the material, the aggregate, bitumen binder and air voids, as highlighted by the arrows. The white specks in the image are metallic features within the aggregate particles.

It is interesting to note that the left and right edges of the specimen appear slightly distorted. This is an effect of the imaging process known as "top hatting" and is related to the scatter of x-rays at the edges of dense materials.
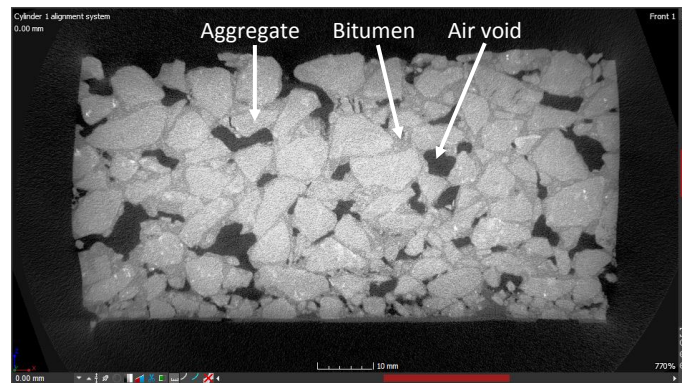
Figure 4-4 Front panel (bottom left) from Figure 4-3

4.3   Image processing

In order to characterise the properties of the specimens, six images were taken from the reconstructions of each specimen. Images were taken from the front perspective of the specimen with the vertical axis set so that it was nominally perpendicular to the surface of the specimen. The depth of the image slice was set so that the middle of the specimen was viewed. This allowed the specimen to be rotated about the vertical axis and images taken at 30 degree increments of rotation. All of the images taken were on the scale of 27 pixels / mm to ensure geometric consistency.

For each of the gathered images the following process was followed in order to determine the area of each image relating to:

- Material, aggregate or bitumen

- A connected air void, an air void that connects to the surface through the network of inter-connected voids

- An isolated air void, an air void that does not connect to the surface, but may be part of a network of inter-connected voids

Cropping and rotation

The first step was to rotate the images so that any variations in the angle of the surface relative to the vertical axis were removed. This was carried out by using the Adobe Photoshop CS2 image processing suite to rotate the image until the surface was horizontal. The image was then cropped so that the following conditions were met:

- The distance between the top of the highest aggregate protrusion and the top of the image was 0.5 mm

- The width of the image represented the middle 90 mm of the specimen

- The height of the image equated to 40 mm

This process ensured that all of the images assessed were representative of the same amount of each specimen. A secondary effect was to reduce the top hating effect by cropping the distorted edges. An example of a captured, and cropped and rotated image is provided in Figure 4-5 and Figure 4-6.
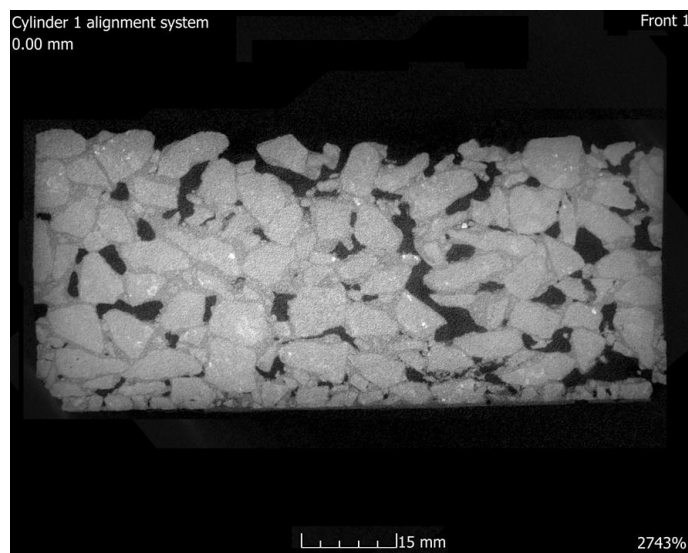
Figure 4-5 Example of a captured image
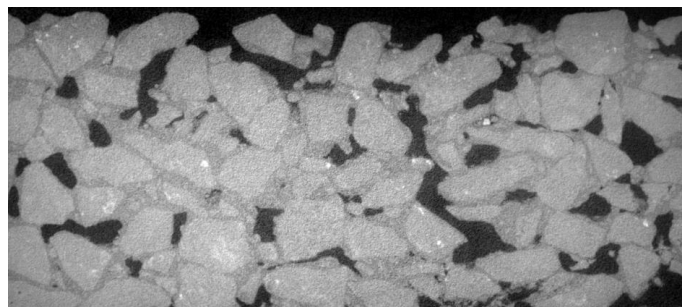
Figure 4-6 Example of a cropped and rotated image

151

TRL

Conversion to a binary image

The cropped and rotated images were then converted to a black and white image such that white areas represented the material and black areas represented air voids. Differences in image contrast between the edges and centre of the image meant that a single threshold could not be applied to identify dark (air voids) and light (material) regions. To overcome this issue a manual operation was used utilising the "Magic wand tool" in the Photoshop CS2 suite. The tool was set to a tolerance of 80% and the middle of an air void region selected. The magic wand tool then selected an area of pixel intensity values within 80% of the selected value. The luminosity of the selected area was then reduced so that the void was represented by an area of zero value intensity pixels.

This procedure was repeated for every air void location in every image. The final step of the procedure was to use the magic wand tool to select every non-zero pixel value (areas representing material). The luminosity of these areas was then increased so that they were represented by areas that were white. This process created a series of images as per the example in Figure 4-7

Figure 4-7 Example of a binary image

Tracing and void characterisation

The final stage of the image processing was to characterise the air voids into connected (a void that connects to the surface) and isolated (a void that does not connect to the surface). This characterisation was carried out manually using a process referred to here as tracing. During the tracing process if a void was identified as connected then it was coloured blue, and if it was identified as isolated it was coloured pink[5]. This created an image as per the example in Figure 4-8.

---

[5] The coloring process was carried out using the "fill" tool in Microsoft paint.

Using the Volume Graphics MyVGL software the tracing process was carried out on the reconstructed CT images using the following process:

- The orientation of the reconstructed specimen and slice depth was set to that of the original image.

- The slice step length was set to 0.10 mm.

- The operator selected a void to assess and incrementally increased the depth of the slice, following the progression of the void through the image until the edge of the specimen was found. If no connection to the surface could be found then the process was repeated but reducing the slice depth.

- If a connection between the selected void and the surface could be found then the void in the binary image was coloured accordingly.

This process was repeated for every void in every image. The resulting collection of traced images therefore contained three pieces of information, the vertical and horizontal geometry of the voids, and a binary representation of their connected states.
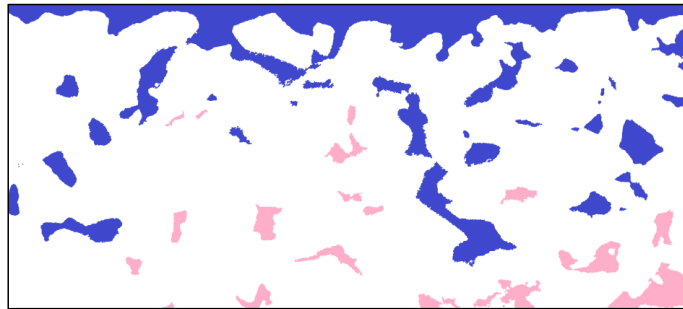
Figure 4-8 Example of a traced image

Conversion to numerical values

Following the image processing stages, the traced images were converted into a matrix of pixel intensity values using a bespoke software package. The matrices were created such that the position of the value in the matrix represented its location in the image and the magnitude of the value related to its colour:

- Blue (connected voids) = 339

- White (material) = 765

- Pink (isolated voids) = 630

153

4.4   Assessment of data

The matrices of pixel intensity values produced by the analysis of the CT images were used to characterise the following material properties for each specimen:

- the amount of material

- the amount of connected voids

- the amount of isolated voids

- the amount of total voids

Each material property was characterised by the average percentage of each image that represented the above properties.   The remainder of this section describes the characterisation process.

4.4.1   Quantification of surface effects

In order to ensure that only the internal structure of the material was included in the characterisations, it was necessary to quantify and remove any surface effects. For the purpose of this exercise a surface effect was considered as any void that could be viewed from a vertical viewpoint above the specimen. This is illustrated in Figure 4-9 which shows a traced image but the surface effects are presented in green.

Figure 4-9 Demonstration of the removal of surface effects

Quantifying these effects was achieved by counting the number of consecutive rows in a column that contained connected voids (a number of 339 in the matrix) starting from the top row. The sum of the row counts for each column provided the quantification of surface effects.

4.4.2 Quantifying the amount of material and void types

For each matrix the number of cells representing material, isolated voids and connected voids, and total voids were calculated by counting the number of cells in the image matrix equating to each of these states:

- Material (M) = number of cells with value "765"

- Isolated Voids (IV) = number of cells with value "630"

- Connected Voids (CV) = number of cells with value "339" minus the contribution of surface effects

- Total voids (TV) = number of cells with value of "339" or "630" minus the contribution of surface effects

Based on these values the Area Of Interest (AOI) (the amount of the image matrix not relating to surface effects) was calculated using Equation 4-1, this will act as a reference against which the percentage of the AOI represented by each of the above variables could be defined.

$$Area\ Of\ Interest\ (AOI) = M + IV + CV$$

$$\%\ of\ AOI\ containing\ variable = \frac{100 \times Variable}{AOI}$$

Equation 4-1 Calculation of AOI for a single matrix and the percentage of each variable that contributes to it

To gain an overall characterisation for each specimen, a mean of the percentage of the AOI represented by each variable was taken for all of the matrices representing a single specimen. These averages are the final characterisations that were used in the analysis stage:

- Average % material

- Average % isolated

- Average % connected

- Average % voids

A full account of the results of the analysis of CT images can be found in Appendix C. The following chapter presents the salient findings.

155

5 The relationship between internally connected voids, flow rate and total void content

The results of the CT imaging and laboratory testing were used to assess the relationship between the horizontal permeability of the specimens and the prevalence of interconnected voids. In addition the relationship between the prevalence of interconnected voids and all voids was assessed in order to further understand the behaviour of porous materials.

5.1 Connected voids and horizontal permeability

The relationship between the horizontal permeability of the specimens and their prevalence for possessing connected voids is shown in Figure 5-1. The black series markers represent the percentage of connected voids calculated from each of the six images taken from a specimen. The blue markers represent the mean of these measurements and the blue line is the line of best fit through the mean values.

There are two key features observed from Figure 5-1, the first is a large amount of scatter in the measurements made on individual images. This is particularly prevalent for the images assessed from the specimen taken from Site 5, Section 1 (permeability closest to the mean) where the percentage of connected voids was calculated between 2.4% and 9.4%. The observed scatter may be a product of the manual analysis of the images that was carried out through the tracing process. A computational approach may yield more repeatable results[6].

The second feature is that despite the scatter in the individual measurements a good correlation is observed between the average percentage of connected voids, and the horizontal permeability. This observation is key as it confirms that the mechanism of horizontal permeability is through the inter-connected void network of the specimens.
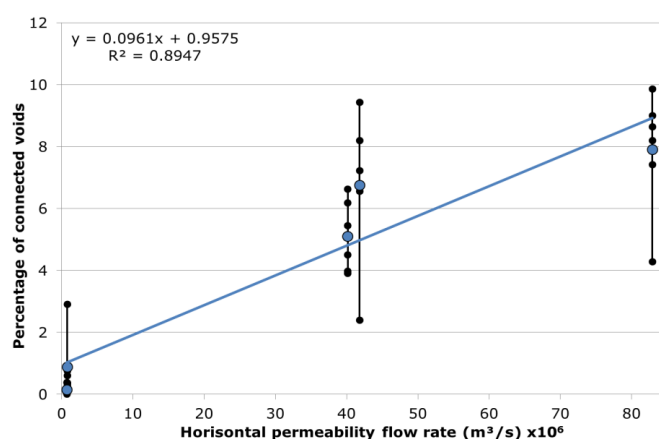
Figure 5-1 The relationship between horizontal permeability and connected voids

---

[6] A computational approach would take computing power several orders of magnitude greater than that which was immediately available and procuring such devices would have exceeded the financial limits of the project.

5.2   Connected voids and total voids

Figure 5-2 presents the relationship between the percentage of all voids in a specimen (connected and isolated) and the percentage of connected voids. The small diamond series represent measurements made on individual images taken from a specimen, and the large circles represent the average of the measurements for a specimen. The black line represents the line of best fit with the average values. The colour of the series is used to identify measurements made on different specimens.

The key observation from Figure 5-2 is an excellent relationship between the average of all voids and connected voids for the materials assessed. This observation suggests that because of the randomly orientated particles in road materials, pavements with high void contents have a greater chance of providing an inter-connected void network. Although this observation is made on a relatively small number of measurements, this could be a potentially valuable insight into the behaviour of porous materials.
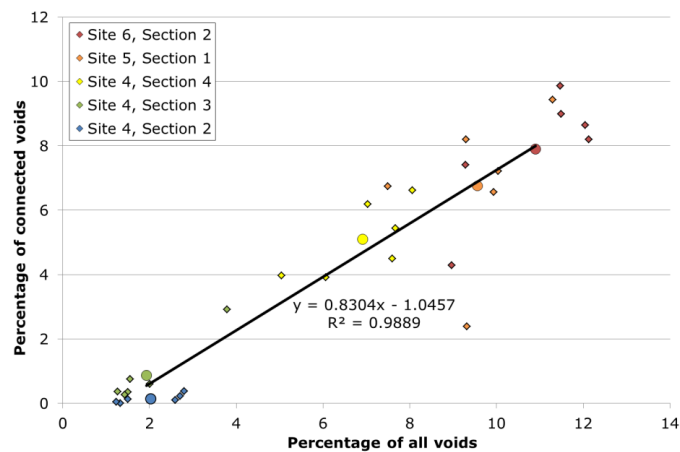
Figure 5-2 The relationship between all voids and connected voids

157

TRL

6 Discussion and conclusions

6.1 Permeability, texture depth and high speed friction

The key hypothesis for this work was that a pavement may remove water from the tyre road interface either via the surface texture depth or through the internal permeability of the surfacing; both mechanisms aid the pavement in providing high speed locked-wheel friction. Through the research tasks listed in chapter 1 this hypothesis has been shown to be valid.

The relationships observed between texture depth, horizontal permeability and high speed friction have demonstrated that the removal of water from the tyre surface interface is a key property in the generation of high speed friction. This has confirmed the previous thinking established in TRL367 (Roe, et al., 1998). For the specimens assessed the CT imaging has shown that the mechanism for the removal of water from the tyre surface interface is through an interconnected network of voids through the pavement structure.

The analysis of the CT images has also demonstrated the possibility that an inter-connected void network is an inevitable result of constructing pavements with a high void content. That is to say that pavements with a high void content will provide some voids which are isolated and some that are connected and that the greater the overall void content the greater the number of connected and isolated voids.

6.2 The characterisation of high speed friction performance

The current methodology used in the UK for mitigating the risks posed to motorists resulting from poor high speed friction relies on the relationship between texture and high speed friction developed in TRL367, which has shown to be inappropriate for some materials. However for the bulk of materials this relationship works well and fails-safe for those materials where the relationship is invalid.

The current methodology means that for certain materials the validation of high speed friction performance must be carried out directly by making measurements using specialist equipment. The methodology used in this work for characterising horizontal permeability may offer an alternative means of characterising the performance of these materials.

An alternative approach would be to allow the option of making measurements of texture depth and permeability in the place of high speed friction. For instance, materials with a texture depth of 0.40 mm SMTD could be accepted if their horizontal flow rate is within a certain range measured according to the technique described in BS EN 12697-19:2012[7].

A re-writing of the standards in this way would require careful consideration as although the relationships described here are robust and should provide a sufficient estimate of high speed friction, there are other properties related to permeability that could produce an adverse effect. One property requiring consideration is the durability of the structure of the pavement. Previous works have shown that porous pavements can be expected to provide lower service lives than non-porous pavements. This is due to the ingress of water into the

---

[7]The technique used to characterize horizontal flow rate for this work

pavement affecting the bonds between pavement particles through the freeze thaw effect or hydraulic pressure.

Another effect worth consideration is the longevity of the porosity of the pavement itself. It is possible that over time, detritus could cause the voids in a porous pavement to become clogged. In this case the ability of the pavement to remove water from the surface may be compromised, negating the benefits for high speed friction. This phenomenon may warrant further research to investigate the potential for this effect in different environments and the timescales evolved.

6.3   Conclusions

From the work carried out the following conclusions can be made:

- A key characteristic influencing high speed locked-wheel friction in wet conditions is the ability of the pavement to remove water from the tyre / road interface.

- The major pathway for water removal from the tyre / road interface is through the surface texture, but the inter-connected void network can provide additional drainage routes.

- There is an indication that pavements with a large percentage of voids inevitably possess a large number of inter-connected voids.

- There is the possibility of amending current standards which require measurements of high speed friction, to allow an inference of high speed friction based on the measurement of texture and permeability.

TRL

Bibliography

ASTM, 2008. *E524-08 Standard Specification for Standard Smooth Tire for Pavement Skid-resistance Tests,* West Conshohocken: ASTM.

ASTM, 2011. *E274/E274M-11 Standard Test Method for SkidResistance of Paved surfaces Using a full-Scale Tire,* West Conshohocken: ASTM.

British Standards, 2004. *BS EN ISO 13473-1:2004 Characterisation of pavement by use of surface profiles - Part 1 - Determination of MPD,* London: BSI.

British Standards, 2010. *BS EN 13036-1. Road and airfield surface characteristics - Test methods. Part 1: Measurement of pavement surface macrotexture depth using a volumetric patch technique,* London: BSi.

British Standards, 2012. *BS EN 12697-19:2012 Bituminous mixtures - test methods for hot mix asphalt part 19: Permeability of specimen,* London: BSI.

Highways England, Transport Scotland, Welsh Government, The Department for Regional Development Northern Ireland, 2008. *HD29/08 - Data for pavement assessment,* London: The Stationery Office.

Highways England, Transport Scotland, Welsh Government, The Department for Regional Development Northern Ireland, 2008. *Manual of Contract Documents for Highway Works (MCHW), Volume 2, Series NG 0900,* London: The Stationery Office.

Highways England, Transport Scotland, Welsh Government, The Department for Regional Development Northern Ireland, 2012. *Interim advice note 154/12,* London: The Stationery Office.

Leu, M. C. & Henry, J. J., 1978. *Prediction of skid resistance as a function of speed from pavement texture measurements,* Washington: Transportation Research Board.

Ordnance Survey, n.d. *Ordnance survey open data.* [Online]
Available at: http://www.ordnancesurvey.co.uk/oswebsite/opendata/
[Accessed 02 09 2011].

Roe, P. G. & Dunford, A., 2012. *PPR564 The skid resistance behaviour of thin surface course systems,* Wokingham: HA / MPA / RBA Collabarative Programme 2008-11: topic 1 prepared for Highways Agency, Minerals Products Association and Refined Bitumen Association.

Roe, P. G., Dunford, A. & Crabb, G., 2008. *PPR324 HA/QPA/RBA Collaborative Programme 2004/07: Surface requirements for asphalt roads,* Wokingham: TRL.

Permeability and high speed friction

Roe, P. G., Parry, A. R. & Viner, H. E., 1998. *TRL367 High and low speed skidding resistance: the influence of texture depth,* Wokingham: Prepared for Pavement Engineering Group, Highways Agency.

Sabey, B. E., 1966. *RRL20 Road surface texture and the change in skidding resistance with speed,* Wokingham: Road Research Laboratory.

Sanders, P. D., Morosiuk, K. & Peeling, J. R., 2014. *PPR727 Road surface properties and high speed friction,* Wokingham: TRL.

Viner, H. et al., 2006. *PPR148, Surface texture measurements on local roads.,* Crowthorne: TRL Ltd.

Appendix A   Site locations

This appendix presents the locations of the sites tested. Each map contains the lengths of each numbered section and the end of the last section, donated by the "E" marker.
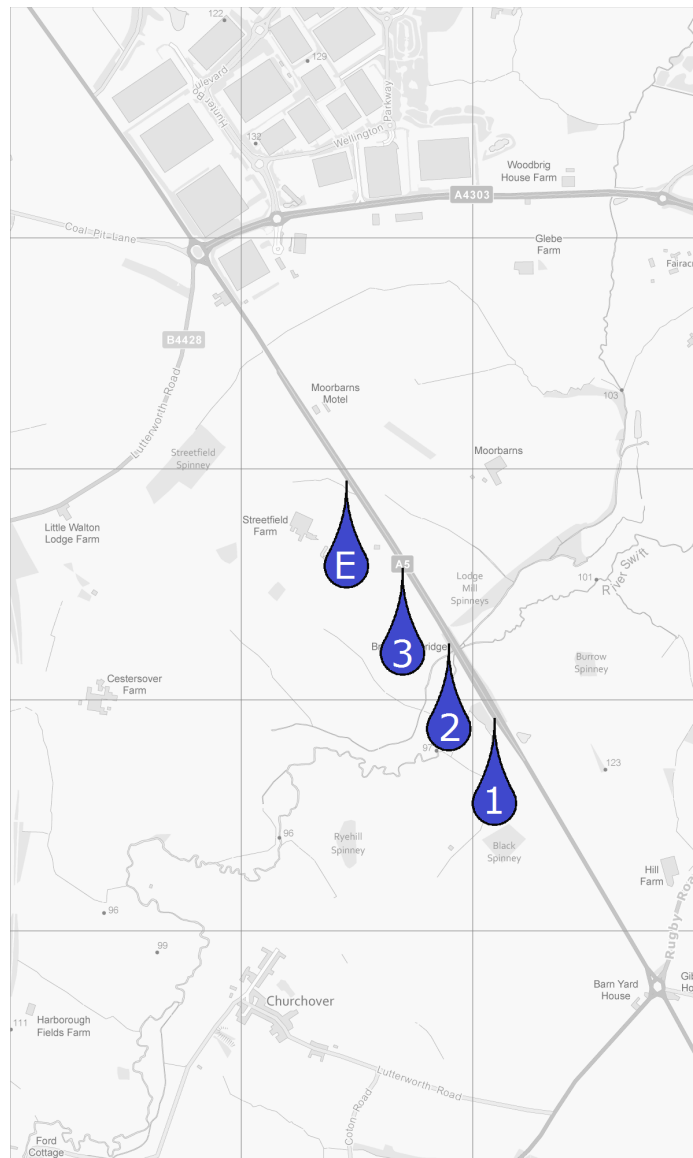
Figure B - 1 Site 1
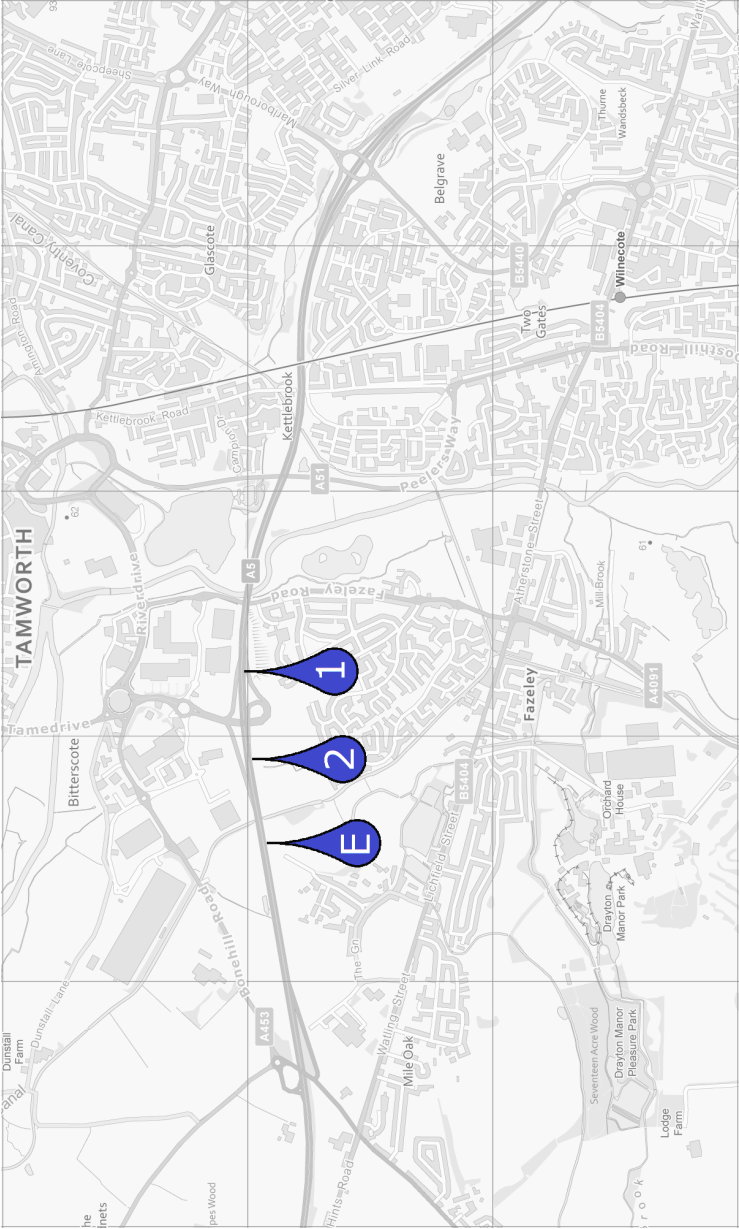
Permeability and high speed friction

Figure B - 2 Site 2

163

Figure B - 3 Site 3

Permeability and high speed friction

Figure B - 4 Site 4

33

Final
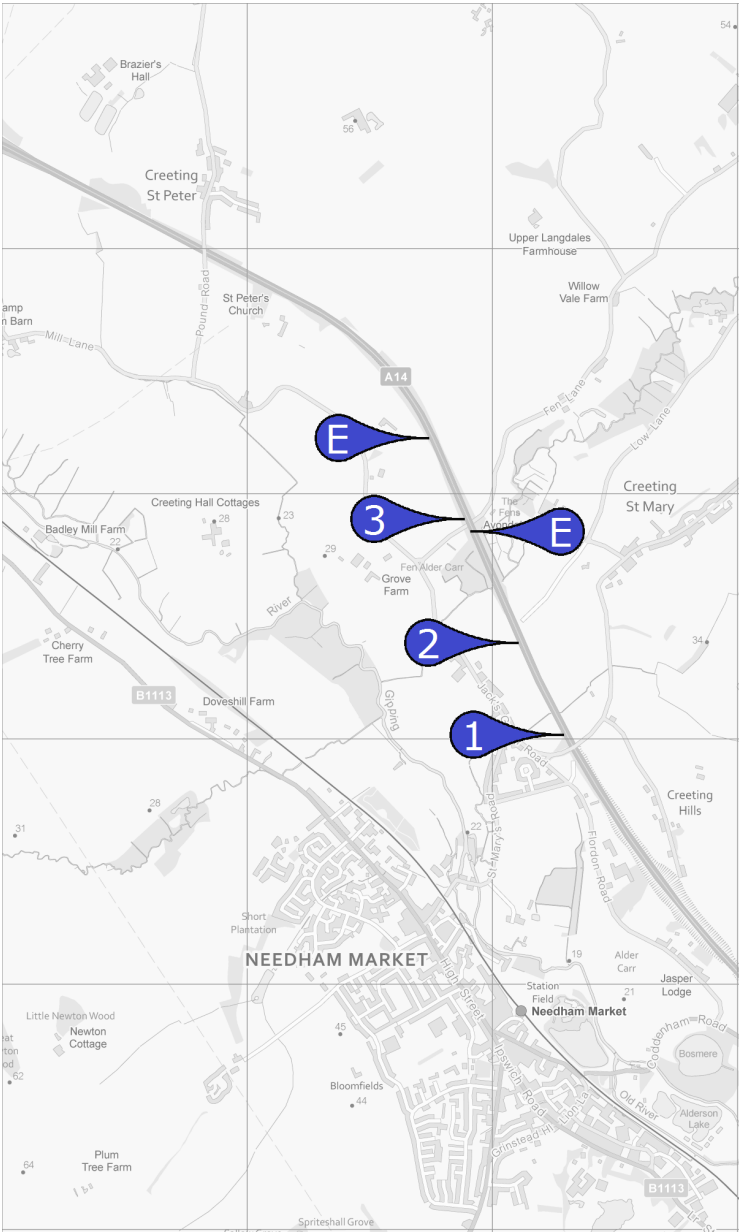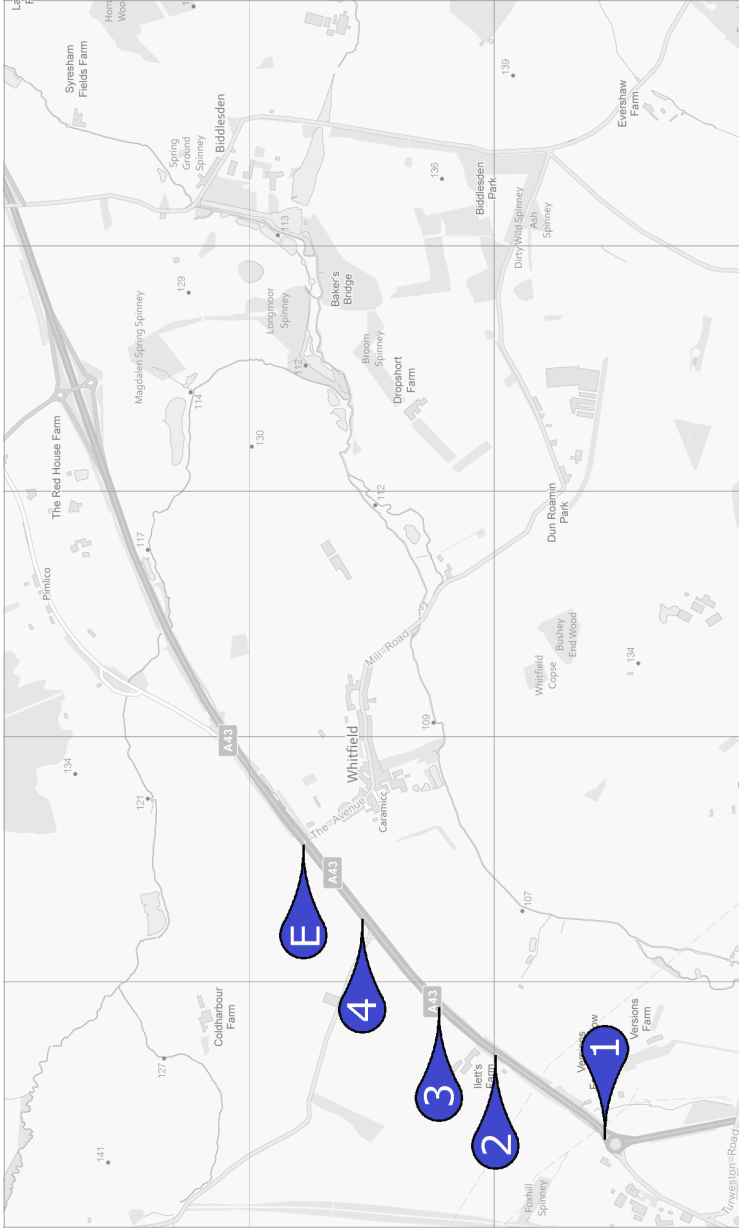
Permeability and high speed friction
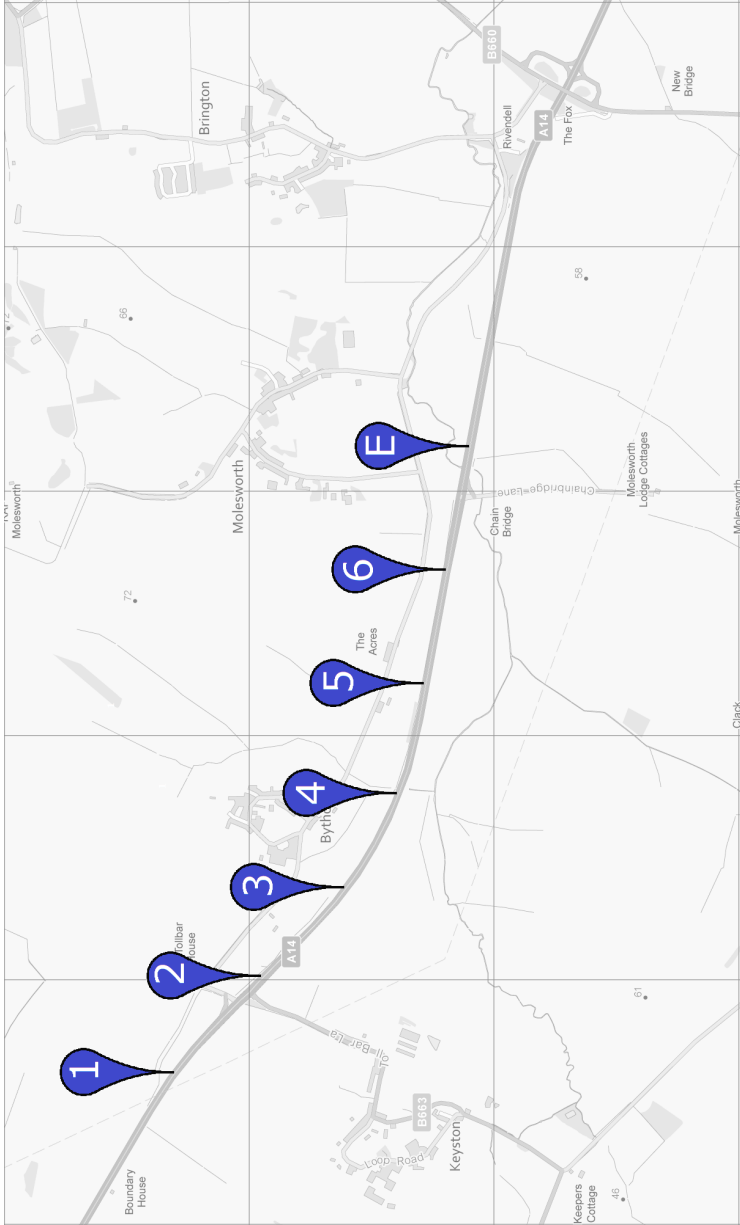
Figure B - 5 Site 5

Permeability and high speed friction

Figure B - 6 Site 6

PPR894

Final
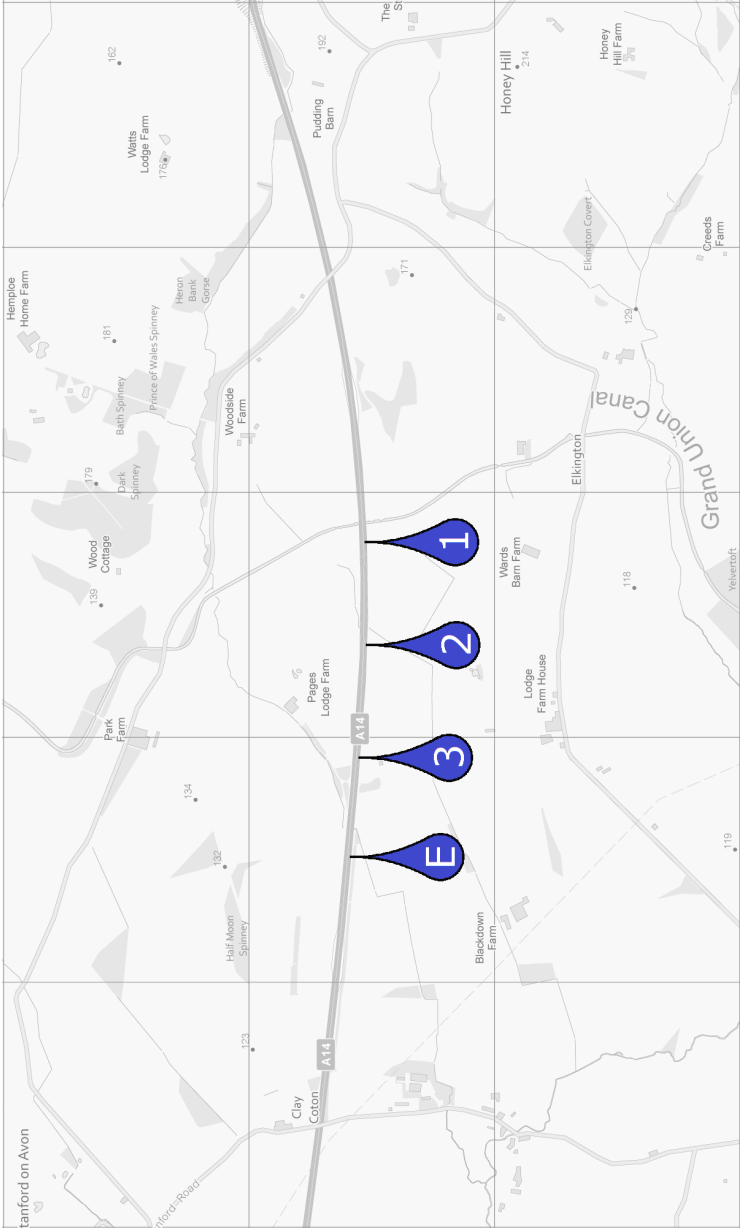
Appendix B   Results of full scale and laboratory measurements

Table B - 1 presents the results of the measurements made as part of the laboratory and full scale assessments. The flow rate for each specimen is provided as are the texture depth, side-force coefficient, and high speed friction values derived for each parent surface.

Table B - 1 Results from full scale and laboratory assessments

Site	Section	Coarse aggregate size (mm)	Lane	Specimen No.	SMTD (mm)	L-Fn100	SR(50)	Flow rate (m³/s)
1	1	10	1	1	0.91	0.40	69.23	1.26E-05
			1	2	0.91	0.40	69.23	2.66E-05
			2	1	1.16	0.42	73.68	1.57E-05
			2	2	1.16	0.42	73.68	4.56E-06
	2	6	1	2	0.62	0.42	72.24	2.31E-05
			2	1	0.75	0.44	73.93	1.19E-05
			2	2	0.75	0.44	73.93	6.29E-06
	3	14	1	1	1.09	0.37	65.17	9.91E-06
			1	2	1.09	0.37	65.17	1.02E-05
			2	1	1.34	0.43	73.93	1.22E-05
			2	2	1.34	0.43	73.93	2.98E-05
2	1	14	1	1	1.17	0.30	57.05	1.65E-05
			1	2	1.17	0.30	57.05	1.39E-05
			2	1	1.64	0.42	62.65	2.98E-05
			2	2	1.64	0.42	62.65	1.25E-05
	2	10	1	1	0.75	0.29	60.21	3.15E-07
			1	2	1.01	0.41	66.87	3.35E-06
			2	1	1.01	0.41	66.87	8.50E-06
			2	2	0.75	0.29	60.21	1.33E-05
3	1	14	1	1	1.17	0.29	55.82	1.28E-05
				2	1.17	0.29	55.82	3.01E-05
	2	10	1	1	0.88	0.31	59.50	3.61E-06
				2	0.88	0.31	59.50	4.52E-06
	3	6	1	1	0.62	0.38	65.90	6.21E-05
				2	0.62	0.38	65.90	2.49E-05
4	1	14	1	1	0.90	0.31	57.24	1.61E-05

				2	0.90	0.31	57.24	1.22E-05
			2	1	1.34	0.31	63.07	1.93E-05
				2	1.34	0.31	63.07	4.40E-05
	2	10	1	1	0.59	0.27	62.27	7.32E-07
			2	1	0.93	0.32	64.93	2.05E-06
				2	0.93	0.32	64.93	4.29E-06
	3	20	1	1	0.84	0.34	59.52	2.44E-05
				2	0.84	0.34	59.52	7.97E-08
			2	1	1.40	0.32	65.31	8.24E-07
				2	1.40	0.32	65.31	6.55E-09
	4	6	1	1	0.59	0.40	68.05	3.58E-05
				2	0.59	0.40	68.05	4.02E-05
			2	1	0.65	0.41	68.33	2.17E-05
				2	0.65	0.41	68.33	2.60E-05
	1	6	1	1	0.39	0.35	57.90	2.73E-05
				2	0.39	0.35	57.90	4.18E-05
	2	10	1	1	0.42	0.29	62.26	6.22E-06
				2	0.42	0.29	62.26	9.66E-06
	3	14	1	1	0.80	0.33	57.65	1.45E-05
5				2	0.80	0.33	57.65	8.83E-06
	4	6	1	1	0.40	0.44	68.79	4.28E-05
				2	0.40	0.44	68.79	4.61E-05
	5	10	1	1	0.42	0.25	72.20	6.45E-06
	6	14	1	1	0.98	0.39	65.67	3.72E-05
				2	0.98	0.39	65.67	5.78E-05
	1	6	1	1	0.54	0.36	67.34	3.13E-05
			2	2	0.70	0.39	59.01	7.10E-05
	2	10	1	1	1.02	0.34	60.12	3.94E-05
				2	1.02	0.34	60.12	5.73E-05
6			2	1	1.18	0.34	58.84	8.29E-05
	3	14	1	1	1.24	0.31	57.82	2.33E-05
				2	1.24	0.31	57.82	1.47E-05
			2	1	1.44	0.33	60.75	3.69E-05
				2	1.44	0.33	60.75	3.66E-06

Appendix C   Results of CT imaging

Table C- 1 Full results from analysis of CT imaging

Specimen	Image angle of rotation (degrees)	% Material	% Isolated voids	% Connected voids	% Total voids	Average % material	Average % isolated voids	Average % connected voids	Average % total voids
	0	90.07	3.37	6.56	9.93				
	30	92.50	0.76	6.74	7.50				
Site 5, Section 1	60	89.96	2.83	7.22	10.04	90.44	2.81	6.76	9.56
	90	88.71	1.86	9.43	11.29				
	120	90.68	6.93	2.39	9.32				
	150	90.70	1.10	8.20	9.30				
	0	87.87	3.93	8.20	12.13				
	30	90.71	1.87	7.41	9.29				
Site 6, Section 2	60	87.96	3.40	8.64	12.04	89.10	3.00	7.90	10.90
	90	88.52	2.49	8.99	11.48				
	120	91.04	4.68	4.29	8.96				
	150	88.53	1.61	9.86	11.47				
	0	98.67	1.32	0.00	1.33				
	30	97.41	2.48	0.11	2.59				
Site 4, Section 2	60	97.30	2.48	0.23	2.70	97.97	1.88	0.15	2.03
	90	97.20	2.42	0.38	2.80				
	120	98.50	1.38	0.12	1.50				
	150	98.77	1.19	0.05	1.23				
Site 4, Section 4	0	92.96	0.86	6.18	7.04	93.09	1.81	5.10	6.91

Permeability and high speed friction

30	92.33	2.23	5.45	7.67
60	92.40	3.11	4.50	7.60
90	91.94	1.44	6.62	8.06
120	93.94	2.15	3.91	6.06
150	94.95	1.07	3.98	5.05
0	98.50	1.15	0.35	1.50
30	97.99	1.41	0.60	2.01
60	98.57	1.16	0.27	1.43
90	96.21	0.88	2.91	3.79
120	98.44	0.80	0.76	1.56
150	98.74	0.90	0.36	1.26

Site 4, Section 3

98.07   1.05   0.87   1.93

Road surface properties and high speed friction - The effect of permeability

Understanding the relationships between road surface properties and high speed friction is key to managing the risk of loss of vehicle control. It is understood that, in wet conditions, texture depth plays an important part in the generation of locked-wheel high speed friction. For the majority of road surfacing materials low levels of texture depth are likely to correlate with low levels of friction. However, this is not the case for all surfaces as previous works have shown there are some surfaces that provide low levels of texture depth and high levels of friction.

The work documented in this report explores the relationship between high speed friction and road surface properties with a view to identifying the mechanisms by which materials can provide low levels of texture depth yet high levels of locked-wheel high speed friction.

Other titles from this subject area

PPR727	Road surface properties and high speed friction. Sanders P D, Morosiuk K, Peeling J R. 2014
PPR564	The skid resistance behaviour of thin surface course systems. Roe P G, Dunford A. 2012
TRL367	High and low speed skidding resistance: the influence of texture depth. Roe P G, Parry A R, Viner H E. 1998
RRL20	Road surface texture and the change in skidding resistance with speed. Sabey B E. 1966

Page left intentionally blank.

Appendix C

Sanders, P. D., Militzer, M & Viner, H. E. (2017b), *PPR815 Better understanding of the surface tyre interface.* **TRL, Wokingham, England.**

PUBLISHED PROJECT REPORT PPR815

Better understanding of the surface tyre interface

P D Sanders, M Militzer and H E Viner

Report details

Report prepared for:	Highways England, Safety, Engineering and Standards
Project/customer reference:	626(4/45/12)
Copyright:	© Transport Research Laboratory
Report date:	February 2017
Report status/version:	Version 3.0
Quality approval:	
(Project Manager) Stuart McRobbie	(Technical Reviewer) Martin Greene

Disclaimer

This report has been produced by the Transport Research Laboratory under a contract with Highways England. Any views expressed in this report are not necessarily those of Highways England.

The information contained herein is the property of TRL Limited and does not necessarily reflect the views or policies of the customer for whom this report was prepared. Whilst every effort has been made to ensure that the matter presented in this report is relevant, accurate and up-to-date, TRL Limited cannot accept any liability for any error or omission, or reliance on part or all of the content in another context.

When purchased in hard copy, this publication is printed on paper that is FSC (Forest Stewardship Council) and TCF (Totally Chlorine Free) registered.

Contents amendment record

This report has been amended and issued as follows:

Version	Date	Description	Editor	Technical Reviewer
1.0	10/10/2016	Working draft	PS/MM	HV
1.1	19/12/2016	Working draft	HV	N/A
1.2	23/12/2016	Working draft	PS	
2.1	05/01/2017	Complete draft for client review	PS/HV	HV
2.2	26/01/2017	Client review	OA	
3.0	09/02/2017	Edits following client review	PS	MG

Document last saved on:	27/07/2017 09:17
Document last saved by:	Sanders, Peter D

Better understanding of the surface tyre interface

Table of Contents

Better understanding of the surface tyre interface

Better understanding of the surface tyre interface

Executive summary

The friction developed between the road surface and vehicles' tyres provides motorists with the reaction forces necessary for manoeuvring. On the English Strategic Road Network (SRN) this is managed through the specification of low speed skid resistance, texture depth and the polishing resistance properties of aggregates.

A combination of changes to the SRN (motorway layout and pavement surface type) and the vehicle fleet (anti-lock braking systems and electronic stability control systems) in recent years makes it appropriate to review the current approach. The work reported here was commissioned by Highways England to investigate how surface characteristics affect the ability of road users to control their vehicles. This was achieved through the completion of the following tasks:

- A literature review was conducted to identify studies assessing the relationship between pavement performance and vehicle demand.

- A methodology was created to define and assess the relationships between friction, wheel slip and vehicle speed using historical friction measurements. This facilitated a more detailed understanding of the characteristics of different surfacing materials than can be obtained from the standardised measurement of skid resistance and texture depth.

- The relationships between friction, wheel slip and vehicle speed were used to identify typical material behaviours and the relationship with texture and low speed skid resistance.

- All the information from the above tasks was combined to determine how significant the low speed skid resistance and texture depth are for road users carrying out braking manoeuvres from different initial speeds.

- A robust approach was developed for estimating the implications of delivering different levels of friction and texture, including a reduction from current requirements.

From the work carried out the following conclusions were made:

- Concrete and asphalt materials exhibit markedly different friction performance. Further work should be undertaken to assess the effect of material design on the friction performance of TSCS materials, which varies considerably.

- The friction prediction model developed performs well overall in predicting friction over a wide range of slip ratio and vehicle speed, from inputs of low speed skid resistance and texture depth. However, it is less accurate at low slip (below 5%) and low, low speed friction (around 0.30 units SC(50)).

- Whilst low speed skid resistance and texture depth both contribute to the braking performance, the importance of texture depth seems particularly significant and texture depth is better able to compensate for lower levels of low speed skid resistance than vice versa.

179

- There appears to be an optimum contribution of low speed skid resistance and texture depth to braking distance, taking account of the vehicle speed and the performance of different surfacing materials.

- The use of driver aids designed to exploit peak friction has a substantial benefit on the braking performance of vehicles. A wide uptake (approaching 100%) of driver aids could allow for a reduction in the friction requirements on the SRN. However, information on the current and projected distribution of vehicles with driver aids would be needed before making changes to specifications.

1   Introduction

The friction developed between the road surface and vehicles' tyres provides motorists with the reaction forces necessary for manoeuvring. Maintaining appropriate and predictable friction conditions is an important contributor to road user safety. On the English Strategic Road Network (SRN) this is managed through the specification of low speed skid resistance (HD28 Skidding resistance, 2015), texture depth, (HD29 Data for pavement assessment, 2008) and (Manual of Contract documents for Highway Works, 2008), and the polishing resistance properties of aggregates (HD36 Surfacing materials for new and maintenance construction, 2006). The requirements have been in place and have remained relatively unchanged for some time.

A combination of changes to the SRN (motorway layout and pavement surface type) and the vehicle fleet (anti-lock braking systems and electronic stability control systems) in recent years makes it appropriate to review the current approach. It is possible that, with the developments to roads and vehicles, the specification of skid resistance and texture measurements may be excessively cautious, or that these characterisations may not be the most appropriate for mitigating risk. Since the texture depth requirement, in particular, is associated with a trade off as regards to the properties of noise, rolling resistance and durability, there could be substantial potential benefits as a result of amending the specifications.

This work was commissioned by Highways England to update the current knowledge of how surface characteristics affect the ability of road users to control their vehicles through the manoeuvres necessary for them to complete their journey (acceleration / braking / cornering). The work comprises a literature review, reported in chapter 4 and an investigation into the friction characteristics of common surfacing materials, and how they could influence vehicle braking characteristics. This is the major part of the study and is reported in chapters 5 to 8. A parallel investigation of the relationship between collision risk and skid resistance is reported separately (Wallbank *et al.*, 2016).

2 Background

The instantaneous friction available for vehicle manoeuvring depends on a complex mix of tyre, vehicle and surface characteristics. Measurements of the road surface contribution to friction are therefore carried out under standardised conditions to eliminate, as far as possible, the variation from other sources. These measurements are denoted "skid resistance" and, in network analyses, relate to average crash rates (Wallbank *et al.*, 2016). However, they do not accurately represent the friction available to road users in a particular situation. This work has been carried out to better understand the relationship between the skid resistance measurements made for asset management purposes, and the friction available to road users for specific manoeuvres.

Skid resistance is typically measured in one of the following ways:

- In side-force tests, a test tyre is angled with respect to the direction of travel, thereby creating a slip between the tyre and road surface, for example SCRIM (BSI, 2006), for which the standard test speed is 50 km/h.

- In fixed-slip tests, a test wheel rotates in the direction of travel and is forced to slip over the road surface at a constant fraction of the vehicle velocity, for example the GripTester (BSI, 2000). Measurements are typically made at 50km/h.

- In locked-wheel tests, such as those made with the Pavement Friction Tester (PFT), measurements are made over a full locked wheel braking cycle. During testing, the tyre/road contact patch is forced through a full braking cycle from instantaneously stationary (free rolling) to moving at the speed of the tow vehicle (fully locked) (ASTM, 2011). High speed friction measurements are typically made at 90km/h.

These skid measurement devices only characterise a limited combination of the vehicle speeds and wheel slips that are available to road users. It is plausible therefore that, depending on the manoeuvre they are attempting to execute, road users may sample combinations of vehicle speed and wheel slip that are not characterised by the standard skid resistance test methodologies.

The work presented in this report will focus heavily on data collected using the Highways England PFT device, Figure 2-1. Measurements made with this device are performed in accordance with the procedure set out in ASTM E-274 (ASTM, 2011) and utilise a smooth treadless tyre as per ASTM E-524 (ASTM, 2008). For each test cycle the test wheel held on the trailer is braked, causing it to lock and skid for approximately two seconds. During a test cycle the vertical and horizontal load forces placed upon the test wheel are recorded, alongside vehicle and wheel speed every 0.01 seconds. Standard tests are conducted in wet conditions by pumping water (from a tank in the tow vehicle), at a controlled rate producing a nominal water film thickness of 1.0mm.

Measurements made with this device can be conducted at any practicable speed, therefore by conducting multiple measurements on the same surface it is possible to capture information at a range of test speeds. It is this methodology which forms the basis of the bulk of the work reported herein.

Better understanding of the surface tyre interface

Figure 2-1 The Pavement friction tester

183

3 Research aims

The key aims of this work are to:

- Conduct a literature review to identify works assessing the relationship between pavement performance and vehicle demand.

- Define and assess the relationships between friction, wheel slip and vehicle speed.

- Use the relationships between friction, wheel slip and vehicle speed to identify typical material behaviours and the relationship with texture and low speed skid resistance.

- Combine the information from the above tasks to determine how significant the skid resistance and texture depth are for road users carrying out different manoeuvres.

- Develop a robust approach to estimating the implications of delivering different levels of friction and texture, including a reduction from current requirements. Provide recommendations to Highways England on changes to current standards and methods for implementation.

4 Literature review

This chapter presents the results of a literature review carried out to inform the understanding of how surface characteristics influence vehicle handling in different manoeuvres. The study started by defining tyre/road friction and exploring its contributory factors. Friction and tyre models used in industry were then explored to gain an insight into the parameters used and how these relate to friction prediction systems. The study concludes with a discussion of driver aids and how these affect tyre/road friction.

4.1 General principles of tyre/road friction

Tyre/road friction is a result of the interaction between the tyre and the road surface, the resistive force (friction) being generated by the movement of the tyre across the road surface. The frictional force is generated at the interface of the tyre and the road, in a direction opposing the direction of travel, and is the interaction which enables vehicle manoeuvres and also determines the stopping distance (Hall *et al.*, 2009).

Friction can be characterised by the non-dimensional coefficient μ, which is determined by the proportion of the horizontal friction force H to the vertical load V as shown in Figure 4-1.
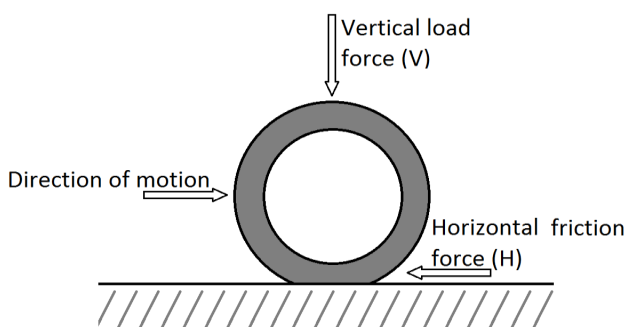
Figure 4-1 Force diagram for a roatating wheel

The speed of the tyre in relation to the pavement surface speed is referred to as slip speed, as described in Equation 4-1. It is also commonly expressed as a ratio or percentage of the vehicle speed.

$$S = V - V_p = V - (0.68 \times \omega \times r)$$

Where:

- S = Slip speed (miles/hour)
- V = Vehicle speed (miles/hour)
- V_p = Average peripheral speed of the tyre (miles/hour)
- ω = Angular velocity of the tyre [rad/sec]
- r = Average radius of the tyre (ft)

Equation 4-1 Calculation of wheel slip (Hall *et al.*, 2009)

The coefficient of friction between a tyre and the pavement changes with varying slip. It increases rapidly with increasing slip to a peak value, known as peak friction, that usually occurs between 10 and 20 percent slip. The friction then decreases to a value known as the coefficient of sliding friction or locked-wheel friction, which occurs at 100 percent slip.

Figure 4-2 Idealised friction versus tyre slip reationship

Peak and sliding friction vary little on dry surfaces and are relatively unaffected by variation in speed. Effects are more marked on wet roads, with locked-wheel friction being lower than peak friction, and both generally decreasing with an increase in speed. These differences depend on vehicle speed and tyre properties, but also on the road surface properties. According to Henry (2000) and Flintsch et al. (2012) measurements made on the left side of the peak (lower slip ratios) are mainly influenced by tyre properties, whereas measurements on the right hand side (higher slip ratios) mainly depend on the macrotexture of the road surface.

4.2 Factors influencing tyre/road friction

As the friction coefficient is defined by the interaction between the road surface and the tyre, the friction depends on various factors which can be grouped into four categories:

- Pavement surface characteristics
- Vehicle operational parameters
- Tyre properties
- Environmental factors

4.2.1 Pavement surface characteristics

The tyre/road friction in wet pavement conditions is greatly influenced by the texture of the road surface. The fine-scale texture on the surface of the coarse aggregate (microtexture)

interacts directly with the tyre rubber to provide adhesion. According to Hall et al. (2009) this component is especially important at low speeds but needs to be present at any speed. In general, in wet conditions, surfaces with greater macrotexture tend to provide better friction at high speeds for the same low-speed friction (Roe and Sinhal, 1998).

Sanders et al. (2014) concluded that, for most surfaces with texture depth below approximately 0.8 mm Sensor Measured Texture Depth (SMTD), friction at high speed increases linearly with texture, and for textures above 0.8 mm SMTD, friction changes little with increasing texture. However this is not always the case: (Roe and Dunford , 2012) found for certain asphalt materials with relatively low texture depth, locked-wheel friction decreases with speed but not to the extent expected from other surfaces with comparably low macrotexture.

This replicates the earlier findings of TRL367 (Roe *et al.*, 1998) which concluded that as friction falls with speed, there is also a relation between friction and texture: friction on low-textured surfaces falls more rapidly than high-textured surfaces. The effect of texture depth on loss of friction was greatest below about 0.7mm SMTD. Above this level, increased texture has a relatively small effect. This work did not assess small-sized aggregate thin surfacings but found that porous asphalt surfacings were providing higher friction levels than expected. It was also found that the texture depth has an impact on friction at low speeds.

4.2.2 Vehicle operating parameters

Vehicle parameters affecting the friction between the tyre and the road are discussed in more detail in section 4.4 and section 4.5.

4.2.3 Tyre properties

Tyre properties such as compound, pattern, tread depth, condition and pressure have an impact on the tyre/road friction. The design of the tyre tread and the condition of the tyre affect the ability of the tyre to remove water from the tyre/road interface. Especially for greater water film thicknesses, the tread depth is important at high speeds when the amount of water accumulating in front of the tyre can be greater than the water that is being removed.

Henry (1983) conducted a study comparing the locked-wheel friction performance of different tyre types. The results of the study demonstrated that locked-wheel friction at 40 miles/hour (64 km/h), measured using a smooth tyre is between 45 and 70 percent of the value measured using a new treaded tyre.

Tyre inflation pressure affects the size and distribution of the tyre/road contact patch. Under-inflation causes an increase in contact area and therefore constricting drainage channels and reducing the average contact pressure on the road surface. As a result, water can become trapped underneath the tyre and the speed at which hydroplaning is likely to occur decreases. Over-inflation however, reduces the trapping effect, reduces the contact area and increases the contact pressure, resulting in a higher hydroplaning speed (Hall *et al.*, 2009). Below hydroplaning speed, Tyrosafe report D10 (Kane et al, 2009) suggests that changes in inflation pressure over relatively wide ranges did not produce significant variations in friction on wet roads, although it did have an effect in dry conditions.

Classically, it has been suggested that two mechanisms, adhesion and hysteresis, are responsible for the generation of friction between rubber and other surfaces, and that the overall friction between tyre and road surface is the sum of these two components (Kummer, 1966). Adhesion is generated at the interface of the rubber and a dry road surface. The polymer chains within the rubber and the surface material interact on a molecular scale, causing distortion of the polymer chains and hence generating friction. This process may even involve the formation and breaking of chemical bonds. Hysteresis arises because energy is lost during the physical deformation of the bulk material by surface asperities. In this process, some of the energy that is used to deform the tyre tread when it slides over the texture is absorbed by the tyre when it returns to its original shape.

4.2.4 Environmental factors

Environmental factors such as temperature and the presence of water, or other contaminants, on the road surface also have an impact on the friction available. As tyres and asphalt road surfacings are made of visco-elastic materials, their properties are affected by temperature.

Water acts as a natural lubricant, which reduces the friction by an amount proportional to the water film thickness. On wet roads, the free rolling tyre/road interface has been characterised in terms of three regions (Moore, 1975). In the sinkage, or "squeeze-film" zone at the forward edge of the tyre/road contact area, the tyre does not make contact with the road, but floats on a thin wedge of water. The depth of water reduces progressively towards the rear of this area, as the water film is squeezed out of the interface by the tyre. In the "draping zone", the tyre makes partial contact with the asperities of the road surface, the water film having been mainly removed by the squeezing action. Finally, at the rear of the contact area, there is an area of actual contact, where most of the friction is generated.

The friction generated depends on the relative areas of these three regions, which is determined by the depth of water, the vehicle speed and the rate at which water can be dispersed from the contact area. As the vehicle speed and the amount of water increase, the contact area becomes progressively reduced until it disappears, at which point the vehicle is said to be hydroplaning.

Further environmental impacts such as the presence of snow and ice also affect the available friction by obscuring the road surface from the tyre and instead presenting the tyre with a low friction contaminant (Hall *et al.*, 2009). The presence of snow and ice is a special case and not directly related to this study.

4.3 Friction models

4.3.1 Road friction models

Several models exist for predicting pavement friction as a function of the vehicle speed and road characteristics. The most commonly reported are:

- The Rado model
- The Penn State model
- The PIARC model

The Rado model

The Rado model, also known as the logarithmic friction model, aims to model the friction path as the tyre proceeds from the free rolling to the locked-wheel condition at a single vehicle speed, Equation 4-2.

$$\mu = \mu_{peak} \times e^{\left[-\frac{ln\left(\frac{V_s}{S_{peak}}\right)^2}{C^2} \right]}$$

Where:

- μ_{peak} = peak friction level
- V_s = the slip speed
- S_{peak} = slip speed at the peak (typically 15% of vehicle speed)
- C = Shape factor – mainly dependent on surface texture

Equation 4-2 The Rado model

The model describes two phases during the braking process. In the first phase, the tyre rotation reduces from free rolling to the peak friction state. Subsequently, the tyre slip speed reduces to the locked-wheel state (100% slip). The corresponding friction coefficient therefore increases to the peak friction level, and then decreases by the increase of the slip ratio (Wang *et al.*, 2010).

The Penn State Model

The Penn State model describes the relationship between friction and slip speed as an exponential function.

$$\mu = \mu_0 \times e^{\left[\frac{PNG}{100} \times S \right]}$$

Where:

- μ_0 = static friction at zero speed
- S = wheel slip speed
- PNG = Percent Normalised Gradient (Equation 4-4)

Equation 4-3 The Penn State model

$$PNG = -\frac{100}{\mu} \frac{\partial \mu}{\partial S}$$

Equation 4-4 Definition of PNG

PNG was discovered to be constant with speed and correlates highly with macrotexture, therefore μ_0 could be predicted by macrotexture. Later versions of this model replaced the PNG/100 by the speed constant S_p (Henry, 2000).

The static friction coefficient μ_0 is related to pavement surface microtexture; and the speed constant is highly correlated with pavement surface macrotexture (Wang *et al.*, 2010).

The PIARC Model

The PIARC model is an adaption of the Penn State model in which the μ_0 term has been replaced to represent the friction at 60 km/h resulting in the following.

$$F(S) = F_{60}\ e^{\frac{60-S}{Sp}}$$

Where:

- F(S) = friction at slip speed S
- F_{60} = friction at 60 km/h
- S_P = IFI Speed Number, see Equation 4-6

Equation 4-5 The PIARC model

$$S_P = a + b \times Txt$$

Where:

- a and b are constants defined in ASTM standards E1845 and E965 (ASTM, 2015)
- Txt = macrotexture measurement (mm)

Equation 4-6 Definition of S_p

The PIARC experiment was conducted in 1992 and aimed to compare and harmonise texture and skid resistance measurements. The experiment resulted in the development of the International Friction Index (IFI), the aim of which was to allow skid resistance to be measured by any methodology and compared on a common scale. Tyrosafe D05 (Vos *et al.*, 2009) reported that although this approach worked to some extent the precision of the resulting common scale was not sufficient for practical application.

The IFI standardizes the way the dependency of friction on the tyre sliding speed is reported. The Speed Number (S_P) measures how strongly friction depends on the relative sliding speed of the tyre and is related to the gradient of the friction values measured below and above 37 miles/hour (60 km/hr). The S_P is reported in the range 0.6 to 310 miles/hour (1 to 500 km/hr) (Hall *et al.*, 2009).

It was confirmed that S_P is strongly influenced by the macrotexture of the surface. Besides macrotexture being a major contributor to friction, the speed number can be used to interpret the condition of the macrotexture as it changes its value over time (Hall *et al.*, 2009).

Combining the Penn State and Rado models

Combining the Penn State and the Rado models allows an approximation of the frictional performance of a surfacing when a vehicle is conducting an emergency braking. Up to the

state where the wheel is fully locked, the friction follows the Rado Model. If the breaking continues after this point, the vehicle speed decreases (being equal to slip speed) and the friction follows the Penn State model up to the point where the vehicle speed is zero (Henry, 2000). This process is shown graphically in Figure 4-3 where an example of the friction estimated by the Penn State and Rado models has been given.
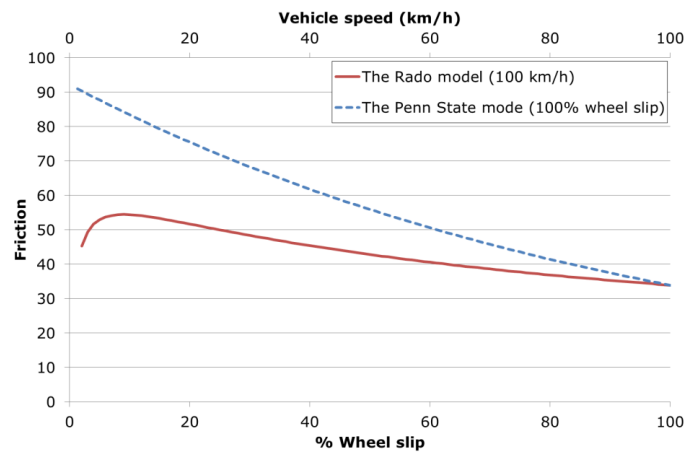
Figure 4-3 Combining the Penn State and Rado models

4.3.2   Tyre/road interaction models

Tyre models are used in vehicle dynamics to predict tyre performance in terms of traction and stability control. Overall, Wong (1993) states that tyre models should consider the composite structure of the tyre, the deformation as well as the near-incompressibility and the non-linearity of rubber material.

Many models describing tyre dynamics have been developed, ranging in complexity from basic models having a single contact point with the road surface to more complex 3-D models which take the deformation, tyre properties such as rim and reinforcements, and pneumatic pressure into consideration (Wang *et al.*, 2010).

Most tyre models are developed for tyre design purposes and aim to predict the level of deformation and the interaction between the tyre components. In 2010 a 3D tyre-pavement interaction model was developed by Wang et al. in order to analyse the forces and stresses generated between the tyre and road surface during vehicle manoeuvring (free rolling, braking/acceleration, and cornering).

Wang defined tyre-pavement interaction as a function of three nonlinear factors: material, geometry and the contact itself. For the simulation the pavement was modelled as a multi-layer structure that has nonlinear material properties for each of the layers. The structure of the tyre is composed of a complex structure including the rubber and the reinforcement. Overall, it was found that, with an increase in surface friction, the lateral contact stresses, at various manoeuvres, and the vertical contact stresses, for cornering manoeuvres, increase.

The model summarised above and all of the other tyre/road interaction models identified as part of this review modelled the road surface contribution to friction as a pre-determined value only. This approach requires the friction of the road surface to be known in advance and so goes little way to adding to the understanding of road surface properties that contribute to friction.

4.4   Active vehicle safety systems

4.4.1   Friction estimation

Friction estimation is used by active vehicle safety systems such as Anti-lock Braking Systems (ABS) or Electronic Stability Control (ESC). Friction estimation systems can be classified into three groups (Singh and Taheri, 2015):

- Vehicle Based Systems - These systems use the longitudinal and lateral motions of the vehicle and the differential speed of the vehicle wheels (wheel slip percentage) as inputs to a friction estimation algorithm.

- Wheel Based Systems - Measurement system that utilises a redundant wheel and is appropriate for heavy duty trucks.

- Tyre Based Systems - Measurement of tyre deformation.

The common feature of all friction estimation systems is that friction is not measured directly, rather inferred from other properties.

FRICTION was an EU funded project aiming to develop an on-board system for measuring and estimating tyre/road friction and therefore to enhance the performance of vehicle integrated and cooperative safety systems. The programme was based on the preceding project APOLLO, which focused on the development of a tyre sensor for the friction estimation (Koskinen and Peussa, 2004).

The FRICTION system works around three parameters: friction currently used (tyre/road forces currently used), friction available (remaining potential) and friction potential (maximum tyre/road friction available), see Figure 4-4.
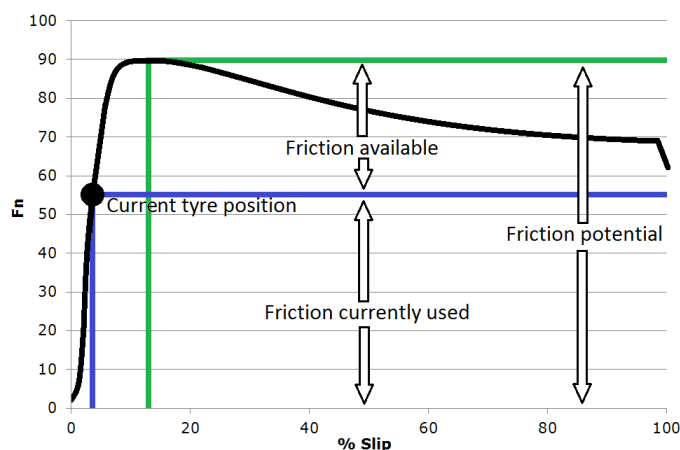
Figure 4-4 Summary of FRICTION parameters

The friction used is estimated using standard vehicle based driving dynamic sensors, such as those used for ABS or ESC systems. The friction potential is estimated using more coarse methods than those used to estimate friction used. The inputs used for the estimation of friction potential are the presence of environmental contaminants such as water or snow and the texture depth of the road surface. Measurement of these properties requires sensors not commonly available on vehicles, such as weather information systems and triangulation lasers.

4.4.2   Vehicle dynamic control

Vehicle dynamics stability control systems regulate the transmitted tyre forces which depend on the slip ratio between the tyre and the road. The primary systems in terms of driving dynamics and driving safety are (Koskinen and Peussa, 2004):

- Antilock Braking System (ABS)
- Traction Control System (TCS)
- Electronic Stability Control (ESC)
- Adaptive Cruise Control (ACC)

This section will discuss each of these systems in more detail focussing on the relationship with friction.

Antilock Braking System (ABS)

Antilock braking systems aim to diminish the loss of friction caused by sliding. It operates at the front side of the peak friction curve and causes the brakes to be applied and released in such a way that the slip is held near the peak. This ensures that the peak friction is not exceeded which would result in a loss of steering control.

193

TRL

The brakes are released before the peak friction is reached and are applied at a set time or percentage slip below the peak, the exact points are subject to propriety manufacturer design.

As described by (Henry, 2000), the ABS friction curve follows the Rado model, described in Equation 4-2, up to a set percentage slip whilst the vehicle speed is reducing. At this point the brake is released and the wheel slip drops, before the brake is reapplied; the cycle then repeating for a lower vehicle speed.

The control of an ABS system is, however, considered a highly nonlinear control problem as the relationship between friction and slip is complex. Furthermore the velocity of the wheel relative to the vehicle, as well as the friction, cannot be measured directly and therefore have to be estimated or inferred by sensor measurements. As a result, different control approaches have been developed (Aly *et al.*, 2011).

Traction Control System (TCS) and Electronic Stability Control (ESC)

Traction control and electronic stability control systems use the same premise of wheel slip detection and control as ABS, controlling individual wheel braking and power delivery to maintain wheel slip and therefore vehicle control. The differentiator between these systems is that ABS is activated only when the vehicle brakes are used manually, whereas TCS and ESC are always active.

The six main components of an ESC system are: wheel speed sensors, a control module, a steering angle sensor, a yaw rate sensor, an accelerometer, and the hydraulic modulator. The hydraulic modulator is the same one used in an ABS system, meaning that ESC adds only the yaw sensor, an accelerometer, and steering angle sensor to a standard ABS system. The control module recognizes the discrepancy between the intended path (communicated by the steering angle sensor) and the actual path (communicated via the yaw rate sensor) and sends a signal to the hydraulic unit, directing it to alter the braking power of individual wheels to achieve the desired response.

For example, if a driver turns the wheel very abruptly to the left, the vehicle may initially under steer. In this case, since the front tyres do not yet have enough traction and they slide, the vehicle therefore continues to move forward rather than turning left. The control module recognizes the discrepancy and directs the hydraulic unit to increase braking power to the left rear wheel. This causes the vehicle to rotate left (the desired response). If necessary, the control module will also reduce engine power by sending a signal to the throttle actuator.

Adaptive Cruise Control (ACC)

Adaptive Cruise Control (ACC) allows the vehicle to keep a constant speed until sensors detect an obstacle ahead. The speed is then adapted in a way that the distance to the obstacle remains constant. The system aims to keep the distance to the obstacle at a level allowing for safe braking in an emergency.

Braking distance can simply be calculated by the velocity and the maximum friction available indicating that, besides speed, the most influencing parameter is friction. If it is generally assumed to be a constant high value, then systems could potentially start braking too late. The calculation of the braking distance could be more precise if information about the road

Better understanding of the surface tyre interface

friction was available (Koskinen & Peussa, 2004), enabling the systems to be used to their full potential.

General

ABS, TCS and ESC already contain friction estimation algorithms and generally their performance is difficult to improve (without better knowledge of the surface characteristics). Knowledge of a more accurate friction potential would aid the operation in their first cycles: ABS would benefit on ice by not braking too hard, and TCS could similarly limit excessive acceleration, especially when switching gears (Koskinen & Peussa, 2004).

A friction estimation system might also improve ESC algorithms by providing more accurate information about the forces and friction potential for each tyre. However, the main benefit of friction estimation system is considered to be preventing dangerous manoeuvres rather than helping to correct them (Koskinen & Peussa, 2004).

In spite of this, it appears that the friction coefficient is generally based on estimation, with no detailed analysis about the interaction between tyre, texture and friction apart from dry, wet and contaminated road surfaces. Even though tyre based algorithms exist, according to Erdogan (2009) none of these systems are mature and reliable enough to be adapted to active safety systems.

4.5   Friction demands for manoeuvring

Rolling resistance

A small amount of friction, rolling resistance, is developed between the tyre and the road surface for a tyre rolling in a straight line, as the contact area is instantaneously stationary. However, for manoeuvres involving change of speed or direction of the vehicle, the application of brakes or steering results in forces developing between the tyre and road that may enable the vehicle to carry out the manoeuvre. Longitudinal friction forces are generated when operating in the constant-brake mode, lateral or side-force friction occurs as a result of steering manoeuvres.

Straight line braking

For a braking manoeuvre the reacting force increases with the increase in braking force up to a point at which the friction available between the road surface and the tyre is exceeded, the peak friction. Flintsch, et. al. suggest that this point occurs generally between 18 and 30 percent slip. The tyre slips over the road as it continues to slow down relative to the vehicle speed. Eventually a locking of the wheel occurs at which time the tyre does not rotate anymore resulting in the skidding of the tyre/road contact patch across the road surface (Flintsch, et al., 2012).

Cornering

For a vehicle steering around a curve or carrying out a lane change manoeuvre an additional force is generated at the tyre/road interface, called lateral (side-force) friction. The relationship between vehicle speed, curvature and friction can be expressed as per Equation 4-7.

$$F_s = \frac{V^2}{15R} - e$$

Where:

- F_S = Side friction
- V = Vehicle speed (miles/hour)
- R = Radius of the path of the vehicle's centre of gravity (also radius of curvature) (ft)
- e = Pavement super-elevation (ft/ft)

Equation 4-7 Calculation of side friction (Hall *et al.*, 2009)

It is important to note that the relationship shown in Equation 4-7 does not describe the absolute friction generated but rather describes the relative change in friction arising from changes in the input parameters. This can be demonstrated by resolving the units of the input parameters.

$$\frac{V^2}{15R} - e = \frac{\left(\frac{distance}{time}\right)^2}{distance} - \frac{distance}{distance}$$

Therefore:

$$\frac{\left(\frac{distance}{time}\right)^2}{distance} - \frac{\cancel{distance}}{\cancel{distance}} = \frac{distance^2}{time^2} \times \frac{1}{distance}$$

Therefore:

$$\frac{distance^2}{time^2} \times \frac{\cancel{1}}{\cancel{distance}} = \frac{distance}{time^2}$$

Equation 4-8 Resolution of the units of the input parameters to Equation 4-7

The resulting unit is one of acceleration which is related to force when the mass of an object is taken into account. Given that the mass of a vehicle remains the same but the mass of different vehicles may differ, the expression in Equation 4-7 therefore reflects the relative friction reaction force to the input parameters for a single vehicle. A more accurate description would therefore be that described in Equation 4-9 which shows friction being proportional to input parameters rather than equating to it.

$$F_s \propto \frac{V^2}{15R} - e$$

Equation 4-9 The relationship between side force friction, vehicle speed, curvature and super-elevation

Combined manoeuvres

Manoeuvres including braking and cornering simultaneously require the [frictional] force to be shared between both [longitudinal and lateral force] mechanisms, meaning that the interaction of the forces leads to a relation in which as one force increases the other decreases by a proportional amount (Flintsch, et al., 2012).

This relationship is shown in the friction circle, Figure 4-5, which shows that for vehicle operations within the vehicle/road friction limits, the braking and turning forces can vary independently on the condition that their vector sum is less than or equal to the limit of friction, defined by the friction circle or friction ellipse. The vector sum of the two combined forces remains constant (circle) or near constant (ellipse). The shape of the friction ellipse (the limit of friction) is defined by tyre and pavement properties and the friction margin is defined by Equation 4-10.
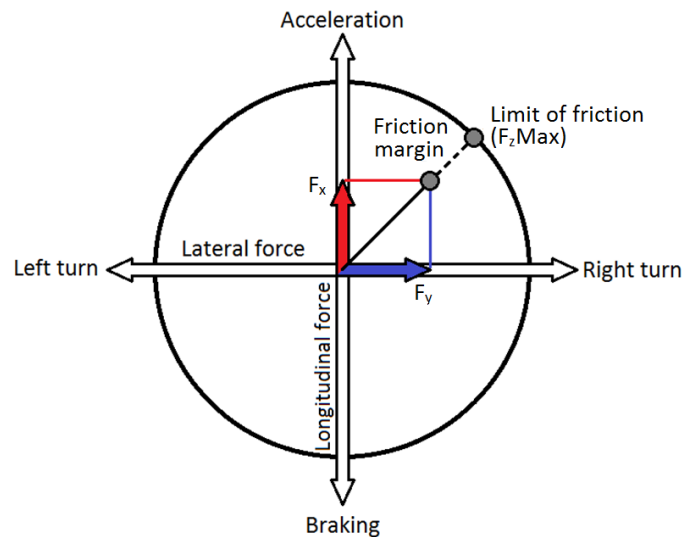
Figure 4-5 Friction circle

$$Friction\ margin = \ F_z Max - \sqrt{F_x^2 + F_y^2}$$

Equation 4-10 (Singh and Taheri, 2015)

For normal driving conditions, where the frictional forces are not fully demanded, the developing forces will be closer to the centre of the circle. With an increase in friction demand, this will move towards the maximum available friction. Therefore determining the friction coefficient is simpler in high demand conditions than for more normal driving conditions when the tyre slip is smaller. For these situations model-based approaches are

generally being used, which estimate the friction coefficient base on tyre force and moment data (Singh and Taheri, 2015).

4.6 Summary

The main points relevant to this work are:

- Road surface texture depth is a major contributor to friction at high levels of wheel slip, whereas tyre properties and road surface microtexture contribute to the generation of friction at lower levels of wheel slip.
- All of the road friction models assessed used an exponential function to describe the change in friction with wheel slip percentage or vehicle speed.
- Vehicle dynamic control systems (anti-lock braking, traction control, electronic stability control and adaptive cruise control), operate in the region of the friction/slip curve around (at comparable slip ratios to) the peak friction.
- These systems contain proprietary algorithms for estimating the friction available. They make use of vehicle based information such as the longitudinal and lateral motions of the vehicle, wheel speed and steering angle but make relatively crude assumptions about the maximum level of friction available. This is in spite of the many models of tyre/road friction available, which are not regarded as mature and reliable enough to be used within active safety systems.
- Both braking / traction and cornering place a demand on the total friction available from the tyre/road interface. If this is insufficient then the wheel will slide unless countered by one of the active safety systems.

5 Defining the vehicle speed, wheel slip and friction relationship

5.1 Approach

A key task of this work was to develop a methodology capable of characterising the friction performance of road surfacing materials in terms of vehicle speed and wheel slip. The approach taken was to model the performance of individual surfaces as a matrix of values where the position of a value in the matrix described its speed and wheel slip and the magnitude of the value represented the tyre/surface friction. This is illustrated in Figure 5-1, where the matrix is plotted as a three dimensional profile, where the x, y and z axes represent the wheel slip, vehicle speed and friction respectively. This will be referred to as a friction profile.
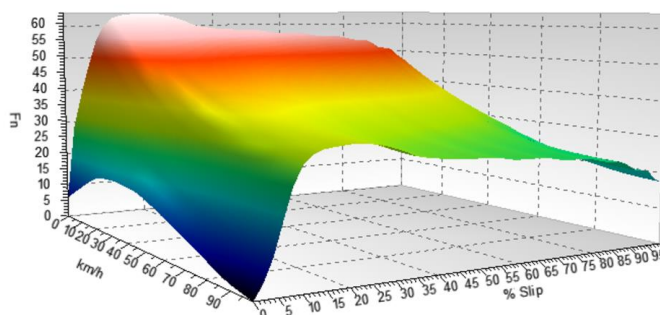
Figure 5-1 Idealised speed (x-axis), slip (y-axis), friction (z-axis) relationship

The matrices were constructed using previous measurements of pavement friction collected using the Highways England locked-wheel Pavement Friction Tester (PFT). Since measurements were collected at different test speeds and were time based, they were combined into a matrix with a consistent spacing in the slip and speed dimensions using the following methodology:

- Collate the individual friction measurements from a surface at different test speeds.
- Perform a linear interpolation on the slip / speed relationship to interpolate data to a resolution of 0.01 units.
- Perform a power regression on the speed, friction relationship to smooth data and interpolate to a resolution of 0.01 units.
- Generate the profile matrices based on the two above interpolations.
- Crop the profile matrices to accept only valid data.

5.2   Collation of friction measurements

Figure 5-2 shows an example of a single locked-wheel measurement. Because the data are collected at fixed time intervals (0.01s) the resulting friction / slip curve (Figure 5-2) has areas where information is highly populated, (60% – 80% slip) or sparse (20% to 30% slip). Furthermore, each measurement is made at a constant test speed (15 km/h in this example). Multiple measurements are made to collect information across the speed range.
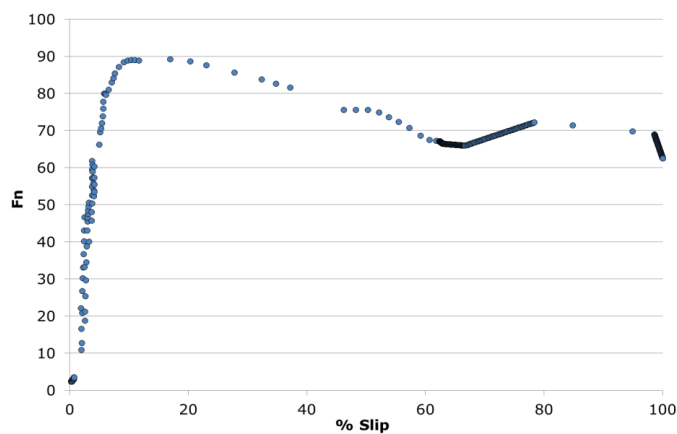
Figure 5-2 Example locked-wheel test

A collection of measurements made on a single surface at different speeds is represented by the data in Figure 5-3. This figure shows how with multiple measurements a 3D profile of the friction performance with respect to vehicle speed and wheel slip can be built.
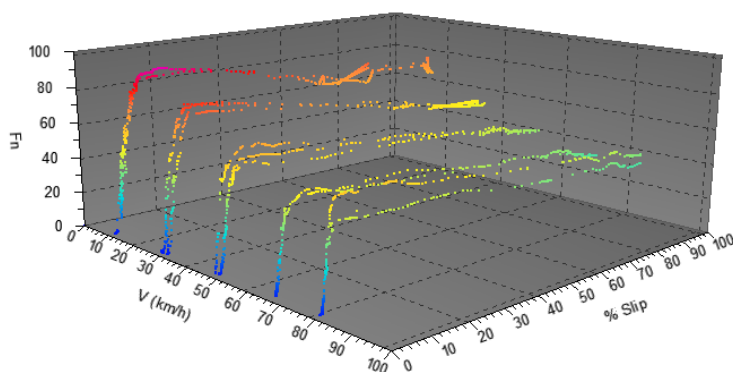
Figure 5-3 Example of measurements made at multiple speeds on a single surface

5.3 Interpolation of the slip/friction relationship

To generate a dense matrix of values describing friction performance, the gaps in Figure 5-3 were filled using interpolation, in two stages. Initially, linear interpolation was used to fill gaps in the % slip/friction direction (x-axis and z-axis respectively), Equation 5-1. This is also shown graphically in Figure 5-4.

$$Fn_x = Fn_0 + \left[(Fn_1 - Fn_0) \times \left(\frac{\% \, Slip_x - \% \, Slip_0}{\% \, Slip_1 - \% \, Slip_0}\right)\right]$$

Where:

- Fn_x = The friction value at $\% \, Slip_x$

- Fn_0 = The closest measured friction value before Fn_x

- Fn_1 = The closest measured friction value after Fn_x

- $\% \, Slip_0$ = The % Slip value at Fn_0

- $\% \, Slip_1$ = The % Slip value at Fn_1

Equation 5-1 Interpolation of friction based on % slip
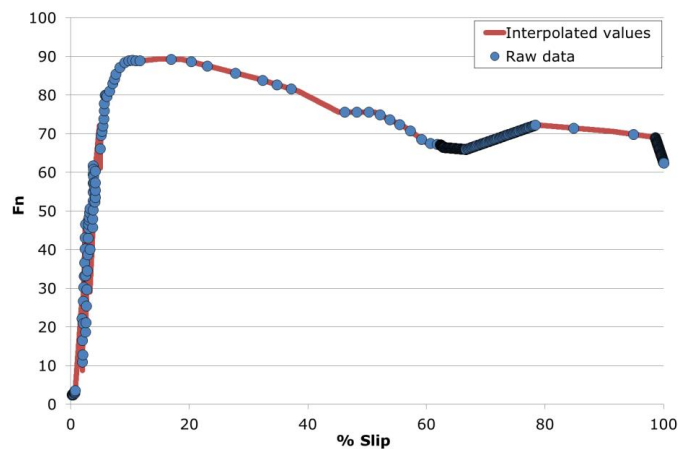
Figure 5-4 Example of interpolation of friction based on % slip

Figure 5-4 shows a typical profile of the % slip and friction relationship recorded using the PFT (the blue series markers) and the interpolated values linking areas where no data were collected (the red line). Below approximately 5% slip the data appear noisy compared to the relatively smooth shape of the rest of the profile. This is because this region contains information from two separate points in the braking cycle, some of these points represent

data collected as the brakes were applied to the test wheel, other points in this area represent data collected as the test wheel was released from its locked state at the end of the test. The points representing post-lockup measurements were included for the following reasons:

- The additional information provided was valuable in assessing the performance of materials at low levels of wheel slip.

- The data from pre and post-lock up provided similar values.

- The amount of interpolation required in this area would be reduced.

- The noise created in the profiles was considered low compared to the overall variation from multiple measurements on the same surface.

5.4 Interpolation of the speed/friction relationship

In the second stage of interpolation, to fill the gaps in measurements between each of the measurement speeds, a model of the friction / speed relationships for each 0.01 % interval on the slip (x) axis was developed. These models were used to populate friction values along the speed (y) axis of Figure 5-3. This also had the effect of smoothing some of the noise that occurs from repeat measurements. An example of this process is shown in Figure 5-5.

The chart shows the equation $y = 168.89x^{-0.374}$ with $R^2 = 0.958$, plotting Fn against Speed (km/h).
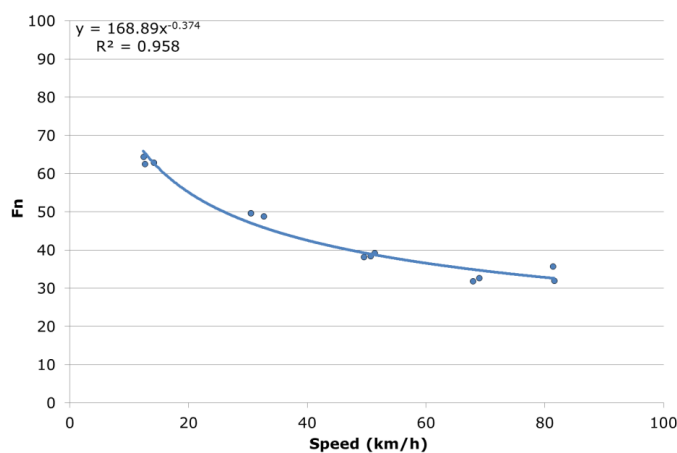
Figure 5-5 Example of interpolation of friction based on vehicle speed

Figure 5-5 shows the speed/friction model for one surface at 100% slip. The relationship between speed and friction for this surface can be described using a power relationship; this was found to be suitable for all the materials tested. Figure 5-5 shows that the use of the power relationship smooths the results and by using the equation describing the relationship, allows friction values at any speed to be interpolated.

5.5 Generation of the friction profile

The interpolation of values allowed a dense matrix of points to be generated describing the friction, speed, slip relationship for individual surfaces. The extent of each matrix was limited as follows:

- Speed ≥ 20 km/h and ≤ 100 km/h, representing the limit of the available data in most cases

- % slip ≥ 2 and ≤ 100, reducing the effect of the noise at very low slip levels from repeat tests on the same surface.

Figure 5-6 is a graphical representation of the matrix generated.
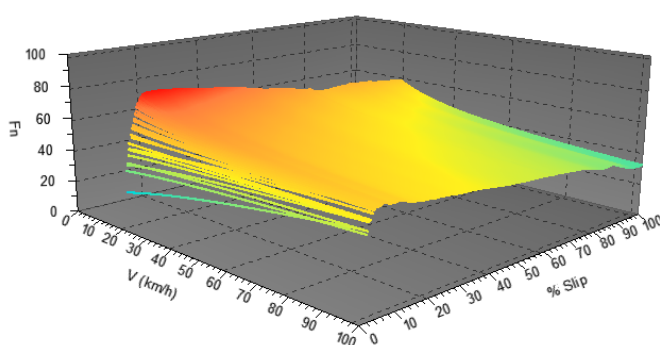
Figure 5-6 Graphical representation of % slip, Vehicle speed, friction matrix

5.6 Verification of profile generation procedure

The approach taken to generate the profiles was validated by defining a minimum requirement for the amount of information used to generate each friction profile, and by comparing the raw data with the generated profiles for a small number of surfaces. The minimum input required measurements made with the PFT at three speeds and three measurements were made per speed. Appendix A provides a summary of the number of individual PFT measurements contributing to each profile.

A comparison between the raw data and that represented by the profiles was carried out by assessing the distribution of the residual values (the profile value minus the measured value) of a small number of profiles generated. The results of this analysis are shown in Figure 5-7 and Table 5-1.

203
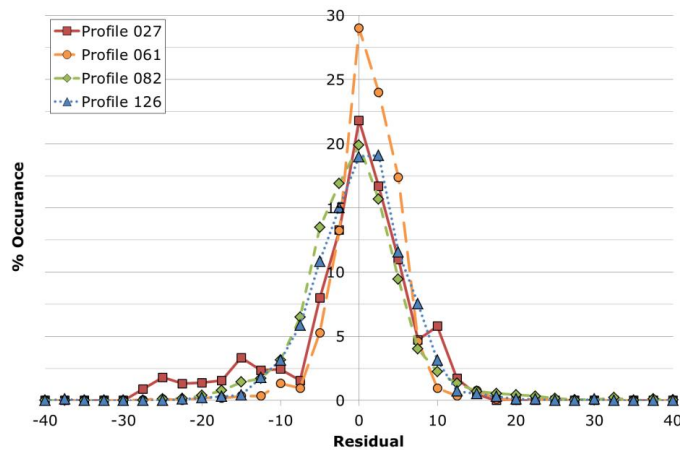
Figure 5-7 Assessment of residual values from profile generation

Table 5-1 Summary of assessed profiles

Profile number	Material	Measurements made	Standard deviation
027	Thin surface course system	15	8.12
061	Brushed concrete	17	4.41
082	Porous asphalt	14	6.77
126	Hot rolled asphalt	15	5.83

Figure 5-7 shows that the distribution of residual values for each profile is normal around zero. The performance of each distribution is similar and although there are variations in the shape of the distributions, these are insubstantial. Table 5-1 shows the standard deviations of the residual values for each profile range between 4.41 and 8.12 inclusive.

The repeatability of the PFT at 100% wheel slip has been identified as between 5.00 and 9.17 inclusive, depending on the speed of the measurement (Brittain and Viner, 2017). The standard deviation of residual values and the repeatability of the PFT are similar and therefore it could be concluded that the methodology used to generate the profiles, closely represents the friction of the surfaces they represent.

6 Assessment of typical material performance

This chapter presents the work carried out to characterise the typical behaviour of different material types.

6.1 Data examined

Friction measurements were made as described by Roe et al. (1998). The dataset used includes data from that original study supplemented by data from later research projects that used the same equipment and equivalent methodology. The data were converted into friction profiles using the methodology detailed in Chapter 5. In total 169 friction profiles were generated for use in this work from 2,494 individual friction measurements made between 1997 and 2013.

To characterise the range of typical performance of each surface type, the friction profiles representing the 5th and 95th percentile of the data were calculated by determining the 5th and 95th percentile of the friction values for individual surfaces within each cell of the slip / speed matrix. In total, data from 113 profiles were used to assess the following material categories:

- Concrete – 41 profiles

- Hot Rolled Asphalt (HRA) – 17 profiles

- Thin Surface Course Systems (TSCS) – 55 profiles combining TSCS materials using the following coarse aggregate sizes:

    o 6 mm – 9 profiles

    o 8 mm – 4 profiles

    o 10 mm – 17 profiles

    o 14 mm – 5 profiles

    o Unknown – 20 profiles

The profiles used in this analysis were identified as having a "normal" relationship between texture and high speed friction.

The results used in this chapter have been further investigated in Chapter 8 to estimate the performance of the surfaces under emergency braking conditions.

Better understanding of the surface tyre interface

6.2   Results

The 5th and 95th percentile profiles for the each material are shown below as 3D plots.

Concrete
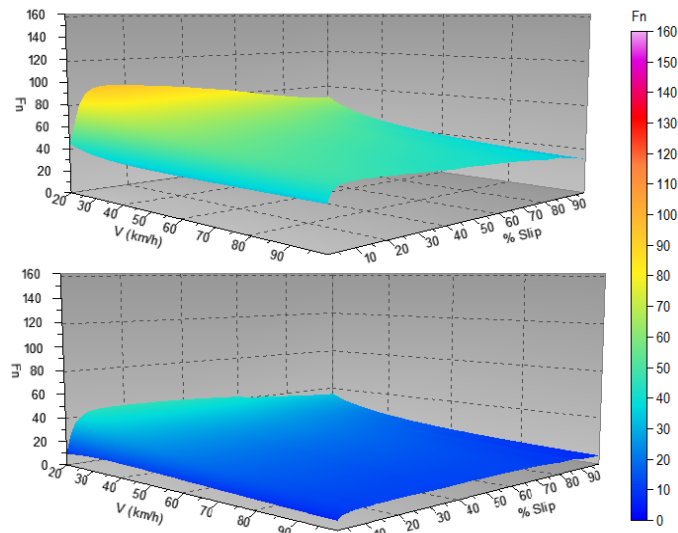
Figure 6-1 5th (below) and 95th (above) percentile profiles for concrete

Hot Rolled Asphalt
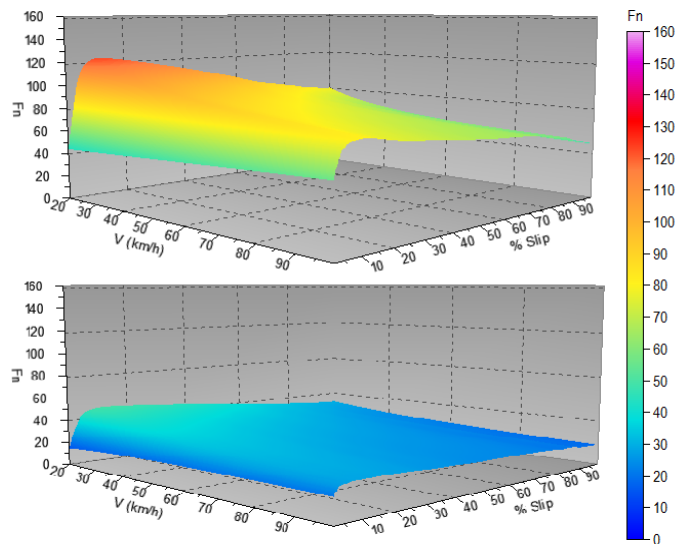
Figure 6-2 5th (below) and 95th (above) percentile profiles for HRA

Better understanding of the surface tyre interface

Thin Surface Course Systems
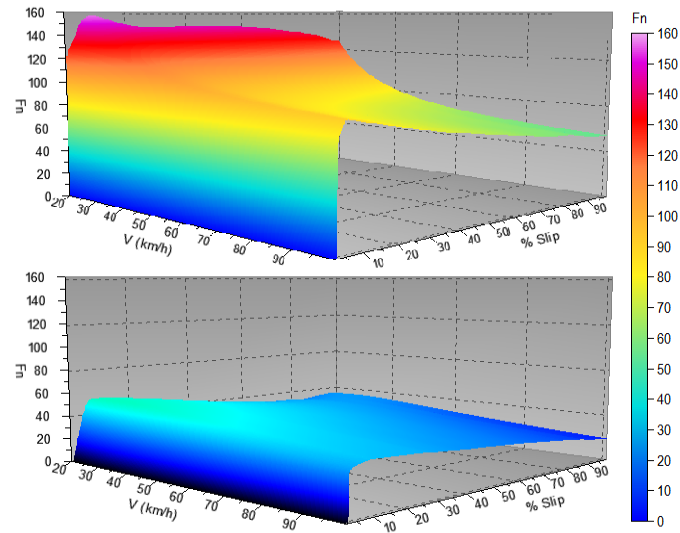
Figure 6-3 5th (below) and 95th (above) percentile profiles for TSCS

6.3 Observations

There is a clear difference in performance between the three materials, the TSCS and concrete materials provide the highest and lowest levels of friction respectively. The 90th percentile range was largest on the TSCS and smallest on the concrete. A low 90th percentile range would be expected on materials with generally low friction properties because there is a greater limitation on the number of possible friction values.

Despite having the greatest friction performance, the 90th percentile range on the TSCS is nevertheless high. An explanation for this could be that this material includes within it multiple sub-divisions of materials that have a wide ranging performance. Unfortunately it was not possible to conduct a similar analysis on these sub-divided materials as there was a limited amount of information available.

7 Development of a friction prediction model

Building on the friction profile matrices developed in Chapter 6, a generic model was developed to predict the friction profile of a surface from measurements of low speed skid resistance and texture depth; referred to as the friction model.

These variables were selected because:

- These were the variables used in previous works to model high speed, locked-wheel friction, reported in TRL367 (Roe *et al.*, 1998), so a direct comparison with this work was possible.

- These parameters are routinely measured on the English SRN as part of the Highways England pavement assessment policy.

- Historical work reported in TRL622 (Parry and Viner, 2005) has shown these parameters to be key indicators of collision risk in certain scenarios.

This section describes how the model was built and validated. In Chapter 8, the friction model is used to assess the significance of low speed friction and texture depth for a vehicle braking manoeuvre.

7.1 Development of the model

The model was built using the multiple linear regression method, in which the overall response (the predicted friction) is modelled as the sum of contributions from variables that are linearly related to the predicted friction. The approach taken can be summarised as:

1. Define assumptions and limitations,
2. Collate data on which the model will be built,
3. Transform the data to produce a linear relationship with friction,
4. Test variables for co-linearity,
5. Perform the regression analysis and define the model.

7.1.1 Assumptions and limitations

The following assumptions and limitations were used for the development of the friction model:

- The model would be based on surfaces with adequate data and displaying a "normal" relationship between texture and high speed friction[A].

- Thereafter, all material types can be modelled together.

- The inputs would be texture depth (SMTD) and low speed skid resistance (SC(50)); it is assumed the variation in friction can be described by these two variables.

[A] To remove surfaces showing effects unexplained by the input variables of the model (see section 7.1.2)

- The limitations of the valid output are 2 – 100 % slip and 20 – 100 km/h speed.

7.1.2   Collation of dataset for modelling

The friction model was built using matrices describing individual surfaces developed in Section 5.5 instead of the raw PFT measurements. The reason for doing so is justified because these matrices are simply mathematical descriptions of the raw measurements that would otherwise be carried out as part of the modelling methodology.

Data from sixteen of the surfaces were removed from the dataset on which the model was built because it was clear from the relationships between texture and high speed friction that a factor other than those used in the model was having a considerable effect on the friction value. This is demonstrated in Figure 7-1 which shows the relationship between texture and locked-wheel friction at 100 km/h (L-Fn100) for the dataset. The points within the red circle represent materials that have been identified as having a substantial contributing factor that would not be captured by the model. Research into the possible factors that contribute to this increase in friction performance is provided in TRL Report PPR727 (Sanders *et al.*, 2014).
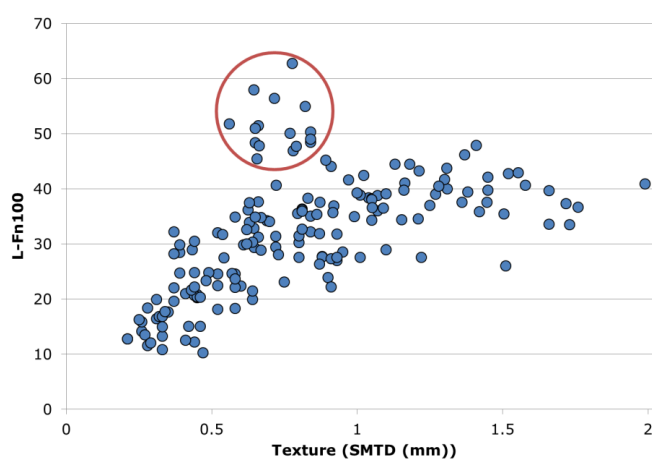
Figure 7-1 Texture and high speed friction relationships

The following information was then collated from all of the remaining friction profiles:

- Profile number
- % slip in 1% increments
- Vehicle speed in 1 km/h increments
- Texture depth (SMTD) associated with the profile number
- Low speed skid resistance (SC(50)) associated with the profile number

- Friction value associated with the % slip / Vehicle speed combination gained from the matrix associated with the profile number

This resulted in a dataset of 6 columns by 1,143,072 rows as per the example in Table 7-1.

Table 7-1 Example of the reference dataset used to develop the model

Profile number	% Slip	Speed (km/h)	SMTD (mm)	SC(50)	Fn
027	2	20	0.52	0.51	22.09
027	3	20	0.52	0.51	48.07
…	…	…	…	…	…
263	100	100	0.81	0.56	35.94

7.1.3 *Variable transformations*

The multiple linear regression analysis method requires the input variables (% slip, vehicle speed, low speed skid resistance and texture depth) to correlate linearly with the predicted variable (friction). In cases where the input variables do not linearly correlate with the predicted variable, it is sometimes possible to carry out a mathematical operation on the input variable to obtain a linear correlation, this is known as a transformation.

Figure 7-2 to Figure 7-5 show the relationships between each input variable and friction, displayed by the blue series. In cases where these do not correlate linearly with friction the transformation required to obtain a linear correlation is shown, the red series.

Figure 7-2 shows the relationship between texture and friction for one vehicle speed, the line of best fit for the relationships is a logarithmic relationship ($y = a \times \log(x) + b$) with a coefficient of determination (R^2 value) of 0.67. Applying a logarithmic transformation to the texture variable results in a linear correlation between the natural logarithm of texture and friction.
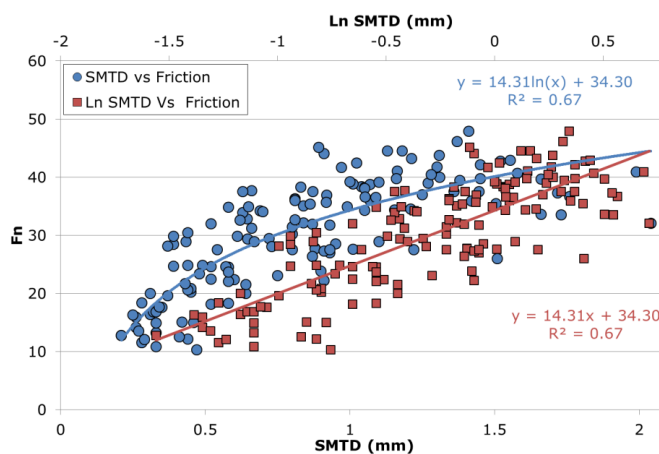
Figure 7-2 Texture and friction relationship

Figure 7-3 shows the typical relationship between vehicle speed and friction for one material, as expected the line of best fit is a power relationship ($y = ax^b$) with an R^2 value of 1. This is expected because this relationship has already been modelled as part of the procedure for generating the matrices from which these data were obtained. Applying a double logarithmic transformation to the speed variable results in a linear correlation between the natural logarithm of the natural logarithm of the speed and friction.
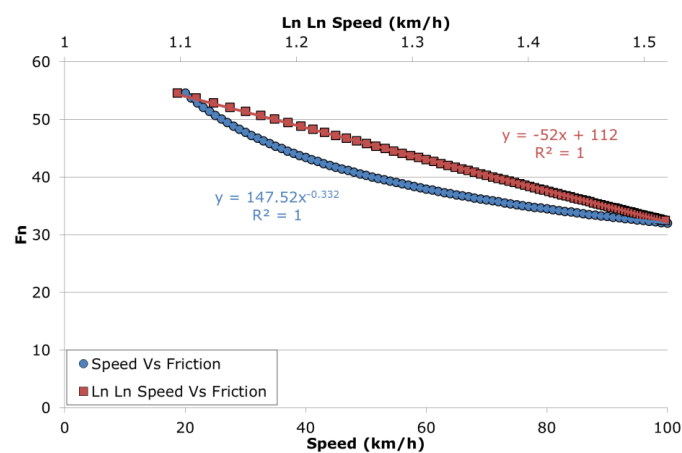
Figure 7-3 Vehicle speed and friction relationship

Figure 7-4 shows the relationship between low speed skid resistance and friction measured at 100% slip and 20km/h, the line of best fit is a linear relationship ($y = m \times x + c$) with an R^2 value of 0.29. As this relationship is already approximately linear, no transformation is required.
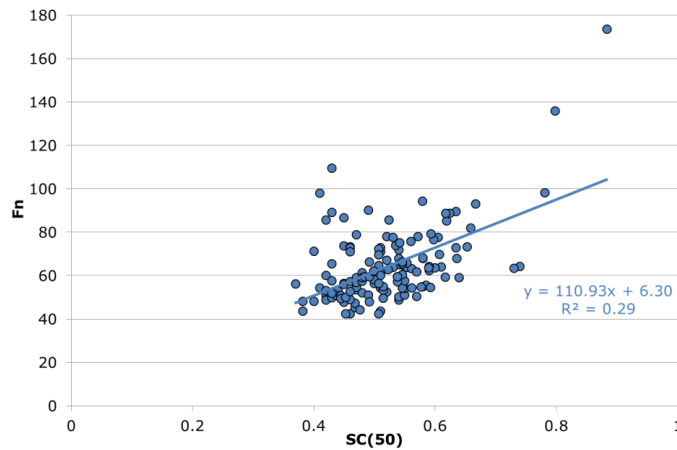
Figure 7-4 Low speed skid resistance and friction relationship

Figure 7-5 shows the relationship between % slip and friction for one material. The line of best fit is a linear relationship ($y = m \times x + c$) with an R^2 value of 0.87. However the use of this relationship is undesirable in the context of this work as doing so would have the potential to inaccurately model the extremes of behaviour. Within the context of this research it is the extremes of behaviour, particularly the very low and very high % slip values that are of interest.

It was therefore decided to remove the % slip variable from the model and instead to model the behaviour at each % slip interval separately. This would create a large table describing the relationship between low speed skid resistance, texture and vehicle speed at each percentage slip interval. This approach was considered preferable to including % slip in the model which would lead to a potentially inaccurate output at the extremes of % slip.
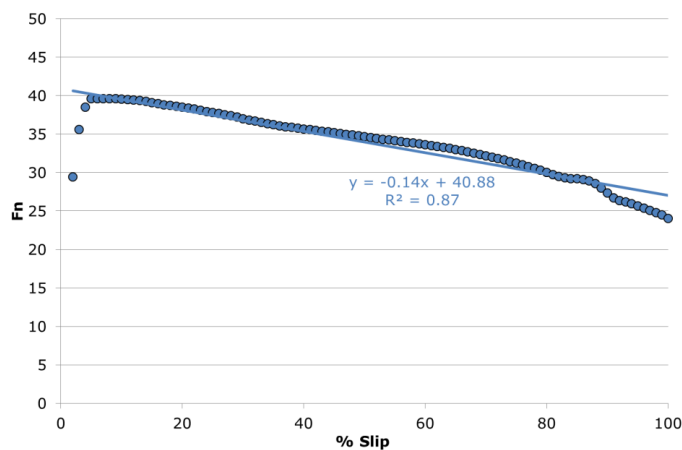
Figure 7-5 % Slip and friction relationship for the reference data

Better understanding of the surface tyre interface

7.1.4 Assessment of collinearity

An assessment of collinearity was carried out to ascertain if any of the input variables were linearly correlated to any of the other input variables. The linear correlation of input variables is undesirable when using the multiple linear regression technique as this can lead to errors occurring in the model predictions.

The assessment of collinearity was carried out by plotting the relationships between all of the input variables separately and analysing the statistics of a linear trend line. Figure 7-6 to Figure 7-8 show the relationships between pairs of the input variables. In each figure the blue series markers represent the variable values, the red line represents the linear trend line and the red text gives the equation of the trend line and the R^2 value. The lower the amount of linear correlation between the two variables assessed the lower the gradient of the trend line and the smaller the R^2 value.

Figure 7-6 and Figure 7-8 show no linear correlation between Ln Ln speed and Ln SMTD, and, SC(50) respectively. Figure 7-7 shows that the linear trend line between Ln SMTD and SC(50) has a gradient of 0.02 and a R^2 value of 0.02. These values are markedly greater than those observed with the other relationships, but not so great as to indicate a collinearity.
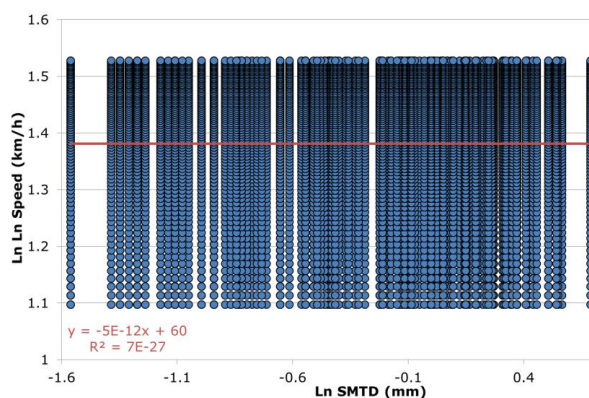
Figure 7-6 Relationship between Ln SMTD and Ln Ln Speed
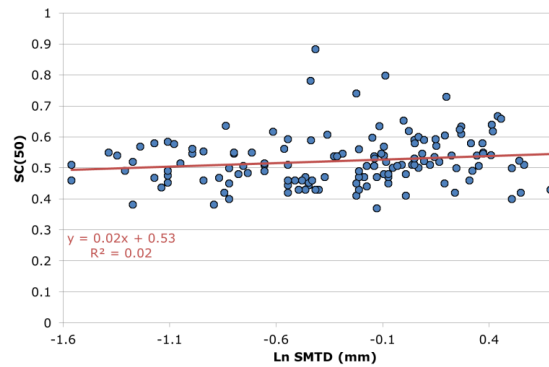
Figure 7-7 Relationship between Ln SMTD and SC(50)
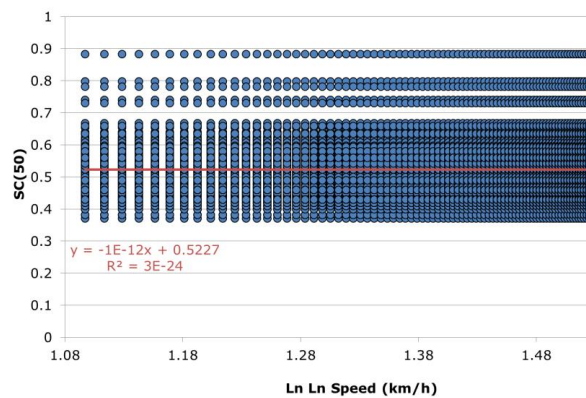
Figure 7-8 Relationship between Ln Ln Speed and SC(50)

7.1.5   Linear regression analysis and model description

Table 7-2 is an example of the dataset on which the regression analysis was carried out; a separate table was produced for each % slip interval. A multiple linear regression analysis was then carried out on each of the tables using the "Regression" tool in Microsoft Excel.

Table 7-2 Example of model variables used

Dependant variable	Independent variables		
Fn	Ln Ln Speed (km/h)	Ln SMTD (mm)	SC(50)
22.09	1.097	-0.65	0.51
48.07	1.097	-0.54	0.51
…	…	…	…
35.94	1.527	-0.21	0.56

The results from the regression analysis allowed the model to be described using Equation 7-1. The model coefficients for each % slip interval are provided in Appendix B.

$$Fn_x = a_x + [b_x \times Ln(Ln(Speed))] + [c_x \times Ln(SMTD)] + [d_x \times SC(50)]$$

Where:

- Fn_x = the friction value at a given % Slip x

- a_x = the model coefficient at % Slip x

- b_x = the speed coefficient at % Slip x

- c_x = the texture coefficient at % Slip x

- d_x = the low speed skid resistance coefficient at % Slip x

Equation 7-1 Description of the friction model

7.2   Model validation

The model predictions were compared with the original, raw friction measurements. (This approach limited the amount of raw data available as the friction model was limited to calculating friction values at integer values of % slip. Corresponding raw measurements comparisons could only therefore be carried out on integer values of % slip. Despite this limitation, 122,018 values were calculated which was considered adequate for validating the model performance.)

Figure 7-9 shows the relationship between the predicted and actual friction values. The relationship is largely linear but a small cluster of values are present below the main cluster, highlighted by the red boundary. A manual assessment of a sample of these points indicated that they have a tendency to be generated at very low values of wheel slip.

This is demonstrated in Figure 7-10 which excludes values relating to a wheel slip below 5%. It can be seen that the majority of values within the red area have been removed.

The line of best fit describing the relationship between predicted and measured friction values, Figure 7-9, is linear with a gradient of 0.98 and an R^2 value of 0.67. These values are encouraging as they indicate a strong relationship between the predicted and actual values.
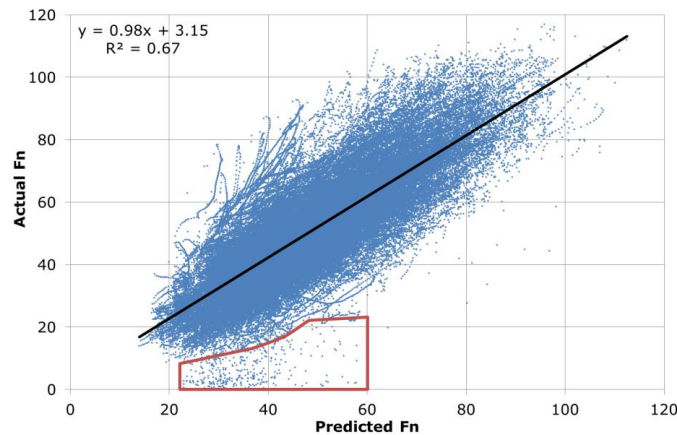
Figure 7-9 Predicted vs. measured friction values
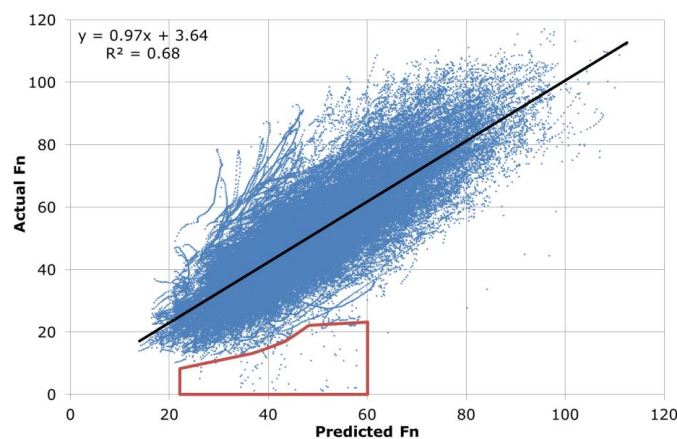
Figure 7-10 Predicted vs. measured friction values, excluding data < 5% slip

The distribution of the residual values (observed friction minus predicted friction) was used to assess the model accuracy. Figure 7-11 shows the distribution of the residual values and the 1, 2 and 3 standard deviation ranges (the red chequered, blue cross hatch and green lined areas respectively). The distribution of residuals forms a bell curve with a mean value of zero. The 1, 2 and 3 standard deviation ranges represent the 68%, 95% and 99.7% likelihood of the residual of any value falling within the ranges indicated by the x-axis. In this case there is a 68%, 95% and 99.7% likelihood that the friction prediction will fall within approximately 10, 20 and 30 units respectively of the actual friction value.

Better understanding of the surface tyre interface
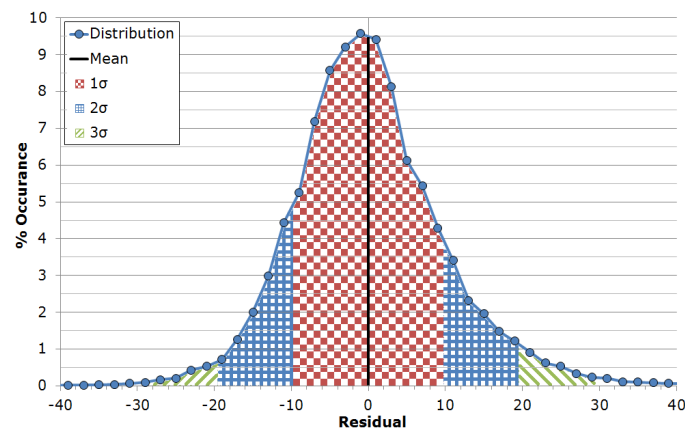
Figure 7-11 Distribution of residual values

To add context to this analysis, a comparative analysis was conducted on the TRL367 model. This consisted of calculating the distribution of the residual values generated by the TRL367 model on the data used to build that model (Roe *et al.*, 1998); the results of this analysis are shown in Figure 7-12. The distribution of residuals of the TRL367 values has 1, 2 and 3 standard deviation ranges of approximately 6, 12 and 18 units. The accuracy of the TRL367 model is therefore greater than that of the friction model. However the TRL367 model is limited to estimating friction at one vehicle speed and one slip speed only.
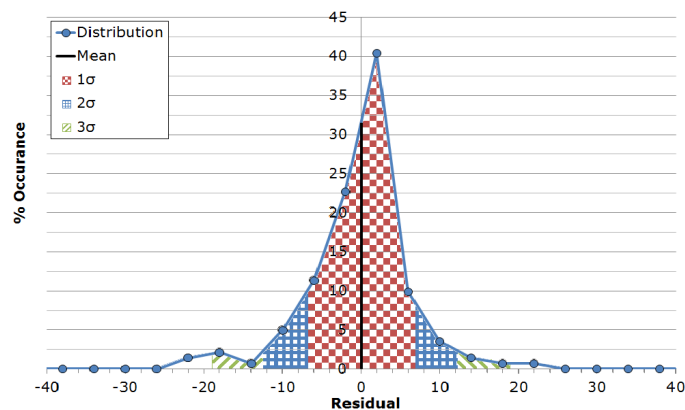
Figure 7-12 Distribution of residual values for model reported in TRL367

A more detailed analysis of the residual values from the friction model was carried out to assess the accuracy of the model for different input variables. The distributions of residual values corresponding to different % slip values are shown in Figure 7-13. This shows that for % slip values greater than 2% the distribution follows closely that of the distribution of

all values. The distribution of values corresponding to very low % slip show a higher propensity to produce lower residuals, indicating that the model has predicted a higher friction value than the value measured. This finding is in line with the observations associated with the highlighted area in Figure 7-9.
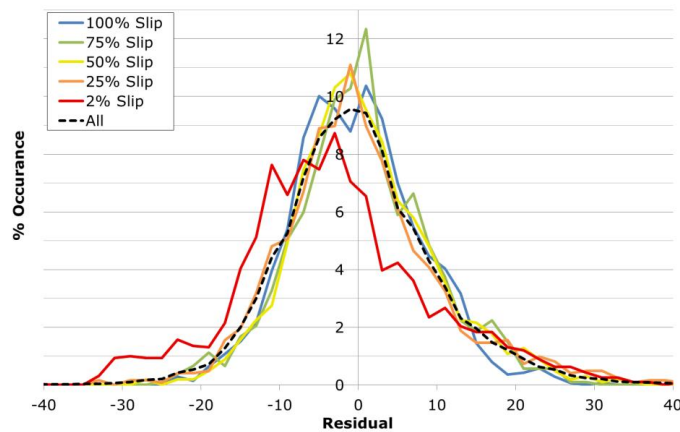
Figure 7-13 Distribution of residual values for different % slip values

The distributions of residual values corresponding to different vehicle speeds are shown in Figure 7-14. The distributions follow a bell curve shape but with different amounts of skew for each vehicle speed. At 50 and 80 km/h there is a slight skew to the right of the mean and at 30 km/h there is a skew to the left of the mean. This suggests the vehicle speed element in the model does not fully represent the effect of speed. However, the level of inaccuracy is relatively small.

Better understanding of the surface tyre interface
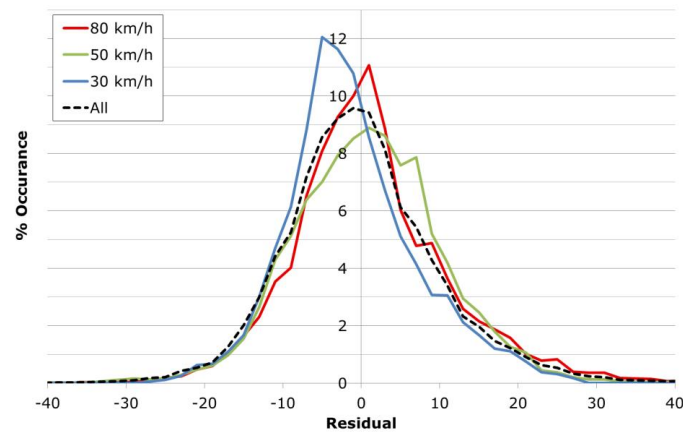
Figure 7-14 Distribution of residual values for different vehicle speeds

The distributions of residual values corresponding to different levels of low speed skid resistance are shown in Figure 7-15. These distributions show a pattern of changing skew of the distribution from positive to negative with increasing low speed skid resistance. The most extreme case is observed at the lowest SC(50) values where the mean of the distribution is approximately 5 units. This indicates that the model is over-predicting the friction properties for materials with very low SC(50) values and, to a lesser extent, under-predicting the friction properties for materials with high SC(50). The over-prediction of values with low SC(50) values is fail-unsafe and so there may be justification for limiting the use of the model for surfaces with low SC(50) values in practice.
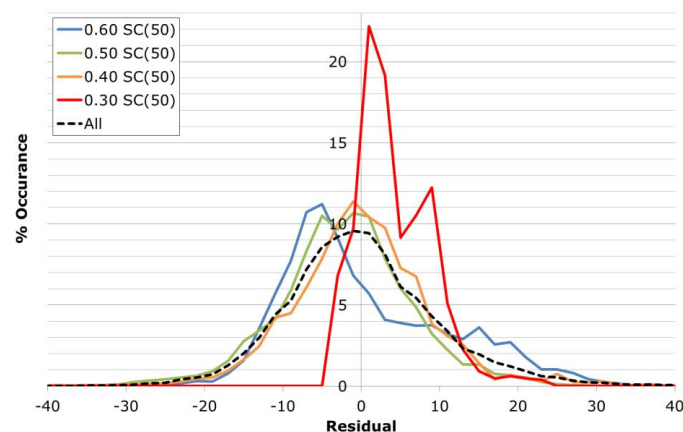
Figure 7-15 Distribution of residual values for different values of low speed skid resistance

Better understanding of the surface tyre interface

7.3 Observations from friction model validation

The following key observations were made from the model validation exercise:

- No colinearity was observed between any of the input variables.

- On average, the model explains nearly 70% of the variation in the observed friction values.

- A small number of input values corresponding to very low values of wheel slip are not predicted well by the model.

- Analysis of the residual values has shown that there is a 68%, 95% and 99.7% likelihood that a residual measurement will fall within approximately 10, 20 and 30 units respectively of the actual friction value.

- The model may over-predict the performance of materials with very low values of SC(50). Otherwise, there is little evidence for systematic bias within the model predictions.

- The friction model is less accurate than the TRL367 model, but is capable of estimating friction across a larger rage of vehicle speeds and wheel slip percentages, whereas the TRL367 model estimates friction at a single vehicle speed and wheel slip percentage.

8 Significance of low speed skid resistance and texture on vehicle manoeuvres

Having, in Chapter 7, developed a friction model to describe the shape of the friction / speed / slip profile seen in Figure 5-1, this section investigates the implications of the shape of the friction profile for an example manoeuvre, vehicle braking.

The performance of surfaces with various nominal levels of low speed skid resistance and texture depth were compared by calculating the distance required for a vehicle to reduce its speed from a specified initial speed to 20 km/h, under emergency braking, with and without ABS. The model built to carry out this analysis will be referred to as the braking model.

8.1 Braking model methodology

The process for developing the braking model can be summarised as:

1. Define assumptions and limitations.

2. Define a method to estimate the time taken to reach peak and locked-wheel friction on surfaces with varying friction characteristics.

3. Specify the initial conditions to be input for each model.

4. Define the iteration process to estimate the braking time and distance.

8.1.1 Definition of assumptions and limitations

The braking model uses an iterative process in which the predicted friction, for the given vehicle speed and wheel slip, is used to determine the instantaneous deceleration and distance travelled within each step of the iteration. The following assumptions and limitations were used for the development of the braking model:

- The deceleration of the vehicle can be characterised by the friction available for braking, defined by the friction model from Chapter 7. This assumes the braking performance of the vehicle is represented by the smooth tyre friction with a 1 mm water film thickness, as used in the original measurements.

- The use of ABS will hold the friction value at the peak friction value.

- The % slip / Speed relationship for the PFT is linear. This is justified in section 8.1.2

- Vehicle speeds below 20 km/h are not considered due to lack of data limiting the extent of validity of the friction model.

8.1.2 Estimate time to reach peak and locked-wheel friction

An estimate of the wheel slip occurring during each iteration is needed to determine the predicted friction level. This was estimated from existing locked-wheel skid test data, by analysing the time taken for the test wheel to reach its peak and locked-wheel states.

Figure 8-1 and Figure 8-2 plot the time taken to achieve locked-wheel and peak friction respectively in each of the individual measurements making up the database used to derive the friction model. These show that the time taken to achieve locked-wheel and peak

friction depends on the friction of the surface measured and the initial speed of the vehicle. A multiple linear regression was carried out on the vehicle speed and friction variables to produce equations that predict the time taken to achieve locked-wheel and peak friction (Equation 8-1 and Equation 8-2). These equations were used to predict the time taken to achieve locked-wheel and peak friction based on the initial conditions of the braking model.
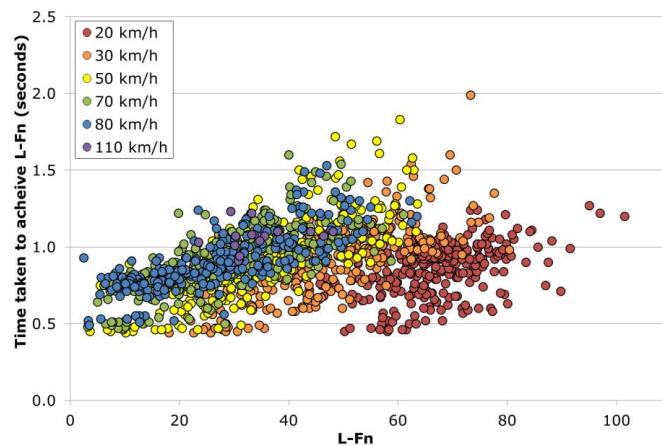
Figure 8-1 Relationship between vehicle speed, locked-wheel friction and the time taken to achieve locked-wheel friction
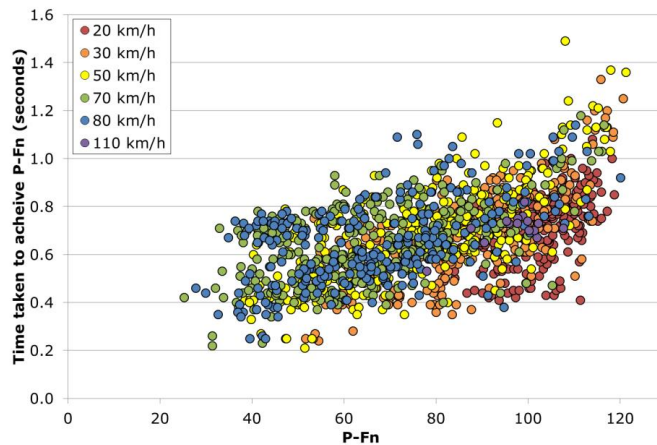
Figure 8-2 Relationship between vehicle speed, peak friction and the time taken to achieve peak friction

Better understanding of the surface tyre interface

$$t_L = 0.140732 + (0.001966 \times S) + (0.005392 \times LFnS)$$

Where:

- t_L = the time taken to achieve locked-wheel friction (seconds)
- S = the average speed of the measurement (km/h)
- LFnS = the locked-wheel friction of the surface at speed S

Equation 8-1 Estimation of the time taken to achieve locked-wheel friction

$$t_P = 0.140732 + (0.001966 \times S) + (0.005392 \times PFnS)$$

Where:

- t_P = the time taken to achieve peak friction (seconds)
- S = the average speed of the measurement (km/h)
- PFnS = the peak friction of the surface at speed S

Equation 8-2 Estimation of the time taken to achieve peak friction

8.1.3 *Specify the initial conditions for the model*

The input conditions required for each model are:

- Initial vehicle speeds (V1) of 50, 75 and 100 km/h were modelled in order to assess the influence of vehicle speed.

- Initial % slip. Set to 2% in all cases, which is the lower limit of the friction model.

- SMTD. Varied between 0.2 and 2.0 to determine the influence of texture depth.

- SC(50). Varied between 0.20 and 0.60 to determine the influence of low speed skid resistance.

- ABS Used. Set to "Yes" or "No" to assess the performance with and without the use of driver aids.

8.1.4 *Define the iteration process used to estimate the braking time and distance*

Starting from the initial conditions, the braking model calculates: the % slip, the vehicle acceleration (from the friction model, given the % slip and the vehicle speed), and the change in vehicle speed and the distance travelled during each iteration. This is continued through iterations of 0.01s until the speed of the vehicle reaches 20 km/h.

% Slip

The % slip of the wheels was derived using the times taken to achieve locked-wheel and peak friction to limit the linear relationships between % slip and time. Equation 8-1 and Equation 8-2 were used to estimate the time taken to achieve peak and locked-wheel friction in the prediction model by exchanging the "S" term in each equation with "V_1". The LFnS and PFnS terms in each equation were then estimated using the friction model.

The values gained were used to estimate the amount of slip experienced at each time interval using linear interpolation, as given in Equation 8-3 to Equation 8-7.

In the case where ABS is not used the following equations are used:

$$\% \, Slip_t = \mathop{\vphantom{\Big[}}\limits_{t \leq t_P}^{t \geq 0} \left[\% \, Slip_0 + \left((\% \, Slip_P - \% \, Slip_0) \times \frac{t}{t_P} \right) \right]$$

Where:

- t = time since brake activation (seconds)
- $\% \, Slip_t$ = The percentage slip estimated at time "t"
- $\% \, Slip_0$ = The percentage slip at time = 0 (this is always 2, given the model restrictions)
- $\% \, Slip_P$ = The percentage slip at peak friction

Equation 8-3 Estimation of the % Slip at any given time before peak friction is achieved and ABS is not used

$$\% \, Slip_t = \mathop{\vphantom{\Big[}}\limits_{t \leq t_L}^{t > t_P} \left[\% \, Slip_P + \left((100 - \% \, Slip_P) \times \frac{t - t_P}{t_L - t_P} \right) \right]$$

Equation 8-4 Estimation of the % Slip at any given time after peak friction is achieved and ABS is not used

$$\% \, Slip_t = \mathop{\vphantom{[}}\limits_{t=\infty}^{t > t_L} [\% \, Slip_L] = 100$$

Equation 8-5 Estimation of the % Slip at any given time after locked-wheel friction is achieved and ABS is not used

In the case where ABS is used the following equations are used:

$$\% \, Slip_t = \mathop{\vphantom{\Big[}}\limits_{t \leq t_P}^{t \geq 0} \left[\% \, Slip_0 + \left((\% \, Slip_P - \% \, Slip_0) \times \frac{t}{t_P} \right) \right]$$

Equation 8-6 Estimation of the % Slip at any given time before peak friction is achieved and ABS is used

$$\% \, Slip_t = \mathop{\vphantom{[}}\limits_{t=\infty}^{t > t_P} [\% \, Slip_P]$$

Equation 8-7 Estimation of the % Slip at any given time after peak friction is achieved and ABS is used

Speed

The vehicle speed throughout the braking cycle was calculated on an iterative basis by using the acceleration experienced during the previous time interval to calculate the speed at the next (Equation 8-8 and Equation 8-9).

$$a = (Fn \times 9.806)/100$$

Where:

a = the acceleration experienced by the vehicle (m/s^2)

Fn = the friction predicted from the friction model given the current vehicle speed and % slip

Equation 8-8 Calculation of vehicle acceleration from friction

$$V_t = V_{t-1} + (a_{t-1} \times \Delta t)$$

Where:

- V_t = the vehicle speed at time interval t
- V_{t-1} = The speed at the previous time interval (m/s)
- a_{t-1} = The acceleration at the previous time interval (m/s^2)
- Δt = The distance between the two time intervals (0.01 seconds in this example)

Equation 8-9 Calculation of speed

Distance travelled

The distance travelled at any time interval is calculated using the standard speed, distance and time relationship, this is shown in Equation 8-10.

$$d_t = V_t \times \Delta t$$

Where:

- d_t = the distance travelled at time interval t (m)
- Vt = the vehicle speed at time interval t (m/s)
- Δt = The distance between the two time intervals (0.01 seconds in this example)

Equation 8-10 Calculation of distance travelled

Summary

The iterative stages were repeated until the vehicle speed reached 20 km/h. The cumulative value of the distance travelled during the previous increments was then reported as the distance required for the vehicle to slow to 20 km/h.

Better understanding of the surface tyre interface

Table 8-1 shows how the process was carried out and how each of the values were calculated using the equations shown in this chapter.

Table 8-1 Example of model

Parameter	Time	Wheel slip	Vehicle speed	Acceleration	Distance travelled	Friction
Unit	(s)	(%)	(m/s)	(m/s^2)	(m)	None
Symbol	t	% Slip	V	A	d	Fn
	0.00	2	V_1	Equation 8-8	Equation 8-10	Calculated from friction model
	0.01	IF ABS = No AND t ≤ t_P THEN Equation 8-3 ELSE Equation 8-4 OR IF ABS = Yes AND t ≤ t_P THEN Equation 8-6 ELSE Equation 8-7	Equation 8-9	Equation 8-3	Equation 8-6	Calculated from friction model
	n	As above	As above	As above	As above	As above

8.2 Assessment of vehicle demand and supply

The braking model was used to conduct a sensitivity analysis of the braking distance based on the friction supplied to motorists at different speeds and under different road conditions. The results have been compared with the braking distances quoted in the Highway Code.

8.2.1 Methodology

The braking model was used to estimate the distances required for a vehicle to slow to 20 km/h from initial speeds of 50, 75 and 100 km/h, with and without ABS, for various skid resistance and texture combinations. This will be referred to as the surface condition analysis.

The braking model was also used to estimate the distance required for a vehicle to slow to 20 km/h on the typical surface ranges defined in Chapter 6. This analysis allowed an investigation of the ability for different surface types in very good and very poor condition to slow a vehicle performing an emergency braking manoeuvre. This will be referred to as the surface type analysis.

For comparison, Figure 8-3 gives the relationship between stopping distance (without thinking time) in wet conditions, for various initial vehicle speeds, from the values given in the Highway Code (Department for Transport, 2004). Since the braking model is not able to estimate the braking distance below 20 km/h, the relationship in Figure 8-3 was

extrapolated, leading to an estimate of 4.71 m for the braking distance from 20 km/h. This was subtracted from the Highway Code braking distances for comparison with the results of the braking model.
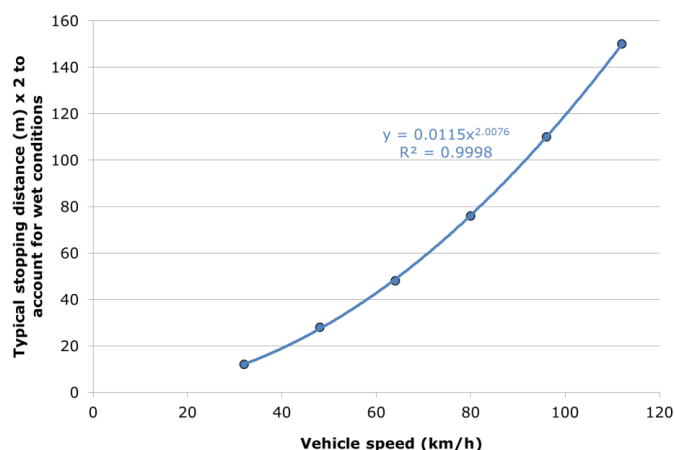
Figure 8-3 The relationship between initial vehicle speed and stopping distance (Department for Transport, 2004)

8.2.2   *Results of the surface condition analysis*

The results from the surface condition analysis are provided in Table 8-2 to Table 8-7. The values in the table cells represent the distance required to reduce the vehicle speed from the initial value to 20 km/h on pavements with the texture depth and low speed skid resistance characteristics represented by the row and column headers. The cells are shaded to indicate if the value is:

- <90% of the distance indicated by the Highway Code (Blue)
- ≥90 <100% of the distance indicated by the Highway Code (Orange)
- ≥ 100% of the distance indicated by the Highway Code (Red)

The texture depth requirement for the English SRN generally requires a level of above 0.8 mm SMTD (HD29 Data for pavement assessment, 2008). The skid resistance requirements are provided for different site categories in HD28 of the DMRB (HD28 Skidding resistance, 2015). Broadly, the site categories can be separated into two groups, high and low risk sites. The skid resistance requirements for low risk sites, such as mainline lengths of Motorways and All Purpose Trunk Roads are generally assigned a minimum Investigatory Level (IL) of 0.35 SC(50). The skid resistance requirements for high risk sites, such as approaches to junctions or roundabouts generally attract an IL of 0.50 SC(50). The texture depth and low speed skid resistance requirements for low and high risk sites are represented in the following tables by the dotted and solid thick lines respectively.

Better understanding of the surface tyre interface

Initial speed 50 km/h

Table 8-2 Vehicle braking distance (m) to 20 km/h (V1 = 50, ABS used = Yes)

SC(50)	SMTD (mm)									
	0.2	0.4	0.6	0.8	1.0	1.2	1.4	1.6	1.8	2.0
0.20	39.07	25.56	20.52	17.98	16.32	15.18	14.52	13.89	13.31	12.89
0.25	34.89	23.15	18.94	16.71	15.26	14.42	13.69	13.09	12.59	12.19
0.30	31.43	21.27	17.55	15.75	14.49	13.59	12.90	12.38	11.96	11.67
0.35	28.47	19.57	16.45	14.72	13.60	12.86	12.25	11.89	11.50	11.19
0.40	25.92	18.13	15.40	13.87	12.87	12.28	11.77	11.37	10.99	10.76
0.45	23.70	16.95	14.40	13.18	12.29	11.69	11.30	11.00	10.70	10.42
0.50	21.58	15.73	13.62	12.48	11.80	11.27	10.89	10.58	10.29	10.08
0.55	19.78	14.79	12.99	11.98	11.28	10.81	10.47	10.18	9.91	9.70
0.60	18.32	14.00	12.31	11.40	10.81	10.39	10.08	9.80	9.58	9.39

Table 8-3 Vehicle braking distance (m) to 20 km/h (V1 = 50, ABS used = No)

SC(50)	SMTD (mm)									
	0.2	0.4	0.6	0.8	1.0	1.2	1.4	1.6	1.8	2.0
0.20	46.24	29.10	23.58	20.73	18.77	17.34	16.55	15.72	15.01	14.42
0.25	40.92	26.66	21.78	19.27	17.50	16.44	15.51	14.72	14.05	13.53
0.30	36.55	24.60	20.31	18.16	16.54	15.41	14.51	13.81	13.22	12.77
0.35	32.97	22.68	19.07	16.92	15.49	14.41	13.61	13.08	12.58	12.11
0.40	30.02	21.03	17.81	15.81	14.50	13.64	12.95	12.37	11.83	11.45
0.45	27.44	19.78	16.59	14.91	13.72	12.86	12.30	11.83	11.38	11.02
0.50	25.20	18.34	15.61	14.00	13.05	12.21	11.66	11.19	10.76	10.42
0.55	23.17	17.18	14.71	13.25	12.28	11.57	11.02	10.58	10.23	9.95
0.60	21.64	16.12	13.82	12.48	11.64	10.99	10.48	10.06	9.77	9.51

Better understanding of the surface tyre interface

Initial speed75 km/h

Table 8-4 Vehicle braking distance (m) to 20 km/h (V1 = 75, ABS used = Yes)

SC(50)	SMTD (mm)									
	0.2	0.4	0.6	0.8	1.0	1.2	1.4	1.6	1.8	2.0
0.20	145.92	81.63	63.21	53.44	47.44	43.37	40.44	38.37	36.55	35.09
0.25	124.52	73.94	57.21	48.79	43.64	40.27	37.70	35.78	34.22	32.94
0.30	107.60	67.31	52.12	44.73	40.43	37.41	35.22	33.52	32.27	31.17
0.35	94.64	59.74	47.57	41.38	37.54	34.95	33.14	31.69	30.47	29.62
0.40	84.20	54.19	43.68	38.36	35.21	32.93	31.41	30.05	29.07	28.19
0.45	75.60	49.26	40.26	35.97	33.14	31.16	29.70	28.60	27.64	26.83
0.50	68.10	44.99	37.64	33.69	31.25	29.46	28.21	27.21	26.56	25.91
0.55	60.76	41.55	35.10	31.71	29.55	28.24	27.09	26.14	25.46	24.80
0.60	54.60	38.49	32.96	30.19	28.27	26.94	25.92	25.07	24.39	23.83

Table 8-5 Vehicle braking distance (m) to 20 km/h (V1 = 75, ABS used = No)

SC(50)	SMTD (mm)									
	0.2	0.4	0.6	0.8	1.0	1.2	1.4	1.6	1.8	2.0
0.20	221.70	102.36	78.04	66.34	59.33	54.42	50.72	48.13	45.80	43.89
0.25	173.87	91.41	71.16	61.15	54.88	50.75	47.51	44.98	42.85	41.11
0.30	143.93	82.49	65.23	56.48	51.17	47.32	44.39	42.07	40.35	38.81
0.35	123.01	74.76	60.05	52.58	47.70	44.20	41.73	39.64	37.94	36.65
0.40	107.46	68.30	55.69	48.89	44.65	41.55	39.32	37.44	35.95	34.65
0.45	95.41	62.80	51.64	45.83	41.93	39.14	36.99	35.34	33.92	32.71
0.50	85.57	57.87	48.27	42.87	39.39	36.82	34.90	33.35	32.28	31.31
0.55	77.22	53.71	45.04	40.23	36.99	34.95	33.20	31.72	30.64	29.65
0.60	70.29	49.93	42.20	38.02	35.16	33.05	31.47	30.17	29.03	28.18

Better understanding of the surface tyre interface

Initial speed100 km/h

Table 8-6 Vehicle braking distance (m) to 20 km/h (V1 = 100, ABS used = Yes)

SC(50)	SMTD (mm)									
	0.2	0.4	0.6	0.8	1.0	1.2	1.4	1.6	1.8	2.0
0.20	411.94	232.18	141.16	129.31	107.82	90.15	83.13	77.95	73.80	70.45
0.25	341.10	207.95	138.79	110.79	97.73	82.50	76.49	71.98	68.44	65.66
0.30	291.16	172.77	123.79	100.12	86.51	75.84	70.78	67.04	64.02	61.50
0.35	254.01	143.32	106.53	91.39	76.18	70.30	66.42	63.11	60.42	58.24
0.40	225.33	127.26	96.64	81.36	71.00	65.87	62.14	59.23	56.91	54.97
0.45	188.47	109.80	88.59	72.47	66.03	61.61	58.34	55.82	53.74	52.05
0.50	165.08	99.30	76.29	67.27	61.76	57.95	55.07	52.79	51.05	49.55
0.55	147.00	90.72	70.89	62.85	58.02	54.63	52.09	50.17	48.56	47.23
0.60	125.34	78.60	65.99	59.41	54.76	51.88	49.59	47.80	46.37	45.15

Table 8-7 Vehicle braking distance (m) to 20 km/h (V1 = 100, ABS used = No)

SC(50)	SMTD (mm)									
	0.2	0.4	0.6	0.8	1.0	1.2	1.4	1.6	1.8	2.0
0.20	>452.31	261.07	184.29	151.31	132.75	119.57	110.57	103.91	98.41	93.95
0.25	>452.31	223.94	164.00	137.38	122.04	110.33	102.53	96.51	91.62	87.79
0.30	452.31	195.98	148.41	125.92	112.27	102.13	95.24	90.08	85.83	82.25
0.35	342.97	173.85	134.83	116.11	103.14	95.01	89.28	84.59	80.71	77.54
0.40	279.19	156.24	123.72	107.07	96.13	88.94	83.58	79.32	75.92	73.01
0.45	236.27	141.40	114.23	98.75	89.71	83.22	78.42	74.60	71.47	68.84
0.50	204.95	129.24	104.64	91.96	83.86	78.12	73.77	70.27	67.55	65.16
0.55	181.14	118.83	97.28	85.92	78.71	73.50	69.48	66.43	63.85	61.66
0.60	161.61	108.89	90.77	80.81	73.93	69.34	65.69	62.78	60.43	58.45

Better understanding of the surface tyre interface

TRL

8.2.3   Results of the surface type analysis

The results from the surface type analysis are provided in Table 8-8. The values in the table cells represent the distance required to reduce the vehicle speed from the initial value (V1) to 20 km/h on the pavement types described by the row headers. The same shading as the previous tables has been used to indicate the surface performance against expected performance.

Table 8-8 Vehicle braking distances on different surface types

Surface type		Vehicle braking distance(m) to 20 km/h from following V1					
		With ABS			Without ABS		
		100	75	50	100	75	50
95th percentile (surface in good condition)	Concrete	69.52	34.85	12.53	91.82	43.32	13.90
	HRA	43.88	23.21	9.10	55.22	26.92	9.16
	TSCS	40.94	20.80	7.87	47.94	22.37	7.87
5th percentile (surface in poor condition)	Concrete	230.28	96.03	28.95	335.49	136.11	38.03
	HRA	116.55	58.59	21.10	172.65	84.44	28.93
	TSCS	83.06	42.32	16.60	134.27	62.04	21.69

8.2.4   Observations from results

From the results of this analysis the following general observations can be made:

- The braking distance is predicted to increase as either the low speed skid resistance or the texture depth decreases. Some combinations (indicated in red in the tables) result in a braking distance that exceeds the values given in the Highway Code.

- As modelled, the use of ABS results in a notable improvement in braking distance. (However, the model is relatively crude, assuming that the peak friction level is maintained throughout braking.)

- The margin between the area of the table corresponding to the friction requirements for Motorways and All Purpose Trunk Roads and the area of the table where the Highway Code braking distances are exceeded reduces with increasing vehicle speed.

- Arguably, pavements may be over specified, in terms of low speed skid resistance and texture, for sites where the speed limit is 50 km/h (30mph).

- The braking distance never exceeds Highways Code values for cases where the greatest texture depth (>= 1.1 mm SMTD) and low speed skid resistance (>= 0.5 SC(50)) requirements apply. This is not always the case for the lower requirements.

- It seems possible to mitigate the risk posed by low values of SC(50) with increasing texture depth, but the converse appears less achievable.

- Surfaces of all types kept in good condition provide lower braking distances than those given in the Highway Code.

- It may be expected for a TSCS in poor condition to provide acceptable braking performance, provided that the vehicle using the surface is equipped with ABS.

These results represent the worst case scenario (a vehicle with bald tyres and where locked-wheel friction is reached as soon as possible) and therefore may not be representative of the majority of the vehicle fleet.

9 Summary, discussion and conclusions

This chapter discusses the results of the work in the context of the research aims listed in Chapter 3.

9.1 Literature review

A literature review was carried out to further the knowledge of the influence of surface characteristics on vehicle handling under different manoeuvres. The study concluded that:

- Texture depth is a major contributor to friction at high levels of wheel slip, tyre properties and road surface microtexture contribute to friction at lower levels of slip.
- The most commonly reported road friction models use an exponential function to describe the change in friction with wheel slip percentage or vehicle speed.
- Driver aids generally operate in the region of the friction/slip curve around (at comparable slip ratios to) the peak friction.
- Vehicle dynamics systems contain proprietary algorithms for estimating the friction available. They make use of vehicle based information to make relatively crude assumptions about the maximum level of friction available.

9.2 Defining the speed, wheel slip and friction relationship

A procedure was developed for defining the friction profile of a road surface as a function of the test speed and wheel slip percentage. This procedure enabled the variation of friction to be observed readily over the range of achievable vehicle speeds and wheel slip ratios for individual surfaces. This is a substantial development as, traditionally, skid resistance is measured at a single vehicle speed and wheel slip percentage.

These three dimensional relationships were developed using historical measurements made using the PFT, available in a database maintained by TRL. In total 2,494 PFT measurements made on 169 surfaces between 1997 and 2013 were used in this study. Each surface was characterised over a speed range of 20 to 100 km/h at slip ratios between 2 and 100%.

The expression of pavement skid resistance as a function of vehicle speed and wheel slip is the first step in understanding the relationship between vehicle behaviour and pavement performance and, hence, assessing road user risk.

9.3 Assessment of typical material performance as a function of texture depth and low speed skid resistance

The friction profiles for different surface types were analysed to assess the typical range of performance for Concrete, HRA and TSCS materials. This was achieved by grouping the results collected from various materials and calculating the 5th and 95th percentiles of the friction values at each speed/slip combination.

This analysis identified a clear difference in performance between the materials. Concrete materials provided the lowest friction values of the three; the performance of the asphalt materials, TSCS and HRA, was generally higher than that of concrete. The 5th percentile

performance of the asphalt materials was similar but the TSCS provided a greater 95th percentile, resulting in a large 90th percentile range. This variation may reflect the variability between TSCS materials, which are diverse and utilise different sizes of aggregate and binder materials.

A valuable sequel to this work would be to collect supplementary measurements of material performance on a variety of TSCS materials. This would enable the assessment of materials with different components or constructions.

It is likely that the overall performance of these materials is largely driven by their texture depth performance. Concrete surfaces tend to possess lower texture depth than asphalt materials, which could potentially lead to a poorer high speed friction performance. The implications for braking performance are discussed below in Section 9.5.

9.4   Development of a friction prediction model

A model was developed to predict the friction performance of materials with respect to wheel slip and vehicle speed, using input variables of low speed skid resistance and texture depth. This model was needed to estimate the implications of delivering different levels of low speed skid resistance and texture depth, which is discussed in Section 9.5.

The results of the modelling exercise were promising in relation to the current Highways England pavement assessment methodology since the parameters routinely measured by Highways England are capable of being used to infer friction performance with a reasonable level of accuracy. However there is scope for improving the model and the distribution of the residual values suggest that there are pavement properties other than texture depth and low speed skid resistance which influence friction generation.

Analysis of the residual values showed some discrepancies between actual and predicted values for very low levels of wheel slip and low speed skid resistance:

- At very low wheel slip, 2 to 5 %, the model has a tendency to under-estimate the amount of friction provided by the road surface.

- At low levels of low speed skid resistance, around 0.30 SC(50), the model tends to over-predict the amount of friction available by approximately 0.05 units.

This suggests that either the form of the equations used within the model is not accurately representing the influence of these parameters over this range, or some other influence is occurring that has not been included in the model. Further assessment of this phenomenon would be a valuable exercise for future work.

An analysis of the residual values from the friction model showed that the model was capable of predicting 95% of the friction values within 20 units. This performance is worse than that of the model reported in TRL367 (Roe *et al.*, 1998), which is capable of predicting 95% of friction values within 12 units. However, the TRL367 model predicts friction for only

one wheel slip and vehicle speed combination[B] whereas the model developed as part of this work is capable of predicting friction over a wide range of vehicle speed and wheel slip.

9.5 Significance of low speed skid resistance and texture for vehicle manoeuvres

A methodology was developed to assess the contribution of pavement texture depth and low speed skid resistance to the performance of vehicles conducting an emergency braking manoeuvre. This uses the deceleration that could be expected based on the friction model as a proxy for vehicle performance, to predict the distance required to slow a vehicle from a specified initial speed to 20 km/h. This exercise was carried out to model surfaces with varying texture depth and low speed skid resistance. The results were compared with the braking distances listed in the UK Highway Code.

The surface performance was analysed in the context of Highways England requirements for pavement texture depth and low speed skid resistance. The results showed that in all cases, the predicted braking performance supplied by pavements which met texture depth requirements of 0.8 mm SMTD and low speed skid resistance criteria of 0.50 SC(50) was within the distances listed in the Highway Code. The results also showed that at low vehicle speeds (50 km/h) the potential friction supply was markedly greater than that which may be demanded. This was, notably, not the case for braking manoeuvres from high speed with no ABS on pavements with lower requirements (0.8 mm SMTD and 0.35 SC(50)). It should be noted that these results represent a worst case scenario (i.e. a vehicle with bald tyres and where locked-wheel friction is reached as soon as possible).

An additional analysis was carried out to assess the performance of Concrete, HRA and TSCS materials in good (95th percentile) and poor (5th percentile) condition. The results of this analysis showed that all of the materials in good condition provided braking distances within those listed in the UK Highway Code. For HRA and Concrete in poor condition, the braking distance is generally predicted to be longer than given in the Highway Code. This is also the case for TSCS for the model without ABS although, notably, even in poor condition the TSCS seems to provide adequate braking with ABS.

While the exact threshold of the Highway Code distances should not be interpreted too literally given the number of assumptions made in the modelling, the observation suggests that in some areas of the network the pavement properties may be over specified whereas in other cases, pavements with low texture depth may not be providing satisfactory performance. Furthermore, the influence of speed is considerable. Speed is taken into account in specifying some site categories and Investigatory Levels within HD28, but this could be developed more thoroughly using this approach. Conversely, the risk on the network could be normalised by reducing traffic speed at high risk locations through the imposition of lower speed limits.

The analysis enabled the relative influence of texture depth and low speed skid resistance on the ability for a vehicle to conduct emergency braking to be assessed. This showed

---

[B] A vehicle speed of 100 km/h and 100% wheel slip (locked-wheel).

texture depth to be the dominant factor in reducing the distance required for a vehicle to slow to 20 km/h. In all of the cases observed, for materials simulated with low values of texture depth, an unrealistic amount of low speed skid resistance would be required to compensate for the loss of braking performance associated with the low texture depth. However for materials simulated with low values of low speed skid resistance, the loss of performance could be mitigated by the provision of, in most cases, an achievable level of texture depth.

This observation has potential connotations for pavement design and maintenance, but the assessment made was limited to a single manoeuvre, using a friction model based on measurements obtained from testing with a smooth tyre and a nominal 1mm water depth. It would be valuable, therefore, to carry out the same analysis for other manoeuvres such as, cornering, lane changes and combined braking and cornering. If similar observations are made then the results could be used to influence design and maintenance standards.

9.6 Conclusions

A procedure was developed, using historical measurements made with the PFT, for defining the friction profile of a road surface as a function of the test speed and wheel slip percentage. The resulting 3-dimensional friction profiles allowed the production of a model capable of predicting road pavement friction based on macrotexture and low speed skid resistance.   The model also facilitates an understanding of how the road surface characteristics influence vehicle performance; in this case this has been studied through considering the effect of skid resistance and texture depth on vehicle braking manoeuvres from different initial speeds. This methodology could be extended to other manoeuvres following the collection of supporting vehicle dynamics information.

From the work carried out the following conclusions can be made:

- Concrete and asphalt materials exhibit markedly different friction performance. Further work should be undertaken to assess the effect of material design on the friction performance of TSCS materials, which varies considerably.

- The friction prediction model developed performs well overall in predicting friction over a wide range of slip ratio and vehicle speed, from inputs of low speed skid resistance and texture depth. However, it is less accurate at low slip (below 5%) and low, low speed friction (around 0.30 units SC(50)).

- Whilst low speed skid resistance and texture depth both contribute to the braking performance, the importance of texture depth seems particularly significant and texture depth is better able to compensate for lower levels of low speed skid resistance than vice versa.

- There appears to be an optimum contribution of low speed skid resistance and texture depth to braking distance, taking account of the vehicle speed and the performance of different surfacing materials.

- The use of driver aids designed to exploit peak friction has a substantial benefit on the braking performance of vehicles. A wide uptake (approaching 100%) of driver aids could allow for a reduction in the friction requirements on the SRN. However,

Better understanding of the surface tyre interface

information on the current and projected distribution of vehicles with driver aids would be needed before making changes to specifications.

237

TRL

References

Aly AA, Zeidan ES, Hamed A and Salem F (2011). *An Antilock-Braking Systems (ABS) Control: A Technical Review* (2011 - 2 - 186-195). Scientific Research, Intelligent Control and Automation .

ASTM (2008). *E524-08 Standard Specification for Standard Smooth Tire for Pavement Skid-resistance Tests*. ASTM: West Conshohocken.

ASTM (2011). *E274/E274M-11 Standard Test Method for SkidResistance of Paved surfaces Using a full-Scale Tire*. ASTM: West Conshohocken.

ASTM (2015). *E1845-15 Standard practice for calculating pavement macrotexture measn profile depth*. ASTM: West Conshohocken.

ASTM (2015). *E965-15 Standard test method for measuring pavement macrotexture depth using a volumetric technique*. ASTM: West Conshohocken.

Brittain S and Viner HE (2017). *PPR818 Development of a high speed friction performance criteriion for asphalt materials* (Wokingham). TRL Limited.

BSI (2000). *BS 7941-2 Surface friction of pavements - Part 2: Test method for measurement of surface skid resistance using the GripTester braked wheel fixed slip device*. British Standards Institution: London.

BSI (2006). *BS 7941-1 Methods for measuring the skid resistance of pavement surfaces. Sideway-force coefficient routine investigation machine*. British Standards Institution: London.

Department for Transport (2004). *The highway code*. Department for Transport: London.

Flintsch GW, McGhee KK, de León Izeppi E and Najafi S (2012). *The little Book of Tire Pavement Friction Version 1.0*. Pavement Surface Properties Consortium.

Gothie M, Parry T and Roe P (2001). The relative influence of the parameters affecting road surface friction. 2nd International colloquium on vehicle tyre road interaction. University of Florence, Civil Engineering Department.

Hall JW, Smith KL, Tirus-Glover L, Wambold JC, Yager TJ and Rado Z (2009). *NCHRP Guide for Pavement Friction.*, National Cooperative Highway Research Program; Transport Research Board of the national academies, Contractor's Final Report for NCHRP Project 01-43.

Hart P (2003). *ABS Braking Requirements*. Hartwood Consulting Pty Ltd: Vistoria.

Better understanding of the surface tyre interface

Henry JJ (1983). *Comparison of Friction Performance of a Passenger Tire and the ASTM Standard Test Tires, ASTM STP 793*. American Society for Testing and Materials (ASTM): Philadelphia, Pennsylvania.

Henry JJ (2000). *Evaluation of pavement friction characteristics*. Transportation Research Board.

Highways England, Transport Scotland, Welsh Government, The Department for Regional Development Northern Ireland (2006). *HD36 Surfacing materials for new and maintenance construction*. The Stationary Office: London.

Highways England, Transport Scotland, Welsh Government, The Department for Regional Development Northern Ireland (2008). *HD29 Data for pavement assessment*. The Stationery Office: London.

Highways England, Transport Scotland, Welsh Government, The Department for Regional Development Northern Ireland (2015). *HD28 Skidding resistance*. The Stationery Office: London.

Kane M, Conter M, Roe P and Schwalbe G (2009). *Report on different parameters influencing skid resistance, rolling resistance and noise emissions*. Deliverable D10 of the FP7 TYROSAFE project, available from http://www.transport-research.info/sites/default/files/project/documents/20120406_002134_64278_TYROSAFE_WP3_D10_ReportOnInfluencingParameters_v2.0_20090824.pdf.

Koskinen S and Peussa P (2004). *FRICTION - Final Report* (FP6-IST-2004-4-027006). Information Society Technologies Programme.

Kummer HW (1966). *Unified theory of rubber and tire friction*. Pennsylvania State University College of Engineering.

Manual of Contract documents for Highway Works. 2008.

Matsuzaki R, Kamai K and Seki R (2015). *Intelligent tires for identifying coefficient of friction of tire/road contact surfaces using three-axis accelerometer*. Smart Materials and Structures, Tokyo University of Science: 025010.

Moore DF (1975). *The friction of pneumatic tyres*. Elsevier Scientific Publishing Company: Amsterdam.

Pacejka HB (2006). *Tire and Vehicle Dynamics; Second Edition.*, SAE Society of Automotive Engineers.

Parry AR and Viner HE (2005). *TRL622 Accidents and the skidding resistance standard for strategic roads in England*. TRL: Wokingham.

Better understanding of the surface tyre interface

Roe PG and Sinhal R (1998). *TRL322 The Polished Stone Value of aggregates and in-service skidding resistance*. TRL: Crowthorne, UK.

Roe PG, Parry AR and Viner HE (1998). *TRL367 High and low speed skidding resistance: the influence of texture depth*. TRL: Wokingham.

Roe PG and Dunford A (2012). *PPR564 The skid resistance behaviour of thin surface course systems*. TRL: Crowthorne, UK.

Sanders PD, Morosiuk K and Peeling J (2014). *PPR727 Road Surface properties and high speed friction*. TRL: Crowthorne.

Singh KB and Taheri S (2015). *Estimation of tire-road friction coefficient and its application in chassis control systems*. Systems Science & Control Engineering, 3:1, 39-61, DOI: 10.1080/21642583.2014.985804.

Vos E, Groenendijk J, Do MT and Roe P (2009). *Report on analysis and findingss of previous skid resistance harmonisation projects*. D05 Tyre and road surface optimisation for skid resistance and further effects.

Wallbank C, Viner H, Smith L and Smith R (2016). *The relationship between collisions and skid resistance on the Strategic Road Network*. TRL Limited: Wokingham.

Wang H, Al-Qadi IL and Staniculescu I (2010). *Effect of Friction on Rolling Tire - Pavement Interaction*. Nextrans.

Wong JY (1993). *Theory of Ground Vehicles.*, John Wiley & Sons, Inc.

Better understanding of the surface tyre interface   TRL

Appendix A Summary of materials assessed and friction profiles generated

Profile number	Date of measurement	Measurements made	Location	Surfacing type
027	01/01/1997	15	A1	Thin Surface Course System
028	01/01/1997	16	A1	Thin Surface Course System
029	01/01/1997	16	A1	Exposed aggregate concrete
030	01/01/1997	16	A1	Exposed aggregate concrete
031	01/01/1997	16	A1	Exposed aggregate concrete
032	01/01/1997	15	A1	Stone mastic asphalt
033	01/01/1997	14	A329M	Hot rolled asphalt
034	01/01/1997	16	A329M	Hot rolled asphalt
035	01/01/1997	14	A329M	Hot rolled asphalt
036	01/01/1997	14	A329M	Hot rolled asphalt
037	01/01/1997	12	A329M	Exposed aggregate concrete
038	01/01/1997	12	A329M	Exposed aggregate concrete
039	01/01/1997	12	A329M	Exposed aggregate concrete
040	01/01/1997	12	A329M	Exposed aggregate concrete
041	01/01/1997	12	A329M	Hot rolled asphalt
042	01/01/1997	10	A329M	Thin Surface Course System
043	01/01/1997	14	M5	Hot rolled asphalt
044	01/01/1997	12	M5	Hot rolled asphalt
045	01/01/1997	14	M5	Hot rolled asphalt
046	01/01/1997	14	M5	Hot rolled asphalt
047	01/01/1997	14	M5	Hot rolled asphalt
048	01/01/1997	14	M5	Exposed aggregate concrete
051	01/01/1997	13	M5	Hot rolled asphalt
052	01/01/1997	13	M5	Hot rolled asphalt
053	01/01/1997	15	A140	Brushed concrete
054	01/01/1997	15	A140	Brushed concrete
055	01/01/1997	15	A140	Brushed concrete
056	01/01/1997	15	A140	Grooved concrete
057	01/01/1997	15	A140	Brushed concrete
058	01/01/1997	17	A140	Brushed concrete
059	01/01/1997	16	A140	Brushed concrete
060	01/01/1997	17	A140	Brushed concrete
061	01/01/1997	17	A140	Brushed concrete

Better understanding of the surface tyre interface

Profile number	Date of measurement	Measurements made	Location	Surfacing type
062	01/01/1997	16	A140	Brushed concrete
069	01/01/1997	18	M40	Porous asphalt
070	01/01/1997	18	M40	Porous asphalt
071	01/01/1997	18	M40	Porous asphalt
072	01/01/1997	18	M40	Porous asphalt
073	01/01/1997	18	M40	Porous asphalt
074	01/01/1997	18	M40	Stone mastic asphalt
075	01/01/1997	18	M40	Stone mastic asphalt
076	01/01/1997	18	M40	Stone mastic asphalt
077	01/01/1997	16	M40	Stone mastic asphalt
078	01/01/1997	15	M40	Stone mastic asphalt
082	01/01/1997	14	A331	Porous asphalt
083	01/01/1997	14	A331	Hot rolled asphalt
084	01/01/1997	15	A322	Surface dressing
085	01/01/1997	15	A322	Surface dressing
086	01/01/1997	14	A322	Surface dressing
087	01/01/1997	15	A322	Surface dressing
088	01/01/1997	13	TRL	Exposed aggregate concrete
089	01/01/1997	12	TRL	Exposed aggregate concrete
091	01/01/1997	9	A249	Brushed concrete
092	01/01/1997	15	A249	Brushed concrete
093	01/01/1997	14	A249	Brushed concrete
094	01/01/1997	15	A249	Brushed concrete
095	01/01/1997	15	A249	Brushed concrete
096	01/01/1997	12	A249	Brushed concrete
097	01/01/1997	13	A27	Brushed concrete
098	01/01/1997	13	A27	Brushed concrete
099	01/01/1997	12	A27	Brushed concrete
100	01/01/1997	13	A27	Brushed concrete
101	01/01/1997	11	A27	Grooved concrete
102	01/01/1997	13	A27	Brushed concrete
103	01/01/1997	12	A27	Brushed concrete
104	01/01/1997	12	A27	Brushed concrete
105	01/01/1997	10	A27	Brushed concrete
106	01/01/1997	11	A325	Surface dressing
107	01/01/1997	12	A325	Surface dressing

Better understanding of the surface tyre interface

Profile number	Date of measurement	Measurements made	Location	Surfacing type
108	01/01/1997	12	A325	Surface dressing
109	01/01/1997	12	A325	Surface dressing
110	01/01/1997	11	A325	Surface dressing
111	01/01/1997	15	A34	Brushed concrete
112	01/01/1997	15	A34	Brushed concrete
113	01/01/1997	15	A34	Brushed concrete
114	01/01/1997	14	A34	Brushed concrete
115	01/01/1997	15	A34	Hot rolled asphalt
116	01/01/1997	15	A90	Surface dressing
118	01/01/1997	15	A90	Surface dressing
119	01/01/1997	15	A90	Surface dressing
121	01/01/1997	15	A766	Hot rolled asphalt
122	01/01/1997	15	A766	Hot rolled asphalt
123	01/01/1997	15	A766	Surface dressing
124	01/01/1997	15	A766	Surface dressing
125	01/01/1997	15	A702	Hot rolled asphalt
126	01/01/1997	15	A702	Hot rolled asphalt
127	01/01/1997	12	A90	Grooved concrete
128	01/01/1997	12	A90	Grooved concrete
129	01/01/1997	14	A90	Brushed concrete
130	01/01/1997	115	A90	Brushed concrete
131	01/01/1997	14	A90	Brushed concrete
132	01/01/1997	15	A90	Brushed concrete
133	01/01/1997	14	A1_H	Stone mastic asphalt
134	01/01/1997	16	A1_H	Stone mastic asphalt
135	01/01/1997	16	A1_H	Stone mastic asphalt
136	01/01/1997	16	A1_H	Stone mastic asphalt
137	01/01/1997	16	A1_H	Stone mastic asphalt
138	01/01/1997	16	A1-M1	Brushed concrete
139	01/01/1997	15	A1-M1	Brushed concrete
140	01/01/1997	15	A1-M1	Brushed concrete
141	01/01/1997	15	A1-M1	Brushed concrete
143	06/12/2005	9	A5	Thin Surface Course System 10mm
144	06/12/2005	9	A5	Thin Surface Course System 14mm
145	06/12/2005	9	A5	Thin Surface Course System 14mm
151	23/06/2006	7	A5	Thin Surface Course System 10mm

243

Profile number	Date of measurement	Measurements made	Location	Surfacing type
152	23/06/2006	12	A5	Thin Surface Course System 14mm
153	23/06/2006	9	A5	Thin Surface Course System 14mm
154	23/06/2006	9	A5	Thin Surface Course System 6mm
155	23/06/2006	8	A5	Thin Surface Course System 10mm
156	23/06/2006	8	A5	Thin Surface Course System 14mm
170	22/06/2006	16	A5	Thin Surface Course System 10mm
171	22/06/2006	20	A5	Thin Surface Course System 14mm
172	22/06/2006	7	A5	Thin Surface Course System 10mm
173	22/06/2006	6	A5	Thin Surface Course System 14mm
174	04/10/2006	18	A5	Thin Surface Course System 10mm
175	04/10/2006	8	A5	Thin Surface Course System 14mm
176	04/10/2006	10	A5	Thin Surface Course System 10mm
177	04/10/2006	10	A5	Thin Surface Course System 14mm
179	02/06/2006	10	A14	Thin Surface Course System 10mm
180	02/06/2006	7	A14	Thin Surface Course System 14mm
181	03/06/2006	16	A14	Thin Surface Course System 6mm
182	03/06/2006	11	A14	Thin Surface Course System 10mm
183	03/06/2006	12	A14	Thin Surface Course System 14mm
186	20/10/2006	17	A14	Thin Surface Course System 14mm
188	12/11/2008	13	M8	Dense Thin Surface Course System 10mm un-gritted
189	12/11/2008	21	M8	Dense Thin Surface Course System 8mm un-gritted
190	12/11/2008	9	M8	Dense Thin Surface Course System 6mm un-gritted
193	12/11/2008	9	M8	Dense Thin Surface Course System 10mm gritted
195	16/11/2008	9	M8	Dense Thin Surface Course System 14mm un-gritted
196	16/11/2008	9	M8	Dense Thin Surface Course System 10mm un-gritted
197	16/11/2008	9	M8	Dense Thin Surface Course System 8mm un-gritted
200	16/11/2008	9	M8	Dense Thin Surface Course System 8mm gritted
220	30/08/2011	24	M27 EB	Pavement quality concrete
221	30/08/2011	9	M27	Pavement quality concrete (fine milling)
222	30/08/2011	19	M27	Pavement quality concrete (shot blasting)

Better understanding of the surface tyre interface

Profile number	Date of measurement	Measurements made	Location	Surfacing type
223	30/08/2011	12	M27	Pavement quality concrete (bush hammering)
224	16/11/2011	11	M27 WB	Pavement quality concrete (fine milling)
227	16/11/2011	11	M27	Pavement quality concrete (shot blasting)
229	16/11/2011	13	M271 N	Pavement quality concrete (fine milling)
230	16/11/2011	24	M271 N	Pavement quality concrete (fine milling)
233	18/09/2012	15	M27 WB	Pavement quality concrete (fine milling)
234	18/09/2012	14	M27 EB	Pavement quality concrete (fine milling)
235	18/09/2012	14	M27	Pavement quality concrete (fine milling)
237	18/09/2012	14	M27	Pavement quality concrete (bush hammering)
238	18/09/2012	13	M271 N	Pavement quality concrete (fine milling)
239	18/09/2012	15	M271 N	Pavement quality concrete (fine milling)
240	18/09/2012	14	M271 S	Pavement quality concrete (fine milling)
241	18/09/2012	15	M271 S	Pavement quality concrete (fine milling)
242	19/06/2013	12	M27 WB	Pavement quality concrete (fine milling)
243	19/06/2013	12	M27 EB	Pavement quality concrete (fine milling)
244	19/06/2013	12	M27	Pavement quality concrete (fine milling)
245	19/06/2013	15	M27	Pavement quality concrete (shot blasting)
246	19/06/2013	13	M27	Pavement quality concrete (bush hammering)
247	19/06/2013	14	M271 N	Pavement quality concrete (fine milling)
248	19/06/2013	12	M271 N	Pavement quality concrete (fine milling)
249	19/06/2013	12	M271 S	Pavement quality concrete (fine milling)
251	01/10/2013	13	M27 WB	Pavement quality concrete (fine milling)
252	01/10/2013	10	M27 EB	Pavement quality concrete (fine milling)
255	01/10/2013	15	M27	Pavement quality concrete (bush hammering)
257	01/10/2013	15	M271 N	Pavement quality concrete (fine milling)
258	01/10/2013	15	M271 S	Pavement quality concrete (fine milling)
259	01/10/2013	15	M271 S	Pavement quality concrete (fine milling)
260	06/11/2012	28	M20/A20 EB	Pavement quality concrete (fine milling)
261	06/11/2012	34	M20/A20 EB	Pavement quality concrete (fine milling)
262	06/11/2012	30	M20/A20 WB	Pavement quality concrete (fine milling)
263	06/11/2012	28	M20/A20 WB	Pavement quality concrete (fine milling)
264	25/09/2013	22	A46	Pavement quality concrete (bush hammering)
265	25/09/2013	18	A46	Pavement quality concrete (longitudinal diamond grinding)
268	25/09/2013	24	A46	Pavement quality concrete (fine milling)

Better understanding of the surface tyre interface

Appendix B Friction model coefficients

% Slip (x)	a	b	c	d
2	34.87	-11.77	10.17	37.70
3	52.24	-23.56	15.00	57.14
4	76.78	-39.48	18.80	67.29
5	100.74	-55.91	21.18	74.68
6	122.14	-70.75	22.79	79.22
7	135.23	-80.16	23.61	82.79
8	142.24	-85.27	23.96	84.82
9	147.32	-88.43	24.02	84.41
10	150.42	-90.29	23.95	83.72
11	152.22	-91.13	23.79	82.36
12	152.93	-91.35	23.64	81.31
13	152.97	-91.26	23.49	80.63
14	153.02	-91.11	23.29	79.62
15	153.23	-91.13	23.10	78.72
16	153.36	-90.94	22.87	77.34
17	153.44	-90.74	22.68	76.05
18	153.24	-90.47	22.41	75.11
19	152.90	-90.05	22.18	74.01
20	152.36	-89.58	21.91	73.12
21	151.96	-89.22	21.64	72.25
22	151.74	-88.96	21.37	71.31
23	151.63	-88.82	21.14	70.49
24	151.64	-88.70	20.90	69.49
25	151.44	-88.46	20.69	68.64
26	151.24	-88.24	20.49	67.83
27	151.05	-88.02	20.28	66.99
28	150.85	-87.81	20.10	66.22
29	150.66	-87.60	19.92	65.42
30	150.49	-87.40	19.78	64.58
31	150.30	-87.22	19.61	63.84
32	149.99	-87.02	19.42	63.32
33	149.83	-86.86	19.23	62.58
34	149.65	-86.67	19.08	61.85

% Slip (x)	a	b	c	d
35	149.37	-86.44	18.91	61.25
36	149.08	-86.17	18.78	60.56
37	148.72	-85.87	18.64	59.95
38	147.99	-85.45	18.49	59.75
39	147.64	-85.14	18.29	59.03
40	147.07	-84.70	18.11	58.41
41	146.20	-84.23	17.94	58.32
42	145.73	-83.88	17.73	57.72
43	145.04	-83.44	17.56	57.34
44	144.16	-82.92	17.39	57.14
45	143.51	-82.54	17.23	56.87
46	142.75	-82.07	17.10	56.58
47	142.22	-81.67	16.94	56.03
48	141.62	-81.31	16.79	55.71
49	141.08	-80.96	16.65	55.34
50	140.65	-80.66	16.52	54.89
51	140.21	-80.34	16.41	54.43
52	139.80	-80.03	16.27	53.94
53	139.29	-79.66	16.14	53.47
54	138.74	-79.24	16.04	52.96
55	138.21	-78.81	15.95	52.40
56	137.83	-78.44	15.82	51.63
57	137.24	-77.97	15.70	51.06
58	136.57	-77.46	15.60	50.52
59	135.91	-76.98	15.49	50.02
60	135.23	-76.47	15.38	49.49
61	134.61	-75.99	15.30	48.89
62	134.01	-75.59	15.21	48.60
63	133.05	-74.97	15.09	48.27
64	132.24	-74.50	14.98	48.05
65	131.73	-74.21	14.90	47.76
66	131.24	-73.90	14.84	47.39
67	130.65	-73.53	14.73	47.05
68	130.27	-73.29	14.66	46.64
69	130.09	-73.16	14.60	46.18
70	130.04	-73.07	14.54	45.61

Better understanding of the surface tyre interface

% Slip (x)	a	b	c	d
71	130.09	-73.01	14.51	44.92
72	129.94	-72.83	14.44	44.22
73	129.84	-72.74	14.35	43.70
74	129.72	-72.72	14.26	43.35
75	129.49	-72.66	14.18	43.09
76	128.98	-72.43	14.10	42.92
77	128.51	-72.26	14.02	42.77
78	127.98	-72.13	13.95	42.87
79	127.37	-71.97	13.88	43.01
80	126.86	-71.96	13.80	43.27
81	126.73	-72.09	13.77	43.33
82	126.57	-72.15	13.70	43.29
83	126.35	-72.09	13.61	43.10
84	126.23	-71.91	13.50	42.47
85	125.97	-71.56	13.34	41.59
86	125.79	-71.32	13.21	40.95
87	125.81	-71.23	13.14	40.24
88	126.42	-71.76	13.12	39.82
89	127.47	-72.78	13.07	39.62
90	128.42	-73.83	13.03	39.65
91	129.86	-75.10	12.97	39.31
92	130.38	-75.66	12.92	39.22
93	130.15	-75.77	12.83	39.51
94	130.26	-75.97	12.82	39.38
95	130.28	-76.24	12.79	39.55
96	129.99	-76.33	12.81	39.86
97	129.67	-76.34	12.85	40.08
98	129.72	-76.63	12.90	40.31
99	129.79	-76.95	12.95	40.56
100	130.89	-77.91	12.95	40.41

Better understanding of the surface tyre interface

TRL

The friction developed between the road surface and vehicles' tyres provides motorists with the reaction forces necessary for manoeuvring. On the English strategic road network this is managed through the specification of low speed skid resistance, texture depth and the polishing resistance properties of aggregates. A combination of changes to the strategic road network (motorway layout and pavement surface type) and the vehicle fleet (anti-lock braking systems and electronic stability control systems) in recent years makes it appropriate to review the current approach. The work reported here was commissioned by Highways England to investigate how surface characteristics affect the ability of road users to control their vehicles.

Other titles from this subject area

PPR806   The relationship between collisions and skid resistance on the Strategic Road Network. Wallbank C., Viner H., Smith L and SmithR. 2016.

PPR727   Road Surface properties and high speed friction. Sanders P. D., Morosiuk K. Peeling J. R. 2014.

TRL662   Accidents and the skidding resistance standard for strategic roads in England. Parry A. R., and Viner H. E. 2005.

TRL367   High and low speed skidding resistance the influence of texture depth. Roe P. G., Parry A. R. and Viner H. E. 1998.

Page left intentionally blank.

Appendix D

Sanders, P. D., Brittain, S. & Premathilaka, A. (2017a), *PPR768 Performance review of skid measurement devices.* TRL, Wokingham, England.

PUBLISHED PROJECT REPORT PPR768

Performance review of skid resistance
measurement devices

P D Sanders and S Brittain (TRL)
A Premathilaka (CH2M)

Report details

Report prepared for:	Highways England, Pavements
Project/customer reference:	300 (4/45/12)
Copyright:	© TRL Limited
Report date:	November 2017
Report status/version:	v6.0
Quality approval:	
P D Sanders (Project Manager)	**Approved**
Martin Greene (Technical Reviewer)	**Approved**

Disclaimer

This report has been produced by TRL Limited (TRL) under a contract with Highways England. Any views expressed in this report are not necessarily those of Highways England.

The information contained herein is the property of TRL Limited and does not necessarily reflect the views or policies of the customer for whom this report was prepared. Whilst every effort has been made to ensure that the matter presented in this report is relevant, accurate and up-to-date, TRL Limited cannot accept any liability for any error or omission, or reliance on part or all of the content in another context.

When purchased in hard copy, this publication is printed on paper that is FSC (Forest Stewardship Council) and TCF (Totally Chlorine Free) registered.

Contents amendment record

This report has been amended and issued as follows:

Version	Date	Description	Editor	Technical Reviewer
1.0	20/01/2015	Initial Draft	PS	MG
2.0	05/02/2015	Draft with AP section	AP	MG
2.7	05/02/2015	Second draft	PS	MG
3.0	12/02/2015	Comments made by MG and Exec summary added	MG	PS
4.0	20/03/2015	Final draft for client comment	PS	MG
5.0	18/05/2015	Issued version addressing client comments	PS	MG
6.0	22/11/2017	Error identified in Figure 3-5, Figure 3-6, Figure 3-8 and Figure 3-10. Error has been rectified and this version supersedes all previous versions.	PS	MG

Document last saved on:	17/07/2020 15:26
Document last saved by:	Peter Sanders

TRL

Table of Contents

Executive Summary

Highways England (HE) are responsible for providing appropriate levels of skid resistance on the English strategic road network in order to manage accident risk. HE manage this risk by undertaking annual Sideway-force Coefficient Routine Investigation Machine surveys. This device was originally developed by the Ministry of Transport at TRL over many years and has subsequently been produced commercially under licence to TRL.

There are, however, a number of other devices and design variants available in the UK that measure skid resistance and friction in different ways. These devices are:

- The Skid Resistance Development Platform (based on a Sideway-force Coefficient Routine Investigation Machine), measuring sideway-force. This device is the backbone of HE's skid resistance strategy.

- The Pavement Friction Tester, measuring locked wheel friction, which is used for research and ad hoc surveys.

- GripTester, measuring fixed slip skid resistance, which is used by HE for research.

In the light of European harmonisation of standards for the measurement of low speed skid resistance, via sideway-force coefficient, there is a need to review HE's use of the Sideway-force Coefficient Routine Investigation Machine. This report provides information:

- To ensure that the device, and the technique, is the most appropriate tool, especially at high risk sites

- That clarifies the status and specification of the devices used by HE, allowing better preparedness for European standard harmonisation

To this end, a test programme was undertaken to assess the performance of skid resistance devices whilst testing; at different speeds, under braking and navigating roundabouts and corners. The results from the testing showed that, for the strategic road network, more accurate or consistent measurement of skid resistance would not be obtained when testing high risk sites with alternative devices to SCRIM. The work also demonstrated that if the lower limit for the existing speed correction was reduced from 25 to 10 km/h then all but a small percentage of sites could be speed corrected and this would reduce the number of high risk sites where valid data are not currently obtained. The results of the testing indicated that applying the speed correction at speeds below 25 km/h would result in an overestimation of the actual skid resistance, i.e. the correction would fail un-safe. However, additional testing on in-service roads is recommended to validate these findings which were derived from measurements on a closed test track.

The report also summarises developments that have been incorporated into the UK SCRIM fleet in recent years such as vertical load measurement, controlled water flow and GPS location referencing that are beyond the key requirements for the device set out in BS 7941-1 (2006). Details of the capabilities of the current fleet are summarised and the implications for the UK fleet of the potential development of a European Standard for measuring the skid resistance of pavements are also considered. There are a number of features available on SCRIM that would be beneficial to include in a future European standard, but the specification and supply of the test tyres will require careful consideration taking into account, the effects on measurement, supply chain and consistency between operators.

TRL

1   Introduction

The work described in this report was carried out in order to gain a better understanding of the performance of the skid resistance measurement devices used by Highways England. In particular the work focussed on the performance of skid resistance devices when testing high risk sites (roundabouts, approaches to pedestrian crossings, junctions, etc…) and characterising the performance of the Sideways-force Coefficient Routine Investigation Machine (SCRIM), the device used for the routine assessment of the English strategic road network. A key aim of this work was to identify if devices other than SCRIM would be more appropriate for the testing of high risk sites.

This report is separated into three parts; the following chapter gives some background information to the current UK skid resistance policy and the main devices available in the UK for characterising pavement skid resistance. The implementation of the current skid resistance policy in terms of the assessment of roads with relation to their site category is discussed. The two main devices used for the assessment of low speed skid resistance, SCRIM and GripTester, are described. In addition the Pavement Friction Tester (PFT) a specialist research tool for the measurement of peak and locked wheel friction at a wide range of speeds is also described.

Chapter 3 concentrates on the work carried out to assess the performance of the devices when testing high risk sites. This chapter opens with the presentation of a desk study carried out to assess the amount of the network for which no valid skid resistance information is collected. The remainder of the chapter concentrates on experimental testing undertaken to assess the performance of skid resistance devices whilst testing; at different speeds, under braking and navigating roundabouts and corners.

In Chapter 4 the current state of the SCRIM fleet is defined and compared with British Standard 7941-1:2006 (British Standards Institution, 2006). Some comment is made regarding the future development of a European skid resistance standard.

TRL

2 Background

2.1 Management of the skid resistance on the HE network

Highways England (HE) are responsible for the management of the English strategic road network (SRN). Part of their remit is to ensure that the skid resistance of the network is maintained to an acceptable standard. To achieve this, HE operates a skid resistance policy, detailed in HD28/15 of the Design Manual for Roads and Bridges (HD28/15 Skidding resistance, 2015). This policy can be summarised as making annual skid resistance measurements of the road network and comparing these with investigatory levels. Lengths of the network that are found to be at or below the investigatory level are then subject to further investigation to determine whether it would be beneficial to improve the skid resistance at these locations.

The investigatory level for any given section of carriageway is defined by the risk posed to road users at that location. Table 2-1 gives the site categories listed in HD28/15 (HD28/15 Skidding resistance, 2015) and the investigatory levels that can be assigned at each of these sites.

Table 2-1 Site category investigatory levels (HD28/15 Skidding resistance, 2015)

Site category and definition		Investigatory level at 50 km/h					
		0.30	0.35	0.40	0.45	0.50	0.55
A	Motorway	□	■				
B	Dual carriageway non-event	□	■	■			
C	Single carriageway non-event		□	■	■		
Q	Approaches to and across minor and major junctions, approaches to roundabouts				■	■	■
K	Approaches to pedestrian crossings and other high risk situations				■	■	■
R	Roundabout				■	■	■
G1	Gradient 5-10% longer than 50 m				■	■	■
G2	Gradient >10% longer than 50 m				■	□	■
S1	Bend radius <500 m – dual carriageway				■	■	■
S2	Bend radius <500 m – single carriageway				□	■	■

Sites defined as category Q, K, R, G1, G2, S1 and S2 are collectively known as high risk sites. High risk sites represent locations where road users are more likely to have to conduct aggressive stopping or steering manoeuvers, and so have higher investigatory levels to reflect the increase in demand for skid resistance.

TRL

2.2   Measurement equipment

There are a number of devices available for the characterisation of pavement skid resistance, a comprehensive list of available, vehicle based devices is given in FEHRL report 2006/01 (FEHRL, 2006) and TYROSAFE report D04 (TYROSAFE, 2008). This section summarises the three main devices used in the UK.

2.2.1   Sideway-force Coefficient Routine Investigation Machine

Sideway-force Coefficient Route Investigation Machines (SCRIMs) are used for routine monitoring of the skid resistance of the English strategic road network. Figure 2-1 shows the Highways England Skid Resistance Development Platform (SkReDeP), which incorporates sideway-force measurement equipment.   Measurements from this device provide information that can be used to compare the performance of surfacings with the requirements for skid resistance laid out in the HE Standards (HD28/15 Skidding resistance, 2015).

Figure 2-1 SkReDeP

SCRIM uses a smooth test tyre installed in the nearside wheel path (NSWP) angled at 20 degrees to the direction of travel, which is mounted on an instrumented axle. The skid resistance value is the average ratio between the measured horizontal and vertical force, multiplied by 100. For the purpose of this study the raw measurements were used from SkReDeP which provide a vertical and horizontal load measurement at a sampling interval of approximately 0.09 m.

2.2.2 GripTester

GripTester is a small trailer based device used by many local authorities for measuring low speed skid resistance (Figure 2-2).

Figure 2-2 GripTester

This device operates under the fixed slip principle, with the test wheel in-line with the direction of travel. The test wheel is mechanically linked via a chain and sprocket to two 'drive wheels', geared so that the test wheel is forced to rotate at a speed slower than that of the drive wheels, thereby generating slip between the test tyre and pavement. Measurements are usually made with GripTester at a test speed of 50 km/h in the NSWP with a sampling interval of 1 m.

2.2.3 Pavement Friction Tester

The Pavement Friction Tester (PFT) is a locked-wheel road surface friction testing device comprised of a tow vehicle and trailer (Figure 2-3). The trailer holds the test wheel, which is mounted on an instrumented axle and can be independently braked. The forces acting upon it are measured to determine the friction between the test tyre and road surface.

Figure 2-3 Pavement Friction Tester

The key difference between the PFT and SCRIM or GripTester, is that during testing, the PFT tyre contact patch slides over the surface at the same speed as the towing vehicle. This device can therefore measure skid resistance at any practical speed up to about 120 km/h. Whilst testing, the load and drag forces on the tyre are measured every 0.01 seconds throughout the three second braking cycle.

From these measurements, the peak[1] and locked[2] friction are determined. Measurements are typically made in the nearside wheel path at a speed of 90 km/h. To characterise the friction of a surface, typically 5 determinations of friction are made and the average of these measurements used. The PFT is used with reference to ASTM standards E274 (ASTM, 2011) and E524 (ASTM, 2008).

---

[1] Peak friction is the maximum friction value reached as the test wheel begins to slip.

[2] Locked friction is the friction value experienced when the test wheel is locked.

3 Skid resistance measurement of high risk sites

The aim of the study was to assess the performance of skid resistance testing devices when operating on high risk sites, and to assess the effectiveness of current methodologies for testing these sites. Testing high risk sites may require devices to operate under conditions different to testing straight-line carriageway such as:

- On bends or roundabouts
- At non-standard speeds in the case of slip roads or approaches to junctions
- Whilst decelerating in the case of stopping at traffic signals or give-way lines.

Testing under these conditions has the potential to affect the measurements made. The effectiveness of speed corrections or effects of load transfer on test wheels could contribute to changes in the measured skid resistance value.

The study was undertaken in two stages, the first was a desk study to assess the percentage of the SRN that is captured by the current procedures. The second was a series of experiments to replicate the conditions of high risk sites and the effects that these have on the measurements made by skid resistance devices. Experiments were set up to mimic sites were; a speed correction may be required, the vehicle may undergo braking, or manoeuvring around roundabouts and sharp corners.

3.1 Desk Study

The objective of the desk study was to define the amount of the network not currently captured by the routine annual SCRIM surveys. When conducting SCRIM surveys the test vehicles aim to travel at a test speed of 50 km/h on single carriageway roads and 80 km/h on dual carriageways and motorways (subject to complying with the prevailing speed limit). Measurements are then corrected to a standard speed of 50 km/h using the speed correction given in HD28/15 (HD28/15 Skidding resistance, 2015). The speed correction can be applied to measurements made between 25 and 85 km/h, which enables variations in speed resulting from traffic levels, road geometry or traffic control to be accounted for. Outside of these limits the speed correction may not be valid and so measurements made outside these limits are ignored. Routine measurements made on the SRN are stored in a central database; the Highways Agency Pavement Management System (HAPMS).

HAPMS was queried to identify the speed of measurements made for each 10 m section of lane 1 on the SRN between 2011 and 2013. The site category for each section was compared with the test speed and the percentage of each site category measured at various speeds was calculated (Figure 3-1).
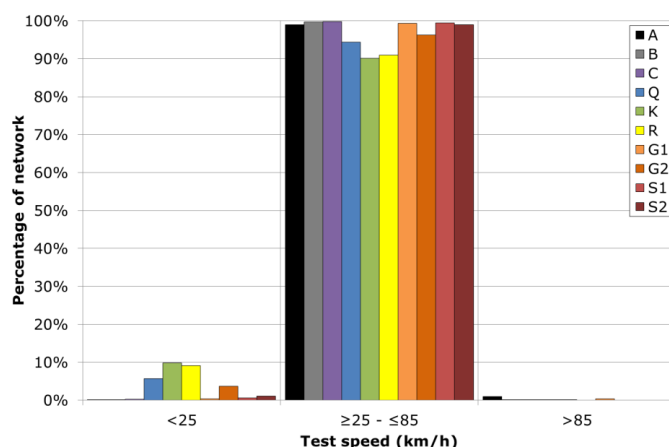
Figure 3-1 Percentage lane 1 measured within survey speed range, 2013

This shows that there is a small yet notable amount of missing information for site categories Q, K, R and G2. The percentages for each of the three years are shown in Table 3-1; this demonstrates that similar percentages are not captured for these site categories in 2012 and 2013. There are also some lengths that have not been surveyed at a valid speed in any of the three years.

Table 3-1 Percentage of lane 1 measured below 25 km/h

Site category	2011	2012	2013	Same site(s) in each year
A	0%	0%	0%	0.1%
B	0%	0%	0%	0.0%
C	0%	0%	0%	0.0%
Q	6%	5%	6%	0.6%
K	11%	8%	10%	1.0%
R	13%	8%	9%	2.0%
G1	0%	0%	0%	0.0%
G2	2%	5%	4%	1.0%
S1	1%	0%	1%	0.1%
S2	1%	1%	1%	0.4%

If the current speed correction could be applied to speeds below 25 km/h then substantially more of the measurements made on high risk sites would be valid. Figure 3-2 shows the same values, measured in 2013, but assumes that the speed correction is valid between 10

and 85 km/h. Figures for site categories A, B and C have been removed as these are not affected by the lower limit of the speed correction.
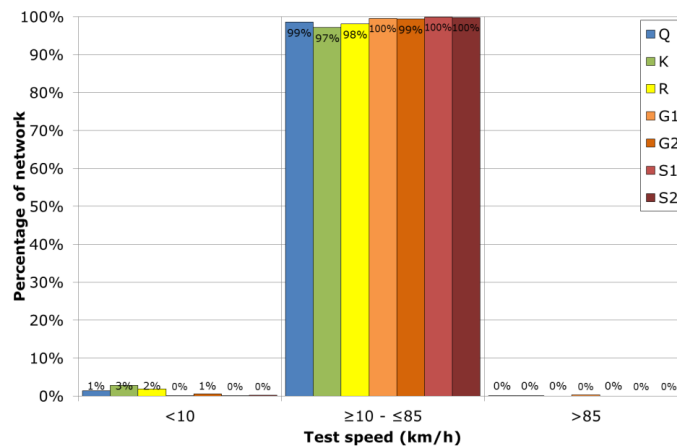
Figure 3-2 Theoretical lane 1 percentage

This shows that if the lower limit of the speed correction could be extended to 10 km/h it would be possible to capture valid information for all but a small percentage of sites.

3.2   Speed correction

Test speed has a considerable effect on skid resistance and therefore most skid resistance standards are written with reference to measurements made at a specific speed. This component of the study was designed to assess changes in the performance of the devices at various test speeds.

SkReDeP, GripTester and the PFT were used to make measurements on the surfaces used for the accreditation of the UK SCRIM fleet at MIRAs proving ground. A description of the surfaces tested is given in Table 3-2. These represent surfaces typically found on the English strategic road network. Unfortunately it was not possible to make measurements on all surface types, for example concrete or surface dressings.

Table 3-2 Description of surfaces tested

Surface	Length (m)	Surface description	Date Laid
Surface 1	130	Normal track surface, thin surfacing.	October 2013
Surface 2	100	A proprietary thin surfacing material using 6 mm coarse aggregate and polymer-modified bitumen.	October 2010
Surface 3	100	A proprietary thin surfacing material using 10 mm coarse aggregate and a fibre-reinforced bitumen.	October 2010
Surface 4	100	A proprietary thin surfacing material using 14 mm coarse aggregate.	October 2010
Surface 5	50	A hot-rolled asphalt with 20 mm chippings	October 2010

Measurements were made on each surface with SkReDeP and GripTester at the following test speeds: 10, 15, 20, 25, 30, 50, 70, 80 and 90 km/h; measurements were made with the PFT at 20, 50, 80 and 100 km/h. Making measurements at a number of test speeds allowed the generation of speed / skid resistance curves for each surface and device.

The speed correction curves were normalised to coalesce at 0.7 units at 10 km/h. Normalising the speed correction curves in this way demonstrates what the equivalent skid resistance values would be at other speeds if a measurement of 0.7 was made at a test speed of 10 km/h. In addition, where existing speed corrections are available the results collected could be compared with them to assess the validity of measurements.

The speed / skid resistance curves derived from PFT measurements are shown in Figure 3-3 and Figure 3-4. These figures show that the form of the speed friction relationships differ to what is normally observed on in-service carriageways. Friction / speed curves for most surfaces typically obey a power, or second order polynomial relationship but the relationships shown here are more linear. This shows that the surfaces measured are displaying different characteristics than would be expected on an in-service carriageway. Caution should therefore be exercised when applying results gathered from these surfaces to in service carriageways.
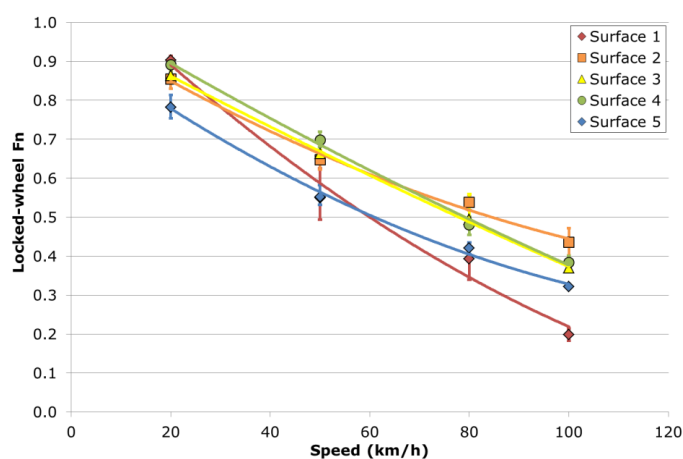
Figure 3-3 Locked-wheel friction / Speed relationship

TRL
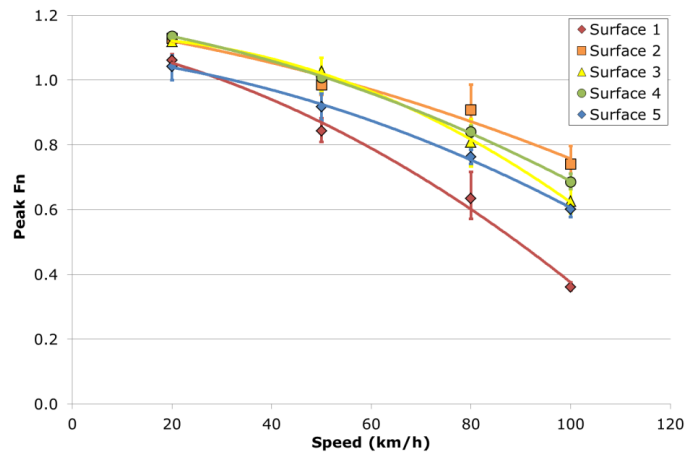
Figure 3-4 Peak friction / speed relationship

The normalised locked-wheel and peak friction curves presented in Figure 3-5 and Figure 3-6 show that Surface 1 is demonstrating a greater change in friction value with speed than any other surface. It is worth noting that Surface 1 was laid in 2013, three years after the other surfaces, and so may be affected by weathering differently to the other surfacings. Between 10 and 50 km/h the normalised values for Surfaces 2 to 5 are in general agreement, however above this speed the values begin to diverge, showing that changes in friction with speed could be, in part, related to the surface type.
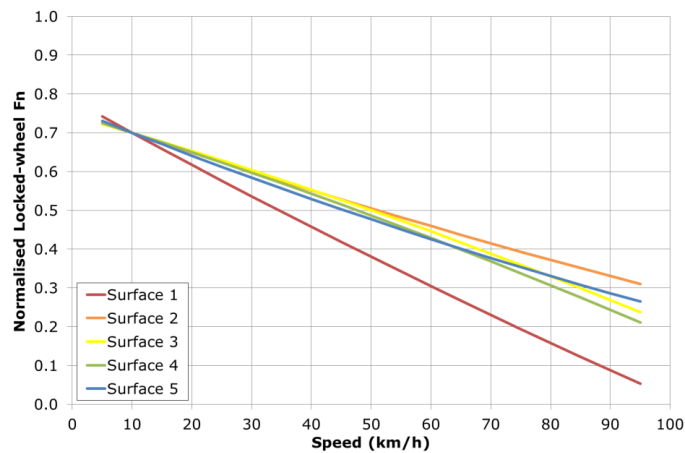
Figure 3-5 PFT Normalised locked-wheel friction / Speed relationship
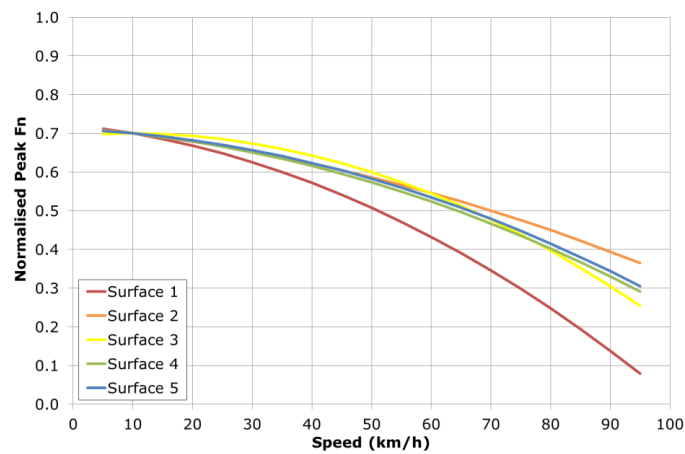
Figure 3-6 Normalised peak friction / speed relationship

Figure 3-7 shows the speed / skid resistance relationships measured using SkReDeP. For the majority of surfaces the results show a reduction in skid resistance with speed. However on Surface 2 this is not the case, and there is relatively little change in skid resistance with speed. This is unusual and further examination of the data revealed that there was a considerable reduction in skid resistance along the length of the section. For this reason the results from Section 2 were excluded from the remainder of the analysis of SkReDeP results.
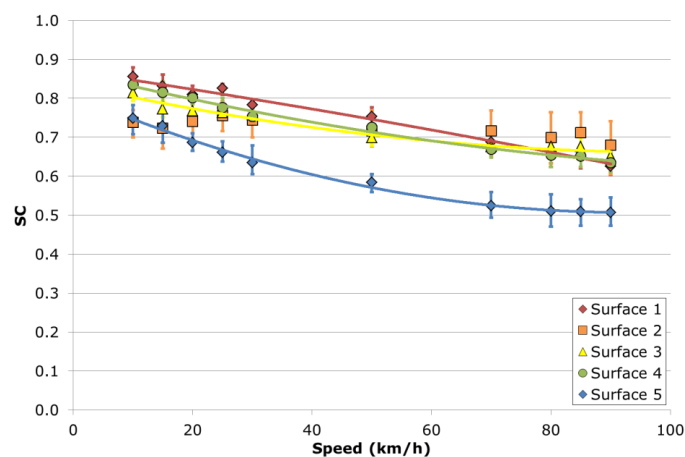
Figure 3-7 Scrim Coefficient / Speed relationship

Figure 3-8 shows the normalised SC curves, included in this figure are values derived from the speed correction formula given in HD28/15 (HD28/15 Skidding resistance, 2015).
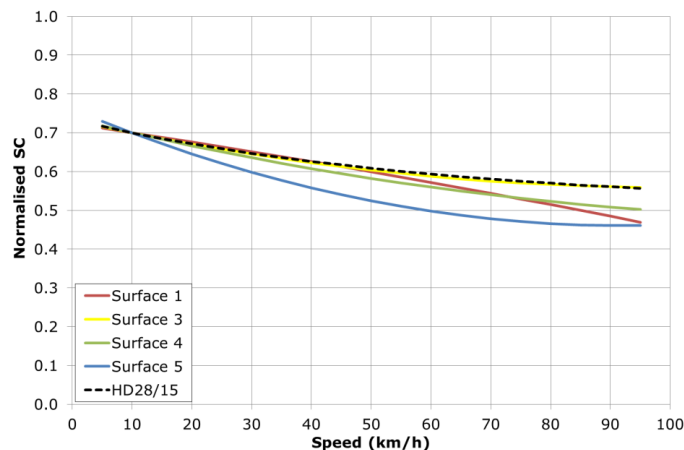
Figure 3-8 Normalised SC / Speed relationships derived using SkReDeP

Figure 3-7 and Figure 3-8 show that between 10 and 50 km/h there is a broad agreement in the performance of surfaces 1, 3 and 4. Surface 5 is a positively textured hot rolled asphalt (HRA) material, whereas the other surfaces are negatively textured thin surface course systems (TSCS). It is possible therefore that the difference in performance is related to the differences in surface types.

Figure 3-8 shows that the normalised SC values derived from the negatively textured materials are generally in agreement with those derived from the speed correction listed in HD28/15 for speeds between 10 and 50 km/h. However, there is a large discrepancy between the behaviour of the speed correction provided in HD28/15 and that observed on Surface 5. Figure 3-8 shows that on Surface 5, the speed correction provided in HD28/15 would overestimate the SC(50) value of a measurement of 0.7 SC made at 10 km/h by approximately 0.08 SC. This is essentially a fail un-safe position and suggests that measurements made below those for which the current speed correction is valid (25 km/h) may have the potential to be overestimated once speed corrected.

The speed / skid resistance relationships from GripTester measurements are shown in Figure 3-9. This clearly shows a different performance in the measurements made on Surface 1 than the other surfaces tested. Interestingly, the same flat performance on Surface 2 that was seen in the SkReDeP results is not observed here which could be due to differences in driving line.
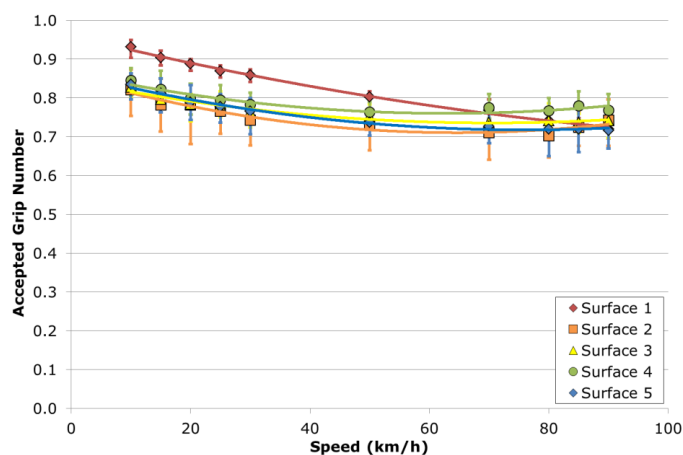
Figure 3-9 GripNumber / Speed relationship
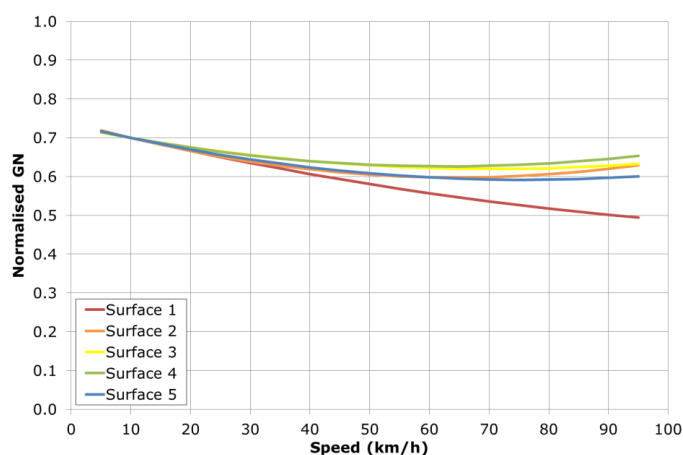
Figure 3-10 Normalised GripNumber / Speed relationship

Figure 3-10 shows that the variation in performance of Surface 1, compared to the other surfaces, is markedly different at speeds over 40 km/h. Below this speed the relative performance of all the surfaces is similar. As with the PFT results this could be related to the difference in material type of Surface 1

3.3   Braking

This component of the study was designed to assess the effects of deceleration on skid resistance devices. Measurements were made with SkReDeP and GripTester on a section of Surface 1 under braking conditions. The braking section was approached at 25, 50 and

80 km/h and the survey vehicles brought to a stop as fast as was deemed safe by the driver. The measurements made under these conditions were then compared to measurements made under normal survey conditions.

The measurements made were analysed in two stages and are presented as a pair of figures for each device. The first set of figures (Figure 3-11 and Figure 3-13) show an example of typical skid resistance and speed values measured on the braking section. The solid coloured lines in these figures represent the skid resistance value, speed corrected to 50 km/h using the speed correction formulae derived for surface 1. The broken coloured lines represent the speed recorded throughout the braking period. The solid black line shows the skid resistance measured at 50 km/h along the length of the section; the reference skid resistance.

The second set of figures (Figure 3-12 and Figure 3-14) shows how deceleration causes the skid resistance value to differ from the reference. The variation in skid resistance from the reference (reference SR – speed corrected SR) is shown against the absolute acceleration being experienced at each nominal approach speed. The red horizontal lines represent the range of skid resistance values measured on the reference surface at a constant speed of 50 km/h.

Figure 3-11 is an example of the skid resistance values measured under braking with SkReDeP. This shows that when braking from 25 and 50 km/h there is a good agreement in values with the reference. A deviation is shown when braking from 80 km/h, but this is slight.
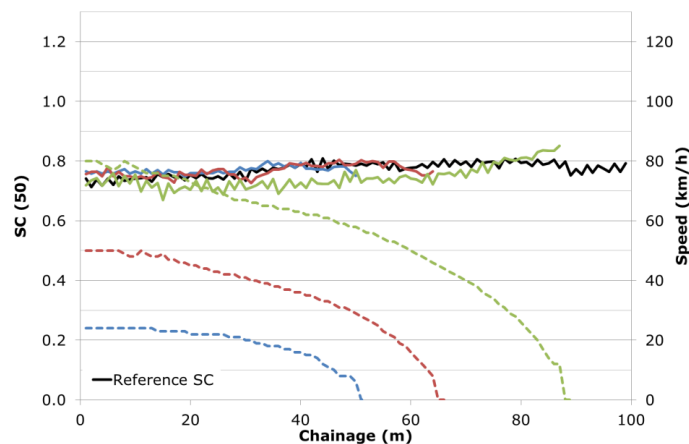
Figure 3-11 Example of SkReDeP skid resistance values under braking
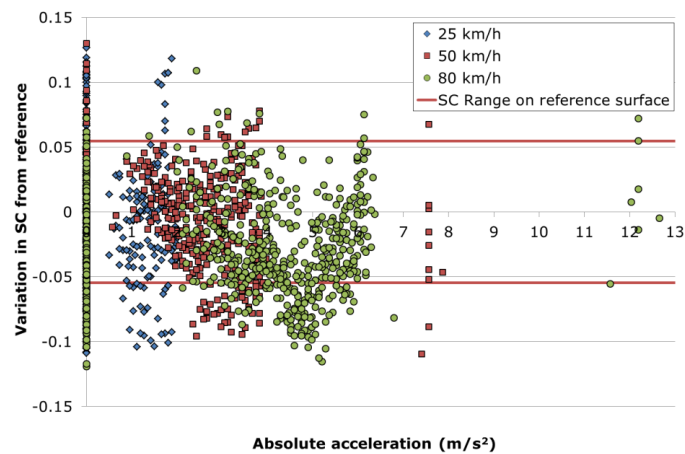
Figure 3-12 SkReDeP Variation from reference

Figure 3-12 shows that the variation in skid resistance measured using SkReDeP under braking is greater than that measured at a constant speed. The range of values measured under braking have a greater range than that of the variation on the reference. However with increasing acceleration there is little correlation with an increase in variation.

The results from GripTester are noticeably different to those from SkReDeP. Figure 3-13 shows that braking from 25 km/h produces a negligible deviation in values from the reference, but braking from 50 and 80 km/h has a marked effect. Observations of the GripTester show that under the influence of the inertial force caused by braking, the trailer pivots on its front wheels which lifts the rear test wheel. Under heavy braking the test wheel can lose contact with the surface entirely which causes the wheel to bounce. The Grip Numbers collected when braking from 80 km/h show that after approximately 50 m the values vary considerably as the force on the load cell exceeds the measurement range of the equipment.
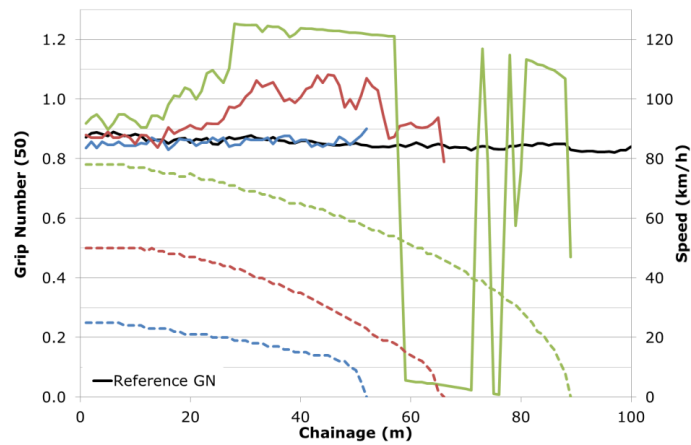
Figure 3-13 Example of GripTester skid resistance values under braking
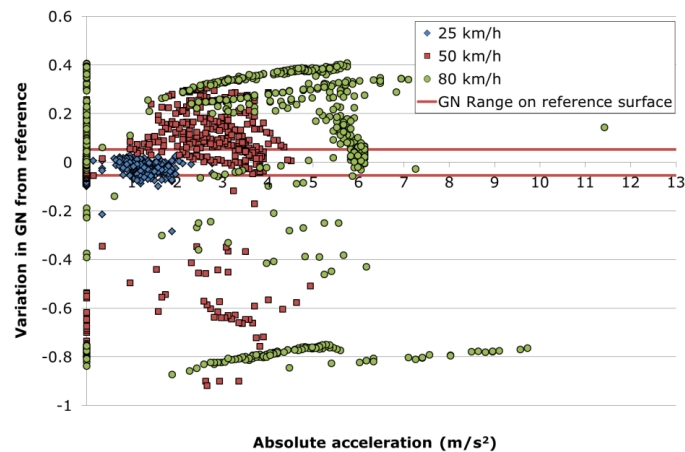
Figure 3-14 GripTester Variation from reference

Figure 3-14 shows that the majority of measurements made when braking from 25 km/h are within the variation expected when testing at a constant speed. Measurements made above a deceleration of approximately 2 m/s^2 rapidly move outside of this range and measurements made at 80 km/h show that the range of the measurement capability of GripTester is being exceeded.

3.4   Roundabouts

SCRIM and GripTester typically make measurements in the NSWP. The use of a test wheel mounted to the side of a vehicle could allow some weight transfer to occur when testing on roundabouts and bends. The testing described in this section was designed to assess the effect of testing a constant radius on skid resistance measurements.

To simulate the conditions of testing on roundabouts SkReDeP and GripTester were used to make measurements in both directions of a circular path with radius 32.9 m on MIRA's steering pad. The measurements were undertaken at speeds between 10 and 35 km/h (35 km/h was the maximum test speed judged safe by the equipment driver) in 5 km/h increments. Typical roundabout radii on the SRN range between 20 and 110 m, a test area with a radius of 32.9 m was the largest area available within the budget constraints of this project.

During testing the vehicle was kept as close to the marked circle as possible as shown in Figure 3-15. The test path therefore differs between the clockwise (CW) and anti-clockwise (ACW) directions.   To account for this, the skid resistance values calculated using an assumed vertical load and the vertical load measured by the device, were compared for each measurement. If lateral load transfer was affecting the skid resistance values it would be expected to see a difference in values calculated from assumed and measured vertical load between the two directions.
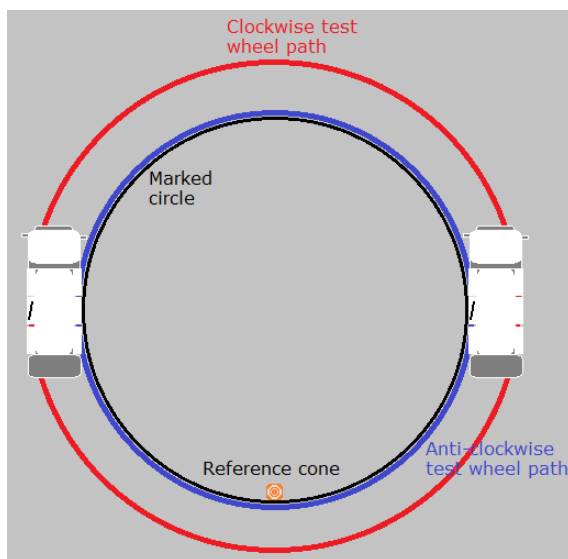
Figure 3-15 Example of roundabouts testing with SkReDeP

The data collected were analysed to produce histograms of the difference in skid resistance calculated using measured vertical load and an assumed constant vertical load. Differences in the histograms between the CW and ACW directions would demonstrate the effects of

load transfer on the skid resistance values. Included with the histograms is the distribution of measurements made in a straight line, so that the performance of the machines testing in both scenarios can be compared.

Histograms for measurements made at 10 km/h and 35 km/h are given to highlight differences in performance due to speed. Histograms for measurements made at intermediate speeds can be found in the appendices.

Figure 3-16 and Figure 3-17 show the distribution of values measured with SkReDeP at 10 and 35 km/h respectively. Both figures show that measurements made in both directions are providing similar distributions. This shows that the effect of load transfer on the results has the same effect regardless of the direction of travel.

The form of the straight line distribution at both speeds is narrower and taller than the distributions measured in a circular path. The straight line distribution at 10 km/h is taller and narrower than that measured at 35 km/h. This shows that measurements made in a circular path are more variable than those made in a straight line as are those made at a higher speed, but the average measurements made in all cases are likely to be similar.
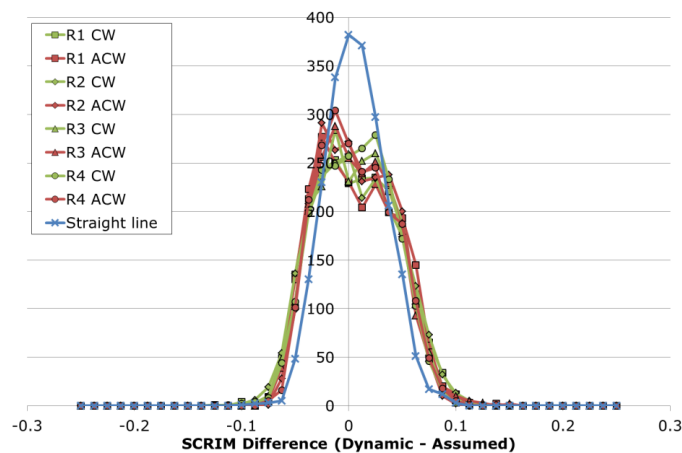
Figure 3-16 SCRIM Difference at 10 km/h
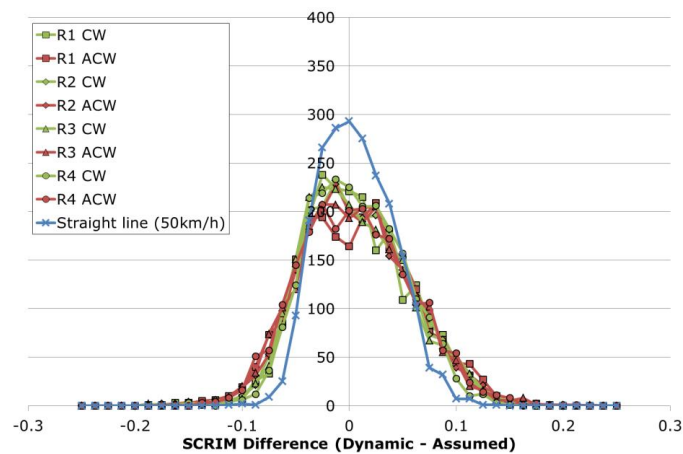
Figure 3-17 SCRIM Difference at 35 km/h

Figure 3-18 and Figure 3-19 show the distribution of values measured with GripTester. Notably these distributions appear to have more noise than the SkReDeP distributions; this is because they are based on fewer points given the averaging lengths used for each machine.

Broadly, the same behaviours are shown in the GripTester results as in the SkReDeP results. There is however an additional phenomenon shown in the results gathered at 35 km/h by the presence of a peak in the ACW results at approximately -0.15 GN Difference. It is possible that this behaviour could be related to an increase in vertical load experienced by some dynamic effects of traveling in an ACW direction with the machine attached on the nearside of the vehicle.
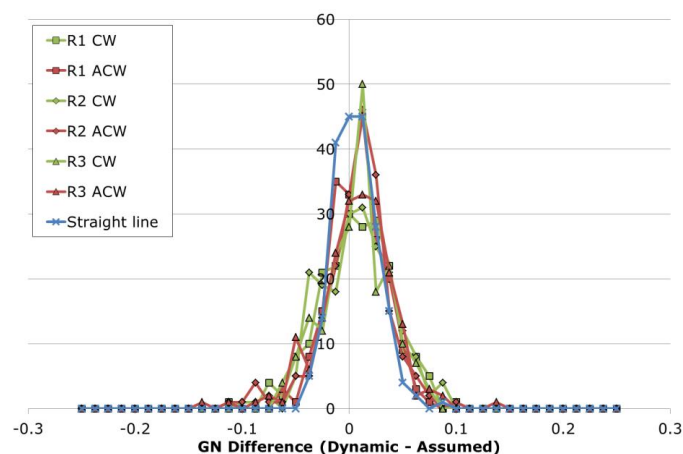
Figure 3-18 Grip Number difference at 10 km/h
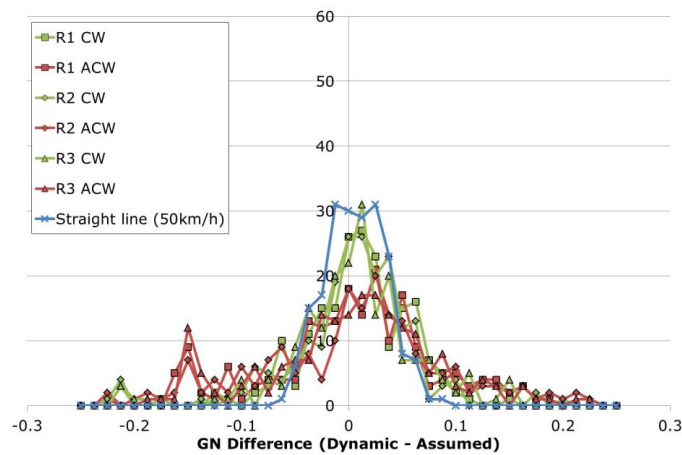
Figure 3-19 Grip Number difference at 35 km/h

3.5 Cornering

Where the testing described in the previous section was carried out to assess the effect of travelling in a circular path, the cornering testing was carried out to investigate the dynamic effects of testing between CW and ACW corners.

The worst case scenario of a vehicle transitioning from a CW to ACW curve was re-created by using a figure of eight test path, as shown in Figure 3-20. MIRA's manoeuvres area provides two marked circles of 12.2 and 13.2 m radii with a distance between the centres of 36.4 m. Measurements were made in each direction of the figure of eight between 10 and 25 km/h in 5 km/h increments.
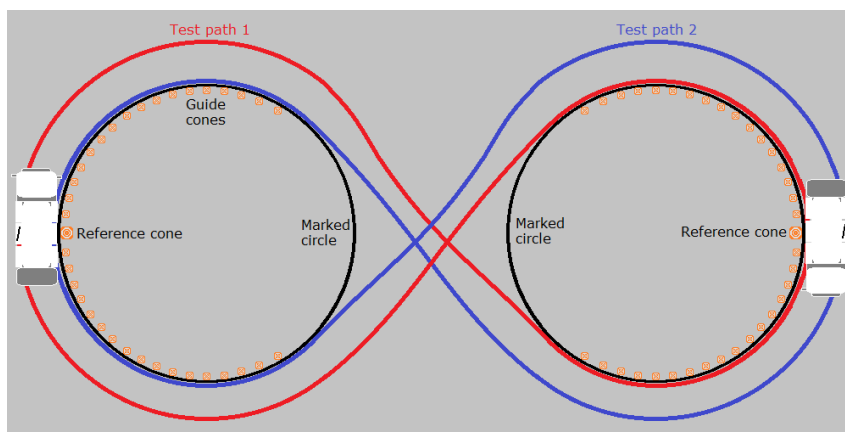
Figure 3-20 Example of cornering testing

As with the roundabouts testing, the wheelpath tested in each direction is different and so a direct comparison between measurements taken in each direction is unadvisable. In addition, because the radius being traversed is not consistent, an analysis equivalent to that carried out for the roundabouts testing is not suitable.

A number of issues arose whilst carrying out the testing, for instance maintaining a constant speed around the whole test path was challenging, especially at one apex where a crash barrier narrowed the test path considerably. Testing at a wide range of speeds was also challenging owing to the geometry of the test path. Because of these issues only broad conclusions can be drawn from this testing and these should be treated with caution.

The results from the figure of eight testing were analysed by comparing the difference in values generated from testing at 10 and 25 km/h along the length of the test path. If load transfer was affecting the results it would be expected to see changes in this difference at the crossover point and apexes of the circles.

The following figures show the difference in skid resistance values measured at 10 and 25 km/h from a single test run, included in the figures are the radius being traversed and values measured in a straight line for reference.

Figure 3-21 shows that the measurements made with SkReDeP in the figure of eight path are relatively consistent and that load transfer does not appear to be a significant issue. An anomaly is shown in test path 1 at 95 m, but this is not shown in test path 2 and is probably due to subtle differences in driving line between the 10 and 25 km/h measurements. There is no obvious change in the overall skid resistance value over the figure of eight path.
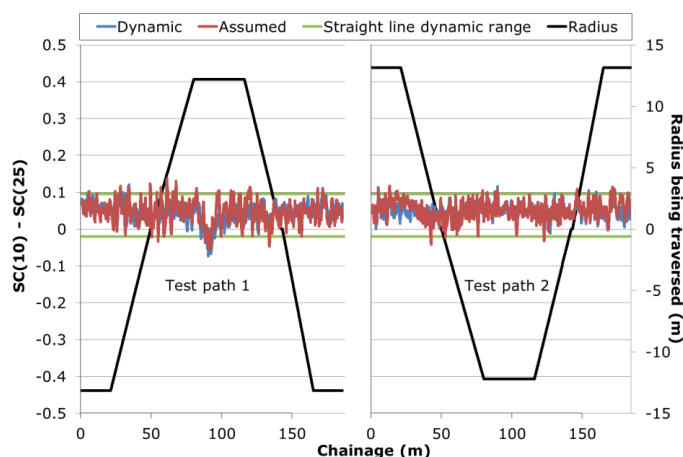
Figure 3-21 SkReDeP Variation

Results gathered using GripTester (Figure 3-22) shows a very noisy profile, with values based on an assumed vertical load being particularly noisy. Despite this there is no obvious trend for the values to change as a result of the figure of eight path.
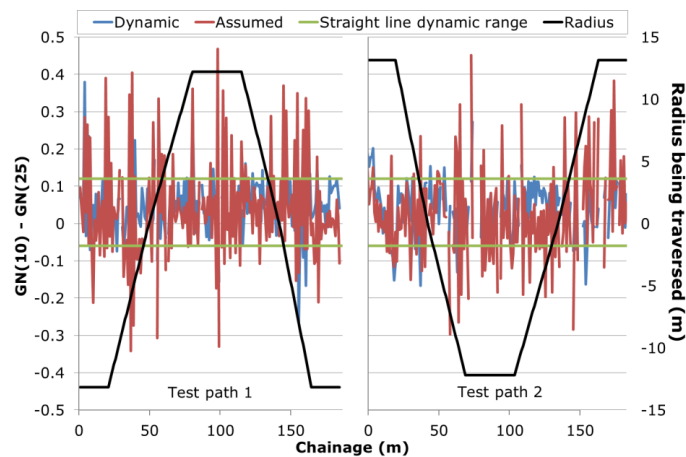
Figure 3-22 GripNumber Variation

3.6 Conclusions

The key conclusions that can be made from the work presented in this chapter are:

- That a considerable amount of skid resistance measurements made on high risk sites are conducted below the current accepted limits for speed correction.

- If the limits of the speed correction could be extended so that they are valid between 10 and 85 km/h then measurements made on all but a small percentage of sites could be used.

- The measurements made with SkReDeP suggest that lowering the current speed correction limit could fail un-safe. However, given the unusual behaviour of the surfaces tested a firm conclusion cannot be made, it is recommended for measurements to be made on in-service carriageways.

- The results gathered from the braking tests have shown that SCRIM values can be successfully speed corrected under braking conditions, but the measurements can be expected to be more variable than travelling at a constant speed.

- The results from GripTester under braking conditions highlighted a mechanical property of the machine that causes the test wheel to rise, affecting the skid resistance measurements

- Measurements made with SCRIM and GripTester made in a circular path can be expected to be more variable than measurements made in a straight line.

- More variable results can be expected when travelling in a figure eight path than measured in a straight line.

- On balance the testing has shown that, for the strategic road network, more accurate or consistent results would not be obtained when testing high risk sites with alternative devices to SCRIM.

- It is therefore recommended that changes should not be made to the current skid resistance survey strategy.

4 Current status of the UK SCRIM fleet

British Standard 7941-1:2006 (British Standards Institution, 2006) (hereto referred to as "the BS") defines the requirements for SCRIM test equipment and operation. Furthermore in the light of the development of European harmonisation of standards (hereto referred to as "the CEN standard") for skid measurement devices, HE are reviewing the current status of the UK SCRIM fleet. This chapter summarises information gathered from the SCRIM manufacturer (W.D.M Limited) about the current status of the development of SCRIM and compares this to the BS. Some comment is also made as to the possible considerations that could be made in developing the CEN standard.

4.1 SCRIM features compared to the British Standard

The BS was first written in 1999 and since then a number of developments have been made to SCRIM with a view to improving the quality and efficiency of measurement. All machines in the UK fleet conform to the BS but a number of significant developments have been made, these are summarised below.

4.1.1 Dynamic vertical load measurement

The BS states that the mass of the test wheel assembly shall provide a static vertical load of (200 ± 8 kg). Furthermore the BS states that the mass acting on the test wheel should be measured using a load cell. The measurement of dynamic vertical load was introduced in the UK in 2004. Machines use one of two types of systems; referred to as the "old system" and the "new system". The old system utilises a sacrificial shear pin which is sensitive to wear, causing it to affect the load measurement. The new system does not use a shear pin and has been found to be more robust and reliable.

Unpublished works carried out into the performance of dynamic vertical load measurement concluded that there are a number of advantages in using dynamic vertical load measurements, namely:

- Less variation between machines, since all would be measuring SFC using the actual applied load at any time

- More precise measurements from individual machines, especially at higher operating speeds

- Better detection of changes in skid resistance previously masked by changes in vertical load

To this end it would be beneficial for the CEN standard to include the requirement for the measurement of vertical load.

4.1.2 Temperature measurement

There is no requirement for the measurement of temperature in the BS. However should such a requirement be introduced in the CEN standard, the fitting of temperature sensors is expected to be straightforward because SCRIM has been designed to allow the addition of this feature if required. If more than two temperatures are required then this may be problematic, especially for machines utilising older style data logging electronics.

The CEN standard may need to address ways to deal with extreme temperatures in some of the countries/regions (for example, limiting surveys to a particular temperature range).

4.1.3   Water application

The BS stipulates the following for water supply and flow control:

- Water is to be controlled by a manual flow valve that can be adjusted to allow different flow rates depending on test speed

- The water control system should activate water flow before the test wheel contacts the ground and should not deactivate until the wheel has left the ground

- The water shall contact the surface 400 ± 50 mm in front of the centre line of the test wheel along the direction of the line of travel.

- The water shall be free from contaminants

- The theoretical water film thickness shall be 0.5 mm at 50 km/h

SCRIM can be fitted with a dynamic control system that adjusts the water flow automatically to ensure that the correct flow rate is achieved at a range of test speeds. The essential elements of a dynamically controlled water flow system are; a flow meter, proportional control valve, and an electronic control system. Either a header water tank or an electric pump is used to ensure that the correct water flow is achievable at high speeds.

Dynamically controlled water flow is appealing from an environmental and resource conservation point of view, but there is as yet no evidence to suggest that measurements are markedly improved as a result.

4.1.4   Test wheel and tyre

The BS specifies the size and resilience of the test tyre; standard test tyres for SCRIM are manufactured by Avon tyres and distributed through the equipment manufacturer who also carries out quality assurance checks. Current standards do not stipulate whether the slip angle of the test tyre (20°) should be in toe-in or toe-out. SCRIM uses the toe-in position; anecdotally, this seems to have been chosen in the early development of the machine to ensure stability of the vehicle when cornering.

In the UK, skid resistance measurements are normally made in the left wheel track of the most heavily trafficked lane, which is usually the leftmost lane. Due to the UK fleet having the test tyre on the nearside of the vehicle (left), they will be unable to test the nearside wheel track on some European roads, and vice-versa for European machines.

Work carried out in 2014 (reported in (Brittain, 2014)) assessed the performance of SCRIM tyres with the equivalent tyres used in Germany (SKM tyres). This work showed a good correlation between the two tyres but the SKM tyres produced skid resistance values approximately 4-8% greater than SCRIM tyres. The specification and supply of test tyres and wheels in the CEN standard will require careful consideration taking into account, the effects on measurement, supply chain and consistency between operators.

4.1.5   Location referencing

Historically location referencing of results has been managed using manually inputted markers at specific locations that can identify points in the results, this is the method of location referencing required in the BS. As technology has developed it has been possible to collect GPS information during surveys and use this information as a location reference. The advantages of GPS over marker input are that (assuming Differential GPS is used) the accuracy of location referencing is improved and data can be automatically matched to a client's road network, assuming that it is pre-defined based on a similar referencing system such as the Ordnance Survey Grid Reference (OSGR).

4.1.6   Data reporting

Below is an excerpt from the BS:

"An electronic recorder shall be provided, capable of measuring the horizontal load, vertical load and distance travelled. The electronic recorder shall display the speed, SR, and length for the subsection and the distance travelled from a predetermined reference point." (British Standards Institution, 2006)

Typically skid resistance results are reported in 10 m averaging lengths after having been corrected for speed and temperature. None of the UK machines automatically correct for speed or temperature, this is carried out as a post process if required (as detailed in HD28 (HD28/15 Skidding resistance, 2015)). However in some cases, if detailed investigations are required, the raw vertical and horizontal load measurements are valuable.

The UK fleet operates using one of two electronics systems, known as the National Instruments (NI) and the 4000 systems. Machines using the NI system are able to output data at intervals of approximately 100 mm and separate the measurements of horizontal and vertical loads. The 4000 systems also make measurements at similar intervals but these are not stored or available for output, the measurements are averaged in real time and output at larger intervals, normally 10 m.

Data processing specifications should be addressed outside of the CEN standard, but it would be beneficial for machines to be able to provide raw data for clients for their own interpretation.

4.1.7   Calibration

The calibration procedure for the horizontal load cell given in the BS is based on the rolling trolley principle; a load is applied to the tyre sidewall which acts in the same direction as the horizontal load cell, but in a different plane.

As with the specification of tyres, the specification of calibration procedures in the CEN standard will require some careful consideration. Alternative procedures such as removal of the load cell for calibration in a laboratory could result in different results compared to the rolling trolley method. This is because the rolling trolley method acts on the tyre and wheel (to replicate the loads applied during testing) whereas in a laboratory the load is applied directly to the load cell. When using the rolling trolley method, subtle differences in tyre or wheel properties, or the surface that the calibration is being carried out on can affect the calibration result.

The calibration method currently used for the vertical load system is different to that described in the current BS. The BS states during calibration the loads should be applied in increasing steps of 20 kg from 0 kg to 200 kg, while the current procedure is to remove load in 20 kg steps from 200 kg to 0 kg.

4.2 The fleet of UK accredited SCRIM machines

The Pavement Condition Information Systems website (PCIS, 2015) holds information on the machines currently accredited to operate on the SRN. Discussions with the equipment manufacturer enabled the production of a high level summary of features available on all machines in operation in the UK (Table 4-1).

Table 4-1 Summary of features in UK SCRIM fleet

Operator	Reg plate	Current accreditation	Test wheels	System electronics	Ability to supply raw data	Vertical load system[3]	Dynamic water flow control	Temp. sensors	Retro-reflective marker input	Water level indication	Forward facing imaging
DoE NI	IKZ 2203	Yes	LHS	4000	No	Old	No	Air & surface	LHS	Discrete	No
Highways Surveyors	AU53 BZM	Yes	LHS	4000	No	Old	No	Air & surface	LHS	Discrete	No
	01-KK-1138	Yes	LHS & RHS	4000	No	Old	No	None	LHS	Discrete	No
PMS Eire	04-G1-3042	Yes	LHS	4000	No	Old	No	Air & surface isolated	LHS	Discrete	No
Suffolk Pavement Evaluation	W965 SVG	Yes	LHS	4000	No	Old	No	Air & surface	LHS	Discrete	No
	YD02 XSN	Yes	LHS	4000	No	Old	No	None	LHS	Discrete	No
Surrey CC	KX07 YXH	Yes	LHS	4000	No	Old	No	Air & surface	LHS	None	No
TRL	WX60 AXN	Yes	LHS	NI	Yes	New	Yes	None	LHS	Continuous	No

[3] Old = shear pin, New = No shear pin

Operator	Reg plate	Current accreditation	Test wheels	System electronics	Ability to supply raw data	Vertical load system[3]	Dynamic water flow control	Temp. sensors	Retro-reflective marker input	Water level indication	Forward facing imaging
	S10 WDM	Yes	LHS & RHS	NI	Yes	New	Yes	Air & surface with display	LHS & RHS	Continuous	Yes
	S11 WDM	Yes	LHS & RHS	NI	Yes	New	Yes	None	LHS & RHS	Continuous	Yes
	S12 WDM	Yes	LHS	NI	Yes	New	Yes	None	LHS	Continuous	Yes
	S13 WDM	Yes	LHS	NI	Yes	New	Yes	None	LHS	Continuous	Yes
WDM	S14 WDM	Yes	LHS	NI	Yes	New	Yes	None	LHS	Continuous	Yes
	S15 WDM	Yes	LHS & RHS	NI	Yes	New	Yes	Air & surface	LHS & RHS	Continuous	Yes
	S16 WDM	Yes	LHS & RHS	NI	Yes	New	Yes	Option	LHS & RHS	Continuous	Yes
	S7 WDM	Yes	LHS	4000	Yes	New	Yes	Air	LHS	Continuous	No
	S800 WDM	Yes	LHS	NI	Yes	New	Yes	Software only	LHS	Continuous	No
	S900 WDM	Yes	LHS	NI	Yes	New	Yes	None	LHS	Continuous	Yes
Yotta	KX07 YVH	Yes	LHS	4000	No	Old	No	Air & surface	LHS	Discrete	No

4.3 SCRIM machines used in other European countries

According to the equipment manufacturer, the following is a summary of the number of SCRIM machines that operate in other European countries.

- Italy – 7
- Spain – 8
- France – 4
- Belgium – 3
- Portugal – 1
- Slovenia – 1

Please note that these numbers indicate those that have been sold to that country, however, they may or may not be in the particular country at the moment. For example, anecdotal information suggests that one SCRIM that was in France is now operating in Spain.

The equipment manufacturer also informs that some of these machines were produced and supplied many years ago, and that some may not be operational at the moment.

The above numbers suggest that SCRIM machines are reasonably widely used in Europe; as such, several countries may wish to see the existing features of SCRIM incorporated into any future European standard for measuring the skid resistance of pavements.

5 References

ASTM. (2008). *E524-08 Standard specification for standard smooth tire for pavement skid-resistance tests.* West Conshohocken: ASTM.

ASTM. (2011). *E274/E274M-11 Standard test method for skid resistance of paved surfaces using a full-scale tire.* West Conshohocken: ASTM.

British Standards Institution. (2006). *BS 7941-1:2006 Measurements for measuring the skid resistance of pavement surfaces - Part 1: Sideways-force coefficient routine investigation machine.* London: BSI.

Brittain, S. (2014). *PPR702 Comparision of SCRIM and SKM sideways-force skid resistance devices.* Wokingham: Transport Research Laboratory.

FEHRL. (2006). *FEHRL Report 2006/01 Harmonisation of European routine and research measuring equipment for skid resistance.* Forum of European National Highway Research Laboratories.

Highways England, Transport Scotland, Welsh Government, The Department for Regional Development Northern Ireland. (2015). *HD28/15 Skidding resistance.* London: The Stationery Office.

PCIS. (2015). Retrieved from Pavement Condition Information Systems: www.pcis.org.uk

TYROSAFE. (2008). *D04 Report on state-of-the-art of test methods.* Tyre and Road Surface Optimisation for Skid Resistance and Further Effects.

Acknowledgements

Appendix A SCRIM Differences
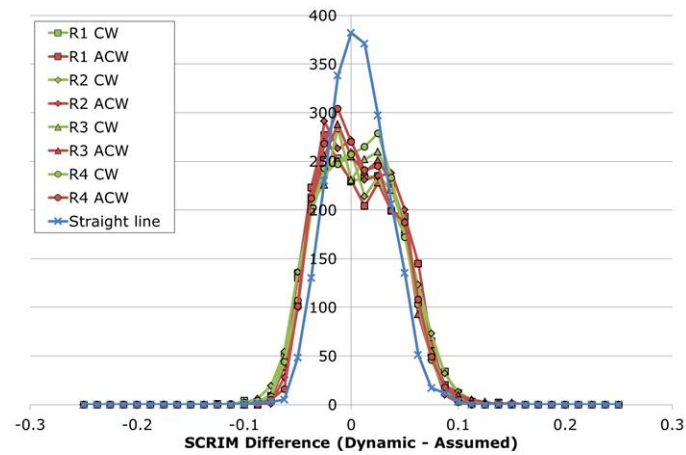
Appendix A 1 SCRIM Difference at 10 km/h
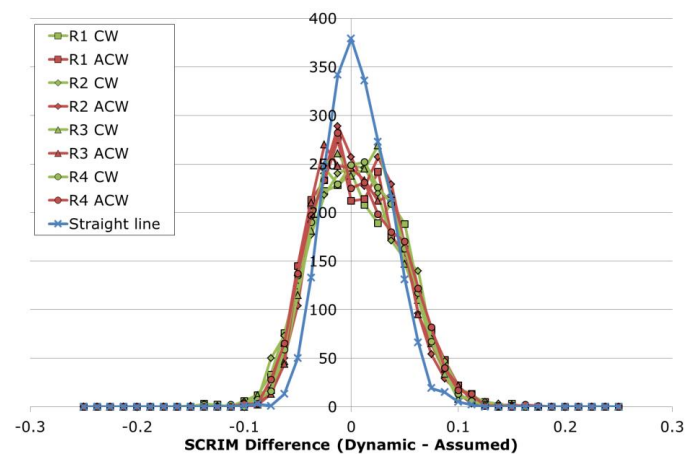
Appendix A 2 SCRIM Difference at 15 km/h

285
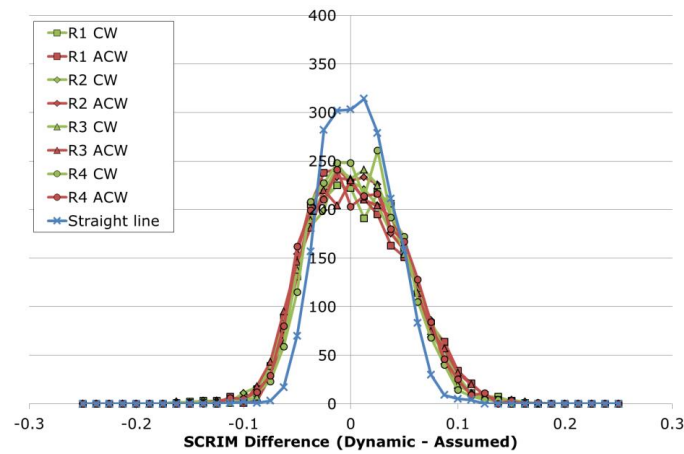
Appendix A 3 SCRIM Difference at 20 km/h
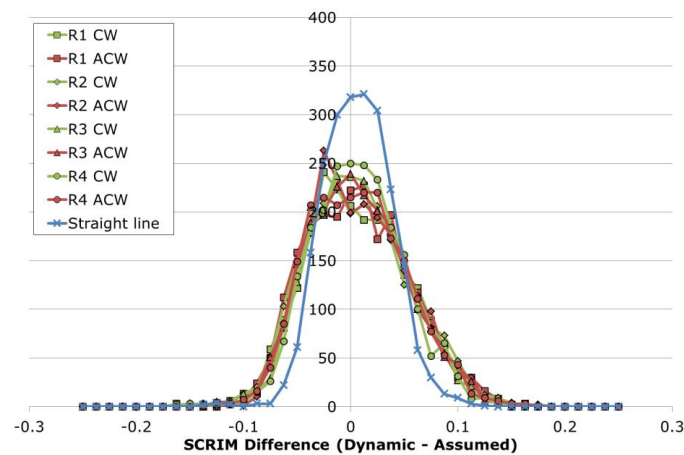
Appendix A 4 SCRIM Difference at 25 km/h
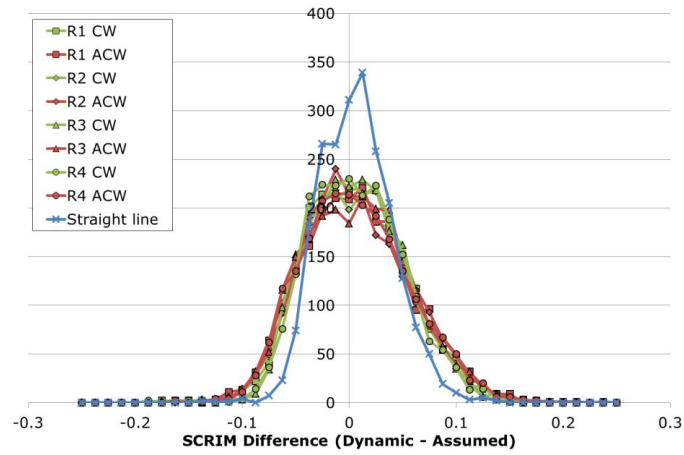
Appendix A 5 SCRIM Difference at 30 km/h
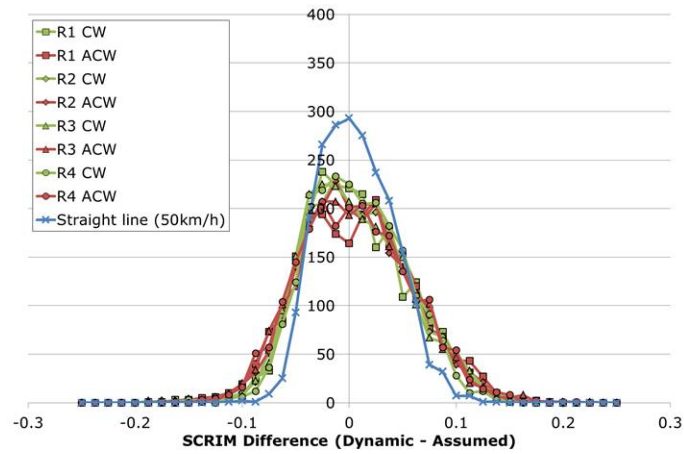
Appendix A 6 SCRIM Difference at 35 km/h

Appendix B GripNumber Difference
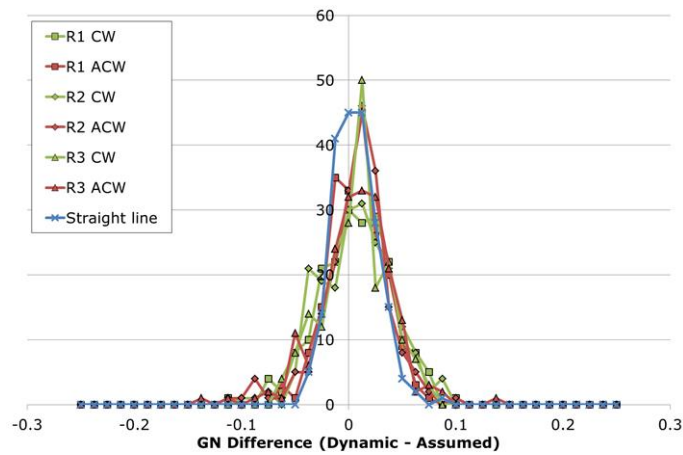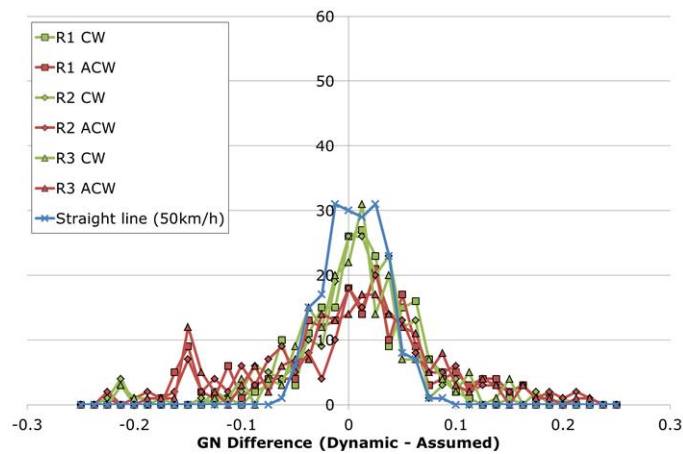

Appendix B 1 GripNumber Difference at 10 km/h
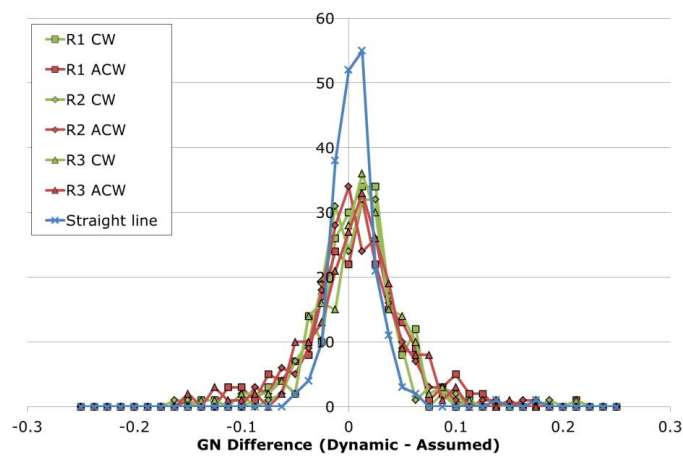
Appendix B 2 GripNumber Difference at 15 km/h
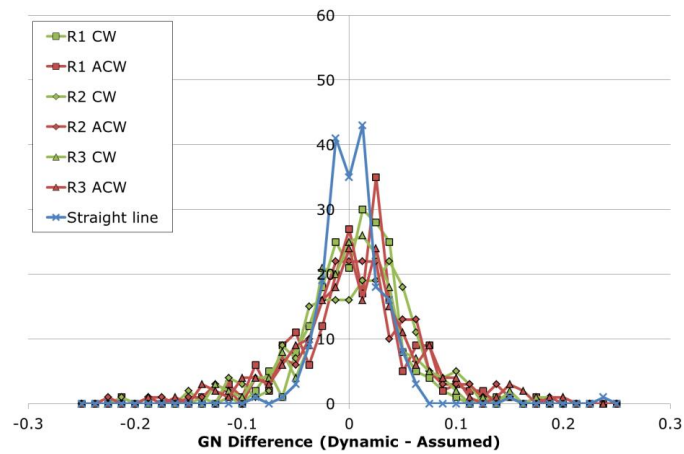
Appendix B 3 GripNumber Difference at 20 km/h
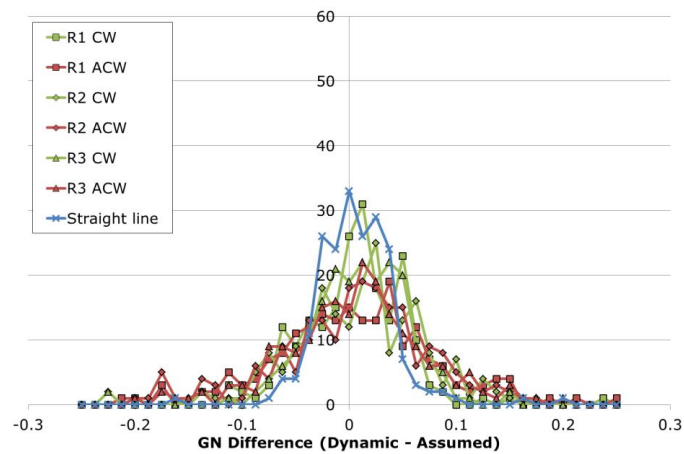
Appendix B 4 GripNumber Difference at 25 km/h
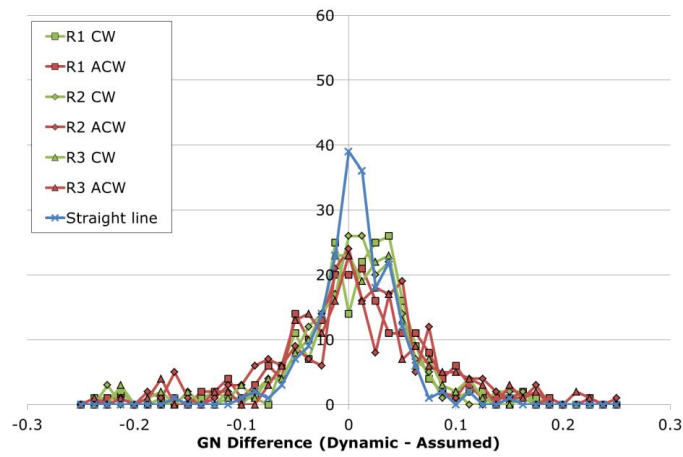
Appendix B 5 GripNumber Difference at 30 km/h

Appendix B 6 GripNumber Difference at 35 km/h

Performance review of skid resistance measurement devices

The work described in this report was carried out in order to gain a better understanding of the performance of the skid resistance measurement devices used by Highways England. In particular the work focussed on the performance of skid resistance devices when testing high risk sites (roundabouts, approaches to pedestrian crossings, junctions, etc…) and characterising the performance of the Sideways-force Coefficient Routine Investigation Machine (SCRIM), the device used for the routine assessment of the English strategic road network. A key aim of this work was to identify if devices other than SCRIM would be more appropriate for the testing of high risk sites.

Other titles from this subject area

PPR702   Comparison of SKM and sideway-force skid resistance devices. S Brittain. 2014

PPR729   Highways England skid resistance policy 2014: a review. A Dunford, P D Sanders, S Brittain, N Sidaway and R Smith. 2015

PPR479   GripTester trial – October 2009 Including SCRIM comparison. A Dunford. 2010

PPR815   Better understanding of the surface tyre interface. P D Sanders, M Militzer and H E Viner. 2017

Page left intentionally blank.

Appendix E

Sanders, P. D. & Browne, C. (2020), *PPR957 Characterising the measurements made by sideways-force skid resistance devices - A desk study and proposal for an experimental study.* TRL, Wokingham, England.

PUBLISHED PROJECT REPORT PPR957

Characterising the measurements made by
sideways-force skid resistance devices

A desk study and proposal for an experimental study

P D Sanders and C Browne

Report details

Report prepared for:	Highways England, Pavements
Project/customer reference:	1-407 Sub-task 2
Copyright:	© TRL Limited
Report date:	July 2020
Report status/version:	Issue
Quality approval:	

A Kaminski (Project Manager)	**Approved**	M Greene (Technical Reviewer)	**Approved**

Disclaimer

This report has been produced by TRL Limited (TRL) under a contract with Highways England. Any views expressed in this report are not necessarily those of Highways England.

The information contained herein is the property of TRL Limited and does not necessarily reflect the views or policies of the customer for whom this report was prepared. Whilst every effort has been made to ensure that the matter presented in this report is relevant, accurate and up-to-date, TRL Limited cannot accept any liability for any error or omission, or reliance on part or all of the content in another context.

When purchased in hard copy, this publication is printed on paper that is FSC (Forest Stewardship Council) and TCF (Totally Chlorine Free) registered.

Executive summary

The effective management of road surface skid resistance is critical for providing a safe means of travel for all road users. The skid resistance on the English trunk road network is managed with the goal of normalising the skidding risk to motorists across areas of varying relative risk (known as site categories). Currently this is undertaken using a correlative approach which compares road surface skid resistance with the prevalence of wet skidding accidents for different site categories. Critically however, it is not understood, even at a fundamental level, how the skid resistance measurements made on the road network physically relate to the fiction properties exploited by vehicles carrying out manoeuvres.

In this paradigm there exists a major potential benefit to road authorities, and road users, in generating this fundamental knowledge, especially in areas of high skid risk. The work reported in this document represents the first stage in a wider programme of research which seeks to fully understand the relationship between the parameters outlined above. The overall result of this programme of work will derive advice to road owners as to how they can best use road surfacing materials in order to:

- Maximise the cost effectiveness of pavement materials used,

- Minimise the skidding risk to road users in areas of varying risk,

- Update the relevant management procedures in order to continually support the above points.

In the UK, the skid resistance properties of the trunk road network are assessed annually using devices utilising the sideways-force measurement principle, the Sideways-force Coefficient Routine Investigation Machine (SCRIM). Currently, a view of the measurement properties of SCRIM is in place. However, this is based on a theoretical analysis of the device, is unsupported by empirical evidence, and, in some cases could be considered contradictory to historical literature. During recent years this view has been challenged and it is the aim of this work to investigate the measurement properties of SCRIM in order to confirm the currently held view, or to provide an alternative.

A desk study produced the following characterisations for SCRIM but was unable to identify a single valid characterisation.

Summary of operating speed and % slip predicted by characterisations

Characterisation	operating speed	% slip
Current	The vehicle speed	34.2
Scalar	The vehicle speed	6.03
Vector	The vehicle speed x Cos(70)	100
Co-Axial	The vehicle speed	11.7

Experimental methodologies for assessing the predictions made by the characterisations are presented.

TRL

Table of Contents

1   Introduction

The effective management of road surface skid resistance properties is a critical factor in providing a safe means of travel. The measurement of skid resistance is a key component in the effective management of skid resistance. In the UK the skid resistance properties of the trunk road network, and many local road networks, are assessed annually using devices utilising the sideways-force measurement principle.

At the time of writing, all of the devices used for characterising the skid resistance properties of the UK trunk road network are Sideways-force Coefficient Routine Investigation Machines (SCRIMs). However, in Germany the SeitenKraftMessverfahren (SKM) is used, and in Belgium the Odoliograph is used, both of which operate under the same sideways-force principles as SCRIM. Understanding the fundamental measurement properties of sideways-force devices would therefore provide a major benefit to UK and international road authorities alike.

Currently, a view of the measurement properties of SCRIM is in place and is widely accepted. However this view is based on a theoretical analysis of the device, is unsupported by practical assessment, and in some cases could be considered contradictory to historical works. During recent years research into road surface skid resistance and friction has progressed in such a way that the specific measurement characteristics of SCRIM have become of particular interest. Owing to this interest, the current view of SCRIM has been challenged and it is the aim of this work to investigate the measurement properties of SCRIM and propose an experimental methodology by which the measurement properties of SCRIM can be confirmed.

2 Background to pavement friction and its influence on vehicle safety and highway management

2.1 Friction as a three dimensional parameter

The friction generated between a road surface and vehicle tyre is highly variable; the concept of a ubiquitous "level of grip" is a misnomer. This is because the friction between a road surface and vehicle tyre, is proportional to, amongst other variables, the speed at which the surface is being traversed, and the amount of slip between the tyre and road surface. Friction is therefore a three dimensional parameter[1]. This is illustrated in Figure 2-1 which presents the typical relationship between friction, operating speed, and wheel slip.
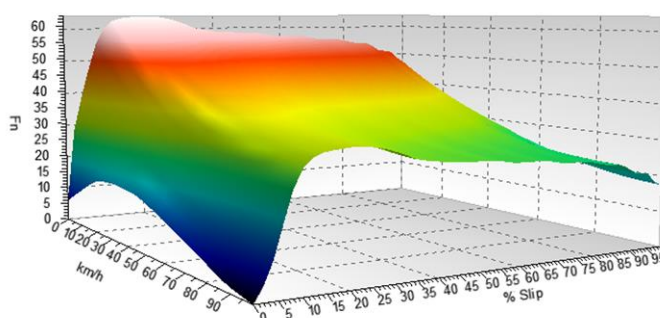

Figure 2-1 An example of the relationship between friction (Fn), operating speed (km/h) and wheel slip (% Slip), the friction profile.

Efforts to normalise the measurement of road friction using standardised devices and test procedures, can allow for the measurement of the roads contribution to friction, the "skid resistance". Skid resistance measurements can be made with reference to the speed and % slip at which the measurement was made for some devices for which these parameters are defined. For SCRIM this is not the case, as the speed and % slip of SCRIM measurements are not known.

2.2 The influence of friction on vehicle safety

Work reported in TRL report PPR815 (Sanders, Militzer, & Viner, 2017) demonstrated that vehicles undertaking a straight line braking manoeuvre use friction at a range of wheel slips and speeds. In other words, vehicles undertaking this manoeuvre use friction values at many

---

[1] In the same way that a map co-ordinate is a two dimensional parameter and that the knowledge of one of the co-ordinates is not meaningful without knowledge of the other.

different points on the profile presented in Figure 2-1. Furthermore, the work demonstrated that if Anti-lock Braking Systems (ABS) are activated, the areas of the friction profile used are markedly different to those used when ABS is not activated. This is illustrated in Figure 2-2 which shows a "plan view" of the profile shown in Figure 2-1 with the areas of the profile used by a vehicle undertaking a straight line braking manoeuvre with and without ABS shown.
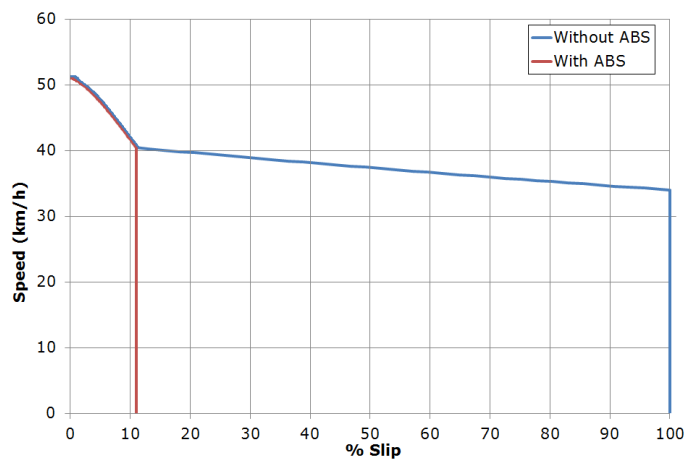

Figure 2-2 Friction used by a vehicle undertaking straight line braking

It is therefore likely that different manoeuvres, cornering or changing lanes for instance, will also use different areas of the friction profile than those illustrated for straight line braking. Clearly, gaining an understanding of the areas on the friction profile demanded by vehicles, and the ability of a road surface to deliver friction in these areas is an important consideration to highways authorities in delivering a safe network.

Sideways-force measurement systems, such as SCRIM, characterise skid resistance continuously, and as such it is a necessity that skid resistance be characterised at a single operating speed, and a single slip speed. To this end, sideways-force measurement systems can be thought of as characterising skid resistance in one dimension, or at a single point on the profile presented in Figure 2-1.

With this in mind, having a firm understanding of where measurements made with SCRIM sit on the friction profile is key in understanding the relationship between SCRIM measurements, vehicle manoeuvres and accident risk.

2.3   The implications for the management of road networks

The UK trunk road network is managed in such a way as to broadly normalise the risk of skidding across the network. To achieve this, the road network is split up into various site categories, which relate to the level of risk posed to road users. Each site category is

assigned a skid resistance Investigatory Level (IL); high risk sites have higher ILs, whereas low risk sites have lower ILs.

The Investigatory Levels are based on measurements made with SCRIM and locations which fall at or below their IL are subject to investigation where other factors such as surface texture, road geometry and collision risk are taken into account to determine whether treatment to improve the skid resistance would be beneficial. Based on the factors outlined in section 0, it may be the case that SCRIM measurements are more relevant[2] in some areas of the network than others.

If these areas could be identified then the decisions made using SCRIM data can be better understood. One way of achieving this may be an adjustment of the width of IL bands to reflect site categories where SCRIM measurements are better or worse predictors of skidding risk. An alternate may be to give SCRIM measurements more or less weight over the maintenance decisions than other parameters such as texture or road geometry.

A third, more radical option, may be to employ other skid resistance assessment methodologies in areas where they make measurements closer to the prevailing skid resistance demand of road users and would be better predictors of collision risk than SCRIM.

---

[2] Better predictors of collision risk

3 Defining the parameters

Skid resistance measurement tools are typically characterised based on their operating principle:

- Longitudinal fixed slip devices. Devices with a test wheel mounted in the same orientation as the vehicle wheels which is forced to rotate at a fixed percentage of the operating speed.

- Longitudinal variable slip devices. Devices with a test wheel mounted in the same orientation as the vehicle wheels which during testing alternates between a freely rotating and a locked-wheel (or peak friction) state.

- Sideways-force devices. Devices with a test wheel mounted at an angle to the vehicle wheels. SCRIM operates under this principle.

Skid resistance measurement devices can be further characterised using the terminology outlined in the following sub sections. The definitions of the parameters detailed in these sub-sections will be used throughout the rest of this document.

3.1 Operating speed

Operating speed is often referred to as vehicle speed, and the two terms are frequently considered synonyms. However, for the purposes of this work it is necessary to introduce a subtle difference in these terms. For this work, vehicle speed is defined as per BS CEN/TS 15901-6-2009, *"Speed at which the device traverses the test surface"* (British Standards Institution, 2009).

Operating speed is defined as the effective vehicle speed of the test device. For two of the three cases considered in this work vehicle speed and operating speed are the same. In one case, which is discussed in Chapter 6, the operating speed differs to that of the vehicle speed.

3.2 Wheel speed

A pre-existing definition of wheel speed could not be identified. Wheel speed is therefore defined here as the tangential speed of the circumference of the test tyre.

3.3 Slip speed, Slip Ratio and Percentage Slip

Slip speed is defined in BS CEN/TS 15901-6-2009 as "relative speed between the test tyre and the travelled surface in the contact area" (British Standards Institution, 2009). This definition can be expressed formulaically using Equation 3-1.

$$Slip\ speed = Operating\ speed - Wheel\ speed$$

Equation 3-1 Definition of slip speed

Slip speed is often expressed as either slip ratio or slip percentage in order to be expressed a relative function of the operating speed. Slip ratio is defined in BS CEN/TS 15901-6-2009 as, "slip speed divided by the operating speed" (British Standards Institution, 2009).

Percentage slip (% Slip) is defined in Equation 3-2. For the purposes of this work, percentage slip will be used in preference to slip ratio.

$$\% \ Slip = \frac{100 \times Slip \ speed}{Vehicle \ speed}$$

Equation 3-2 Definition of % Slip

3.4 Vertical and horizontal load

Skid resistance is a unit-less parameter calculated as the ratio between vertical and horizontal load. For all skid resistance measurements systems, vertical load is the load acting on the test wheel in the direction of gravity. The definition of horizontal load however differs depending on the specific measurement device. In the case of SCRIM, horizontal load is defined as the load acting on the test tyre along the axis of rotation. These properties are illustrated in Figure 3-1.
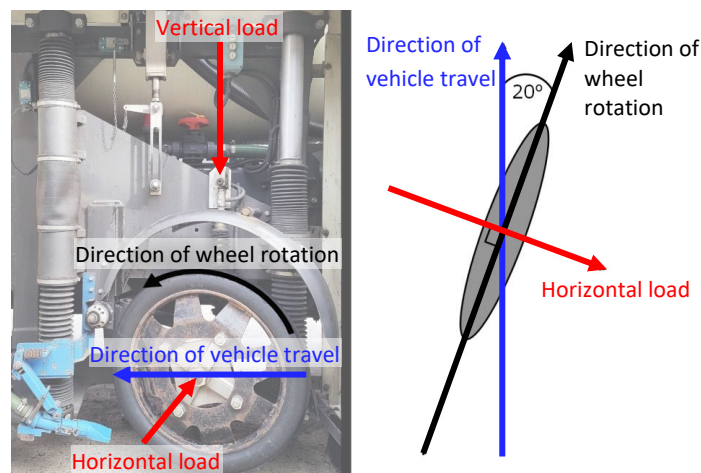

Figure 3-1 Image of the SCRIM measurement system with annotations (Left), diagram of the SCRIM measurement system in plan view

4 The currently accepted view, 34.2 % slip at 50 km/h operating speed

In order to demonstrate the currently held view of sideways-force skid resistance devices, a literature review was carried out and presented below are a selection of extracts from documents which report either the % slip, slip speed, wheel speed and/or operational speed for SCRIM.

Highways Agency (now Highways England) standard HD28/04 (which has since been superseded by CS 228) states "Because the test wheel is set at an angle to the direction of travel, the effective slip speed of the test tyre is much slower than the vehicle operating speed. The measurement is therefore one of low-speed skid resistance: at a 50 km/h standard test speed, the slip speed is approximately 17 km/h." (Department for Transport, 2004)[3].

The National Cooperative Highway Research Program (NCHRP) document "Evaluation of pavement friction characteristics" states under the heading "Side Force Devices" that "The relative velocity between the rubber and the pavement surface for these devices is approximately V Sin (α) (where α = yaw angle, and V = vehicle speed)." (Henry, 2000).

TRL report PPR564 states "At the standard test speed of 50 km/h, the test tyre contact patch slips over the road surface at about 17 km/h." (Roe & Dunford, 2012)

The NSW Roads and Maritime Services QA Specification R423 states "The parameter measured by the SCRIM. Generally the test wheel operates at an angle of 20° giving a 34% slip ratio and about 97% maximum friction." (NSW Roads and Maritime Services, 2013)

Work reported in Deliverable D1.1 of the European ROSANNE project states that "Three devices operate on the sideways-force friction principle and use test wheels which are set at an angle to the direction of travel: SCRIM, SKM and Odoliograph. The angle of the test wheel is 20° for all three devices which equates to a slip ratio of 34 %." (Greene, Viner, Cerezo, Kokot, & Schmidt, 2014)

Highways England standard HD28/15 states "The slip ratio is the ratio of the speed at which the test tyre slides over the surface (the slip speed), to the speed of the survey vehicle (the survey speed), normally expressed as a percentage." And "…For example, when a sideways-force coefficient routine investigation machine (slip ratio 34%) carries out a test at 50 km/h, the test wheel is sliding at a slip speed less than 20 km/h." (Department for Transport, 2015).

Figure 4-1 and Equation 4-1 present the current view of SCRIM in graphical and mathematical forms respectively, these are based on the definitions provided by (Henry, 2000). Equation 4-2 demonstrates that if the "relative velocity between the rubber and the pavement surface" is considered orthogonal to the wheel direction then an operational

---

[3] It is interesting to note that this text was omitted in later versions of this standard HD28/15 (Department for Transport, 2015) and CS 228 (Highways England, Transport Scotland, Welsh Government, Department for Infrastructure, 2019).

speed of 17.1 km/h and a slip percentage of 34.2 % (the currently held view of SCRIM) can be derived using Equation 3-2.
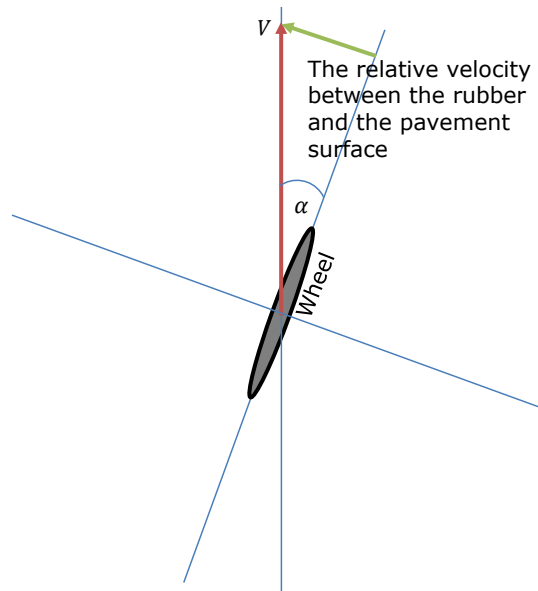

Figure 4-1 Calculation of the relative velocity between the rubber and the pavement surface presented by (Henry, 2000)

$$The\ relative\ velocity\ between\ the\ rubber\ and\ the\ pavement\ surface = V \times Sin(\alpha)$$

$$The\ relative\ velocity\ between\ the\ rubber\ the\ pavement\ surface = 50 \times Sin(20)$$
$$= 17.1\ km/h$$

Where:

- V= the vehicle speed (for SCRIM this is standardised at 50 km/h) (British Standards Institution, 2006)

- α = the angle between the direction of travel and direction of rotation of the test wheel (for SCRIM this is 20 degrees)

Equation 4-1 Calculation of the relative velocity between the rubber and the pavement surface presented by (Henry, 2000)

Therefore using Equation 3-2:

$$\% Slip = \frac{100 \times 17.1}{50} = \mathbf{34.2}\ \%$$

Equation 4-2 Derivation of % Slip based on characterisation presented by (Henry, 2000)

5 Scalar characterisation, 6.04 % wheel slip at 50 km/h operating speed

If the definitions presented in Chapter 3 are directly applied to SCRIM without any other consideration it can be shown that the system measures skid resistance at 6.04 % slip and an operating speed of 50 km/h.

5.1 Operating speed

The operating speed is equal to the vehicle speed which is standardised at **50 km/h**.

5.2 Wheel speed

The linear wheel speed has been assumed to be the component of the vehicle speed acting in the direction of the test wheel. This is shown in Figure 5-1 and can be calculated using Equation 5-1.
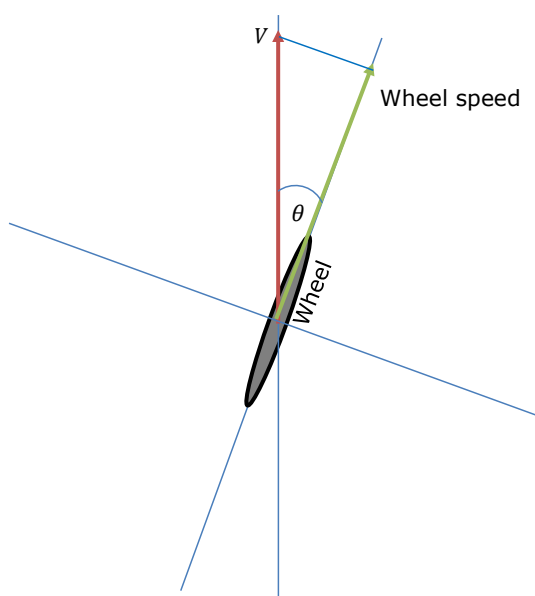
Figure 5-1 Diagram representing calculation of wheel speed (not to scale)

$$Wheel\ speed = VCos(\theta)$$

Where:

- V = the operating speed of the vehicle (km/h)
- θ = the angle between the test wheel and direction of vehicle travel

Equation 5-1 Calculation of wheel speed based on vehicle speed and wheel angle

The wheel speed can therefore be calculated as:

$$50Cos(20) = 46.98 \text{ km/h}$$

5.3   Slip speed and slip percentage

Slip speed = $50 - 46.98 = 3.02\ km/h$ from Equation 3-1

Slip percentage = (100 x 3.02) / 50 = **6.02 %** from Equation 3-2

5.4   Discussion

The analysis in this chapter has presented the case for characterising sideways-force skid resistance measurement devices as making measurements at an operating speed of **50 km/h**, and a slip percentage of **6.02%**.

This scalar characterisation of skid resistance measurement devices may be appropriate for those devices (the PFT or GripTester for instance) that make measurements (with the exception of vertical load) in a single direction. That is, those devices which measure wheel speed, horizontal load and vehicle speed in the same direction, the direction of travel.

Sideways-force devices, however, add a vector component into the fabric of the measurement system through the angled nature of the test tyre. Chapter 6 explores how sideways-force skid resistance measurement devices may be characterised using a vector rather than scalar analysis.

6 Vector characterisation, 100% wheel slip at 17.1 km/h operating speed

By considering the inherent directionality of SCRIM, and by reviewing some historical literature, it can be shown that the system measures skid resistance at 100 % wheel slip and an operating speed of 17.1 km/h.

6.1 Historical evidence to support 100% wheel slip

The following excerpts were taken from historical documentation referring to sideways-force measurement devices preceding SCRIM.

Ministry of Transport document TP2 presents an analysis of the factors affecting skid resistance measurement. "It has been pointed out that the sideway force coefficient/speed relations shown in Fig. 1 were obtained with the angle theta of the sidecar wheel set above a critical value. It is now necessary to consider the meaning of the critical angle and the values of sideway force coefficient measured at a range of angles covering it. When the motor-cycle is driven along a road surface with the sidecar wheel out of alignment, the tyre on this wheel is subject to forces which produce lateral distortion. The distortion increases from nothing at zero wheel angle, up to a maximum, which occurs at critical value of wheel angle. Within the range of zero to critical angle, the sideway force coefficient is therefore dependent on tyre distortion; above the critical angle, when tyre distortion has attained its maximum and true sliding occurs, the coefficient is dependent, as has been seen, only on road characteristics." (Bird & Miller, 1937)

A Road Research Laboratory (a predecessor to TRL) document on the interpretation of measurements made with the Road Research Laboratory's motorcycle skidding machine states that "To measure skidding resistance, this wheel is set at an angle of about 18 degrees with the direction of travel of the machine, this being the minimum angle necessary to ensure that the tyre is skidding sideways and delivering the full sideways force." (Grime, 1953)

Whilst not explicitly stating it, these documents heavily suggest that the test wheel for sideways-force devices, once beyond a critical angle enters a "true sliding" phase, this has been interpreted by the author as equating to a locked wheel (100% slip) friction phase.

6.2 The effect of the direction of measurement

For this analysis the effect of the direction of individual measurements made is crucial. For instance, most sideways-force measurement devices measure the following properties in the following orientations[4]

- Operating speed = 0 degrees (rotated around the vertical axis)

---

[4] Where the vertical axis is that which acts in the direction of gravity, and the longitudinal axis acts along the direction of vehicle travel.

- Wheel speed = N/A (not measured)

- Horizontal load = 70 degrees (rotated around the vertical axis)

- Vertical load = 90 degrees (rotated around the longitudinal axis)

In contrast, longitudinal devices measure the following properties:

- Operating speed = 0 degrees (rotated around the vertical axis)

- Wheel speed = 0 degrees (rotated around the vertical axis)

- Horizontal load = 0 degrees (rotated around the vertical axis)

- Vertical load = 90 degrees (rotated around the longitudinal axis)

The agreement in the measurement direction of operating speed, wheel speed and horizontal load for longitudinal devices means that a simple scalar assessment is appropriate. However, for sideways-force devices, because the horizontal load is measured at an angle to the direction of travel it is necessary to resolve the vectors so that the magnitude of vehicle speed and wheel speed agree with the direction of measurement of horizontal load.

This is analogous to measuring the weight of an object on an inclined plane using a platform scale. If the scale is placed on the plane, and can only measure weight perpendicular to the plane, then the weight of the object will be underestimated owing to a proportion of the weight acting in the direction of gravity. To ascertain the actual weight of the object, the angle of the plane must be considered to resolve the gravitational force and allow the true weight of the object to be calculated Figure 6-1.
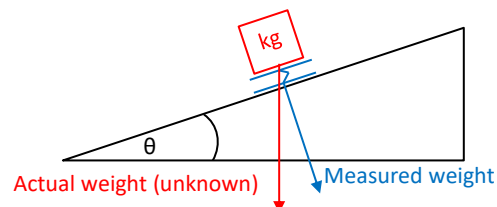

Figure 6-1 Resolving forces on an inclined plane to determine the actual weight of an object

6.3   Operating speed

The operating speed can be resolved in the direction of measurement as shown in Figure 6-2 by using Equation 6-1[5].
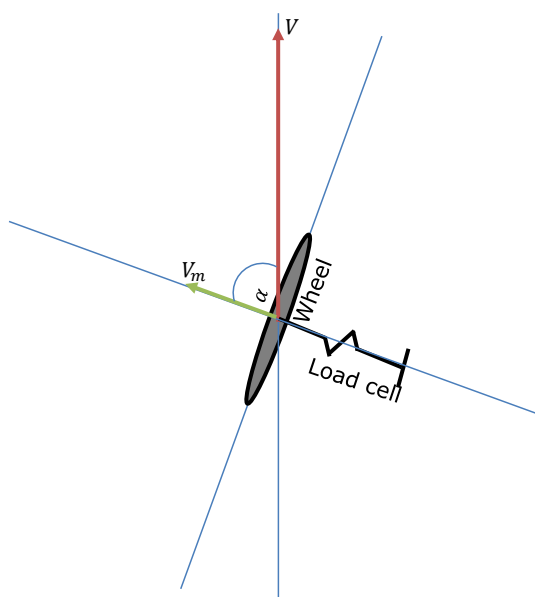

Figure 6-2 Diagram representing the operating speed and the direction to be resolved (not to scale)

$$V_m = VCos(\alpha)$$

Where:

- V_m = The vehicle speed resolved into the direction of measurements (km/h).
- V = The unresolved vehicle speed (km/h).
- α = The angle between the direction of travel and measurement.

Equation 6-1 Resolving operating speed

---

[5] It is interesting to note that this is very similar to the analysis reported in (Henry, 2000) that it is believed formed the basis of the current view. However in this case the results of the analysis are being considered as the operating speed, rather than the wheel speed as is reported in (Henry, 2000).

For the case of SCRIM:

- V = 50 km/h
- α = 70 degrees
- Therefore, $V_m = 50Cos(70) = \mathbf{17.1\ km/h}$

6.4   Wheel speed

For the purpose of this work it has been assumed that the wheel speed is the component of the vehicle speed acting in the direction of the test wheel. This has been calculated in section 3.2 as 46.98 km/h.

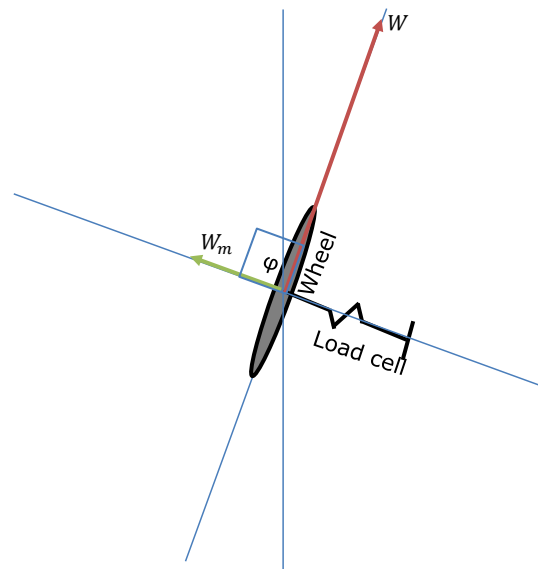The wheel speed can be resolved in the direction of measurement by using Equation 6-1.

Figure 6-3 Diagram representing the wheel speed and the direction to be resolved (not to scale)

$$W_m = WCos(\varphi)$$

Where:

- W_m = The wheel speed resolved into the direction of measurements (km/h).
- W = The unresolved wheel speed (km/h).
- φ = The angle between the wheel rotational direction and the direction of measurement.

Equation 6-2 Resolving wheel speed

For the case of SCRIM:

- W has been assumed to be 46.89 km/h

- φ = 90 degrees

- Therefore, $W_m = 46.89 Cos(90) = 0.0 \; km/h$

6.5 Slip speed and slip percentage

Now that vehicle and wheel speed have been resolved into the correct direction, Equation 3-1 and Equation 3-2 can be used to calculate slip speed and slip percentage.

Slip speed = $17.1 - 0 = \textbf{17.1} \; \textbf{\textit{km}/\textbf{h}}$ from Equation 3-1

Slip percentage = 100x17.1/17.1 = **100 %** from Equation 3-2

6.6 Discussion

The analysis in this chapter has presented the case for characterising sideways-force skid resistance measurement devices as making measurements at an operating speed of **17.1 km/h**, and a slip percentage of **100%**.

7 Validating the characterisations

Owing to the highly theoretical nature of the work and as an addition to the normal TRL quality assurance procedures, the desk study reported in the previous chapters was independently validated. This verification was carried out by one of TRLs physicists, not familiar with SCRIM or the operation thereof, and without knowledge of the work presented in the previous chapters. The question which is the theme of this work was posed, and a brief explanation of the operation of SCRIM was provided, after which the physicist carrying out the verification was not corresponded with until their findings were presented.

The full verification is presented in Appendix A but can be summarised here as having fully replicated the characterisations presented in the above chapters and generated a fourth characterisation. The characterisations developed in Chapters 1 – 6 are summarised in Table 7-1; the additional characterisation developed as part of the verification process has also been included in Table 7-1 and has been called "Co-Axial".

Table 7-1 Summary of operating speed and % slip predicted by characterisations

Characterisation	Operating Speed	Operating Speed (km/hr)	% slip
Current view	Vehicle speed	50	34.2
Scalar	Vehicle speed	50	6.03
Vector	Vehicle speed x Cos(70)	17.1	100
Co-Axial (from verification process)	Vehicle speed	50	11.7

In addition to quantifying the different possible operating speeds and slip percentages for SCRIM, the theoretical analysis carried out demonstrates that describing the performance of SCRIM cannot be carried out purely theoretically. This is because each one of the characterisations describes the same underlying physics. Identifying which characterisation is correct can therefore only be carried out by physical experimentation.

8   Support for characterisations in the existing literature

In order to assess if historical data could be used to support one or another of the characterisations summarised in Chapter 7 a literature review was carried out identifying pertinent historical literature and data referring to the function of SCRIM. This chapter presents the results of that review.

8.1   Observations of tyre striations from SCRIM testing

TRL operatives carrying out standard SCRIM testing have reported that worn SCRIM tyres possess striations which run at 90 degrees to the direction of rotation. This was shown to be the case for all the SCRIM tyres in TRL's stock and was present regardless of tyre age, or amount of use[6]. An example of this is shown in Figure 8-1 where the presence of the striations has been highlighted with white paint.
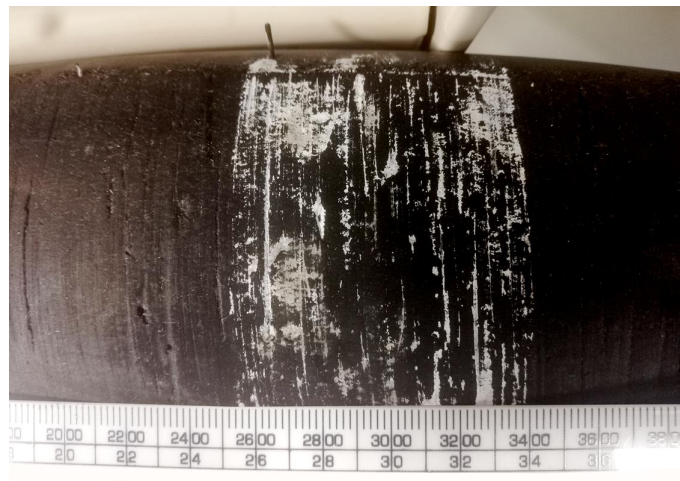

Figure 8-1 Striations observed on a SCRIM tyre due to testing

This observation is clear evidence that the tyre/road interface moves at 90 degrees to the direction of tyre rotation, or in other words, in the direction of horizontal load measurement. This seems to suggest that any characterisation that does not consider slip in this direction cannot be considered credible. Unfortunately from this evidence alone, it is not possible to infer the direction in which operational speed should be considered and so it adds equal weight to each of the characterisations in Table 7-1.

---

[6] So long as the tyre had been subject to the standard run-in process

8.2 (Bradley & Allen, 1930-31)

Fundamental work assessing the forerunner to modern SCRIMs was carried out by Bradley & Allen in 1930 and 1931. That work used a motorcycle and sidecar with an adjustable angle wheel, Figure 8-2. The sidecar wheel was fitted with sensor equipment capable of measuring the vertical load, horizontal load (along the axis of wheel rotation) and longitudinal load (in the direction of wheel rotation).
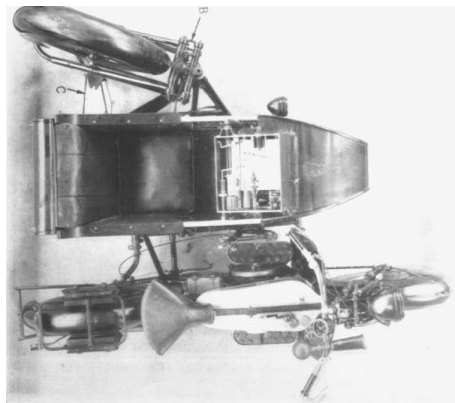

Figure 8-2 Test apparatus used by (Bradley & Allen, 1930-31)

Measurements were made using this device on materials of different types, including concrete, asphalt and wood blocks, with the device in two different configurations:

1. The configuration shown in Figure 8-2 with the sidecar wheel extended to an angle (relative to the direction of motion) of 20 degrees.

2. A configuration with the sidecar wheel retracted to an angle of zero degrees relative to the direction of travel[7] and where the sidecar wheel could be progressively braked using a manual hydraulic brake to induce different levels of wheel slip.

Measurements were also made using two different tyre types (tyre H and tyre B), neither of which reflect those used by today's SCRIM devices. In configuration 1 measurements were made at a variety of test speeds, and in configuration 2 at a range of % wheel slips, (Bradley & Allen, 1930-31) do not state at which test speed measurements were made in configuration 2.

The results from the measurements made are replicated in Figure 8-3. The relationship between speed and sideways-force coefficient was obtained making measurements in configuration 1. Of note here is that in some cases there is a positive relationship between

---

[7] (Bradley & Allen, 1930-31) did not explicitly state that this was the case and so this has been assumed.

speed and sideways-force coefficient. This is something that is commonly thought of as being a physical impossibility and so these findings are more likely to be related to the nature of data collection, rather than the actual skid resistance performance of the materials tested.

The relationship between % Slip and braking force coefficient was obtained using configuration 2. These results also demonstrate an odd behaviour as there is no evidence of a locked-wheel friction being achieved on any of the materials[8] as would be expected through long established observations. This is also likely an oddity of the measurement technique and could be due to a reduced vertical load force, or an artefact of the specific sensor equipment used.
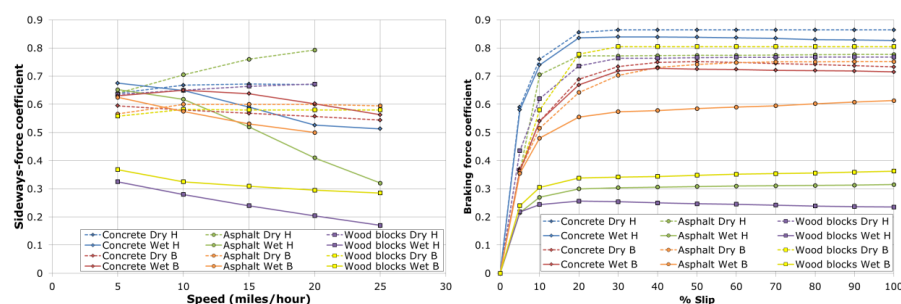

Figure 8-3 Replication of results reported in (Bradley & Allen, 1930-31)

Despite the limitations of this work, some insight can be provided by assessing the relationship between the measurements made using the two system configurations. To this end, the absolute difference between the braking force coefficient, and the sideways-force coefficient measured at 20 miles/hour, for each % slip was calculated for each material/tyre/wetting combination. The results of this analysis are presented in Table 8-1, the lowest values for each set of measurements assessed represent the best agreement in results between the two system configurations and these have been highlighted in green.

Table 8-1 Difference between braking force coefficient and sideways-force coefficient measured at 20 miles/hour

Material	Concrete				Asphalt				Wood blocks			
Dry / Wet	Dry	Wet	Dry	Wet	Dry	Wet	Dry	Wet	Dry	Wet	Dry	Wet
Tyre	H	H	B	B	H	H	B	B	H	H	B	B

---

[8] That is, there is no substantial difference between measurements made between 10 − 20 % slip and those made at 100 % slip.

% Slip	Absolute difference between braking force and sideways-force coefficients at 20 miles/hour											
0	0.67	0.53	0.56	0.60	0.79	0.41	0.60	0.50	0.67	0.20	0.58	0.30
5	0.08	0.05	0.19	0.24	0.43	0.20	0.24	0.15	0.24	0.01	0.22	0.06
10	0.09	0.21	0.02	0.06	0.09	0.14	0.09	0.02	0.05	0.04	0.00	0.01
20	0.19	0.31	0.13	0.07	0.02	0.11	0.04	0.06	0.06	0.05	0.20	0.04
30	0.19	0.31	0.18	0.12	0.02	0.11	0.10	0.07	0.09	0.05	0.23	0.05
40	0.19	0.31	0.19	0.13	0.02	0.10	0.13	0.08	0.09	0.05	0.23	0.05
50	0.19	0.31	0.20	0.12	0.02	0.10	0.14	0.09	0.09	0.04	0.23	0.05
60	0.19	0.31	0.19	0.12	0.02	0.10	0.15	0.09	0.10	0.04	0.23	0.06
70	0.19	0.31	0.19	0.12	0.02	0.10	0.15	0.10	0.10	0.04	0.23	0.06
80	0.19	0.30	0.19	0.12	0.02	0.10	0.15	0.10	0.10	0.04	0.23	0.06
90	0.19	0.30	0.18	0.12	0.02	0.10	0.15	0.11	0.10	0.03	0.23	0.06
100	0.19	0.30	0.18	0.11	0.02	0.10	0.15	0.11	0.10	0.03	0.23	0.07

It can be observed from Table 8-1 that in all but two cases the best agreement between the sideways-force coefficient and braking force coefficient is achieved between 5 and 20 % slip. In the other two cases the best agreement is observed at 100% slip. This lends some credence to the scalar characterisation as this characterisation predicts that SCRIM makes measurements at 6.03% slip.

8.3 (Bird & Miller, 1937)

In the late 1930s, Bird & Miller continued the work of Bradley & Allen into the development of sideways-force coefficient measurement technology. They conducted a series of experiments assessing the relationship between the angle of the sidecar device and the skid resistance value on different surfaces and at different speeds. The conclusions of this work act as the basis for defining the SCRIM wheel angle at 20 degrees.

The work carried out by Bird & Miller is best summarised by Figure 8-4 which in the interest of clarity has been replicated from the original text. Figure 8-4 presents the skid resistance values measured on three materials of different nominal friction levels, made at various test speeds. The general form of the results collected on each surface / test speed combination can be summarised as, a linear increase in skid resistance that reduces slightly once a critical wheel angle is met.
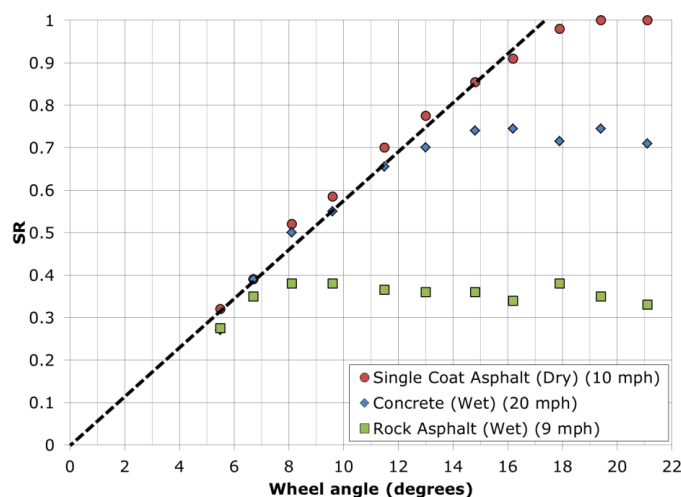
Figure 8-4 Replication of results presented in (Bird & Miller, 1937)

One of the key observations from Figure 8-4 is that regardless of surface type, test speed or the presence of water, the initial friction values from all of the tests carried out conform to the same straight line (represented by the broken line) until a critical wheel angle is met. Below is an excerpt from Bird & Miller explaining this observation.

"When the motor-cycle is driven along a road surface with the sidecar wheel out of alignment, the tyre on this wheel is subject to forces which produce lateral distortion. The distortion increases from nothing at zero wheel angle, up to a maximum, which occurs at the critical value of wheel angle. Within the range of zero to critical angle, the sideway force coefficient is therefore dependent on tyre distortion; above the critical angle, when tyre distortion has attained its maximum and true sliding occurs, the coefficient is dependent, as has been seen, only on road characteristics." (Bird & Miller, 1937)

This effect is demonstrated in Figure 8-5. In this figure a single particle is imagined approaching a SCRIM wheel, and then contacting the tyre in two cases. The case on the left of Figure 8-5 (small blue dots) shows a particle related to a "low grip" surface where the critical angle of the wheel is met. In this case the particle approaches the wheel in the direction of vehicle travel. As it makes contact with the tyre, it slides (is transposed due to the rotational action of the wheel) across the tyre in a direction perpendicular to the direction of travel.

The case on the right of Figure 8-5 (large red dots) shows a particle related to a "high grip" surface where the critical angle of the wheel is not met. In this case as the particle makes contact with the wheel it does not slide along the surface, rather, it grips the tyre and deforms it in the direction of rotation. In this case, in order to achieve full sliding, the energy applied to the tyre needs to be increased by either, increasing the wheel angle, or, increasing vehicle speed.
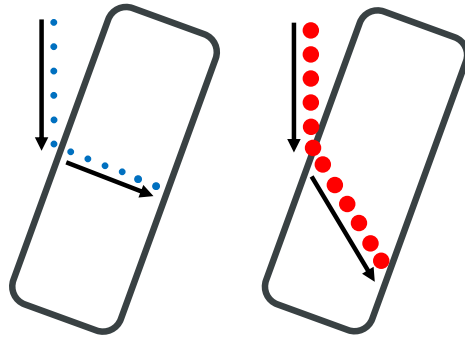
Figure 8-5 Measurements made on a "low grip" surface (left) and a "high grip" surface (right)

This observation, and explanation for it, seems to suggest that wheel angle and percentage slip are correlated. This is because the increase in skid resistance value to a peak, and a subsequent levelling off (Figure 8-4) is convincingly similar to the generation of friction with increasing wheel slip shown in Figure 8-3. However, the observations shown in Bird & Miller show that the relationship between maximum friction value reached with increasing wheel angle is correlated to the nominal friction value of the surface.

This is contrary to the observations of peak friction made by Bradley & Allen Figure 8-3 which show that maximum friction, percentage slip and nominal friction are not correlated. The observations of Bradley & Allen can be corroborated by more recent friction measurements made with the PFT which show that the peak friction of a material is independent at the percentage slip at which that friction is measured (Figure 8-6[9]).

Figure 8-6 shows that the correlation between Peak friction and the % Slip at which peak friction was measured is very poor. The box drawn with broken lines represents approximately 95% of the data present and it is approximately 15% wide. This shows only a very general trend for higher slip percentages to be present with increasing peak friction. Figure 8-4 however shows a very definite relationship between these two variables.

---

[9] Figure 8-6 shows data collected using the PFT, a locked wheel friction tester which reports levels of Locked-Wheel Friction (L-Fn) and Peak Friction (P-Fn).
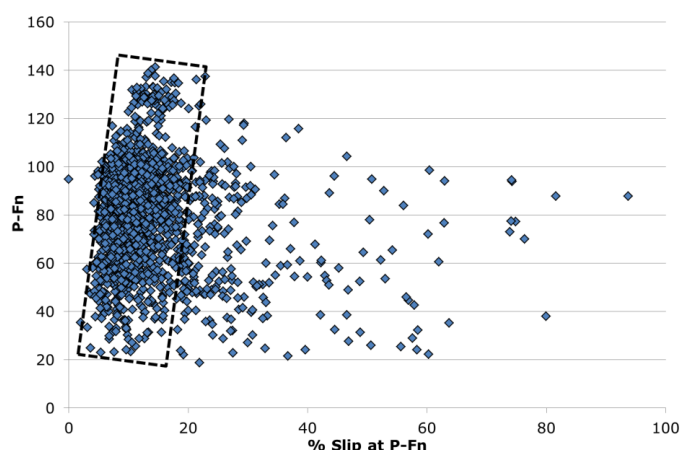
Figure 8-6 Relationship between Peak friction values and the % Slip at peak friction for 1883 individual friction measurements made using the PFT

The critical wheel angle observed by Bird & Miller must therefore be related to the properties of the tyre and is therefore not related to the peak friction of the surface. The results of Bird & Miller therefore lend themselves equally to supporting all of the characterisations of SCRIM reported in the previous chapter.

There is an important note based on the observations made in this chapter, whilst not strictly within the scope of this work, which is provided in Appendix B.

8.4 (Nordström & Åström, 2001)

During the late 1990s and early 2000s the Swedish National Road and Transport Research Institute, VTI, sought to update their skid resistance test device, the BV12. The updates made to the BV12 and an initial study into its performance are reported in (Nordström & Åström, 2001).

The update allowed the device to assess the skid resistance characteristics of road surfaces under combined turning and braking conditions. To achieve this VTI modified their BV12 to include an instrumented wheel capable of being held at an angle relative to the direction of travel and simultaneously braked. The wheel was instrumented such that the load applied to it could be measured in three directions, these were:

- Along the vertical axis,
- Along the axis of wheel rotation, referred to as the y-axis (such as that measured by sideways-force devices)
- In the direction of wheel rotation, referred to as the x-axis (such as that measured by longitudinal friction devices)

An initial set of measurements were gathered to explore the friction coefficients measured by the device in various testing configurations. A single test run was carried out whereby the test wheel was angled at 0, 5 and 10 degrees to the direction of travel. At each angle the test wheel was then braked and the friction forces acting in line with the direction of wheel rotation, and perpendicular to it were calculated for each percentage slip achieved by the wheel. Measurements were made at a test speed of 60 km/h with a nominal water thickness of 0.8 mm. It has been assumed that all of the measurements were made on a relatively homogeneous surface.

The original data referring to this work were not available in the literature assessed and so an approximation of the data has been re-constructed using the graphical representations of the data within (Nordström & Åström, 2001). The re-constructed data is presented in Figure 8-7 and in the interest of clarity data not pertinent to this work have been omitted.

Figure 8-7 presents friction coefficient measurements made with the updated BV12 with the test wheel at 0, 5 and 10 degrees to the direction of travel. For the 0 degree case, friction coefficients are presented for the full slip curve. For the angled cases, friction coefficients are presented for the 0 slip case, i.e. where the test wheel is not braked. Figure 8-7 therefore presents the comparative friction coefficients for a longitudinal test device, and a side force device with a test wheel at 5 and 10 degrees.

Based on the re-constructed data from (Nordström & Åström, 2001) three of the characterisations presented in Table 7-1 (the current view, scalar and co-axial[10]) can be tested. This can be achieved by comparing the friction coefficients measured at 5 and 10 degrees wheel angle at 0 % slip (free rolling), with those made with a 0 degrees angle at various levels of wheel slip.

---

[10] The Scalar characterization cannot be tested because this predicts that changes in wheel angle equate to changes in operational speed. The work reported by (Nordström & Åström, 2001) used a single vehicle speed of 60km/h and so the change in friction coefficient with operational speed is unknown.
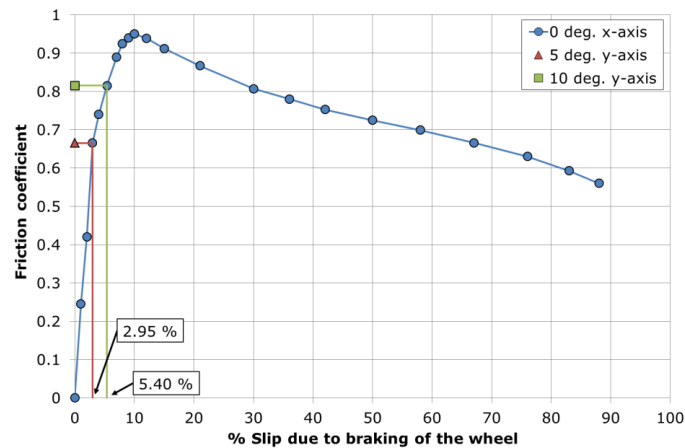
Figure 8-7 Re-construction of data from (Nordström & Åström, 2001)

The percentage slips calculated from the above exercise can then be compared to the percentage slips associated with wheel angles of 5 and 10 degrees for each of the three characterisations. This calculation has been carried out and is shown in Figure 8-7 by the red and green lines for 5 and 10 degrees wheel angle respectively. If the percentage slips defined by one or more of the characterisations match those shown in the data then this will support that/those characterisations.

The results of this analysis are shown in Table 8-2 and it can be seen that none of the characterisations that could be tested predict the % slips that were calculated from the data. One possible explanation for this is that the critical wheel angel for the surface being assessed was not reached at 5 or 10 degrees.

Table 8-2 Comparison of % slip for different wheel angles predicted by characterisations and calculated from (Nordström & Åström, 2001)

Characterisation	% slip	% slip at wheel angle (degrees):	
		5	10
Current view	Sinθ	8.72	17.36
Scalar	1-Cosθ	0.38	1.52
Co-Axial	Sin²θ	0.76	3.02
% Slip calculated from (Nordström & Åström, 2001)		2.95	5.40

Figure 18 of (Nordström & Åström, 2001), presented here in Figure 8-8, suggests that this could be the case for 5 degrees, but shows that this was not the case for the 10 degree wheel angle. Figure 8-8 shows a similar behaviour to that observed by Bradley & Allen,

namely a linear increase in friction (represented by the broken red line) with wheel angle until a critical angle is reached (the solid red line). It has been assumed that the data reported in Figure 8-8 was collected from measurements made using the same surface / tyre combination as those data in Figure 8-7. Figure 8-8 shows that measurements made at 10 degrees are clearly above the critical angle. Measurements made at 5 degrees however seem to have been made in some transitional space that does not conform to the linear broken line, nor the solid red line.
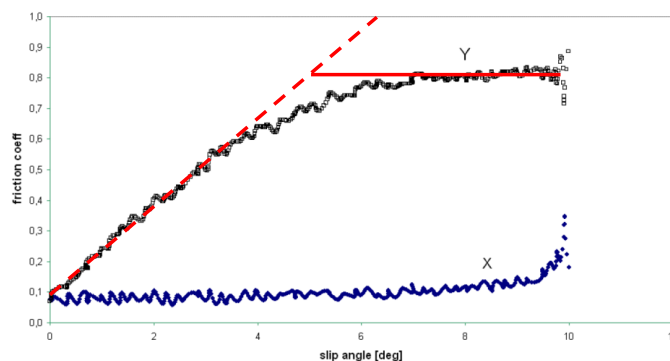
Figure 8-8 Relationship between wheel angle and friction coefficient for the updated BV12 device (Nordström & Åström, 2001)[11]

This analysis does not therefore support any of the characterisations developed which predict that changing the wheel angle of a sideways-force device is analogous to altering the percentage slip.

8.5   Summary of literature review

Based on the historical literature there is no justification for supporting any one of the characterisations summarised in the previous chapter. The literature has also shown that SCRIM can only be properly characterised when it is operating above the critical angle (when the tyre is undergoing full sliding) for any given surface. In order to properly characterise the measurement characteristics of SCRIM it is therefore necessary to collect empirical evidence comparing the performance of SCRIM with that of another measurement device.

---

[11] The solid and broken red lines have been added for clarification.

9 Challenging the characterisations

This chapter outlines experimental methodologies for empirically assessing the measurement characteristics of SCRIM.

9.1 Measuring the test tyre rotational speed

A key assumption of the scalar and vector characterisations is that the test wheel speed is equal to the component of the vehicle speed in the direction of rotation. Challenging this assumption is therefore critical in gaining confidence in these characterisations. One of the features of the current view is that at the standard vehicle speed of 50 km/h the linear test wheel speed is 46.98 km/h. This feature can also be examined using the methodology outlined below.

In order to challenge this assumption the rotational speed of the test wheel should be directly measured using a wheel speed sensor. Measurements made on surfaces with different nominal SC levels should be carried out at different vehicle speeds. If the assumption is correct then the linear speed of the wheel should follow the relationship defined in Chapter 5.

9.2 Full scale methodology

This section presents a full scale experiment utilising the Skid Resistance Development Platform (SkReDeP)[12], and another device, the Pavement Friction Tester (PFT)[13].

9.2.1 The experimental procedure

The data collection exercise for assessing operating speed and slip percentage is the same and is summarised in the following bullet points:

- Install a SCRIM wheel and tyre on the PFT and adjust the trailer weight to match that of the vertical load on SkReDeP,

- Make measurements using the PFT at different operating speeds on surfaces with different nominal friction levels,

- Make measurements with SkReDeP on the same surfaces and at the same vehicle speeds.

For each surface the measurements collected from the PFT can be used to build a surface profile. These surface profiles can then be interrogated and compared with the predictions of operating speed and % slip derived from the characterisations as summarised in Table 7-1.

---

[12] SkReDeP is a device owned by Highways England for the purpose of conducting skid resistance research and contains SCRIM equipment.

[13] The pavement friction tester is a device capable of making friction measurements over the full wheel slip percentage range at up to operating speeds of 130 km/h.

9.2.2 Data assessment

To assess the predictions of operating speed and % slip made by each of the characterisations, the change in friction measurements at various percentage slips with speed made using the PFT can be compared to the change in friction measurements made using SkReDeP. This analysis should be carried out for each of the surfaces assessed and in order to gain full confidence in the characterisations, a similar relationship should be observed regardless of the material being assessed.

To gain confidence in the current view, the change in friction with vehicle speed for the SCRIM should closely match the change in friction with vehicle speed of the PFT at 34.2 % wheel slip. To gain confidence in the scalar characterisation, the change in friction with vehicle speed for the SCRIM should closely match the change in friction with vehicle speed of the PFT at 6.03 % wheel slip.

To gain confidence in the vector characterisation, the change in friction with vehicle speed for SCRIM should closely match the change in friction with the vehicle speed multiplied by Cos(70) at 100 % wheel slip.

Idealised results of this analysis presenting hypothetical relationships demonstrating confidence in the current view and vector characterisation are shown in Figure 9-1.
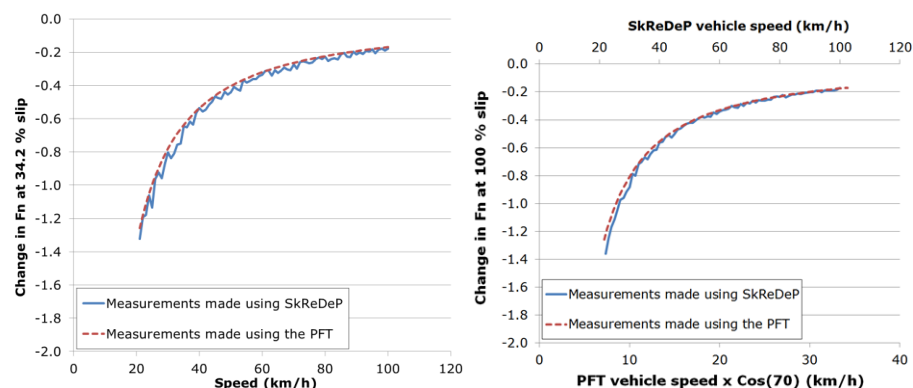

Figure 9-1 Idealised analysis results demonstrating confidence in the current view (left) and vector characterisation (right)[14]

Work reported in TRL report PPR815 (Sanders, Militzer, & Viner, 2017) demonstrated that the rate of change in friction with operating speed at various % slips is markedly different. Furthermore, the relationship between the rate of change in friction with operating speed

---

[14] This figure is an idealised representation of theoretical relationships and was NOT derived from test data.

differs for measurement s made on materials with different nominal levels of skid resistance. An analysis of this type should therefore be robust.

9.3 Laboratory methodology

The author of the verification work (Appendix A) presents a laboratory methodology for characterising the performance of SCRIM.

9.3.1 The experimental procedure

A laboratory experiment is proposed whereby a statically held, but rotating wheel, is loaded onto a conveyer belt. The following aspects of this system can be controlled:

- The angle between the wheel and conveyer belt

- The slip speed of the test wheel relative to the conveyer belt

- The speed of the conveyer belt

- The nominal friction of the belt through the use of different belt materials

The following aspects of the system would be measured:

- The vertical load applied to the test wheel

- The load in the direction of wheel rotation (the longitudinal friction)

- The load at right angles to the direction of wheel rotation (the horizontal friction)

This experimental setup will allow each of the characterisations in Table 7-1 to be independently challenged. To challenge the characterisations, measurements should be made under the following conditions using all of the different belts (belts with different friction characteristics):

1. With the wheel set to have a zero angle with the conveyor belt:

    1.1. At belt speeds of 10, 20, 30, 40 and 50 km/h

    1.2. For each belt speed, at % slips of 34.2, 6.03, 11.7 and 100

2. With the wheel set to an angle of 20 degrees with the conveyor belt:
    2.1. At belt speeds of 10, 20, 30, 40 and 50 km/h
    2.2. The test wheel should be allowed to freely rotate
3. With the wheel set to an angle of 90 degrees with the conveyor belt:
    3.1. At belt speeds of 3.42, 6.84, 10.26, 13.68 and 17.01 km/h

9.3.2 Data assessment

In order to challenge each of the characterisations, the longitudinal friction measurements made with the wheel angle at zero degrees should be compared to the horizontal friction measurements made with the wheel at a 20 degree angle. In order for a characterisation to be considered valid the friction values should match for the longitudinal friction measurements made at the corresponding percentage slip. In addition, in order for the

scalar characterisation to be valid, horizontal friction measurements made with a wheel angle at 90 degrees and the augmented belt speeds should also match the other friction values gathered.

10 Summary and conclusions

The work presented in this report has summarised three theoretical characterisations of the measurement properties of sideways-force coefficient skid resistance test devices. An experimental methodology for the assessment of these characterisations has been presented. In addition, historical works have been reviewed which add some credence to two of the characterisations.

From the work carried out the following conclusions can be made:

- The current view of SCRIM characterises its performance as having an operating speed the same as the vehicle speed and a % slip of 34.2.

- The scalar characterisation of SCRIM demonstrates an operating speed the same as the vehicle speed and a % slip of 6.03.

- The vector characterisation of SCRIM demonstrates an operating speed as the vehicle speed multiplied by Cos(70) and a % slip of 100.

- Work carried out by (Bradley & Allen, 1930-31) goes someway to supporting either the scalar or vector characterisations, but is limited in its scope.

- The experimental study presented should be carried out to identify if any of the characterisations match the measured performance of SCRIM.

- Identifying the correct performance of SCRIM is critical in designing appropriate safety standards for highways.

Appendix A   Verification of the desk study

The following analysis seeks to understand what SCRIM measures based on its configuration and the forces acting on it. The goal is to express the SCRIM configuration in language which can be equally applied to the other friction testing devices to enable a direct comparison.

This analysis has been carried out by me (Dr. Cormac Browne, July 2019) after receiving an explanation of the configuration of SCRIM and how the device operates. This is an independent note to be read in conjunction with the analysis carried out by P. D. Sanders. Both documents were produced by the respective authors without knowledge of the other's methods or definitions until after both notes were produced.

A.1   SCRIM Test Configuration

For clarity I have included a conversion from the terminology that I would employ to the language of slip percentages which is standard within the topic.
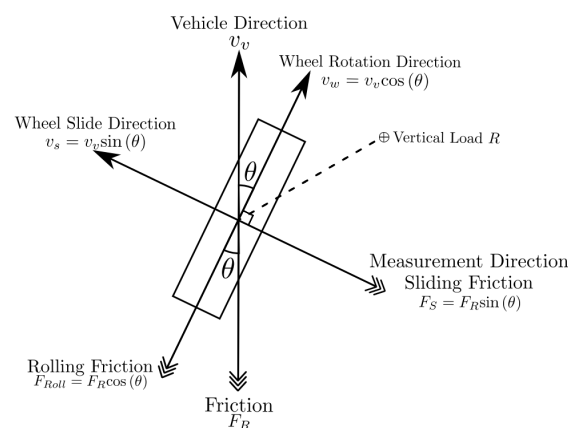
Figure A - 1 Diagram displaying the velocities and forces that act on the SCRIM test wheel

As a summary, my understanding of the SCRIM device is as follows:

1. To simulate the worst case scenario SCRIM utilises a smooth tyre and applies water to achieve an approximately constant thickness film.

2. The wheel can freely rotate around a fixed axle, and is held at an angle of $\theta = 20^0$ relative to the direction of vehicle travel.

3. During testing the vehicle travels at a constant v_v = 50 km/hr (13.8 m/s) and a constant Vertical Load R = 200g, where g is the acceleration due to gravity, is applied through the centre of the wheel and orthogonal to the axle.

4. I assume that the only source of opposing force in the system is due to the Friction F_R generated between the tyre and the road surface.

5. On the fixed axle is a load cell to measure the component of friction in the direction of the axle, which I am calling the Sliding Friction F_S.

6. SCRIM reports using the Sideways-force Coefficient $\mu s \equiv \frac{F_s}{R}$.

A.2   Interpreting the Configuration

SCRIM provides an indirect measurement of coefficient of friction that is experienced by the tyre. This can be seen using the fact that $F_R = \mu R$, meaning:

$$\mu s = \frac{F_s}{R}$$
$$= \frac{F_R \sin(\theta)}{R}$$
$$= \frac{\mu R \sin(\theta)}{R}$$
$$= \mu \sin(\theta)$$

Equation A - 1

Figure A - 1 shows how the velocity of the vehicle v_v and the vertical load R create a resultant friction F_R which can be resolved in to an 'along wheel' component and an 'in axle' component. All frictions are dependent upon the relative velocity between the surfaces causing the friction. To characterise the action of the SCRIM device it is important to fully describe these velocities and the relationship between them. There are 3 velocities which are natural to consider in the configuration - the vehicle velocity v_v, the linear velocity of the wheel v_w (along the axis of rotation), and the sliding velocity of the wheel v_s.

To enable comparison with other devices (particularly the Pavement Friction Tester which is a longitudinal friction tester) we wish to define an Operating Speed u_{op} and a Slip Speed u_{slip} experienced by the system. It is standard to use the Slip Percentage $S_\% \equiv \frac{u_{slip}}{u_{op}} \cdot 100\%$ to refer to the slip speed in relation to the operating speed.
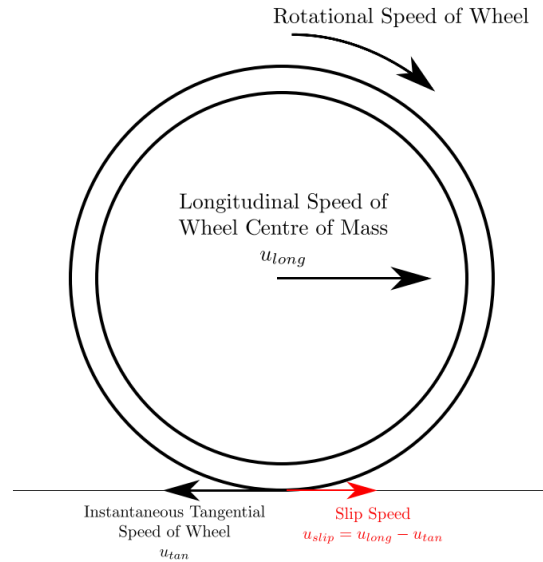
Figure A - 2 Diagram showing how slip speed is defined for a longitudinal friction tester

In the case of a longitudinal friction tester (LFT) there are natural values to associate with each of these parameters, see Figure A - 2. The operating speed can be defined as the longitudinal speed of the wheel's centre of mass u_{long}. This allows us to define the slip speed as the difference between u_{long} and the instantaneous tangential speed of the wheel u_{tan}:

$$u_{slip} = u_{long} - u_{tan}$$

Equation A - 2

Hence we can see that the slip percentage S% of the system is:

$$S_\% = \frac{u_{slip}}{u_{op}} \cdot 100\%$$

$$= \frac{u_{long} - u_{tan}}{u_{long}} \cdot 100\%$$

$$= \left(1 - \frac{u_{tan}}{u_{long}}\right) \cdot 100\%$$

Equation A - 3

Returning to the SCRIM device, we can see that there are range of possible definitions that could be employed to understand the SCRIM configuration. These definitions will produce different values for the slip percentage and are evaluated below. However, the fundamental

source of the measured friction remains the relative velocity between the pavement and the tyre in the direction of the measurement.

A.2.1 *Sliding Velocity Relative To Vehicle Velocity*
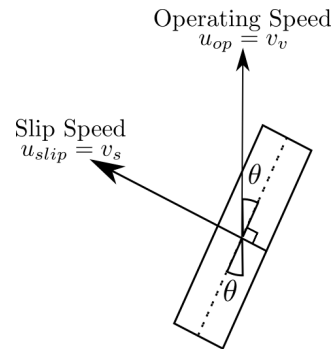

Figure A - 3 Sliding velocity relative to vehicle velocity

To attempt directly mapping the definitions for the LFT we can define the operating speed to be the vehicle speed: u_{op} = v_v. Considering the slip speed as defined for the LFT to be targeting the component of the longitudinal velocity of the tyre centre of mass that is due to sliding the tyre and not due to its rotation leads to the closest analogue being the sliding velocity so we have u_{slip} = v_s. Choosing these definitions allows us to see that the slip percentage $S_\%$ will have no dependence on the vehicle speed, and purely depends on the angle between the tyre and the vehicle direction:

$$S_\% = \frac{u_{slip}}{s_{op}} \cdot 100\%$$
$$= \frac{v_v \sin(\theta)}{v_v} \cdot 100\%$$
$$= \sin(\theta) \cdot 100\%$$
$$= 34.2\%$$

Equation A - 4

A.2.2   *Wheel Rotation Velocity Relative to Vehicle Velocity*
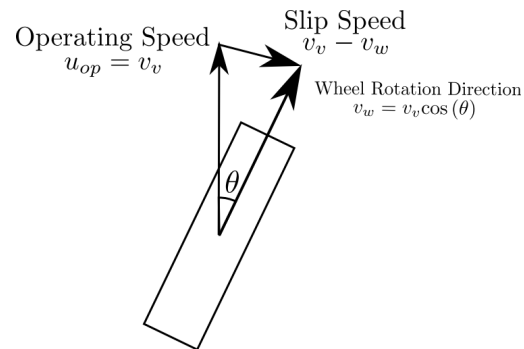

Figure A - 4 Wheel rotation relative to vehicle velocity

For the LFT the slip speed is calculated from the difference between the vehicle speed and the tangential velocity of the tyre. Applying this strict definition, using the equivalent terms for SCRIM leads to $u_{slip} = v_v - v_w$, and using this to calculate slip percentage gives:

$$S_\% = \frac{u_{slip}}{u_{op}} \cdot 100\%$$

$$= \frac{v_v - v_w}{v_v} \cdot 100\%$$

$$= \frac{v_v - v_v \cos(\theta)}{v_v} \cdot 100\%$$

$$= \big(1 - \cos(\theta)\big) \cdot 100\%$$

$$= 6.03\%$$

Equation A - 5

However an insurmountable flaw in this definition is that the SCRIM does not measure any forces in this direction. The friction measured is in an orthogonal direction to the wheel's rotation and so characterising the slip percentage in these terms is misleading.

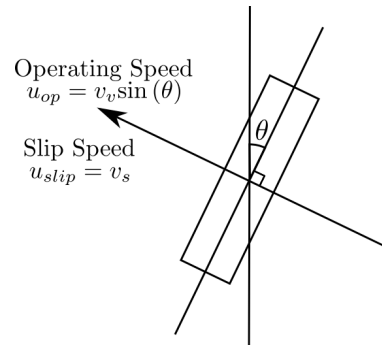### A.2.3 Velocities Co-Axial to the Slip Direction

Figure A - 5 Velocities co-axial to the slip direction

An alternative interpretation of the LFT setup is that all the velocities are defined such that they are co-axial with the slip direction. That is, the operating speed is defined to be the vehicle velocity in the direction of the slip and the slip speed is defined as the difference between wheel rotation speed in the direction of slip and the sliding speed. As the wheel is rotating about a fixed axle that is in the same direction as the slip direction it is clear that the slip speed is then just the sliding speed. Thus the slip percentage is simply:

$$S_\% = \frac{u_{slip}}{u_{op}} \cdot 100\%$$

$$= \frac{v_s}{v_v sin(\theta)} \cdot 100\%$$

$$= \frac{v_v sin(\theta)}{v_v sin(\theta)} \cdot 100\%$$

$$= 100\%$$

Equation A - 6

A.2.4   Velocities Co-Axial to the Vehicle Direction
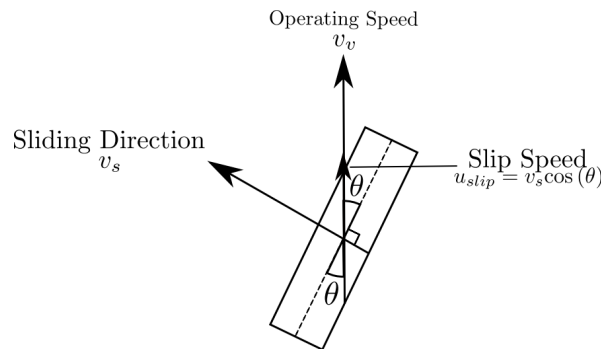

Figure A - 6 Velocities co-axial with the vehicle direction

Similarly, as the only source of friction in the system is due to the motion of the vehicle one could choose to 're-resolve' the velocities of interest to be co-axial with the direction of interest. Here we define the operating speed to be the velocity of the vehicle. Then the slip speed can be defined as either:

1. The sliding velocity resolved in the direction of the vehicle's travel.

$$u_{slip} = v_s sin(\theta)$$
$$= v_v sin^2(\theta)$$

Equation A - 7

2. The difference between the vehicle speed and the tangential speed of the tyre resolved in the direction of the vehicle's travel.

$$u_{slip} = v_v - v_w cos(\theta)$$
$$= v_v - v_v cos^2(\theta)$$
$$= v_v\big(1 - cos^2(\theta)\big)$$
$$= v_v sin^2(\theta)$$

Equation A - 8

As can be seen both definitions produce the same slip speed as can be expected - the amount of slip in the direction of travel should be the same no matter how you choose to calculate it. The slip percentage using this set of definitions is:

$$S_{\%} = \frac{u_{slip}}{u_{op}} \cdot 100\%$$

$$= \frac{v_v sin^2(\theta)}{v_v} \cdot 100\%$$

$$= sin^2(\theta) \cdot 100\%$$

$$= 11.7\%$$

Equation A - 9

The flaw in this interpretation is that measurement is not co-axial to the vehicle direction - thus we are characterising the measurement using parameters which contain components that the measurement does not interact with. One can also consider the act of 're-resolving' the forces to be an arbitrary choice that is ill justified although I would argue it does tell you the amount of slip an element of rubber would experience in the direction of travel. The measurement of friction occurs at an angle of $\frac{2}{\pi} + \theta$ relative to the direction of travel of the vehicle. As such it may be necessary to scale the measurement result by $(sin(\theta))^{-1}$ when comparing to other friction testers.

A.2.5   *Summary Table of Interpretations*

Operating Speed u_{op}	Operating Speed Value (km/hr)	Slip Speed u_{slip}	Slip Speed (km/hr)	Slip Percentage %
v_v	50	v_s	17.1	34.2
v_v	50	v_v-v_w	3.02	6.02
$v_v sin(\theta)$	17.1	v_s	17.1	100
v_v	50	$v_s sin(\theta)$	5.85	11.7

A.3 Testing the Interpretations

There is some mathematical justification for using any of the above interpretations. I would argue Interpretation 2 is not an accurate representation of the SCRIM and is unlikely to produce results which can be compared to other devices.

The other three interpretations are different methods of representing the same underlying physics. If each definition is applied correctly it will result in the same resolution of the forces and produce the same relative velocity between the road surface and the tyre. Friction arises in the system due to the vertical load and this relative velocity producing a resistive force to oppose the vehicle's motion.

To test each of these interpretations there are two complimentary methodologies which can be employed:

1. Recreate each configuration using a longitudinal friction tester and measure the resulting coefficients of friction.

2. Recreate the SCRIM configuration and measure wheel velocity, slip speed, and the dependence on angle and operating velocities.

To implement Method 2, I would propose using a moveable conveyor belt system with a surface of known frictional properties applied to the belt. This makes use of the fact that there is no difference between a vehicle traversing a road surface at some velocity and a surfacing being moved relative to the vehicle at the same velocity. Such a system would allow for measurements of the resultant forces in all relevant directions (co-axial with the "vehicle" motion, the axis of rotation of the wheel, and the direction of rotation of the wheel) and for the relative angle between the direction of travel and the wheel to be varied.

The advantage of such a setup is all degrees of freedom in the system can be controlled and investigated. It is possible to set up any measurement configuration and iterate between them to fully map how the SCRIM depends on the different parameters and to determine at what points different kinds of friction become important. Should it be desired a more detailed methodology can be drafted and proposed.

Appendix B   Note on the determination of SCRIM critical angle

The only work that was identified referring to the calculation of the SCRIM critical angle, was that work carried out in the 1930s by (Bradley & Allen, 1930-31) and (Bird & Miller, 1937). Both pieces of work were carried out using the motorcycle and sidecar device which was the precursor to modern SCRIM devices. It is not known to the authors if further work investigating the critical angle was carried out between the 1930s and when SCRIM was developed in the 1960s the results of which were not reported or have been lost over time.

Since 1937 numerous changes to the sidecar and motorcycle device have been made, the most notable of which are:

- The vertical load applied to the test wheel has been standardised at 200 kg

- The vehicle chassis has been updated to improve stability

- The test tyre compound has been changed, at least twice

- The vehicle test speed has been standardised at 50 km/h

- The application of water to the tyre surface interface has been standardised at a nominal depth of 0.5 mm

- The test wheel itself has been changed from a spoke to solid plate design

All of the changes listed above will have had a dramatic effect on the sideways-force system and could therefore also affect the critical angle. For example, increasing the vertical load on the wheel would increase the sideways force applied to the wheel for a surface of the same skid resistance[15]. According to Figure 8-4 and Figure 8-5 this would require the critical angle, or vehicle speed to be increased to overcome the additional force applied to the tyre from the road.

It may be the case therefore, that current SCRIM devices are operating using a wheel angle which is below the critical angle for some materials and above it for others. For materials where SCRIM operates below the critical angle, this would have the effect of producing a lower skid resistance measurements on these surfaces than would have been measured using a greater wheel angle. Crucially, these measurements are most likely to be made on materials with a high nominal friction level, which are typically installed on the highest risk sites, where accurate skid resistance characterisation is crucial for motorist safety.

It is therefore strongly recommended that a review is carried out to identify if critical angle was further investigated since 1937 and if not, the experiments of Bird & Miller repeated using a modern SCRIM device to assess if modern SCRIMs are operating above critical angle for all of the material types present on the UK road network, in particular for High Friction Surfacings that were not present on the UK road network in the 1930s.

---

[15] Because, skid resistance = horizontal force / vertical force

Bibliography

Bird, G., & Miller, R. A. (1937). *TP2 Studies in road friction II. An analysis of the factors affecting measurement.* Department of scientific and industrial research and Ministry of Transport.

Bradley, J., & Allen, R. F. (1930-31). Factors affecting the behaviour of rubber-tyred wheels on road surfaces. *Institute of automobile engineers proceedings*, pp. 63-92.

British Standards Institution. (2006). *BS 7941-1-2006 Methods for measuring the skid resistance of pavement surfaces – Part 1 SCRIM.* London: BSi.

British Standards Institution. (2009). *DD CEN/TS 1509-6:2009 Part 6: Procedure for determining the skid resistance of a pavement surface by measurement of the sideway force coefficient (SFCS): SCRIM.* London: British Standards Institution.

Department for Transport. (2004). *HD 28/04 Skidding resistance.* London: DfT.

Department for Transport. (2015). *HD 28/15 - Skid resistance (DMRB 7.3.1).* London: The Stationery Office.

Greene, M., Viner, H., Cerezo, V., Kokot, D., & Schmidt, B. (2014). *ROSANNE Deliverable D1.1 Definition of boundaries and requirements for the common scale for harmonisation of skid resistance measurements.* N/A: ROSANNE.

Grime, G. (1953). *RN_2029_GG The interpretation of measurements made with the road research laboratory's motorcycle skidding machine.* Road research laboratory.

Henry, J. J. (2000). *Evaluation of pavement friction characteristics.* NCHRP.

Highways England, Transport Scotland, Welsh Government, Department for Infrastructure. (2019). *CS 228 Pavement inspection and assessment - Skidding resistance.* London: Highways England.

Nordström, O., & Åström, H. (2001). *Upgrading of VTI friction test vehicle BV12 for combined braking and steering tests under aquaplaning and winter conditions .* Florence: 2nd International Coloquium on Vehicle Tyre Road Interaction .

NSW Roads and Maritime Services. (2013). *QA Specification R423 Measurement of surface friction by sideways-force coefficient routine investigation machine (SCRIM).* NSW Roads and Maritime Services.

Roe, P. G., & Dunford, A. (2012). *PPR564 The skid resistance behaviour of thin surface course systems.* Wokingham: TRL.

Sanders, P. D., Militzer, M., & Viner, H. E. (2017). *PPR815 Better understanding of the surface tyre interface.* Wokingham: TRL.

Characterising the measurements made by sideways-force skid resistance devices

TRL

The effective management of road surface skid resistance properties is critical for providing a safe means of road travel. The measurement of skid resistance is a key component in the effective management of road surface skid resistance. In the UK the skid resistance properties of the trunk road network are assessed annually using devices utilising the sideways-force measurement principle, the Sideways-force Coefficient Routine Investigation Machine (SCRIM).

Currently little is understood about the fundamental measurement characteristics of SCRIM. The relationship between the skid resistance properties of the UK road network, and the friction characteristics exploited by vehicles conducting various manoeuvres, is, by extension, also not fundamentally understood. In generating this fundamental knowledge, there therefore exists major potential benefits in terms of reducing vehicle incidents, reducing cost, and maximising the efficiency of road management.

This document presents the results of a desk study into the properties of SCRIM devices with the goal of characterising the measurement properties of SCRIM in terms of the fundamental properties of skid resistance devices, namely; the percentage slip and operational speed. Four equally valid characterisations were generated, and an outline experimental procedure for determining that which is related to SCRIM devices is presented.

Other titles from this subject area

PPR737   Performance review of skid measurement devices. Sanders P D, Brittain S and Premathilaka A. 2015

PPR850   Optimisation of water flow depth for SCRIM. Brittain S, Sanders P D and Viner H E. 2017

PPR702   Comparison of SCRIM and SKM sideway-force skid resistance devices. Brittain S. 2014

PPR815   Better understanding of the tyre surface interface. Sanders P D, Militzer M and Viner H E. 2017

Page left intentionally blank.

Appendix F

Sanders, P. D. (2021), *PPR980 Characterising the measurements made by sideways-force skid resistance devices - An experimental study.* TRL, Wokingham, England.

Sanders, P. D. (2021), *PPR980 Characterising the measurements made by sideways-force skid resistance devices - An experimental study.* TRL, Wokingham, England.

PUBLISHED PROJECT REPORT PPR980

Characterising the measurements made by
sideways-force skid resistance devices

An experimental study

P D Sanders

Report details

Report prepared for:	Highways England, Pavements
Project/customer reference:	1-407 Sub-task 2
Copyright:	© TRL Limited
Report date:	January 2021
Report status/version:	Draft
Quality approval:	
A Kaminski (Project Manager)	**Approved**		M Greene (Technical Reviewer)	**Approved**

Disclaimer

This report has been produced by TRL Limited (TRL) under a contract with Highways England. Any views expressed in this report are not necessarily those of Highways England.

The information contained herein is the property of TRL Limited and does not necessarily reflect the views or policies of the customer for whom this report was prepared. Whilst every effort has been made to ensure that the matter presented in this report is relevant, accurate and up-to-date, TRL Limited cannot accept any liability for any error or omission, or reliance on part or all of the content in another context.

When purchased in hard copy, this publication is printed on paper that is FSC (Forest Stewardship Council) and TCF (Totally Chlorine Free) registered.

Contents amendment record

This report has been amended and issued as follows:

Version	Date	Description	Editor	Technical Reviewer
1.0	07/01/2021	Final version issued to client	PS	MG

Document last saved on:	11/01/2021 15:53
Document last saved by:	Peter Sanders

Executive summary

The effective management of road surface skid resistance is critical for providing a safe means of travel for all road users. The skid resistance on the English trunk road network is managed with the goal of normalising the skidding risk to motorists across areas of varying relative risk (known as site categories). Currently this is undertaken using a correlative approach which compares road surface skid resistance with the prevalence of wet skidding accidents for different site categories. Critically however, it is not understood, even at a fundamental level, how the skid resistance measurements made on the road network physically relate to the friction properties exploited by vehicles.

In this paradigm there exists a major potential benefit to road authorities, road users, and vehicle manufacturers, in generating this fundamental knowledge, especially in areas of high skid risk. The work reported in this document represents part of a programme of research which seeks to fully understand the relationship between the parameters outlined above. The overall result of this programme of work will provide advice to road owners as to how they can best use road surfacing materials in order to:

- Maximise the cost effectiveness of pavement materials used,

- Minimise the skidding risk to road users in areas of varying risk,

- Update the relevant management procedures in order to continually support the above points.

In the UK, the skid resistance properties of the trunk road network are assessed annually by devices utilising the sideways-force measurement principle, the Sideways-force Coefficient Routine Investigation Machine (SCRIM). Currently, a view of the measurement properties of SCRIM is in place. However, this is based on a theoretical analysis of the device, is unsupported by empirical evidence, and, in some cases is contradictory to historical literature. During recent years this view has been challenged and it is the aim of this work to investigate the measurement properties of SCRIM in order to confirm the currently held view, or to provide an alternative.

A desk study produced the following characterisations for SCRIM but was unable to identify a unique valid characterisation.

Summary of operating velocity and % slip predicted by characterisations

Characterisation	operating velocity	% slip
Current	The vehicle speed	34.2
Scalar	The vehicle speed	6.03
Vector	The vehicle speed x Sin(20)	100
Co-Axial	The vehicle speed	11.7

As a result, the following research questions were prompted:

- What is the speed of the SCRIM test tyre, and how does this relate to the vehicle speed?

- What factors influence the speed of the SCRIM test wheel?

- What is the operational velocity for SCRIM?

- At what percentage slip does SCRIM characterise road surface friction?

- What factors influence the operational velocity and percentage slip?

This report presents an experimental study which was designed to answer these questions. From the work carried out, the following conclusions can be made:

- SCRIM measurements are made at an operational velocity of 17.1 km/h and 100% Slip, when measurements are made at the standard vehicle speed of 50 km/h.

- Aquaplaning or near aquaplaning of the SCRIM tyre occurs on materials with a nominal low speed skid resistance.

- There is evidence that on materials with high nominal skid resistance levels, the critical wheel angle for SCRIM (i.e. the angle above which skid resistance measurements no longer increase) may not be being achieved.

TRL

Table of Contents

TRL

1 Introduction

The effective management of road surface skid resistance properties is a critical factor in providing a safe means of travel for all road users. The measurement of skid resistance is a key component in the effective management of skid resistance. In the UK the skid resistance properties of the trunk road network, and many local road networks, are assessed annually using devices utilising the sideways-force measurement principle.

At the time of writing, all of the devices used for charactering the skid resistance properties of the UK motorway and trunk road network are Sideways-force Coefficient Routine Investigation Machines (SCRIMs). However, in Germany the SeitenKraftMessverfahren (SKM) is used and in Belgium the Odoliograph is used, both of which operate under the same sideways-force principles as SCRIM. Understanding the fundamental measurement properties of sideways-force devices would therefore provide a major benefit to UK and international road authorities in better interpreting the measurements made and how they relate to manoeuvres and friction demand of the vehicle fleet.

Currently, a view of the measurement properties of SCRIM is in place and is widely accepted. However, this view is based on a theoretical analysis of the device, is unsupported by practical assessment, and in some cases could be considered contradictory to historical works. During recent years, research into road surface skid resistance and friction has progressed in such a way that the specific measurement characteristics of SCRIM have become of particular interest. Owing to this interest, the current view of SCRIM has been challenged and it is the aim of this work to investigate the measurement properties of SCRIM and to undertake experimental programme of measurements by which the measurement properties of SCRIM can be confirmed.

2 Background to pavement friction and its influence on vehicle safety and highway management

2.1 Friction as a multi-dimensional parameter

The friction generated between a road surface and vehicle tyre is highly variable; the concept of a ubiquitous "level of grip" is a misnomer. This is because the friction between a road surface and vehicle tyre, is dependant upon, amongst other variables, the speed at which the surface is being traversed, and the amount of slip between the tyre and road surface. Friction is therefore a three-dimensional parameter[1]. This is illustrated in Figure 2-1 which presents the typical relationship between friction, operating velocity, and wheel slip.
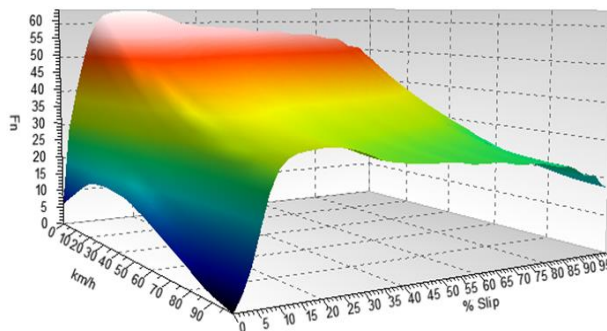

Figure 2-1 An example of the relationship between friction (Fn), operating velocity (km/h) and wheel slip (% Slip), the friction profile.

Efforts to normalise the measurement of road friction using standardised devices and test procedures, can allow for the measurement of the road's contribution to friction, the "skid resistance". Skid resistance measurements can be made with reference to the speed and % slip at which the measurement was made for some devices for which these parameters are defined. For SCRIM this is not the case, as the speed and % slip of SCRIM measurements are not known.

2.2 The influence of friction on vehicle safety

Work reported in TRL report PPR 815 (Sanders, Militzer, & Viner, 2017) demonstrated that vehicles undertaking a straight line braking manoeuvre use friction at a range of wheel slips and speeds. In other words, vehicles undertaking this manoeuvre use friction values at many

---

[1] In the same way that a map co-ordinate is a two dimensional parameter and that the knowledge of one of the co-ordinates is not meaningful without knowledge of the other.

different points on the profile presented in Figure 2-1. Furthermore, the work demonstrated that if Anti-lock Braking Systems (ABS) are activated, the areas of the friction profile used are markedly different to those used when ABS is not activated. This is illustrated in Figure 2-2 which shows an idealised view of the areas on the friction profile used.
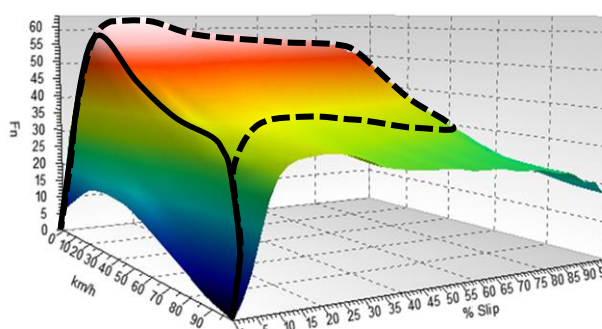

Figure 2-2 Friction used by a vehicle undertaking straight line braking, the solid line represents ABS use and the broken line represents braking without ABS

It is likely that different manoeuvres, will use different areas of the friction profile than those illustrated for straight line braking. Gaining an understanding of the areas on the friction profile demanded by vehicles, and the ability of a road surface to deliver friction in these areas is therefore an important consideration to highways authorities in delivering a safe network.

2.3 The implications for the management of road networks

The UK trunk road network is managed such as to broadly normalise the risk of skidding across the network. To achieve this, the road network is split up into various site categories, which relate to the level of risk posed to road users. Each site category is assigned a skid resistance Investigatory Level (IL).

Investigatory Levels are based on measurements made with SCRIM and their relationship to collision risk, with locations which fall at or below their IL being subject to investigation to determine whether treatment to improve the skid resistance would be beneficial. Based on the factors outlined in section 2.2, it may be the case that SCRIM measurements are more reflective of the friction demanded by vehicles in some areas of the network than others.

This view is supported by the outcomes of studies to assess the relationship between skid resistance and collision risk on the network; (Wallbank, Viner, Smith, & Smith, 2016) showed that the relationships were stronger for some situations, such as bends, than others, e.g. non-event motorway. Therefore a better understanding of where SCRIM measurements sit on the friction, slip, speed profile would lead to improvements in how skid resistance is managed on the network.

3   Definition of parameters

Skid resistance measurement tools are typically characterised based on their operating principle:

- Longitudinal fixed slip devices. Devices with a test wheel mounted in the same orientation as the vehicle wheels which is forced to rotate at a fixed percentage of the operating velocity.

- Longitudinal variable slip devices. Devices with a test wheel mounted in the same orientation as the vehicle wheels which during testing alternates between a freely rotating and a locked-wheel (or peak friction) state.

- Sideways-force devices. Devices with a test wheel mounted at an angle to the vehicle wheels. SCRIM operates under this principle.

Skid resistance measurement devices can be further characterised using the terminology outlined in the following sub sections. The definitions of the parameters detailed in these sub-sections will be used throughout the rest of this document.

3.1   Operational velocity

Operational velocity is often referred to as the vehicle speed, and the two terms are frequently used interchangeably. However, for the purposes of this work it is necessary to introduce a subtle difference. For this work, vehicle speed (V_v) is defined as the speed at which the test device traverses the test surface.

In PPR 957 (Sanders & Browne, 2020) operational velocity was described as operating speed with the following definition:

"Operating speed is defined as the effective vehicle speed of the test device." - (Sanders & Browne, 2020)

To add further clarity, a more detailed definition of operational velocity[2] is given below. The practical use of the terms "Operational velocity" in this report and "Operating speed" in PPR 957 are identical.

Operational velocity (V_o) is the speed at which the rotational axis of the test tyre moves with respect to the direction of friction measurement.

3.2   Wheel speed

Wheel speed (V_w) is defined as the tangential linear speed of the circumference of the test tyre.

---

[2] The term "velocity" is used in preference to "speed" as the definition of operating velocity makes reference to a specific direction.

3.3   Slip speed, Slip Ratio and Percentage Slip

Slip speed (V_s) is defined as "relative speed between the test tyre and the travelled surface in the contact area (British Standards Institution, 2009). This definition can be expressed formulaically using Equation 3-1.

$$V_s = V_o - V_w$$

Where:

- V_s = Slip Speed
- V_o = Operational velocity
- V_w = Wheel speed

Equation 3-1 Definition of slip speed

Slip speed is often expressed as either slip ratio or slip percentage in order to be expressed a relative function of the operational velocity. Percentage slip (% Slip) is defined in Equation 3-2. For the purposes of this work, percentage slip will be used in preference to slip ratio.

$$\% \, Slip = \frac{100 \times V_s}{V_v}$$

Where:

- V_s is the slip speed
- V_v is the vehicle speed

Equation 3-2 Definition of % Slip

3.4   Vertical and horizontal load

Skid resistance is a unit-less parameter calculated as the ratio between vertical and horizontal load. For all skid resistance measurement systems, vertical load is the load acting on the test wheel in the direction of gravity. The definition of horizontal load however differs depending on the specific measurement device. In the case of SCRIM, horizontal load is defined as the load acting on the test tyre along the axis of test wheel rotation (Figure 3-1).
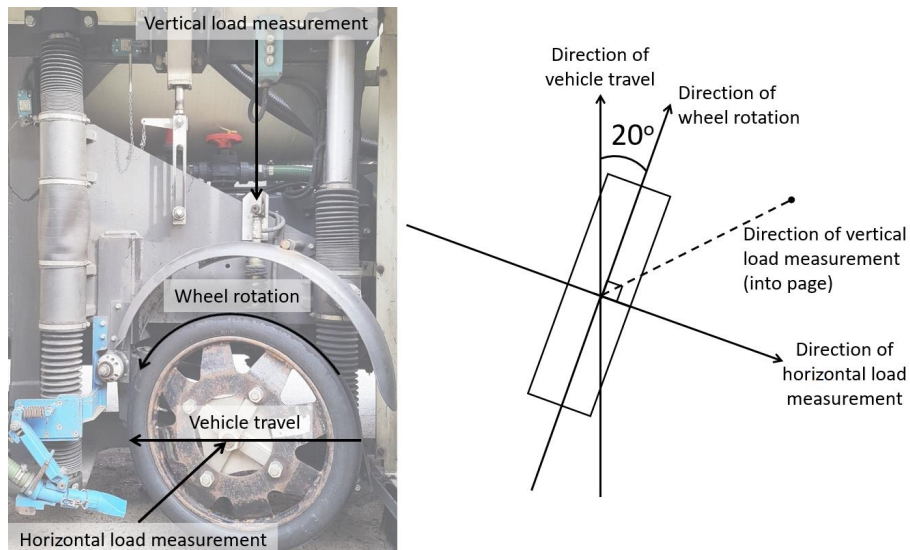
Figure 3-1 Image of the SCRIM measurement system with annotations (Left), diagram of the SCRIM measurement system in plan view

3.5   Critical wheel angle

Whist the wheel angle for SCRIM is fixed at 20 degrees, for some of the later discussion in this report, the concept of Critical Wheel Angle (CWA) is important. The CWA for SCRIM devices was derived by Bird and Miller in their 1937 work (Bird & Miller, 1937) which assessed the skid resistance of various surfaces and at different wheel angles. The results of this work have been replicated in Figure 3-2. As wheel angle increases the Skid Resistance (SR) value increases linearly, until such point as no further substantial change is observed. This point is the CWA.

It should be noted that the CWA is surface dependant and appears to be related to the nominal SR of the surface. For example, on the Rock Asphalt surface, the CWA is met at approximately 8 degrees, and on the Single Coat Asphalt it is met at approximately 20 degrees.
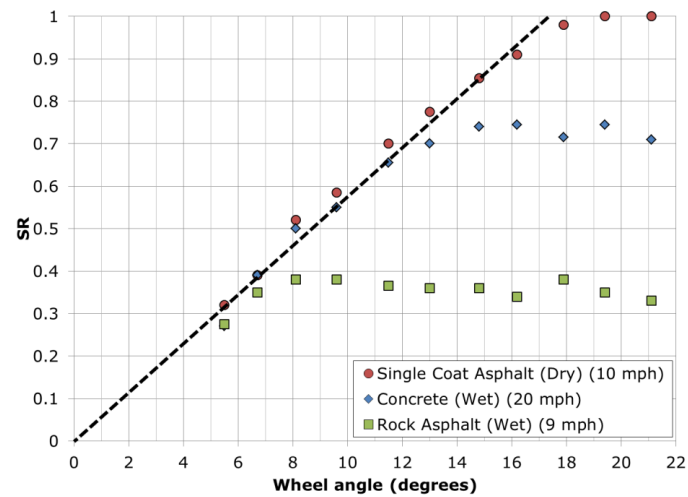
Figure 3-2 Replication of results presented in (Bird & Miller, 1937)

4 Summary of the desk study

The desk study preceding this experimental work is presented in full in (Sanders & Browne, 2020). The characterisations of sideways-force skid resistance measurements devices derived from that work have been summarised in this chapter. It is important to note that these characterisations were based on the assumption that SCRIM is always operating above the CWA. The goal of this desk study was to derive different characterisations of the operation of SCRIM, using the language of operational velocity, slip speed, and slip percentage. Hence the different characterisations arise from considering the impact of varying which aspects of the wheel motion are treated as the operational velocity and slip speed.

4.1 The currently accepted view, 34.2 % slip at 50 km/h operational velocity

In the currently accepted view, the operational velocity is considered to be the vehicle speed, and the slip speed is considered to be the vehicle speed resolved orthogonal to the direction of wheel rotation. Figure 4-1 presents the currently accepted view of SCRIM in graphical and mathematical forms, these are based on the definitions provided by (Henry, 2000).
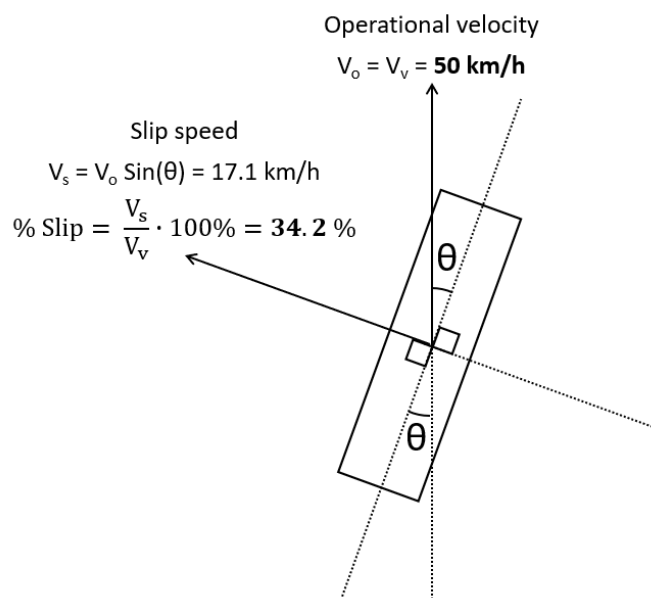
Operational velocity

$V_o = V_v = \textbf{50 km/h}$

Slip speed

$V_s = V_o \, \text{Sin}(\theta) = 17.1 \text{ km/h}$

$\% \, \text{Slip} = \dfrac{V_s}{V_v} \cdot 100\% = \textbf{34.2 \%}$

Figure 4-1 Derivation of the currently accepted view

4.2 Scalar characterisation, 6.04 % wheel slip at 50 km/h operational velocity

The scalar characterisation applies the definitions presented in Chapter 2 directly. The operational velocity is therefore considered as the vehicle speed, and the slip speed is calculated from the wheel speed (which is calculated by resolving the vehicle speed in line with the direction of wheel rotation), and vehicle speed (Figure 4-2).
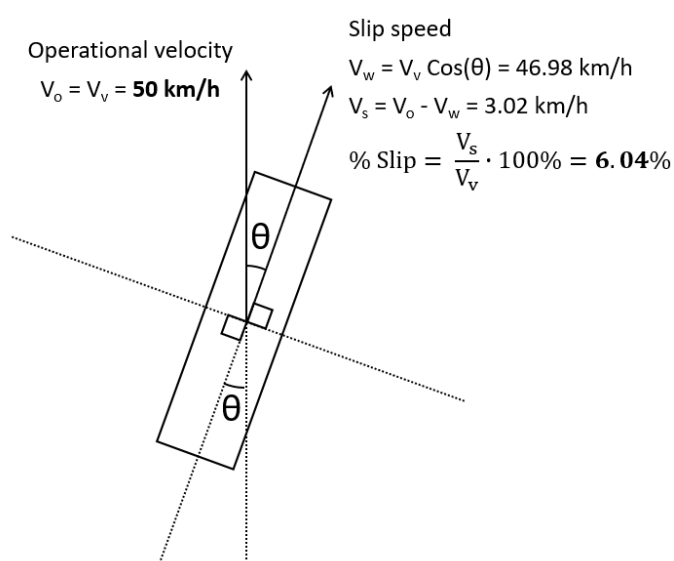
Operational velocity

$V_o = V_v = $ **50 km/h**

Slip speed

$V_w = V_v \, Cos(\theta) = 46.98$ km/h

$V_s = V_o - V_w = 3.02$ km/h

$\% \, Slip = \dfrac{V_s}{V_v} \cdot 100\% = \mathbf{6.04}\%$

Figure 4-2 Derivation of the scalar characterisation

4.3 Vector characterisation, 100% wheel slip at 17.1 km/h operational velocity

The vector characterisation considers the operational velocity and slip speed to act in the direction orthogonal to the direction of wheel rotation. This is owing to the direction of measurement of horizontal force for the majority of side-force skid resistance measurement devices (Figure 4-3).
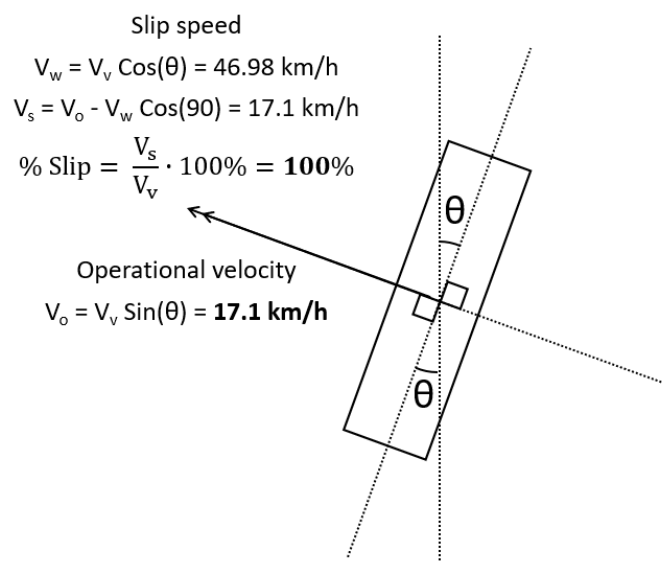
Slip speed

$$V_w = V_v \cos(\theta) = 46.98 \text{ km/h}$$

$$V_s = V_o - V_w \cos(90) = 17.1 \text{ km/h}$$

$$\% \text{ Slip} = \frac{V_s}{V_v} \cdot 100\% = \mathbf{100\%}$$

Operational velocity

$$V_o = V_v \sin(\theta) = \mathbf{17.1 \text{ km/h}}$$

Figure 4-3 Derivation of the vector characterisation

4.4 Co-axial characterisation, 11.7% wheel slip at 50 km/h operational velocity

The co-axial characterisation 're-resolves' the velocities of interest to be co-axial with the direction of interest. Here the operational velocity is defined as the velocity of the vehicle and the wheel speed re-resolved into the direction of travel (Figure 4-4).
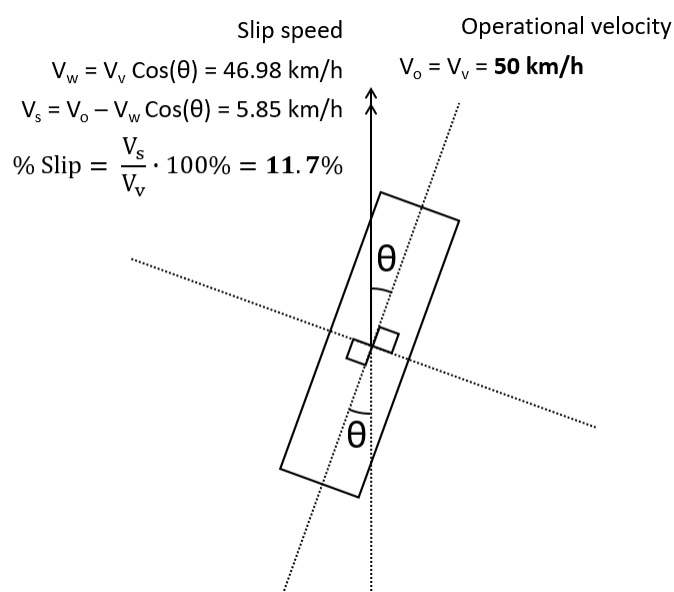
Slip speed

$V_w = V_v \, Cos(\theta) = 46.98 \text{ km/h}$

$V_s = V_o - V_w \, Cos(\theta) = 5.85 \text{ km/h}$

$\% \, \text{Slip} = \dfrac{V_s}{V_v} \cdot 100\% = \mathbf{11.7\%}$

Operational velocity

$V_o = V_v = \mathbf{50 \text{ km/h}}$

Figure 4-4 Derivation of the co-axial characterisation

4.5   Summary

The results of the desk study are summarised in Table 4-1, the relative positions of these results are presented on an idealised friction profile in Figure 4-5. When presenting the results in this way, the importance in understanding the measurement characteristics of SCRIM, with regard to manoeuvres carried out by motor vehicles, becomes clear.

Table 4-1 Summary of desk study

Characterisation	Operational velocity	% slip
Current	The vehicle speed	34.2
Scalar	The vehicle speed	6.03
Vector	The vehicle speed x Sin(20)	100
Co-axial	The vehicle speed	11.7
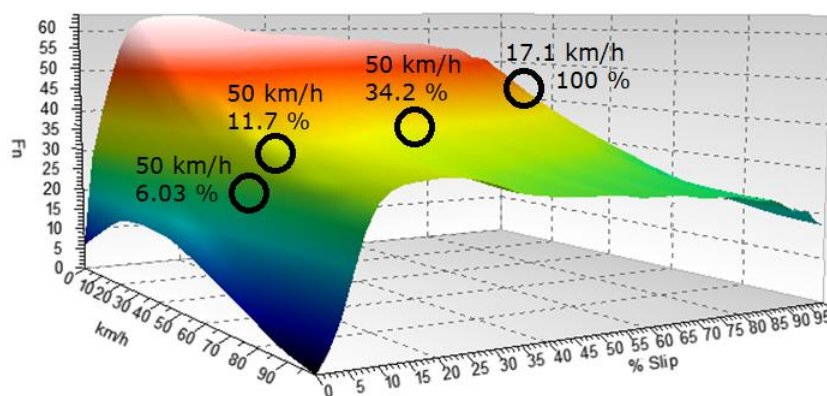
Figure 4-5 Results of desk study as positions on friction profile

As clear conclusions could not be drawn from the results of the desk study, the following research questions were prompted:

- What is the speed of the SCRIM test tyre, and how does this relate to the vehicle speed?
- What factors influence the speed of the SCRIM test wheel?
- What is the operational velocity for SCRIM?
- At what percentage slip does SCRIM characterise road surface friction?
- What factors influence the operational velocity and percentage slip?

The remainder of this document presents an experimental study which was designed to answer these questions, the approach to which can be summarised as follows:

TRL

- A wheel speed rotation sensor was installed on the Highways England Skid Resistance Development Platform (SkReDeP),

- SCRIM wheels and tyres were installed on the Highways England Pavement Friction Tester (PFT) and the trailer weight adjusted to reflect that of the vertical load on SkReDeP,

- Friction measurements were made using the PFT at different operational velocities on surfaces with different nominal friction levels,

- Comparable measurements were made using SkReDeP on the same surfaces and at the same vehicle speeds as those carried out by the PFT.

5 Measurement devices used

5.1 The Skid Resistance Development Platform

Sideway-force Coefficient Route Investigation Machines (SCRIMs) are used for routine monitoring of the skid resistance of the English strategic road network. Figure 5-1 shows the Highways England's Skid Resistance Development Platform (SkReDeP), which incorporates sideway-force measurement equipment.

Figure 5-1 SkReDeP

SCRIM uses a smooth test tyre installed in the nearside wheel path angled at 20 degrees to the direction of travel, which is mounted on an instrumented axle. The Skid Resistance (SR) value is the average ratio between the measured horizontal and vertical force, multiplied by 100.

For this work, SkReDeP was used in its standard configuration with the only modification being the addition of a wheel speed rotation sensor, measurements were therefore made in accordance with BS 7941-1-2006 (British Standards Institution, 2006).

5.2 The Pavement Friction Tester

The Pavement Friction Tester (PFT) (Figure 5-2) is a locked-wheel road surface friction testing device owned by Highways England and operated on their behalf by TRL. The PFT is comprised of a tow vehicle and trailer. The trailer holds the test wheel, which is mounted on an instrumented axle. The test wheel can be independently braked and the forces acting upon it measured to determine the friction between the test tyre and road surface.

During testing, the load and drag forces on the tyre are measured every 0.01 seconds throughout the braking cycle and from this the friction provided at each percentage slip can

be determined. Combining tests made at different operational velocities can yield data that can be combined to create friction profiles such as that presented in Figure 2-1.

Figure 5-2 Pavement friction tester

As alluded to in the previous chapter, substantial modifications were made to the PFT trailer and as such, measurements made with the PFT did not follow the standards required for PFT tests. These modifications were made in order to make the PFT "look" as much like a SCRIM device as possible (same test tyre and vertical load) such that a direct comparison between the measurements made by both devices could be made. The modifications made are detailed in the following sections.

5.2.1 The addition of SCRIM wheels and tyres

For direct comparison of PFT and SkReDeP measurements, it was necessary to fit the PFT with SCRIM tyres and to set the vertical load on the test wheel to 200kg. To achieve this, interference plates were designed to allow two SCRIM tyres to be installed on to the PFT side by side[3]. These alterations are shown in Figure 5-3.

---

[3] Four SCRIM tyres were therefore installed on the PFT, two per side.

Figure 5-3 SCRIM tyres installed on the PFT

Two SCRIM tyres were required to be used on the PFT because the PFT trailer weight could not be reduced sufficiently to achieve the 200 kg per tyre weight used on SCRIM (see following section). To this end it was necessary to use two tyres, per side, on the PFT with a 400 kg vertical load on each pair of tyres. Note that in its standard operating mode, there is a 500kg vertical load on each of the wheels on the PFT trailer.

5.2.2 *Alteration of trailer weight*

As stated in the previous section, the PFT trailer weight was adjusted to reflect the weight on a SCRIM wheel; this was achieved by the removal of steel ballast plates within the trailer and a warning sign assembly that is required for on road testing. To this end the trailer weight was adjusted until 400 kg was applied to each trailer wheel assembly (i.e. set of two SCRIM tyres).

To ensure that this setup would not introduce error in the results, a preliminary study was carried out comparing the friction measurements made with the PFT using one SCRIM tyre at 300 kg per wheel load, with measurements made using two SCRIM tyres at 600 kg load. This study is detailed in 0 and the conclusions can be expressed as the relationship shown in Equation 5-1.

$$Fn_{m\,t} = Fn_{m2\,t2}$$

Where:

- $Fn_{m\,t}$ is the friction measured on surface x at mass m and using one tyre, and,
- $Fn_{m2\,t2}$ is the friction measured on surface x at mass 2m and using two tyres.

Equation 5-1 Relationship between friction measurements made with one tyre and x1 mass, and two tyres and x2 mass

6 Materials assessed and measurements made

The experimental work required the determination of the friction properties of materials with different nominal friction levels, at a wide range of vehicle speeds, and with multiple measurements being made at each vehicle speed. To this end measurements were made on a closed test track such that the experimental conditions could be controlled, and multiple measurements made in a safe and efficient manner.

The straight line wet grip area at the HORIBA-MIRA proving ground was selected as the test site as it met all of the necessary experimental requirements. This facility has the additional benefit of containing surfaces used in the annual accreditation of sideways-force skid resistance devices in the UK.

Figure 6-1 shows the layout of the straight line wet grip area with the nominal friction values[4] of the materials assessed. For this study, measurements were made on the following materials using the regime summarised in Table 6-1:

- Basalt tiles (BT) – A smooth surface constructed from basalt tiles,

- DeluGrip 1 (DG1) – An asphalt surface designed to have high friction values,

- ISO Braking asphalt 1 (ISO1) – An asphalt surface used in standardised braking tests,

- Bridport Pebble (BP) – An asphalt material with bridport pebble aggregate,

- ISO Braking asphalt 2 (ISO2) - An asphalt surface used in standardised braking tests,

- DeluGrip 2 (DG2) - An asphalt surface designed to have high friction values,

---

[4] Reported as values of SC, the standard friction characterisation for SCRIM devices.

TRL

Lane 1	Asphalt	Ceramic tiles	
Lane 2	Basalt tiles SC = 0.131		
Lane 3	DeluGrip 1 SC = 0.383	ISO Braking asphalt 1 SC = 0.365	
Lane 4	Bridport Pebble SC = 0.215	ISO Braking asphalt 2 SC = 0.376	
	Deli grip 2 SC = 0.491		
Lane 5	Glass plate	Smooth Concrete	Aquaplaning area

Figure 6-1 Layout of the HORIBA-MIRA straight line wet grip area

Table 6-1 Summary of measurements made

Material	Measurement runs made with SkReDeP at the following vehicle speeds:			Measurements made with the PFT at the following vehicle speeds:		
	30	50	80	30	50	80
BT	8	10	8	24	28	43
DG1	8	8	7	27	26	22
ISO1	8	8	8	20	26	25
BP	8	8	8	16	13	4
ISO2	8	8	8	27	27	18
DG2	6	5	6	39	46	42

Measurements were made in such a way as to minimise the effects of track conditioning[5]. This was achieved by using an alternating test programme where measurements were made in rotation such that track conditioning effects would be averaged out in the data analysis.

---

[5] The act of making a friction measurement alters the friction of the surface.

7 Data processing and analysis

7.1 The calculation of operational velocities for SkReDeP

Data collected using SkReDeP was used as the main data set for this work and against which data collected using the PFT were compared. Comparisons were made in line with the characterisations of SCRIM derived from the desk study (Table 4-1). In order to make these comparisons it is necessary to calculate the operational velocity of the SkReDeP measurements made in line with these characterisations.

For the current, scalar and co-axial characterisations of SCRIM, the operational velocity is equal to the vehicle speed and so no calculation of operational velocity is required. For the vector characterisation, operational velocity is defined as Sin(20) of the vehicle speed. As part of the data analysis an additional column of data was calculated for the measurements made using SkReDeP which performed this operation.

7.2 The generation of friction profiles

To generate comparative data, it was necessary to calculate the friction provided by each surface at each operational velocity / % slip combination, this calculation is referred to as a friction profile. The procedure for generating friction profiles from data collected using the PFT is detailed in Chapter 5 of TRL report PPR 815 (Sanders, Militzer, & Viner, 2017). This procedure can be summarised as:

- Consider the individual measurements made on a given surface at different vehicle speeds,
- interpolate the % slip / friction relationship for each individual measurement to a resolution of 1 % slip,
- interpolate the operational velocity / friction relationship at each % slip using a line of best fit adhering to the power relationship and calculate the friction measurement at each 1 km/h interval using the coefficients of the line of best fit.

The results of this process yielded a friction profile for each material tested. These profiles are presented in 0 and, as an example, the profile generated for the ISO2 material is presented in Figure 7-1.
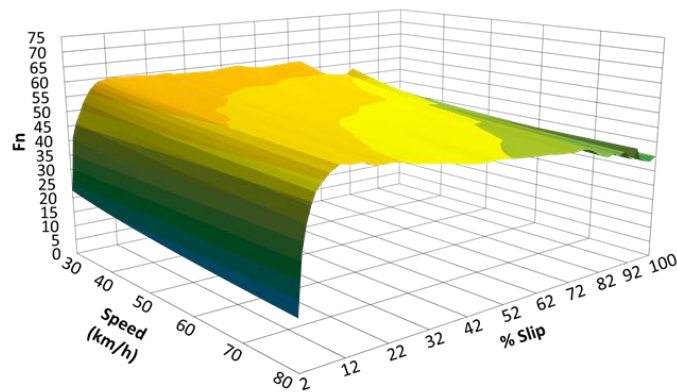
Figure 7-1 Friction profile generated for the ISO 2 material

7.3   The comparison of SkReDeP and PFT data

To compare data collected using SkReDeP and the PFT, measurements of SR were averaged for each target speed and plotted with respect to the operational velocity for each of the characterisations identified in PPR 957 (Sanders & Browne, 2020). Alongside these data, friction measurements collected using the PFT were plotted which corresponded to the locations on the friction profile representative of the characterisations identified in PPR 957 (Sanders & Browne, 2020).

An example of this for the ISO 2 material and the vector characterisation is shown in Figure 7-2 where:

- the solid series markers represent the average friction or SR value for the operational velocity,

- the shaded series markers represent the individual friction or SR data,

- the solid lines represent lines of best fit through the average friction and SR values individually (the solid series markers), and

- the broken black line represents the line of best fit through all average data collectively.

When assessing the figures comparing measurements made with SkReDeP and the PFT, the R^2 value of the lines of best for the broken black lines are primarily used to assess the amount of agreement between the two datasets.
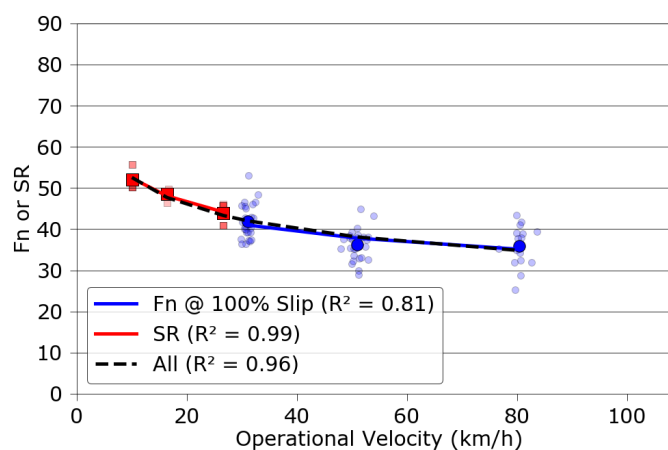
Figure 7-2 A comparison of SR and Friction data for the ISO 2 material and vector characterisation of SCRIM[6]

Comparisons of friction and SR data were carried out for each of the characterisations listed in Table 4-1. To contextualise these data, comparisons were also made between SR data (at both operational velocities) and the closest matching friction data.

To achieve this, a regression analysis was carried out whereby friction measurements made at each % Slip were compared to SR data. The R^2 value of the line of best fit for all average data (the black broken line) was calculated for each SR / friction data pairing, the data relating to the greatest R^2 value were considered the closest matching data. An example of this is shown in Figure 7-3.

The case shown in Figure 7-3 shows SR data where the operational velocity is equal to Sin20 of the vehicle speed. In these cases, the operational velocity of the SR data and friction data do not overlap. This is owing to the limitations on vehicle speeds of the SkReDeP and PFT devices. The minimum vehicle speed of the PFT (for which valid measurements are produced) is 30 km/h. The maximum vehicle speed of SkReDeP is 90 km/h; Sin20 of this speed is 31 km/h.

---

[6] Note that the data presented refer to the operational velocity, not the vehicle speed and as such the SR data range between 10 km/h and 27 km/h despite measurements having been made at vehicle speeds between 30 km/h and 80 km/h.
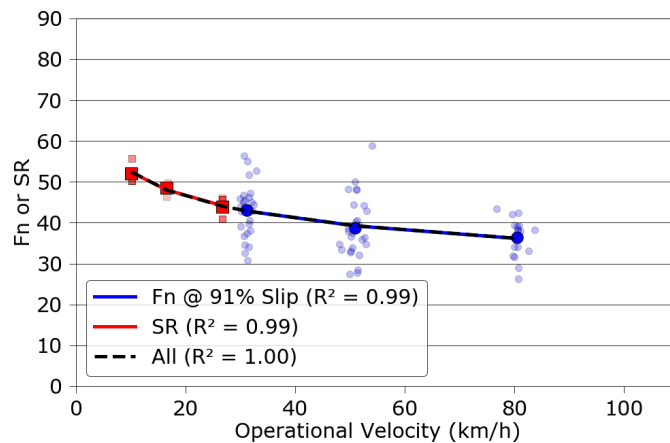
Figure 7-3 A comparison of SR data and closest matching friction data for the ISO 2 material and an operational velocity for SkReDeP equal to Sin(20) of the vehicle speed[7]

7.4 The calculation of test wheel speed

In Chapter 9 two aspects of the tyre rotation are presented, namely the linear speed and angular speed of the tyre. The angular speed of the tyre is measured using the wheel speed encoder installed on the SkReDeP test wheel and is expressed as a function of degrees of rotation with respect to time.

The linear speed of the tyre is the instantaneous speed of the tyre tangential to the direction of rotation. The linear speed of the SkReDeP test wheel was calculated by multiplying the angular speed of the tyre by its measured radius (Equation 7-1)

$$V = \omega \cdot r$$

Where:

- V is the linear speed of the test wheel

- ω is the angular speed

- r is the radius of the tyre measured from the centre of the axis of rotation to the ground under normal loading[8]

Equation 7-1 Calculation of linear velocity

---

[7] Note that the % slip value shown in the legend does not equal that of any of the characterisations in Table 4-1.

[8] To account for any compression of the tyre.

The calculated linear wheel speeds were compared with the estimated wheel speeds for each material and each test speed. The difference between these two speeds is presented in Chapter 9 as a percentage of the vehicle speed[9]. For clarity the equation used to derive these values is presented in Equation 7-2

$$\% \, res = 100 \cdot \frac{V_w - V_v Sin(20)}{V_v}$$

Where:

- % res (residual value) is the difference between the measured and estimated wheel linear speeds as a percentage of the vehicle speed

- V_w is the linear speed of the wheel (Equation 7-1)

- V_v is the speed of the vehicle

Equation 7-2 Calculation of the difference between the measured and estimated wheel linear speeds as a percentage of the vehicle speed

[9] To remove the scaling effects of higher vehicle speeds.

8   Results - Assessment of friction measurement characteristics

This chapter presents the friction measurements as described in the previous chapter. Owing to the amount of data presented, and for clarity, each group of six plots generated for each material have been presented as single figures.
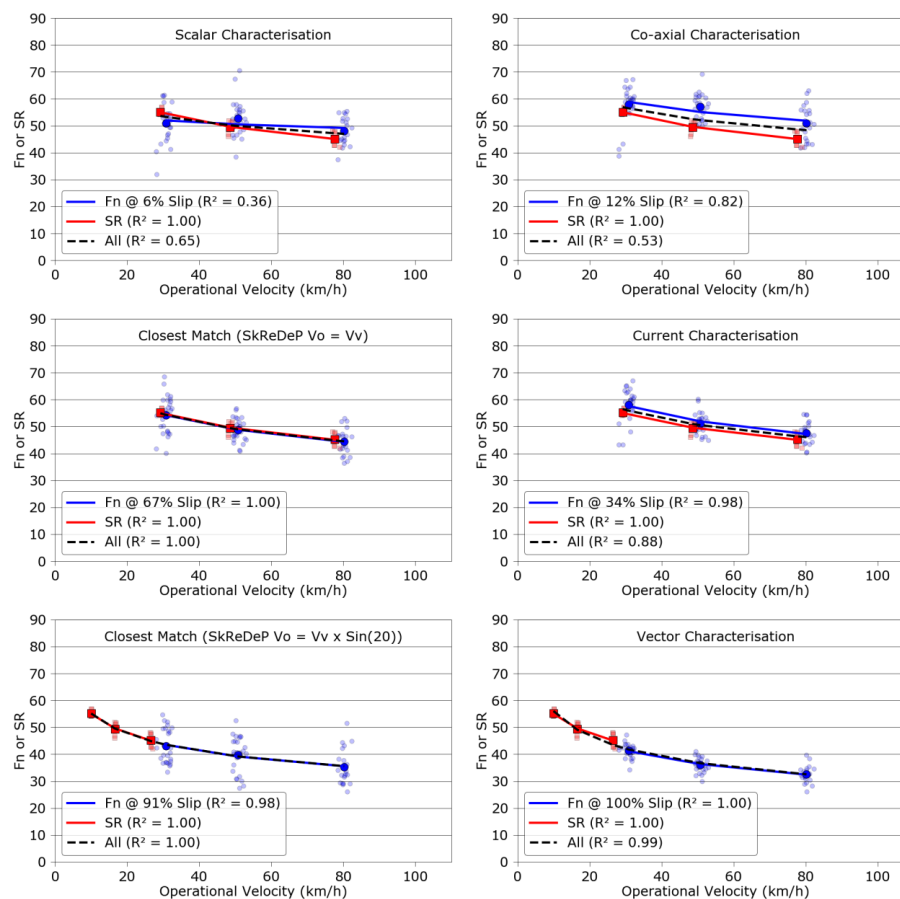
Basalt Tiles
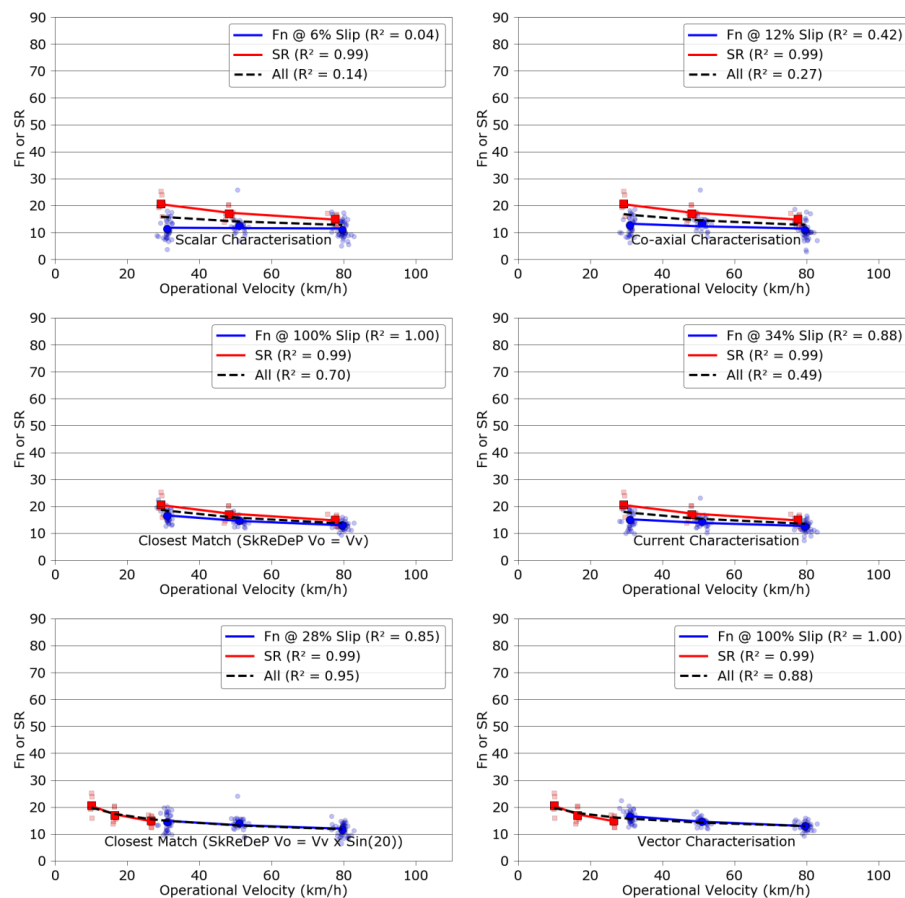
Figure 8-1 Friction measurements made on the Basalt Tiles material

Figure 8-1 shows that, with an R^2 value of 0.88, of the 4 characterisations assessed, the **Vector** characterisation provided the closest agreement between the two test devices. The closest matching data were observed at a SkReDeP operational velocity equal to Sin(20) of the vehicle speed and at 28% slip.

DeluGrip 1

Figure 8-2 Friction measurements made on the DeluGrip 1 material

Figure 8-2 shows that, with an R^2 value of 0.99, of the 4 characterisations assessed, the **<u>Vector</u>** characterisation provided the closest agreement between the two test devices. The closest matching data were observed at a SkReDeP operational velocity equal to Sin(20) of the vehicle speed and at 91% slip.
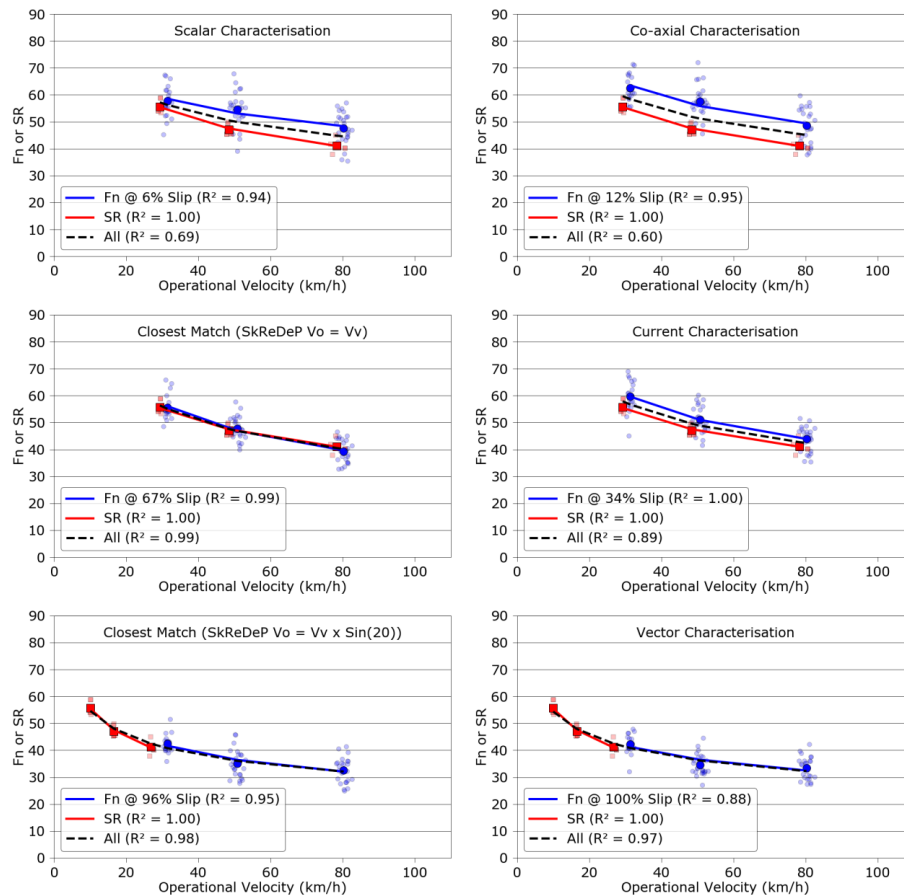
ISO Asphalt 1

Figure 8-3 Friction measurements made on the ISO Asphalt 1 material

Figure 8-3 shows that, with an R^2 value of 0.96, of the 4 characterisations assessed, the **Vector** characterisation provided the closest agreement between the two test devices. The closest matching data were observed at a SkReDeP operational velocity equal to Sin(20) of the vehicle speed and at 96% slip, and at a SkReDeP operational velocity equal to the vehicle speed and 82% slip.
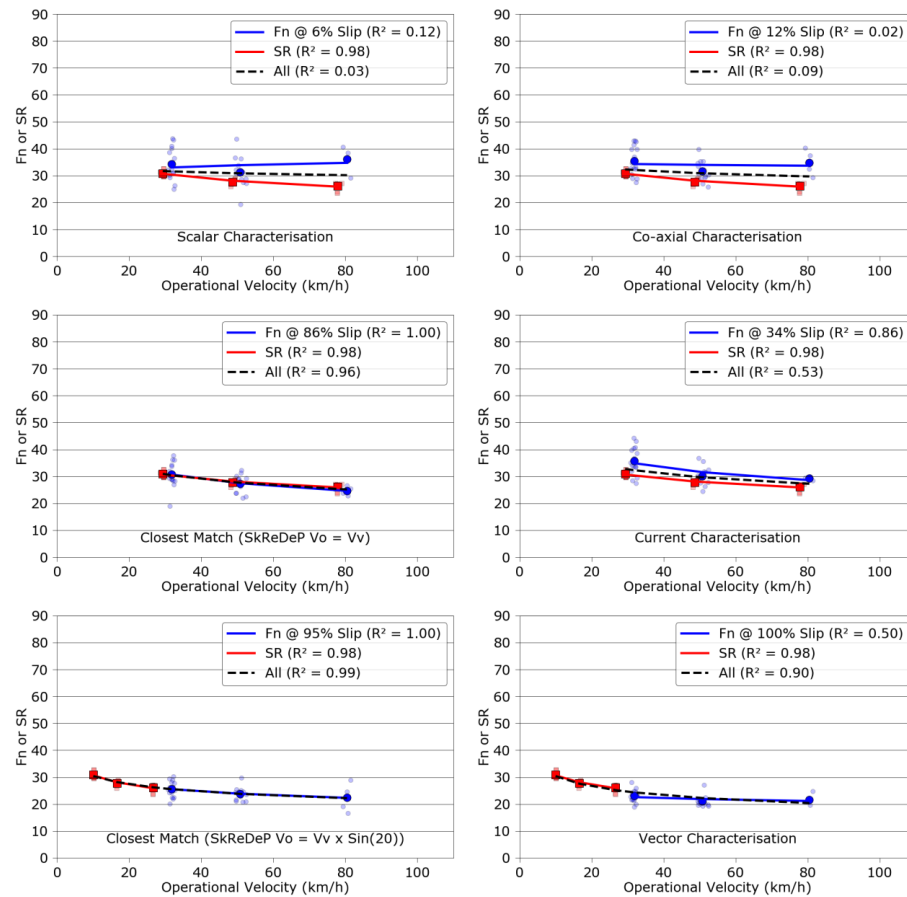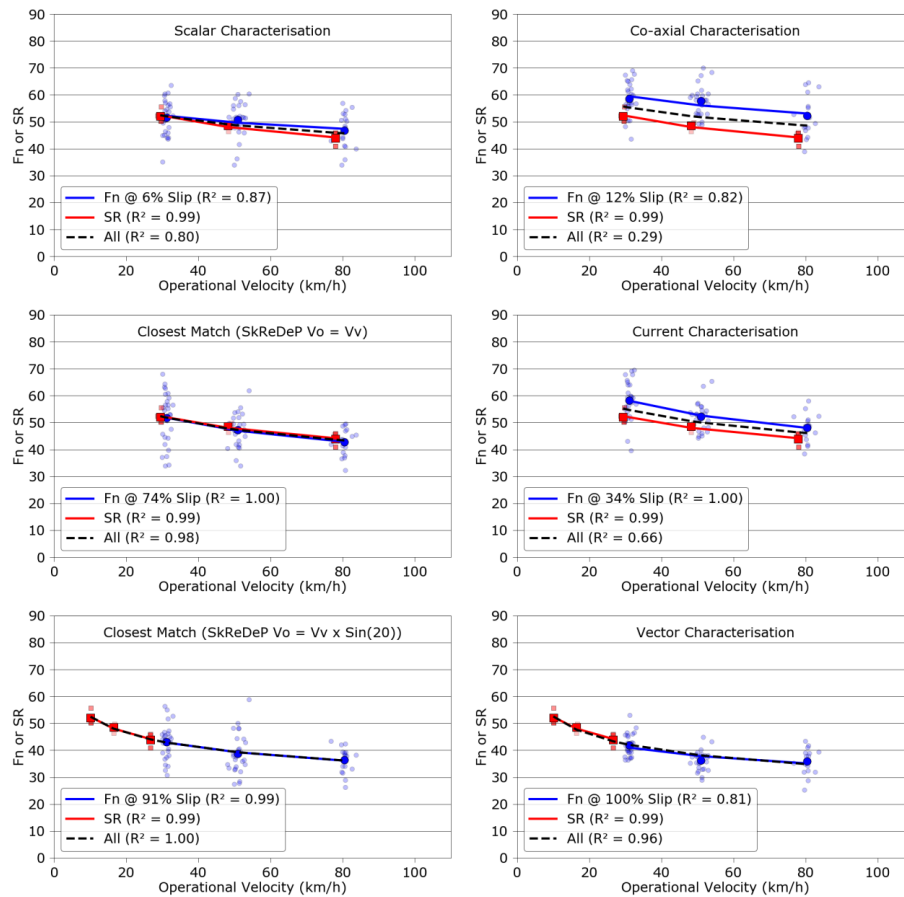
Bridport Pebble

Figure 8-4 Friction measurements made on the Bridport Pebble material

Figure 8-4 shows that, with an R^2 value of 0.90, of the 4 characterisations assessed, the **<u>Vector</u>** characterisation provided the closest agreement between the two test devices. The closest matching data were observed at a SkReDeP operational velocity equal to Sin(20) of the vehicle speed and at 95% slip.

TRL

ISO Asphalt 2

Figure 8-5 Friction measurements made on the ISO Asphalt 2 material

Figure 8-5 shows that, with an R^2 value of 0.96, of the 4 characterisations assessed, the **Vector** characterisation provided the closest agreement between the two test devices. The closest matching data were observed at a SkReDeP operational velocity equal to Sin(20) of the vehicle speed and at 91% slip.
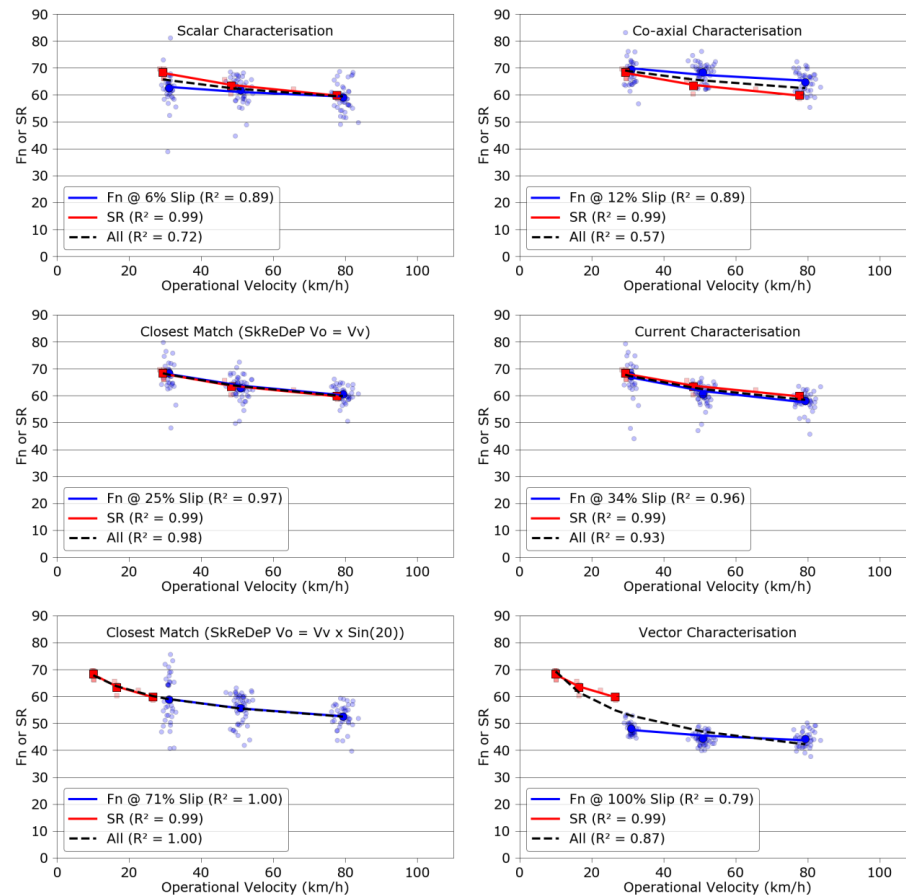
DeluGrip 2

Figure 8-6 Friction measurements made on the DeluGrip 2 material

Figure 8-6 shows that, with an R^2 value of 0.93, of the 4 characterisations assessed, the **Current** characterisation provided the closest agreement between the two test devices. The closest matching data were observed at a SkReDeP operational velocity equal to Sin(20) of the vehicle speed and at 71% slip.

This is the only case of the 6 where the vector characterisation did not provide the closest match and may demonstrate something fundamental about the measurements made by side-force skid resistance measurement devices on this type of surfacing.

From the results presented in this chapter, the following observations can be made:

- The vector characterisation provides the closest agreement between measurements made using the PFT and SkReDeP on all but one of the surfaces assessed.
- Of these surfaces, the agreement observed by the vector characterisation is markedly greater than the agreement observed by the next closest characterisation.
- On the DeluGrip2 surface (the highest friction surface) the closest agreement between data collected using the PFT and SkReDeP was observed at % slips lower than 100%.

TRL

9   Results - Assessment of tyre rotational speed

This chapter presents the results of the test wheel rotational speed measurements. Figure 9-1 presents the Average % res[10] of the tyre rotational speed for each material assessed and each vehicle speed. The data have been presented with the sites ordered relating to their nominal friction values.

Figure 9-1 shows that on the Basalt Tiles (BT) material the actual rotational speed of the tyre is markedly lower than its expected rotational speed, and, that this discrepancy increases with vehicle speed. This may provide evidence that the tyre is aquaplaning, or near to aquaplaning. The physical explanation for this is that the friction between the tyre and surface is not great enough to force the tyre to spin at the estimated rotational speed, rather that the tyre is slipping relative to the surface (in addition to the slipping in the direction of the axis of rotation).

Figure 9-1 also shows that for measurements made at 30 km/h, the average % res for the majority of the materials tested, namely the BP, ISO1, ISO2 and DG1 materials, here forth referred to as "the middle four" is approximately zero. However, with increasing speed, the average % res decreases. At 50 km/h the middle four produce an average % res of -0.14 and at 80 km/h, -0.81%.
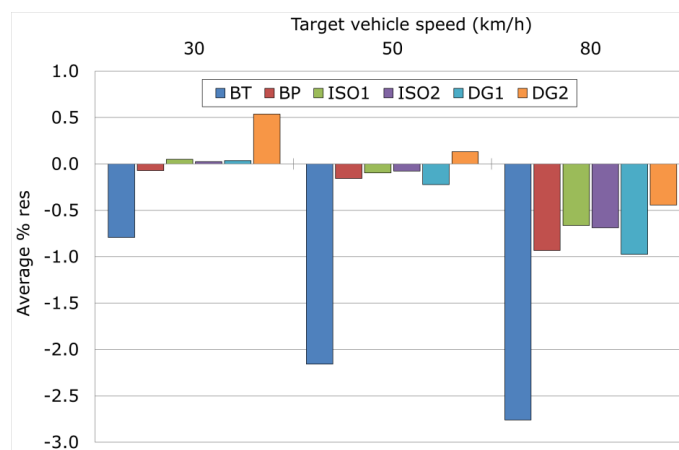

Figure 9-1 The average residual values for wheel linear speed as a percentage of vehicle speed

The final key observation from Figure 9-1 is that the average % res measured on the DG2 material, the highest friction material, is greater than the middle four for each vehicle speed. Pertinent to this observation are the data presented in Figure 9-2 which show the

---

[10] The difference between measured and predicted linear wheel speed as a percentage of the vehicle speed.

average rotational speed of the test wheel for each material and vehicle speed, expressed as a percentage of the average rotational speed for all materials at each speed.

Figure 9-2 Average rotational speed of the test wheel for each material and speed, expressed as a percentage of the average rotational speed for all materials at each speed.

Figure 9-2 shows that the rotational speed of the tyre on the Basalt Tiles material is markedly lower than that measured on all other materials. This is consistent with the theory that aquaplaning, or near aquaplaning, occurred on this material.

Figure 9-2 also shows that the rotational speed of the tyre on the DeluGrip 2 material is similar to that measured on the middle four. Combining this observation with that showing lower comparative linear speeds, the following argument can be formed:

1. Linear wheel speeds on the DG2 material were greater than those of the middle 4,

2. rotational wheel speeds on the DG2 material were similar to those of the middle 4,

3. linear wheel speed is dependent upon the radius of the tyre,

4. the radius of the tyre can change if the tyre deforms due to vertical load, or stretching due to the friction between tyre and the road,

5. given the relationship between tyre rotational and linear speed given in Equation 7-1[11], to satisfy points 1 and 2, the conclusion follows that the tyre stretched less (producing a greater radius) on the DeluGrip2 materials than on the middle four.

6. a hypothesis for this conclusion is that the tyre is in a pre-locked condition, in other words, measurements are being made below the critical angle for this material.

---

[11] Linear speed = Rotational speed x Radius

TRL

10 Summary and conclusions

10.1 Characterising SCRIM measurements

Comparative measurements made using a modified PFT and SkReDeP have shown that in five of the six cases tested, the characterisation produced by the literature review which most closely matched observation was the 17.1 km/h operational velocity and 100% Slip case. For the sixth case, where measurements were made on the material with the highest skid resistance of those assessed, a markedly different pattern to the friction data, and wheel rotation data were observed; this is discussed further in Section 10.3.

10.2 Aquaplaning or near aquaplaning

The use of an encoder allowed the wheel rotational speed to be measured, and compared to the predicted value which was calculated as wheel speed = vehicle speed x Sin(20). The results for the tests carried out at 30 km/h and 50 km/h showed for materials BP, ISO1, ISO2, and DG1 that this relationship held, indicating the wheel was experiencing the full friction of the road and was not sliding in the direction of travel.

However, for all of the tests carried out on surface BT and for the tests carried out at 80 km/h the measured wheel speed was lower than the predicted wheel speed. This indicates that the friction between the tyre and road surface is not sufficient to cause the tyre to rotate at the predicted speed, and instead it is (partially) sliding in the direction of travel, i.e. it is aquaplaning or nearly aquaplaning.

10.3 Critical wheel angle

The measurements carried out on surface DG2 exhibited a markedly different relationship between the measured friction and vehicle speed to the other surfaces. This was further investigated by considering the linear wheel speed as calculated from the measured rotational wheel speed, and the differences between measured rotational wheel speeds between surfaces.

At low speeds the measured linear wheel speed exceeded the value that would be predicted from the vehicle operational velocity – this indicates that either the angle between vehicle and tyre has changed (unlikely to consistently occur only on surface DG2) or that the radius used in calculating the linear wheel speed from the measured rotational wheel speed is incorrect. As the measured rotational wheel speeds for the materials were similar it can be concluded that the latter is most likely to be the reason for the different behaviour on DG2, and hence the radius of the tyre was greater than expected.

The radius of the tyre results from the combination of the deformation of the tyre due to the vertical load and the stretching of the tyre that results from friction between the tyre and pavement surface. Since the vertical load was kept constant for all tests we can conclude that the tyre must have experienced a different degree of stretching, which we hypothesise is due to the tyre being in a pre-locked condition – i.e. the measurements have been made below the critical angle for this surface.

10.4 Conclusions

From the work carried out, the following conclusions can be made:

- SCRIM measurements are made at an operational velocity of 17.1 km/h and 100% Slip, at the standard vehicle test speed of 50 km/h.

- Aquaplaning or near aquaplaning of the SCRIM tyre occurs on materials with a nominal low skid resistance.

- There is evidence showing that on materials with high nominal skid resistance levels, the critical wheel angle, above which skid resistance measurements no longer increase, may not be being achieved.

Bibliography

ASTM. (2008). *ASTM E1337 - 90 Standard Test Method for Determining Longitudinal Peak Braking Coefficient of Paved Surfaces Using Standard Reference Test Tire.* ASTM.

ASTM. (2011). *ASTM E274 E274M-11 Standard Test Method for Skid Resistance of Paved Surfaces Using a Full-Scale Tire.* ASTM.

ASTM. (2012). *ASTM E524 - 08 Standard smooth tyre for pavement skid resistance tests.* ASTM.

Bird, G., & Miller, R. A. (1937). *TP2 Studies in road friction II. An analysis of the factors affecting measurement.* Department of scientific and industrial research and Ministry of Transport.

Bradley, J., & Allen, R. F. (1930-31). Factors affecting the behaviour of rubber-tyred wheels on road surfaces. *Institute of automobile engineers proceedings*, pp. 63-92.

British Standards Institution. (2006). *BS 7941-1-2006 Methods for measuring the skid resistance of pavement surfaces – Part 1 SCRIM.* London: BSi.

British Standards Institution. (2009). *DD CEN/TS 1509-6:2009 Part 6: Procedure for determining the skid resistance of a pavement surface by measurement of the sideway force coefficient (SFCS): SCRIM.* London: British Standards Institution.

Department for Transport. (2004). *HD 28/04 - Skid resistance (DMRB 7.3.1).* London: The Stationery Office.

Department for Transport. (2004). *HD 28/04 Skidding resistance.* London: DfT.

Department for Transport. (2015). *HD 28/15 - Skid resistance (DMRB 7.3.1).* London: The Stationery Office.

Greene, M., Viner, H., Cerezo, V., Kokot, D., & Schmidt, B. (2014). *ROSANNE Deliverable D1.1 Definition of boundaries and requirements for the common scale for harmonisation of skid resistance measurements.* N/A: ROSANNE.

Grime, G. (1953). *RN_2029_GG The interpretation of measurements made with the road research laboratory's motorcycle skidding machine.* Road research laboratory.

Henry, J. J. (2000). *Evaluation of pavement friction characteristics.* NCHRP.

Highways England, Transport Scotland, Welsh Government, Department for Infrastructure. (2019). *CS 228 Pavement inspection and assessment - Skidding resistance.* London: Highways England.

TRL

Nordström, O., & Åström, H. (2001). *Upgrading of VTI friction test vehicle BV12 for combined braking and steering tests under aquaplaning and winter conditions .* Florence: 2nd International Coloquium on Vehicle Tyre Road Interaction .

NSW Roads and Maritime Services. (2013). *QA Specification R423 Measurement of surface friction by sideways-force coefficient routine investigation machine (SCRIM).* NSW Roads and Maritime Services.

Roe, P. G., & Dunford, A. (2012). *PPR564 The skid resistance behaviour of thin surface course systems.* Wokingham: TRL.

Sanders, P. D., & Browne, C. (2020). *PPR957 Characterising the measurements made by sideways-force skid resistance devices - A desk study and proposal for an experimental study.* Wokingham: TRL.

Sanders, P. D., Militzer, M., & Viner, H. E. (2017). *PPR815 Better understanding of the surface tyre interface.* Wokingham: TRL.

Wallbank, C., Viner, H., Smith, L., & Smith, R. (2016). *The relationship between collisions and skid resistance on the Strategic Road Network. TRL Published Project Report PPR806.* Wokingham: TRL.

The double wheel experiment

The aim of the double wheel experiment was to test the assumption that the friction generated between a surface and a vehicle comprising a given mass and given number of tyres per axle, is the same as the friction generated between the same surface and a vehicle with twice the mass and twice the number of tyres per axle. This is shown in Equation A - 1.

$$F_{mt} = F_{2m2t}$$

Where:

- F = The friction generated between a vehicle and surface

- m = The mass of a vehicle

- t = the number of tyres per axle of a vehicle

Equation A - 1 Definition of the null hypothesis H_0 for the double wheel experiment

A.1   Experimental procedure

The experiment was carried out with the PFT modified to accept SCRIM wheels. The study consisted of making multiple measurements of friction on a single surface at the Longcross test track with the PFT trailer in two configurations, namely:

1. With a single SCRIM wheel per axle, and a per axle weight of 260 kg, and,

2. With two SCRIM wheels per axle, and a per axle weight of 520 kg.

The PFT measurements were made at a range of test speeds. Table A - 1 summarises the measurements made.

Table A - 1 Measurements made

Configuration	Number of measurements	Test speed (km/h)
1 (tyre "A")	Eight tests at each speed	30, 50 and 80
1 (tyre "B")	Eight tests at each speed	30, 50 and 80
2 (tyres "A" and "B")	Eight tests at each speed	30, 50 and 80

To account for variations in tyre performance the same tyres were used for all of the measurements. Both the "A" and "B" tyres were used for the configuration 2 testing, and, configuration 1 testing was carried out with the "A" and "B" tyres separately.

The SCRIM tyres used in configuration 2 were mounted to the PFT in a "back to back" configuration such that the wheel offsets force the tyres away from the PFT trailer hub. Furthermore, during the configuration 1 testing, the positions of the "A" and "B" tyres matched the positions of those tyres in configuration 2.

A.2   Data handling and assessment

Data from both configurations, were plotted on a single graph and a one sample student's t-test using an alpha level of 5% was carried out. The t-test was carried out for each friction type (P-Fn and L-Fn) and speed pair. This was achieved using Equation A - 2.

$$t = \frac{\bar{x}_2 - \bar{x}_1}{\left(\sigma_2 / \sqrt{n_2}\right)}$$

Where:

- t = the "t" value, a separate t-value will be calculated for each speed

- $\bar{x}_1$ = the population mean, the mean value from the configuration 1 testing

- $\bar{x}_2$ = the sample mean, the mean value from the configuration 2 testing

- σ_2 = the sample standard deviation, the standard deviation from the configuration 2 testing

- n_2 = the number of tests carried out during the configuration 2 testing

Equation A - 2 Calculation of students t-test "t" value

The t values were compared with the appropriate statistical critical values in order to accept or reject the hypothesis that mesurements made in configuration 1 and 2 are the same (H_o).

The results of this study are presented in Figure A - 1 which shows that in all cases H_o was accepted. It is possible to state with some confidence therefore that $F_{m_a t_b} = F_{m_{2a} t_{2b}}$.
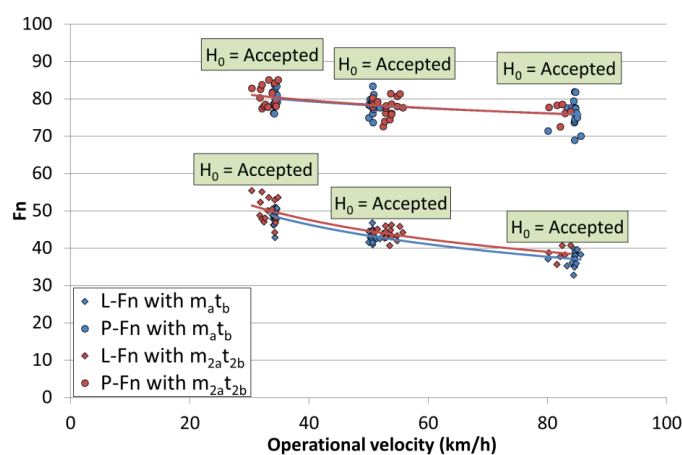

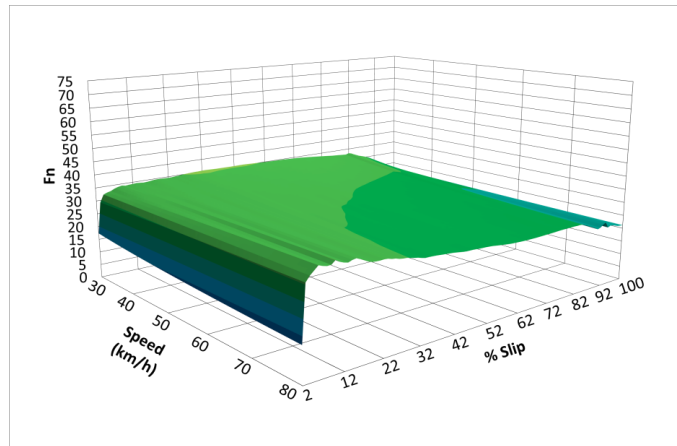**Figure A - 1 Results of the double wheel experiment**

Friction profiles

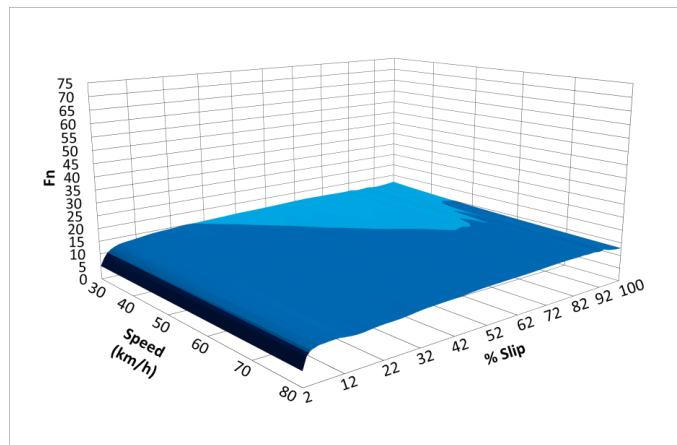**Figure B - 1 Friction profile generated for the Bridport pebble material**

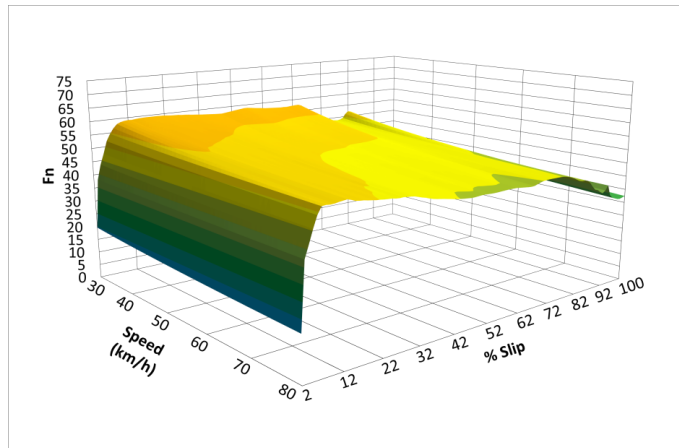**Figure B - 2 Friction profile generated for the Basalt tiles material**

Figure B - 3 Friction profile generated for the DeluGrip 1 material
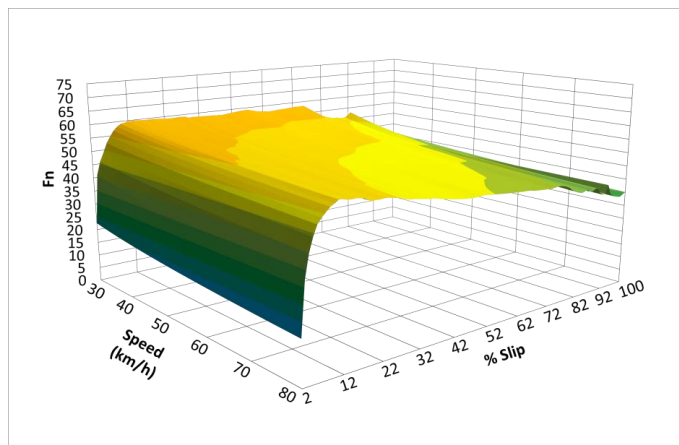

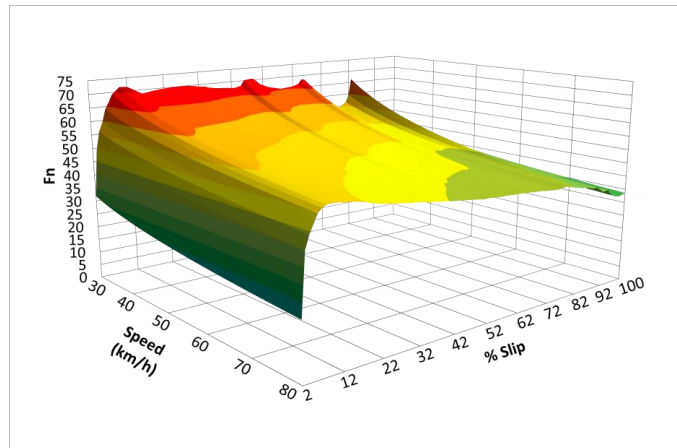**Figure B - 4 Friction profile generated for the ISO2 material**

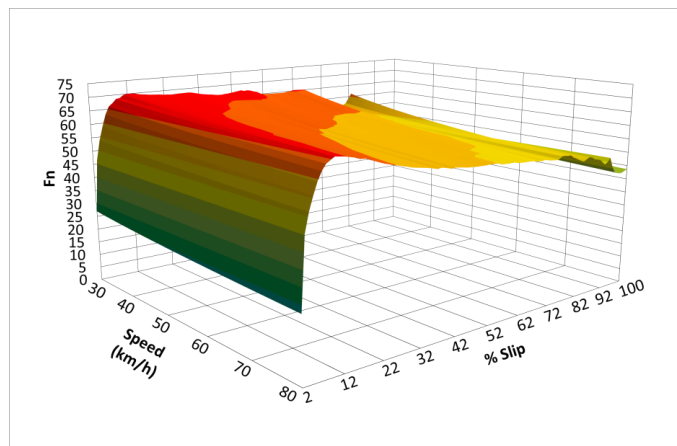**Figure B - 5 Friction profile generated for the ISO1 material**

Figure B - 6 Friction profile generated for the DeluGrip 2 material

Characterising the measurements made by sideways-force skid resistance devices

TRL

The effective management of road surface skid resistance is critical in providing a safe means of road travel. The measurement of skid resistance is a key component in the effective management of road surface skid resistance. In the UK the skid resistance properties of the trunk road network are assessed annually using devices utilising the sideways-force measurement principle, the Sideways-force Coefficient Routine Investigation Machine (SCRIM).

Currently, the fundamental measurement characteristics of SCRIM, its percentage slip and operational velocity, are not known. This document presents the results of an experimental study which characterises the measurement properties of SCRIM in terms of percentage slip and operational velocity.

Other titles from this subject area

PPR957   Characterising the measurement characteristics of sideways-force skid resistance mea-surement devices - A desk study and proposal for an experimental study. P D Sanders and C Browne. 2020.

PPR768   Performance review of skid measurementdevices. P D Sanders, S Brittain and A Premathilaka. 2017.

PPR815   Better understanding of the tyre surface interface. P D Sanders, M Militzer and H E Viner. 2017

PPR727   Road surface properties and high speedfriction. P D Sanders, K Morosiuk and J R Peeling. 2014.